IMPACT OF EXTERNAL SHADING STRATEGY ON ENERGY PERFORMANCE OF HOTEL BUILDINGS IN MEDITERRANEAN CLIMATE

A THESIS SUBMITTED TO
THE FACULTY OF ARCHITECTURE AND ENGINEERING
OF
EPOKA UNIVERSITY

BY

GRIDI HIMÇI

IN PARTIAL FULFILLMENT OF THE REQUIREMENTS
FOR
THE DEGREE OF MASTER OF SCIENCE
IN
ARCHITECTURE

JULY, 2021

Approval sheet of the Thesis

This is to certify that we have read this thesis entitled **"Impact of external shading strategy on energy performance of hotel buildings in Mediterranean climate"** and that in our opinion it is fully adequate, in scope and quality, as a thesis for the degree of Master of Science.

____

Dr. Edmond Manahasa
Head of Department
Date: July, 23, 2021

Examining Committee Members:

Assoc. Prof. Dr. Sokol Dervishi (Architecture) _________________

Dr. Artan Hysa (Architecture) _________________

MSc. Artemis Hasa (Architecture) _________________

I hereby declare that all information in this document has been obtained and presented in accordance with academic rules and ethical conduct. I also declare that, as required by these rules and conduct, I have fully cited and referenced all material and results that are not original to this work.

Name Surname: Gridi Himçi

Signature: _______________

ABSTRACT

IMPACT OF EXTERNAL SHADING STRATEGY ON ENERGY PERFORMANCE OF HOTEL BUILDINGS IN MEDITERRANEAN CLIMATE

Himçi, Gridi

M.Sc., Department of Architecture

Supervisor: Assoc. Prof. Dr. Sokol Dervishi

The tourism sector accounts for 10.4% of global GDP and 319 million jobs, one of fastest rates of growth of all sectors worldwide. Hotels are one of the many actors that play a vital role in the industry as a whole. With this considered, it is necessary setting up viable operational practices as well as educating consumers on sustainable behaviors. External shading system is considered as one of the main passive elements providing environmental and socio-economic benefits but also aesthetic values in buildings. However, researches on this topic have been mostly conducted for office buildings, and there is a literature gap regarding the impact of SDs on hotel buildings. The aim of this study is to further estimate the impact of SDs on the thermal efficiency of hotel buildings in the Mediterranean climate. Several parameters in the design, such as window-to-wall ratio, orientation of the building, and climate are considered essential for determining efficient placement of SDs. The results highlight the efficiency of SDs strategies achieving a significant range of energy reduction from 20% up to 80 % for 100% window-to-wall ratio scenario, with 2.7 °C up to 5 °C indoor air temperature decrease in the summer period. The significance of this study lies in providing results providing a fundamental framework for early design decision-making phases.

Keywords: *External shading devices, hotel buildings, energy optimization, passive design, thermal performance, simulation*

ABSTRAKT

IMPAKTI I SISTEMEVE TE JASHTME TE HIJEZIMIT NE PERFORMANCEN TERMIKE TE HOTELVE NE KONTEKSIN MESDHETAR

Himçi, Gridi

Master Shkencor, Departamenti i Arkitektures

Udhëheqësi: Assoc. Prof. Dr. Sokol Dervishi

Sektori i turizmit përbën 10.4% të PBB-së (Prodhimi i Brendshëm Bruto) globale dhe 319 milion vende pune, një nga normat më të shpejta të rritjes së të gjithë sektorëve në të gjithë botën. Hotelet janë një nga shumë faktorët që luajnë një rol jetësor në industrinë në tërësi. Duke marrë parasysh këtë, është e nevojshme vendosja e praktikave praktike operacionale, si dhe edukimi i konsumatorëve për sjelljet e qëndrueshme. Sistemi i hijes së jashtme konsiderohet si një nga elementët kryesorë pasivë që ofron përfitime mjedisore dhe socio-ekonomike, por edhe vlera estetike në ndërtesa. Sidoqoftë, hulumtimet mbi këtë temë janë kryer kryesisht për ndërtesat e zyrave, ekziston një hendek i literaturës në lidhje me ndikimin e hijezuesve në ndërtesat e hoteleve. Qëllimi i këtij studimi është të vlerësojë më tej ndikimin e hijezuesve në efikasitetin termik të ndërtesave hoteliere në klimën mesdhetare. Disa parametra në dizajn, të tilla si raporti dritare në mur, orientimi i ndërtesës dhe klima konsiderohen thelbësore për përcaktimin e vendosjes efikase të hijezuesve. Rezultatet theksojnë efikasitetin e strategjive SDs duke arritur një gamë të konsiderueshme të reduktimit të energjisë nga 20% në 80% për skenarin e raportit 100% dritare në mur, me 2.7 ° C deri në 5 ° C ulje të temperaturës së brendshme në periudhën e verës. Rëndësia e këtij studimi qëndron në sigurimin e rezultateve që ofrojnë një kornizë themelore për fazat e hershme të vendimmarrjes në dizajn.

Fjalët kyçe: *Pajisjet e hijëzimit të jashtëm, ndërtesat e hoteleve, optimizimi i energjisë, dizajni pasiv, performanca termike, simulime*

TABLE OF CONTENTS

LIST OF TABLES

LIST OF FIGURES

CHAPTER 1

INTRODUCTION

1.1 Issues regarding hotel building approach towards energy consumption problem

Energy efficiency is now recognized as one of the fastest and suitable approaches to reduce any energy related emissions associated with, air pollution, global warming and climate change (Dincer, 1998). Buildings are expected to achieve energy efficient status by most nations, which could be achieved through active or passive design strategies. The biggest percentage of energy consumption for any building in hot climate is for air conditioning (Iqbal et.al, 2007). Hotels represent 11% of non-residential total floor space in the EU. (Lapillonne, B., et al, 2013) Ranked among top five, hotels are considered as the most energy consuming among non-residential buildings. Based on various studies data combinations, hotel energy use varies in the range of 200-400 $kWh/m^2/yr$ (Solutions, 2011). For example, the extensive use of glass (very common in office buildings of large European and North American cities) directly affects the energy needs of the building and its level of internal thermal comfort (Gratia and De Herde, 2003). This condition is critical in climates such as the Mediterranean climate that have high solar radiation with moderate temperature winters and warm summers. In this sense, the coordinated performance of HVAC systems, shading devices and electric lighting, based on advanced control strategies, improve energy efficiency by minimizing heating and cooling loads, electric lighting consumption, and assuring visual and thermal user comfort. As a result, the type of construction used in the facade is a key factor in determining the energy performance of a building and therefore its level of sustainability (Fernández Hernández et al., 2017)

Besides enhancing the aesthetic appearance to the buildings, shading devices on the building facades help to minimize energy consumption in the building. Good shading strategy can make a remarkable difference to project's cost, energy efficiency, and environmental impact. To prevent improper applications, designers need accurate and detailed information to ensure choosing the correct shading devices techniques. The success of shading device design depends entirely on building’s use and local climatic conditions. Additionally, a full understanding of the weather data for the site and the needs of the local climate conditions is required (Aldawoud, 2012). Although the shading systems have already been integrated into building facades enhancing aesthetic appearance, their application as a technology to regulate internal building temperatures is a novel. Therefore, more research is required in establishing a more comprehensive knowledge of the shading system's benefits as passive design strategies.

1.2 Thesis Objective

Despite the fact that shading systems have been used and integrated into different types of buildings as an aesthetic and sustainable solution, a literature gap regarding their quantitative effects on hotel building’s thermal performance in Mediterranean climate. The contribution of the present study is therefore to evaluate, considering different forms of shade design, the impact shading systems have on energy savings and interior thermal comfort.

1.3 Organization of the thesis

This thesis is divided in 6 chapters. The organization is done as follows:

In Chapter 1, the problem statement, thesis objective is presented. Chapter 2, includes the literature review. Chapter 3, consists of the methodology followed in this study. In Chapter 4, the simulated results are presented. The discussion session is presented in Chapter 5 when the main results are evaluated. Conclusions and recommendations for further study are presented in Chapter 6.

CHAPTER 2

LITERATURE REVIEW

2.1 Theoretical background

2.1.1. Definition

As practical and low maintenance elements, SDs (shading devices systems) are increasingly used to block direct solar heat impact. The target of SDs is to enlarge the shading ratio, especially on glazing, to keep spaces conditioned, lower energy demands and reduce glare levels (J.enbuild et al., 2016).

2.1.2 Typologies of SDs (Shading Devices Systems)

Numerous studies have categorized shading devices on the basis of the building's orientation, the angle of the shading devices and the geographical position (climate).

Some studies include: J.enbuild et al. (2016) and Kirimtat et al. (2016) classify shading devices as external and internal. External SDs have a higher performance than internal ones (Atzeri et. al., 2014) and fixed SDs are economical solutions, as they do not require manual adjustments (Freewan, 2014).

A general division of shading Rungta (2011) shows the different types of external SDs from simple designs to and complex designs. In simple design he categorized horizontal overhang or panel, horizontal louvers (outrigger system), vertical outer panel, horizontal light shelve, horizontal multiple blades or panels, unfilled eggcrate, and complex filled eggcrate with panels, and complex filled eggcrate with horizontal louvre, vertical slanted fins or panels, horizontal panel and vertical louvers, vertical panels and horizontal louvers, and cantilever.

Several authors provide details of shading devices how daylight regulation can be done with a great variety of shading devices (blinds, overhangs, venetian blinds, louvers, roller shades, etc.). Fernández Hernández et al. (2017), Bellia et al. (2014) and Kirimtat et al. (2016) highlight the complexity of classifying the shading devices but suggest a simple classification based on its place in the building (external or internal) and if it is fixed or movable (manual or automatic). Meerbeek et al. (2014) show the complexity of the interaction between an automation control of motorized exterior blinds with users in Dutch offices. Lee et al. (1998) describes an experimental case of an Oakland (EEUU) office with automatic control of internal venetian blinds, obtaining energy savings of 15 % and 50 %, respectively, with an optimal 45 º slat angle in cooling and electric lighting.

Complex shading device Azar Arifin et al. (2015) made part of his study and consequently the complexity of the shading design egg-crate design result in reducing and controlling the daylight more than vertical design and horizonal respectively. All shading devices performances in indoor air temperature and relative humidity are considered acceptable. But the research outcome shows that the office building with egg-crate shading device is the most appropriate as it has the closest value of indoor air temperature and relative humidity based on the recommended standard guideline.

Al-Tamimi (2011) make another highlight of external shading devices such as overhangs, louvers, and egg crates as architectural elements, should be encouraged to cover building envelopes and occupants from solar radiation. However, egg-crate devices are the best in reducing indoor air temperature and decreasing the number of discomfort hours because of their configuration (i.e., combination of overhangs and fins devices), which avoids solar radiation from varied sun angles.

While the effects of shading devices in visual and thermal comfort depend on different parameters. Shen et al. (2012) investigate the balance between daylight and solar gain control in offices with internal blinds according to orientation and WWR. With a WWR of 30-50 70%, they attain optimum advantages in southern orientation. In terms of the optimum configuration of louvers parameters, Datta (2001) illustrates how fixed and external horizontal louvers can minimize the cooling demand by 70%: length, distance between louvers and tilt angle.

In general, several authors describe the case of an integrated approach for exterior shading as the most successful, but this also has its limits Cho et al. (2014). Datta (2001) insisted that the optimization of the shading devices was done with respect to primary energy demands for the whole year, and the optimum design was found to depend on location and weather conditions. The shading factor was also identified to vary with the time of day, and is different for summer and winter.

2.1.3 SDs variation with building orientation

The orientation of the building that is most affected by solar heat is generally the south façade in subtropical climates, but also a general knowledge tool is provided from various studies that could be the best alternatives not only for this façade orientation, but also for other directions. This study can be further explored by varying the orientations and the building form, the size or depth of the shading devices as well as the materials of the shading devices as different types of materials have different thermal insulation. It is important to take into account the design requirements of each shading system as a guideline prior to its implementation on the façade of the building. External shading devices will act as a passive design strategy for the building thus, planning for this at the early phase of the design is very important (Shahdan et al., 2018).

Fernández Hernández et al. (2017) suggested horizontal louvers for the south façade with a fixed angle of 0 ° and vertical louvers for the east façade with different slat tilt angles. From the daylight guidelines provided by the Department of Building Technologies at the Lawrence Berkeley National Laboratory, also Kirimtat et al. (2016) recommend this louver configuration. The north facade is not shaded because very little direct solar gain is obtained from it. The horizontal louvers in the south-facing wall reduce the demand for cooling by more than 100 kWh/m^2·year, a decrease of around 60%. The effect of slat angles in the central and southern areas is not found to be crucial, so the effect of slat angles in the eastern zone alone should be studied. In addition, in the east region, cooling demand is measured in terms of the angle of the louvers of the slats. The angles of 60 (facing north) and -60 (facing south) are more effective in the reduction of cooling demand, but also affect negatively in daylight increasing the electric energy consumption. The 30 and -30 angles are a better option, giving a reasonable balance between cooling requirement, visual comfort and the consumption of electric light.

Appropriate shading options for the north, south, north-east, north-west, south-east and south-west facades were proposed according to the building's base design geometry. This shading conforms to the recommendation of US DOE to provide vertical fins and horizontal louvers for shading east-south and west-east facing windows. Abanomi and Jones (2005) also suggested suitably orienting the vertical fins on east and west facades for effectively blocking the direct solar radiation in morning and afternoon.

In 2007, Wong et al. (2007) studied the effectiveness of window shading devices on cooling energy consumption for east and west windows in Singapore. The study shows that 2.62%–3.24% of the energy cooling load can be saved by applying a simple 30 cm-deep horizontal shading device to the window. Wong and Li's research, however, considered only east and west orientations and did not take into account other parameters such as opening width, opening height, horizontal shadow angle, and vertical shadow angle Al-tamimi et al. (2011). Alhuwayil et al. (2019) analyzed various alternatives of overhangs and fins attached to an elementary school's south, west and east façades. The use of overhangs with fins on south, west and east facades could yield a savings of up to 13.62 % in the annual energy consumption and 12.5 % in total energy cost.

In regards to the orientation of the building, in general, that there are facade solutions that work particularly well for each particular orientation. However, it can be argued that for cooling demand, the west orientation stands out as the most problematic, while the north orientation is the most favorable due to its lower demands. It is necessary to design the facade with the lowest possible FSg (Overall solar factor of the façade) to reduce and equalize the cooling demands for different orientations of the building C.Planas et al. (2017)

Dutta et al. (2017) also studied the effect of building orientation on building energy consumption, and found that heat-gain through south oriented windows is maximum followed by East, West and North bound windows in a tropical climate of northern hemisphere.

In the summer season, in comparison to the south orientation, the east and west orientations are generally known to have a superior solar radiation blocking effect with vertical shielding devices rather than horizontal overhangs (Cho et al., 2014)

North-facing windows are usually thought not to need shading, although this depends on the position of the building. For instance, to reduce heat gain during the year, maximum shade on all sides of the building is needed in tropical and hot-dry climates. In the northern hemisphere, at mid-latitudes (normally from 200N to 600N), the morning and afternoon sunrays hit obliquely on the north façade from north-west and north-east directions in summer (Alhuwayil et al., 2019).

2.1.4 Impact on buildings and energy efficiency

Several studies have investigated the impact of shading devices systems on the building environment and the energy performance. J.enbuild et al. (2016) mention some fundamental mechanisms to be considered in the application of shading devices as passive systems for energy savings; shading effect, thermal insulation, thermal/daylighting/visual comfort, aesthetical expression also as economical solution.

Energy-saving potential: According to Cho et al. (2014) a cooling consumption decreasing until 23.2% can be reached by paying attention to the location of the blinds, the blinds color, the opening of the double-skin. The maximum cooling effect of a shading system is observed during the summer period, and better efficiency is found in locations with higher solar radiation (Pérez et al., 2015). Energy efficiency and human comfort are the main priorities of the users in the building operation. In this sense, the coordinated performance of HVAC systems, shading devices and electric lighting, based on advanced control strategies, improve energy efficiency by minimizing heating and cooling loads, electric lighting consumption, and assuring visual and thermal users' comfort (Fernández Hernández et al., 2017). In the present fast-growing building construction scenario, the potential for tremendous savings in the nation's energy, and the associated economic and environmental benefits, are quite obvious, through the implementation of appropriate passive design strategy for the new buildings (Alhuwayil et al., 2019).

Insulation effect: Shading devices in façade is defined normally as a pair of glass walls which are separated by an air gap. This gap works as insulation against noise, wind with high velocity (especially in high rise buildings), and mainly temperature. It also forces airflow next to the exterior glazing that can be used as natural ventilation for the interior spaces (Azarbayjani, 2013).

Cost Analysis: The potential for enormous energy savings in the country, and the related economic and environmental benefits, are very evident in the current fast-growing building construction scenario, through the introduction of an effective passive design strategy for new buildings. The proposed shading by Alhuwayil et al. (2019) for a multi-story hotel building the payback time for the additional investment required to incorporate the passive shading strategy is projected to be 2 years and without shading is unacceptable long with polyurethane in walls and roof and triple low-e glazed shows) (84 years). The application of exterior shading devices is expected to replace the use of expensive, high-performance glass (Cho et al., 2014) The results of building energy modeling based on exterior shading devices showed a simple payback period of about 3.4 years for the horizontal overhang, and 8.7 years for the vertical panel.

Thermal, Daylighting and Visual comfort: The results demonstrate the importance of shading devices in thermal and visual comfort of building users and the viability of them in relation to important parameters as the type of glazing or the weather (Fernández Hernández, 2017). They found that significant improvement in daylighting quantity and quality for visual comfort could be achieved by simple modification of window glazing and shading device (Lim et al., 2012).

Aesthetical expression: Modern buildings are often characterized by large openings glazing material. With the increased usage of glazed areas increase heat gain and cooling loads in buildings. Shadings are important as integral components of fenestration systems in order to reduce the building's cooling load and discomfort due to glare (Ghosh et al., 2018). Using experimental aesthetics these facade's components are encouraged in such a way as to achieve a harmonious composition (Belakehal et al., 1996).

2.1.5 Glazing types impact

The selection of the glass type has a major impact on the building and on the proposal of shading systems, as it has a direct effect on the energy and cooling use in the building during operation. Therefore, in their simulations, many authors also attempt to provide meaning to this variable to give a general context that has the best utility by being studied in parallel with other variables that they use in their studies, such as geographical position types or shading systems, etc.

The case of study is an office building called Málaga Business Park located in Málaga, Spain. Malaga has a Mediterranean climate: hot and dry summers and warm winters. Other cities are selected. They belong to different climatic zones: London (oceanic climate) and Milan (subtropical climate). The windows properties values have been taken from International Glazing Database (IGDB) LBNL (2016). The window is a double (6/8/6) glazing (see ***Figure 1***). The sensitivity analysis is performed with respect to the base case in order to emphasize the requirement of shading devices. Two different parameters are analyzed: type of glazing and weather.

Glazing type	Dimensions (mm)	U (W/m^{2}K)	Windows solar factor (g)	Solar transmittance (Ts)	Solar reflectance (*Rf*)	Visible Transmittance (Tv)
Reflective	6/8/6	2.76	0.46	0.377	0.322	0.299
Solar Control	6/8/6	2.76	0.40	0.260	0.111	0.365
Low-e	6/8/6	2.46	0.724	0.627	0.135	0.815

Figure 1. Type of glazing. Simulation parameters

The comparison between heating and cooling demand in Malaga shows that heating demand is less important than cooling demand; therefore, the best option adopted in the study in a Mediterranean climate will be the most favorable with regard to decrease the cooling demand. In Milan and London, the thermal results are opposites. Cold winters make the solution of glazing façades more suitable than in a

Mediterranean climate and the installation of shading devices in these cities is a solution less necessary, focused to visual comfort and avoid possibility of glare.

In a Mediterranean climate, buildings with glass façades lead to a high cooling demand. Indeed, solar control or reflective windows, with low solar and visible transmittances properties, guarantee less cooling demand than conventional or low-e windows. On the contrary, this type of building is usual in cities with oceanic or continental climates (London or Milan), where the cooling demand is low and solar gains are favorable for reducing the heating demand. The most adequate glazing in this case is low-e glazing, with higher values of solar transmittance. According with these results, we can conclude that low-e windows is more appropriate in northern countries where the annual light exposure is lower than in Mediterranean countries, where reflective and solar control windows integrated with shading devices are a good solution to achieve a good equilibrium between daylight, electric lighting consumption and thermal comfort (Fernández Hernández et al., 2017) (refer to ***Figure 2***)

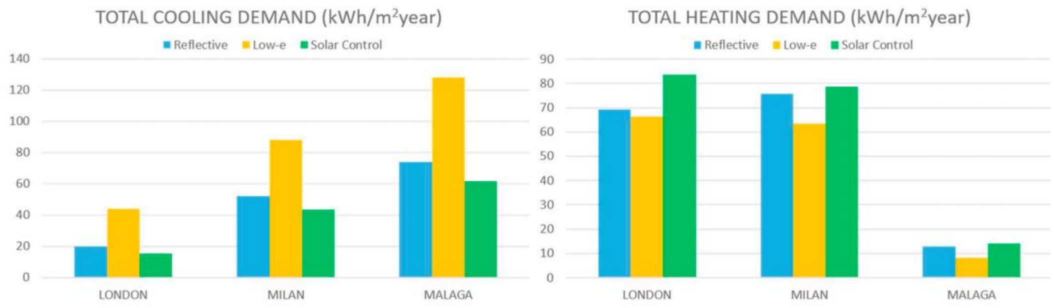

Figure 2. Total cooling and heating demand in terms of type of glazing and location

A more detailed examination according to selection of glass type is represented from Alhuwayil et al. (2019) for a multi-story hotel building in a typical hot-humid climate of Saudi Arabia. The energy saving potential and economic viability of implementing external passive shading strategy have been analyzed. The thermal insulation (in walls and roof) and glazing (DG window) of the baseline building meet the requirements of Saudi Building Code-601. This study shows that the annual energy consumption of the baseline building can be reduced by 20.5% by implementing the proposed passive shading strategy. The additional cost incurred for the passive shading can be recovered in 2 years. It is also worth noting that improving the baseline insulation and glazing (with polyurethane in walls and roof and triple low-e glazed shows, without shading) can save only 5% of annual energy consumption, and the payback period is too long (84 years) owing to the significantly higher costs of polyurethane and triple low-e glazing (Alhuwayil et al., 2019)

Generally, many other studies Cho et al. (2014), Fahmy et al. (2019), Ghosh et al. (2018), Gratia et al. (2007) and Mandalaki et al. (2012) has taken glass variable constant in their simulations. Cho et al. (2014) presents an integrated approach for exterior shading design analysis about energy performance and economic feasibility in a high-rise residential building (Seoul, Korea). First, exterior shading devices, depending on the shading method, shape, size and depth, were combined with three orientations; and the commercial software was used to analyze the annual shading masks and the direct radiation for each combination. Second, based on the sun-shading performance analysis results, practically applicable alternatives were determined, and economic feasibility based on a consideration of the cooling energy demand reduction and installation cost was analyzed, through the process of energy modeling. The glass was chosen with those parameters window (glass) 2.4W/m^2 K SC: 0.86.

A detailed overview of the identified contributions is summarized in ***Table 1.***

Table 1. Reviewed scientific literature concerning urban and building scale benefits of shading devices systems

Contribution area	Authors	Description
Urban environment and sustainability	Fernández Hernández et al. (2017)	As an environmentally friendly solution, a shading control strategy based on vertical and horizontal louvers is used.
	Fahmy et al. (2019)	A double skin facade can also be supported by shading device to control the heat gain. This adds a value to the environmental aspect where the double skin façade minimizes the heat gain of the interior spaces and help achieving natural ventilation.
	Ghosh et al. (2018)	Glazed facades are being increasingly used in modern buildings in order to improve the daylight availability in the interiors, offer better external views and also add to the architectural beauty of the building. However, this increased usage of glazed facades is leading to higher solar gain inside the building which is becoming a major issue in hot climatic regions.
	Gratia et al. (2007)	In recent years, there has been a great deal of interest in double-skin facades with shading devices due to the advantages claimed for this technology in terms of energy saving in the cold season, protection from external noise and wind loads and their high-tech image. In that case, air conditioning system will not be necessary, which will result in considerable energy and cost savings. It will also indirectly reduce the burden on the environment, since the use of energy is always associated with the production of waste materials.
Shading potential	Kim et al. (2012)	Kim et al. conducted a series of simulations by an energy analysis program, IES VE, which revealed that their experimental shading device promises the most efficient performance, with various adjustments of the slat angle.
	Nyuk Hien et al. (2003)	Shading devices can be utilized to block the solar radiation before it reaches the indoor environment. The reduction ranges between 0.5 deg C to 1 deg C or 1.3% to 2.8%. Horizontal shading devices (Shad.H90 or Shad.LH90) have reduction in a range of 0.61 deg C to 0.88 deg C. The vertical shading device (Shad.HV90) reduces the temperature by 0.98 deg. for a residential building in Singapore. The evaluate the use of shading devices within a naturally ventilated DSF's cavity. The results showed enhancement in thermal comfort when integrating shading devices with naturally ventilated DSF. This enhancement includes lower mean OT (operative temperature) compared to ambient OT that could reach 1.85 Celsius degrees difference in West facade.
Energy-saving potential	Fernández Hernández et al. (2017)	Analyzing the effects of the louvers in the cooling demand, it is important to note that horizontal louvers give cooling demand savings of about 68% in south zone with respect to the base case. Besides, cooling demand in the east zone is evaluated in terms of the angle of the slat's louvers.
	Imessad et al. (2014)	A study on Algerian buildings with typical Mediterranean climate has found that the combination of both natural ventilation and horizontal shading devices improved the thermal comfort and significantly reduced the cooling load.
	Al Tamimi et al. (2011)	Studied the effectiveness of window shading devices on cooling energy consumption for east and west windows in Singapore. The study shows that 2.62%–3.24% of the energy cooling load can be saved by applying a simple 30 cm-deep horizontal shading device to the window.
	Choa et al. (2014)	We see that a cooling consumption decreasing until 23.2% can be reached by paying attention to the location of the blinds, the blinds color, the opening of the double-skin.

	Gratia et al. (2007)	Proper use of building shading devices can only improve the thermal comfort in indoor environment. The cooling energy saving potential was about 20% while the reducing of solar heat gain by the two exterior shading devices (the horizontal overhang and the vertical panel) would lead to a decrease of the cooling energy demand 19.7% and 17.3%, respectively.
	Alhuwayil et al. (2018)	The effect of louver shading devices (both horizontal and vertical) on energy consumption of the building, for different latitudes. It was shown that the louver shading devices could yield significant savings in energy consumption compared to a building without shading.
	Cho et al. (2014)	The cooling energy saving was about 20%, while the reduction of solar heat-gain by the combination of horizontal overhang and vertical panel could decrease the cooling load by 19.7% and 17.3% respectively.
Insulation effect	Fahmy (2019)	Evaluate the use of shading devices within a naturally ventilated DSF's cavity as a thermal buffer, reducing the heat loss through the building envelope and at the same time optimizing air temperature and wind speed.
	Azarbayjani (2013)	A double skin façade is defined normally as a pair of glass walls which are separated by an air gap. This gap works as insulation against noise, wind with high velocity (especially in high rise buildings), and mainly temperature. It also forces airflow next to the exterior glazing that can be used as natural ventilation for the interior spaces.
	Alhuwayil et al. (2018)	The payback period for the additional investment required for incorporating the passive shading strategy is estimated to be 2 years and the payback period without passive shading is unacceptably long (84 years).
Cost Analysis	Cho et al. (2014)	The simple payback period calculation results for the residential units facing various orientations by exterior shading type showed the horizontal overhang to have a minimum simple payback period of 3.4 years, and the vertical panel, although somewhat less advantageous than the horizontal overhang, to have a period 8.7 years, indicating sufficient economic feasibility for these alternatives. The two exterior shading types are deemed to be rational alternatives that can be applied to the facade design of high-rise residential buildings.
	Hong et al. (2017)	Hong conducted the non-linearity analysis of the shading effect on the technical-economic performance of building-integrated photovoltaic blind (BIPB).
Aesthetical expression	Belakehal et al. (1996)	Using experimental aesthetics these facade's components are ordered in such a way as to achieve a harmonious composition.
	Ghosh et al. (2018)	Modern buildings are often characterized by large windows of glazing materials. With the increased usage of glazed areas, the heat gain in the buildings also increase leading to larger cooling load. Thus, shadings are essential as integral parts of fenestration systems in order to reduce the cooling load of the building as well as discomfort due to glare.
	Fernández Hernández (2017)	The results demonstrate the importance of shading devices in thermal and visual comfort of building users and the viability of them in relation to important parameters as the type of glazing or the weather.
	Lim et al. (2012)	They found that significant improvement in tropical daylighting quantity and quality for visual comfort could be achieved by simple modification of window glazing and shading device.

Thermal, Daylighting and Visual comfort	Al Tamimi et al. (2011)	The horizontal single overhang and vertical panel, which satisfy both conditions of applicability and sun-shading/daylighting performance, can serve as rational alternatives.
	Kim et al. (2012) / Wong et al. (2003) / Nielsen et al. (2003)	Thermal comfort aspects have been included in terms of calculation constraints by Nielsen et al. [16] who calculated the energy demand and the daylight level of a single office comparing different situations of shading, imposing an internal setpoint for heating/cooling and air flow rates for mechanical ventilation required for comfort class II in the Standard EN ISO 15251:2007.
	Nyuk Hien et al. (2003)	The study also concluded that vertical shading devices are not effective in enhancing daylighting and natural ventilation.
Building geometry	Rendón et al. (2016)	SDs on rectangular buildings were found to be very effective in reducing space cooling and performed better.
	Dutta et al. (2017)	The effect of building orientation on building energy consumption, and found that heat-gain through south oriented windows is maximum followed by East, West and North bound windows in a tropical climate of northern hemisphere. A Programmable Logic Controller (PLC) based movable shading device could yield energy savings up to 14.9% with annual average of 9.8%; also, the economic analysis showed a payback of 6 months.
	C.Planas et al. (2017)	In regards to the orientation of the building, it cannot be asserted, in general, that there are facade solutions that work particularly well for each particular orientation. However, it can be asserted that the west orientation stands out as the most problematic for cooling demand, while the north orientation is the most favorable because of its lower demands.
Natural ventilation	Wong et al. (2003)	From the natural ventilation aspect, the shading device can be used as wind catcher. However, it must be designed and located in the right place, which otherwise can become a barrier to wind flow (wind breaker). Vertical shading devices are not effective in enhancing daylighting and natural ventilation.
	Fahmya et al. (2013)	Using naturally ventilated double skin facades could enhance energy performance of buildings through heat dissipation. Also, using shading devices could lower down energy consumption by blocking undesired solar heat gain.
	Alahmed. (2013)	The researcher concluded in his research that the wider the cavity, the lower energy the building will consume. Also, he concluded that at the western façade which had the best results, multistory type succeeded to reduce the energy by 5.02% compared to the base model and 4.05% when compared to the base model with shading devices. The corridor type façade results were 7.71% and 4.43% energy reduction when compared to the base model and the base model with shading devices respectively. While, the box window type showed 8.05% and 4.78% energy savings when compared to the base model without and with shading, respectively
Acoustical Performance	Lee et al. (2015)	The proper controls of shading devices inside a DSF air cavity can contribute to thermal and acoustical comfort with avoiding overheating and noise transmission. This study aimed at evaluating the correlation between natural ventilation potential and noise transmission loss based on the degree of orientation and thickness of vertical shading devices inside a DSF air cavity.
	De Salis et al. (2002)	Reviewed various noise control techniques in naturally ventilated buildings, and they introduced louvers as noise barriers by screening the direct sound path using angled blades for ventilation openings.

2.2 Previous related study

To develop a better predictive framework for the shading devices system's thermal performance, scientific literature is reviewed as summarized in ***Table 2.***

Table 2. Data available in scientific literature for shading devices systems (please, note that SDs is Shading Devices System)

Authors	Year	Type of SDs	SDs application	SDs details	Program	Case study model	Location
Shahdan et al.	2018	1.Horizontal single/double panel. 2.Horizontal inclined double panel. 3.Horizontal louvers. 4.Vertical fins. 5.Vertical slanted fins.	Glazing	Not specified	Building Information Modelling (BIM)	3-storey school building	Shah Alam,Malaysia.
Manzan	2014	Horizontal inclined double panel	Glazing	Two different horizontal inclined double panel with two different angles	Software tool ESP-r (computing thermal loads) DAYSIM(illuminance) FRONTIER(optimization)	Hypothetical office room 2.7 m high, 5.0 m wide and 4.0 m deep, a south facing window 4.0 m wide and 1.5 m high.	Rome and Triestre, Italy
Saranti et al.	2015	Horizontal inclined double panel	Glazing	Two types shut (up) and open (down). The second is the moving SD with integrated PV.	No program used.	Physical model of 1/10 scale. A typical room of 3.5 m 5.4 m 2.9 m is used as a reference.	Chania Crete
Mendis et al.	2020	Horizontal inclined single panel	Glazing	Horizontal inclined 30 panel PV integrated shading at a distance-to-length ratio of 4	EnergyPlus, RADIANCE, Daysim, and OpenStudio	Central commercial building in urban block.	Colombo, Sri Lanka

Valladares-Rendón et al.	2016	Horizontal overhangs applied together, as single, edge and layer	Glazing	Not specified	Not mentioned	In a rectangular building.	Taipei, Taiwan
Alhuwayil1, et al.	2019	Horizontal inclined Overhang, Fins, and Louvers	Glazing	Case1: Fins perpendicular to the wall and fixed on the edges of windows Case 2: Overhang with louvers (number of blades 20, vertical spacing 0.35 cm, angle 10, Distance from window 0.30 cm) Case 3: fins and overhangs attached to one edge of each window a inclination of 45 while horizontal (triangular) overhangs connected the fins with the bottom of windows in each floor. Case 4: all the options were combined.	DesignBuilder	A 10-story hotel building. Floor height 4.2 m. Window height 4m. No. of rooms 308. Window to wall ratio 60.4%	Dhahran, Saudi Arabia.

2.3 Aim and originality of the study

A highly dynamic process containing a large number of possible architecture variables are present in literature review, illustrating efficiency of the application of shading for optimization of energy and daylight. Even though substantial researches have been done on shading devices in buildings around the globe, it provides original contributes on the integration of external shading devices into the envelope of hotel buildings, at the early design stage involving main potential design variables under the influence of Mediterranean climate.

Previous research does not conduct a detailed simulation of buildings model, which examined factors (building orientation, HVAC operation, occupancy, internal gains, shading devices parameters, and WWR). The energy demand and visual comfort of an actual office building in a Mediterranean city with a high window wall ratio (WWR) was measured by Fernández Hernández et al. (2017). South-oriented facades receive a very high solar gain that the current HVAC system cannot manage the cooling demand. He claims that the effects of shading devices in visual and thermal comfort depend on different in the simulation process. In this context, in a Mediterranean climate, only one modeling analysis is carried out but only offers data for the typology of office buildings. Accordingly, the basic focus of Alhuwayil et al. (2019), is therefore to determine the effect of the exterior shading approach on the total energy consumption of the building and, by considering a multi-story hotel building in KSA, to study its economic viability. But shading devices are provided in the proposed strategy in such a way that they help to shape a self-shading envelope, thus reducing heat gain. Shen et al. (2012) examine the balance between daylight and solar gain control in orientation-based internal blinds offices and 30% -50% WWR achieving optimum benefits in southern orientation. Wong et. al., (2007) investigated the efficacy of window shading systems on cooling energy usage for east and west windows in 2007, finding that by adding a basic 30 cm deep horizontal shading system to the window, 2.62 %-3.24 % of the energy cooling load can be saved. When the depth of the shading reaches 90 cm, the cooling load of the room is reduced by 8.27%–10.13% but study considered only east and west orientations, without taking into account other parameters such as the width of the openings, height of the openings, horizontal shadow angle, and vertical shadow angle.

Different locations are identified in the papers reviewed: Saudi Arabia Alhuwayil et al. (2019), Malaysia Al-Tamimi et al. (2011), Rome Italy Atzeri et al. (2014), Barcelona Spain C.Planas et al. (2017), Chania Crete Saranti et al.(2015), Colombo, Sri Lanka Mendis et al. (2020), Qatar Al Touma, et al. (2018), Málaga, Spain Fernández Hernández et al. (2017). Generally, are analyzed places in hot and Mediterranean climates where demands are high. In this context, researches on this topic have been mostly conducted for office buildings, and we have a lack of studies in hotel building typology.

Only one of the shading systems simulation studies analyzed developed by Fernández Hernández et al. (2017) evaluates the energy demand and visual comfort with wide which examined different parameters but also it stands on the office building typology.

CHAPTER 3

METHODOLOGY

3.1. Overview

The main objective of this research is to point out the impact of shading devices on energy performance of hotel buildings. Alternative hypothetical hotel shape is proposed in different Mediterranean locations. The goal is that by achieving precise, accurate, comparative data and results, to provide guides that can easily be used from architects in early design stages of hotels, not only in Mediterranean basin but in similar climatic regions as well. Computational evaluations will clearly show how shading device system affects indoor thermal energy performance of hotel buildings in diverse locations within the Mediterranean context (refer to ***Figure 3***).

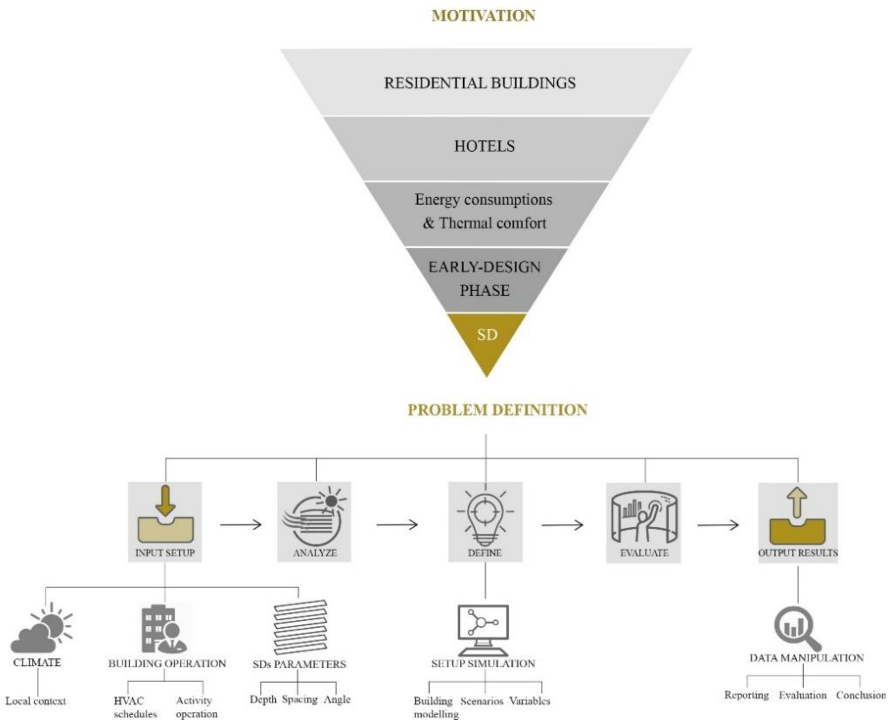

Figure 3. The study's methodological framework

3.2 Climate

Under the Köppen-Geiger system classification Mediterranean climate classified as “Csa” is characterized with mild wet winters, dry and hot summers. (Kottek, M., Rubel, F., 2020). Towards having a broader understanding, aiming to constitute more accurate evaluations of hotels energy performance in this region, four contrasting locations are selected. The locations (see ***Figure 4***) are chosen intentionally based on various temperatures, solar radiation and other different attributes each location possess. The climate data inputs are taken from “Meteonorm 7.3” (Meteotest, 2020). ***Figure 5.*** Illustrates the average temperature for the case of Antalya, Almeria, Naples and Tirana.

Figure 4. The selected locations in the Mediterranean region

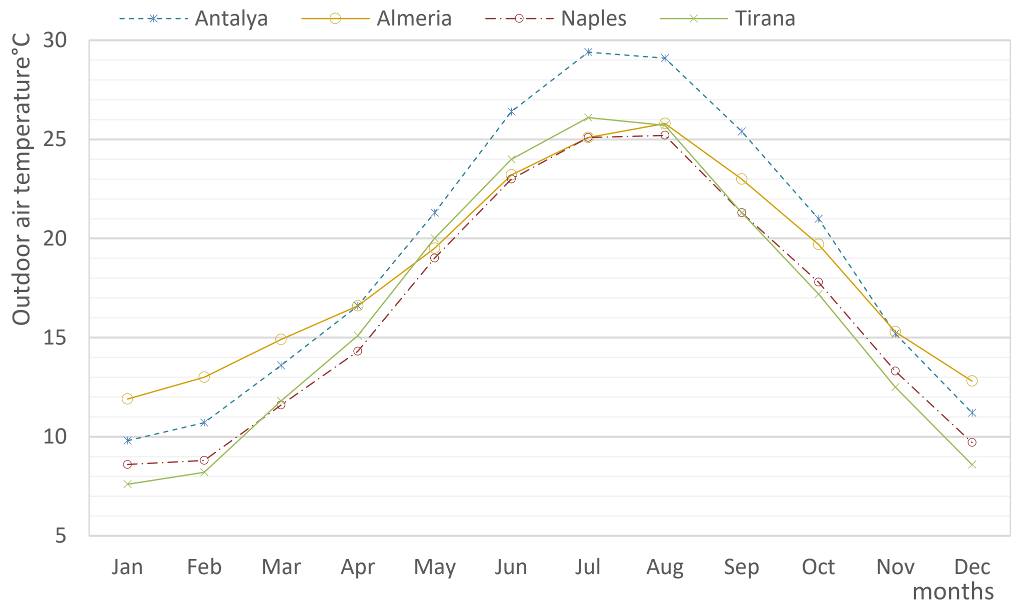

Figure 5. Average outdoor air temperature data for selected locations

3.2.1. Tirana, Albania

The climate of Tirana defined by the Köppen climate classification like Cfa, is Mediterranean, with mild, rainy winters and hot, sunny summers. Tirana is located at 41.33 o latitude north and 19.82 o longitude east and 113 m above sea level. The average annual temperature is 14.8 °C | 58.6 °F. Temperatures vary throughout the year, from an average of 5.2 °C | 41.4 °F in January to 24.7 °C | 76.4 °F in August. With a high-temperature of 9.8 °C | 49.6°F and a low-temperature of 1.5 °C | 34.6 °F, January is the coldest month. With a high-temperature of 29.9 °C | 85.9°F and a low-temperature of 18.9 °C | 66 °F, August is the warmest month. ***Figure 6.*** Illustrates the climate for the case of Tirana.

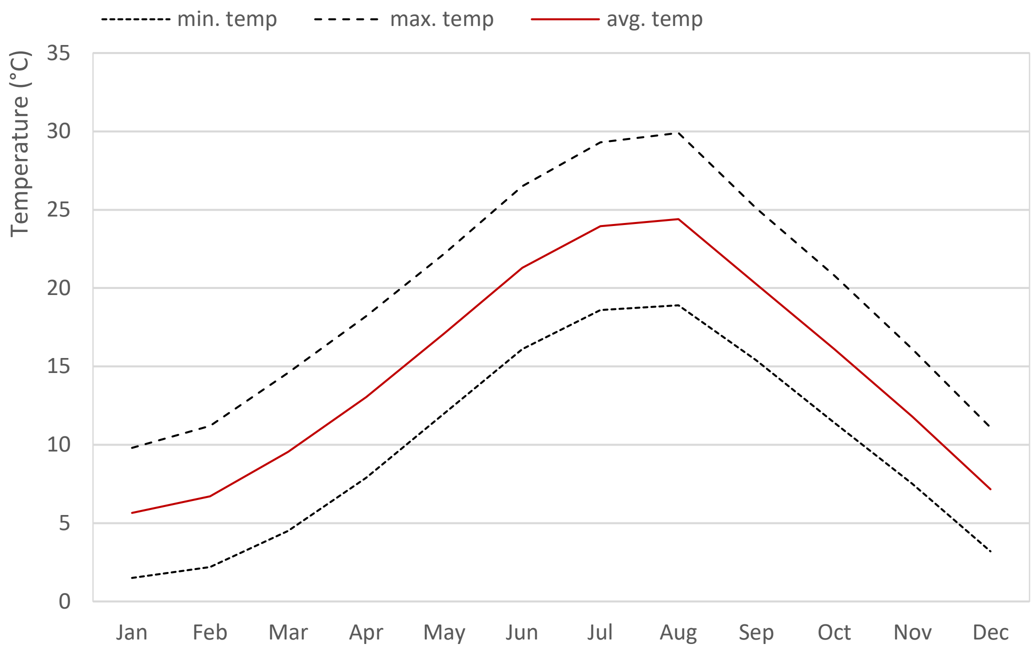

Figure 6. Monthly maximum, minimum average temperatures in Almeria

3.2.2. Almeria, Spain

The climate in Almeria is classified as “Csa-BSk” by the system of Köppen-Geiger. Almería is the only city in Europe with a true hot desert climate (*BWh*) according to the Köppen climate classification, bordering a hot semi-arid climate (*BSh*). It is one of the driest zones on either shore of the Mediterranean coast. Almeria is located at 36.83 o latitude north and 2.46 o longitude west and 43 m above sea level. The average annual temperature is 17.4 °C | 63.4 °F. Temperatures vary throughout the year, from an average of 9.8 °C | 49.7 °F in January to 26.1 °C | 79.0 °F in July. With high-temperature of 14.4 °C | 58 °F and low-temperature of 9.8 °C | 49.7 °F, January is the coldest month. With a high-temperature of 30.5 °C | 86.9 °F and a low-temperature of 26.1 °C | 58 °F, July is the warmest month. (CLIMATE-DATA.ORG, 2021) ***Figure 7.*** Illustrates the climate for the case of Almeria.

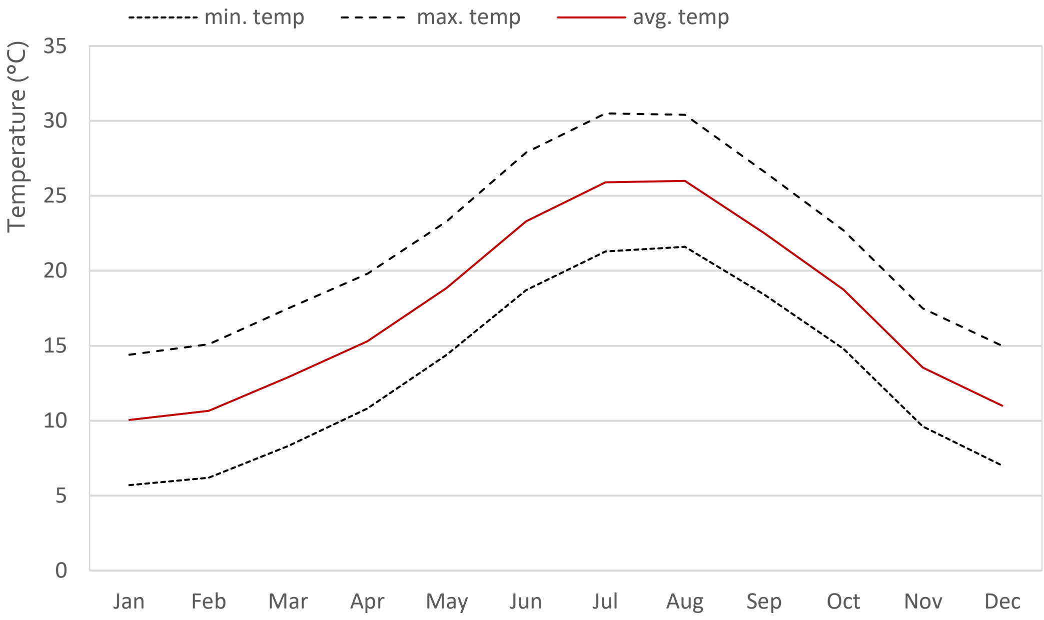

Figure 7. Monthly maximum, minimum average temperatures in Almeria

3.2.3. Antalya, Turkey

The climate in Antalya is classified as "Csa" by the system of Köppen-Geiger. As a Mediterranean climate, it has "humid" dry-summer subtropical climate and mild rainy winter. Antalya is located at 36.89 o latitude north and 30.71 o longitude east and 61 m above sea level. The average annual temperature is 17.8 °C | 64.0 °F. Temperatures vary throughout the year, from an average of 7.7 °C in January to 29.3 °C in July. With high-temperature of 12 °C and low-temperature of 4 °C, January is the coldest month. With high-temperature of 35.9 ° C and low-temperature of 22.5 °C, July is the warmest month. (CLIMATE-DATA.ORG, 2021) ***Figure 8.*** Illustrates the climate for the case of Antalya.

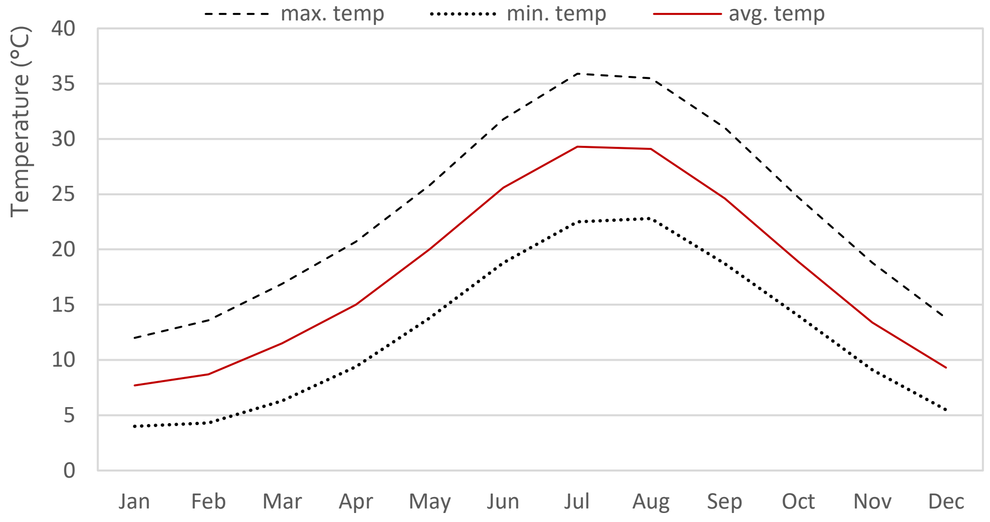

Figure 8. Monthly maximum, minimum average temperatures in Antalya

3.2.4. Naples, Italy

Naples has a borderline Mediterranean climate (*Csa*) and a humid subtropical (*Cfa*) in the Köppen climate classification, since only two summer months have less than 40 mm (1.6 in) of rainfall, preventing it from being classified as solely humid subtropical. Naples is located at 40.85 o latitude north and 14.26 o longitude east and 70 m above sea level. The average annual temperature is 16.5 °C | 61.6 °F. Temperatures vary throughout the year, from an average of 9.0 °C | 48.3 °F in January to 25.2 °C | 77.4 °F in August. With a high-temperature of 11.6 °C | 52.8 °F and low-temperature of 6.5.8 °C | 43.6 °F, January is the coldest month. With a high-temperature of 28.7 °C | 83.7 °F and a low-temperature of 21.6 °C | 70.9 °F, August is the hottest month. (CLIMATE-DATA.ORG, 2021) ***Figure 9.*** Illustrates the climate for the case of Naples.

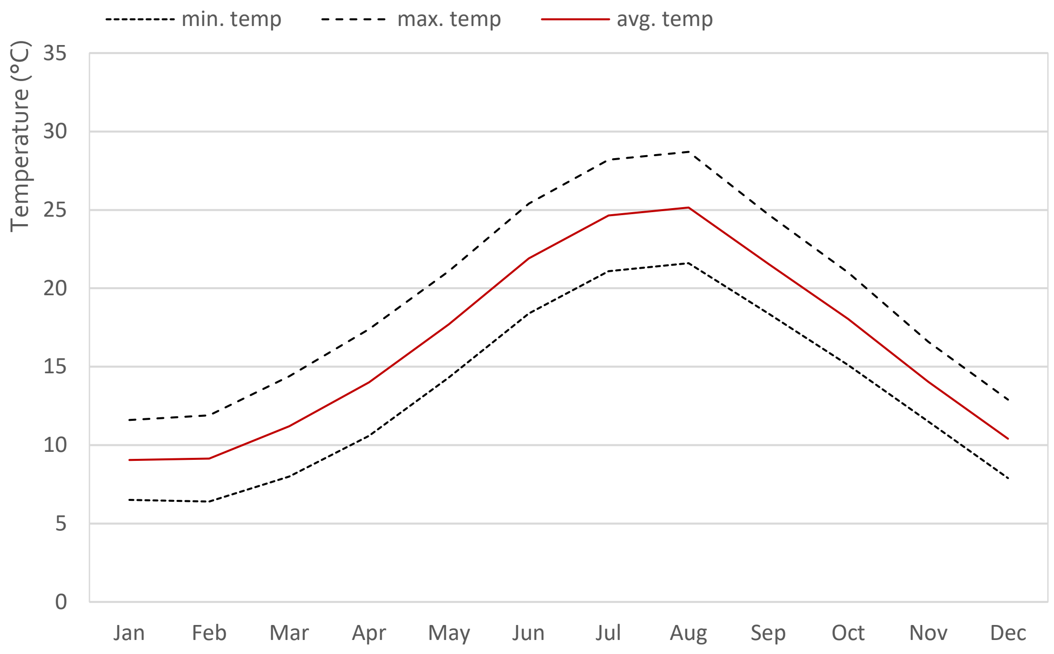

Figure 9. Monthly maximum, minimum average temperatures in Naples

3.3 Model development (Base case)

For the purpose of investigating the effects of external shading devices on indoor air temperature in the case study is proposed a three-story hotel building in rectangular shape. Nine identical room cells are selected facing a single direction. The reference case used in the study is a generic plan for a 36 m2 hotel room (8x4.5 m) (Fahmy, 2019) characteristic of hotel room. The width of a cell room is 4.5 m (100% WWR glass opening) and the length 8 m. Therefore, this room is chosen to be given flexibility in daylighting and visual comfort, as it has also function of a living room accommodating other activities working as well (Saranti et al., 2015). The other three walls are opaque. In this scenario, we have a total of nine room cell spaces, all of which have one 100% WWR (window to wall ratio) face positioned in the same direction. This block of nine cell rooms will be rotated in three different orientations south, east and west in different subtypes of the Mediterranean climate context. Rather, the present study analyzes the impact of different typologies shading systems with associated parameters on energy performance. ***Table 3***, ***Table 4***, ***Table***

5, Table 6 and ***Table 7*** demonstrate the same construction parameters, HVAC template, glazing type, lighting, internal loads and local shading data.

Table 3. Construction properties

		Density [kg/m³]	Conductivity [W/m °C]	Specific heat [J/kg °C]	Thickness [m]
External wall	Stone – hard stone	2880	3.49	840	0.03
U-value= 0.381 [W/m^2. K]	Air gap				0.03
	MW Stone Wool	40	0.38	840	0.07
	Brick	1920	0.72	840	0.25
	Cement/plaster/mortar	1760	0.72	840	0.02
Insulated roof					
U-value= 0.347 [W/m^2. K]	Asphalt – reflective coat	2300	1.2	1700	0.005
	Floor/Roof Screed	1200	0.41	840	0.05
	XPS Extruded Polystyrene	35	0.034	1400	0.08
	Cast concrete (lightweight)	1200	0.38	1200	0.10
Internal floor					
U-value= 0.383 [W/m^2. K]	Timber Flooring	650	0.14	1200	0.02
	Floor/Roof Screed	1200	0.41	840	0.07
	Cast Concrete	2000	1.13	1000	0.3
	XPS Extruded Polystyrene	35	0.034	1400	0.06

Table 4. Input parameters for HVAC operation

Input parameters	
Fan coil unit	(4 pipe) water cooled chiller, waterside economizer
Heating	Natural Gas
Cooling system	Electricity from grid
Heating system seasonal [CoP]	2.00
Cooling system seasonal [CoP]	2.00
Heating setpoint temperature [ºC]	22
Heating set back [ºC]	18
Cooling setpoint temperature [ºC]	24
Cooling set back [ºC]	28
Natural ventilation setpoint [ºC]	15

Base scenario (BC) is developed (see ***Figure 10***) incorporating one window-to-wall ratio (WWR) 100%. ***Figure 11*** shows plan (left) and ***Figure 12*** section (right) of the hotel room cells.

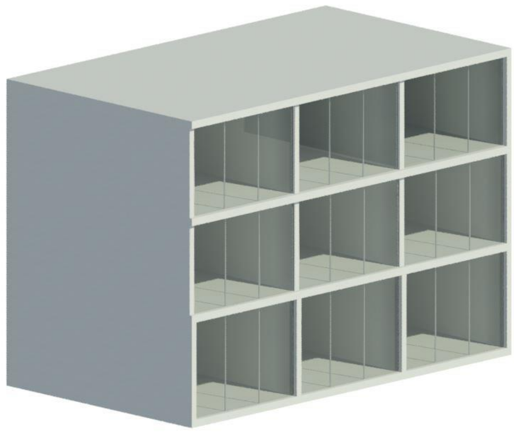

Figure 10. 3D modeling of the base case scenario with WWR 100%

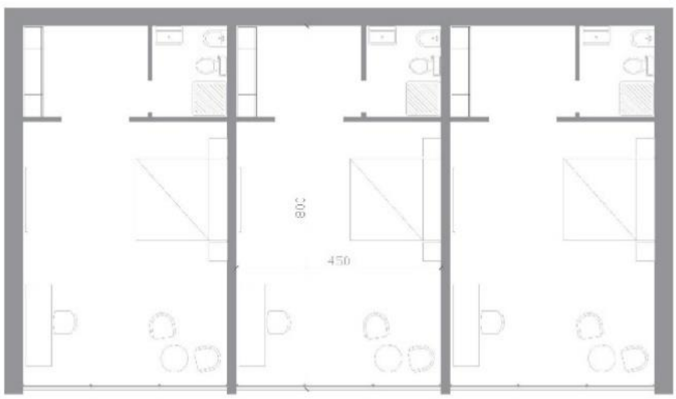

Figure 11. Plan of the hotel room cells

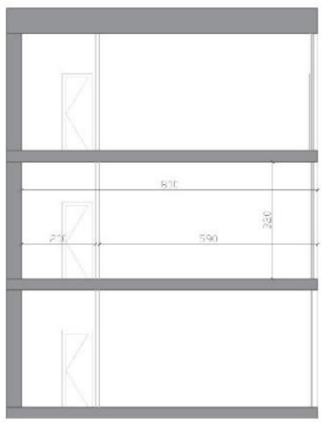

Figure 12. Section of the hotel room cells

The above-mentioned scenario will serve as a reference for analyzing the thermal performance of shading systems applied in facade with 100% window-to wall ratio. ***Table 5*** illustrates the glazing properties for all the simulated scenarios.

Table 5. Glazing properties for window to wall ratio 100% scenario

Glazing properties	WWR 100%
Glazing type	Double LoE(e2=1) Clr 6mm/13 mm air
Frame properties	Aluminum window frame with thermal break
SHGC (Total solar transmission)	0.568
U-value [W/m^2. K]	1.679
Opening position	center
Glazing area opens [%]	50
Airtightness [ac/h]	0.5

Table 6. Input parameters for internal heat gain conditions

Input parameters	
Occupancy density [P/m^2]	0.05
Latent fraction	0.5
Metabolic factor	1
Lighting [W/m^2]	11.8
Workday profile [h]	(0:00-24:00) Mon-Sun

Table 7. Local shading data

Shading Data	
Material	Aluminum
Thickness (m)	0.02
Conductivity (W/m-K)	160
Specific Heat (J/kg-K)	880
Density (kg/m3)	2800
Surface properties	
Thermal absorptance (emissivity)	0.3
Solar absorptance	0.3
Visible absorptance	0.3
Roughness	Smooth
Color	grey

3.4 Simulation software

The process of environmental simulation is the common of all studies involving building physics Yu et al. (2008). In order to analyze the impact of external shading systems on indoor air temperature, the following content used Design Builder interface version 6 (Tindale, 2005) and Energy Plus (Doe, 2013) computer modeling techniques, which have been commonly marketed as an important and accurate tool to optimize the building design phase. The average monthly temperatures of these regions are extracted from the Meteonorm 7.3 software.

3.5 Typologies proposed for design strategy

A series of scenarios are set out to demonstrate the effect of shading systems on the thermal efficiency of the hotel building. As specified in ***Table 7***, Horizontal, Vertical and Overhanging shading devices are main “Categories” typologies with their subtypes (scenarios).

Table 8. Description of the simulated scenarios

Category	Code	Scenario	Description
I	HO	WWR 100%, horizontal overhang shading device	Horizontal overhang slabs with depth=1.5 m and thickness=0.2 mm
	VO	WWR 100%, vertical overhang shading device	Vertical overhang walls with depth=1.5 m and thickness=0.2 mm
	EC1	WWR 100%, egg-crate shading device	Intersection of horizontal overhang slabs with depth=0.75 m and vertical walls overhang walls with depth=1.5 mm
	EC2	WWR 100%, egg-crate shading device	Intersection of horizontal overhang slabs with depth=1.5 m and vertical walls overhang depth=0.75 mm
II	H1	WWR 100%, Horizontal inclined multiple shading device	Multiple louvers with depth=0.3 m, spacing=0.6 m and angle (30°)
	H2	WWR 100%, Horizontal multiple shading device	Multiple louvers with depth=0.3 m and spacing=0.6 m
III	V1	WWR 100%, Vertical inclined (left) multiple fins shading device	Multiple fins with depth=0.3 m, spacing=0.6 m and angle (30°)
	V2	WWR 100%, Vertical inclined multiple fins shading device	Multiple fins with depth=0.3 m, and spacing=0.6 m
	V3	WWR 100%, Vertical inclined (right) multiple fins shading device	Multiple fins with depth=0.3 m, spacing=0.6 m and angle (30°)

3.5.1. "I Category" Overhanging shading design

"I Category" represents the base case with its respective scenarios according to the construction material properties as specified in Section 3.3. Specifically, HO, VO, EC1 EC2 are the scenarios of "Category I" (see ***Figure 13***) Section details and plans are illustrated below in ***Figure 14*** for HO scenario, ***Figure 15*** for VO scenario, ***Figure 16*** for EC1 scenario and ***Figure 17*** for EC2 scenario.

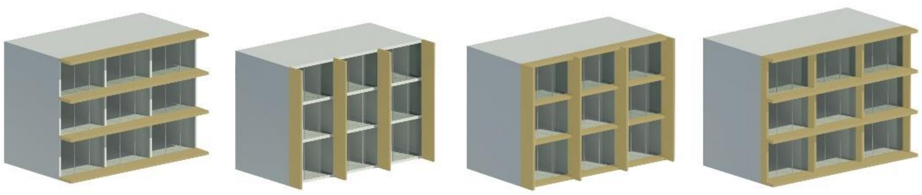

Figure 13. Scenarios of "Category I"

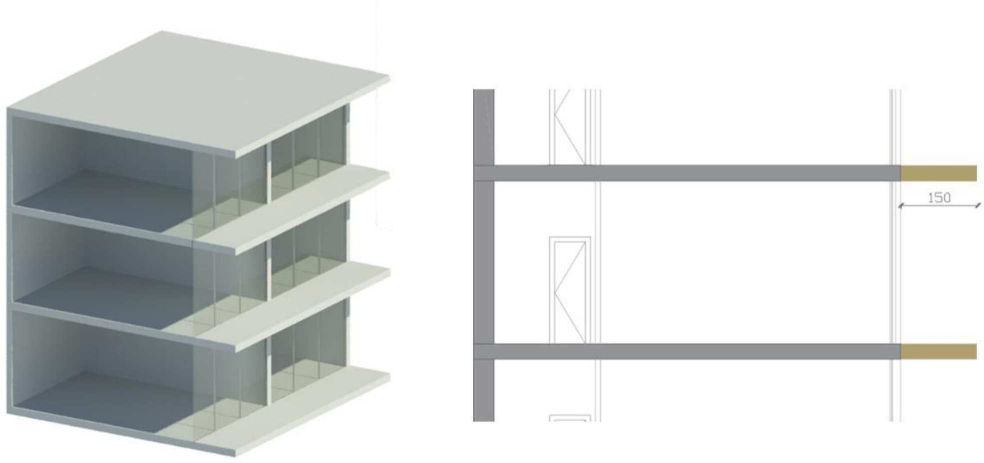

Figure 14. Section detail for HO (horizontal overhang) scenario with horizontal depth (1500 mm)

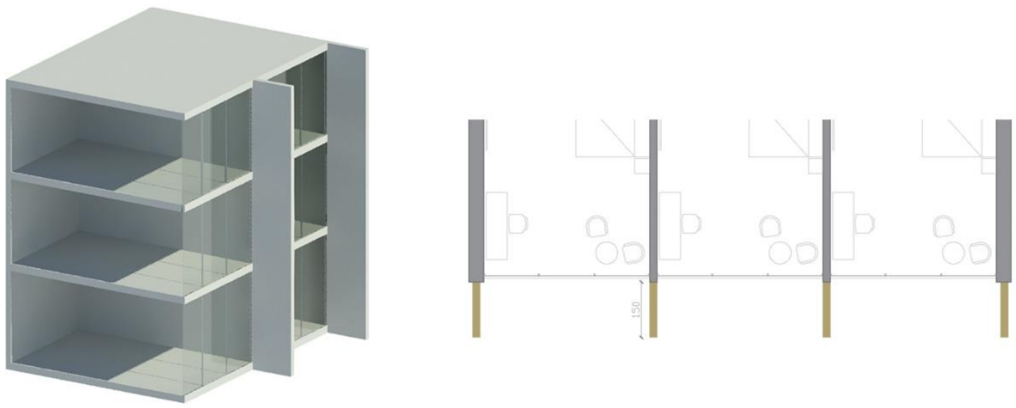

Figure 15. Plan detail for VO (vertical overhang) scenario with vertical depth (1500 mm)

Figure 16. Section detail for EC1 (egg-crate 1) scenario with horizontal depth (750 mm) and vertical depth (1500 mm)

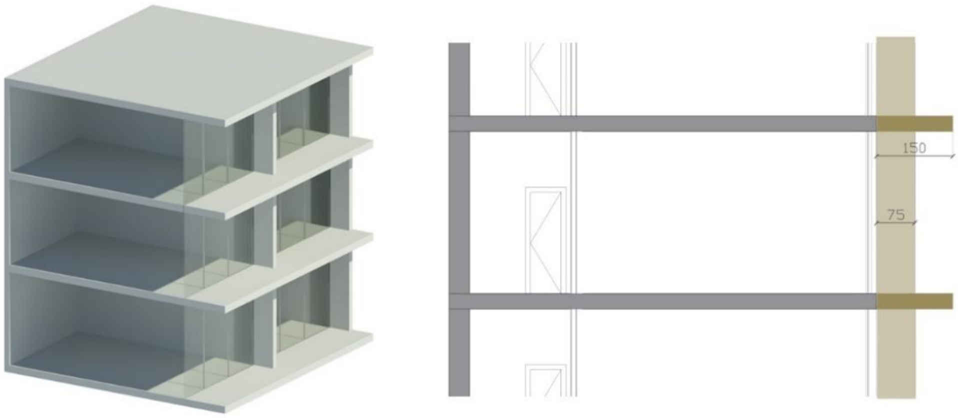

Figure 17. Section detail for EC2 (egg-crate 2) scenario with horizontal depth (1500 mm) and vertical depth (750 mm)

3.5.2. "II Category" Horizontal (louvers) shading design

"II Category" represents the base case with its respective scenarios according to the construction material properties as specified in Section 3.3. Specifically, H1, H2 are the scenarios of “Category II” (see ***Figure 18.***) Section details are illustrated below in ***Figure 19.*** for H1 scenario, and ***Figure 20***. for H2 scenario.

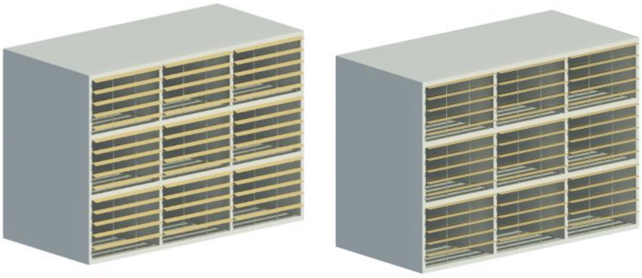

Figure 18. Scenarios of "Category II"

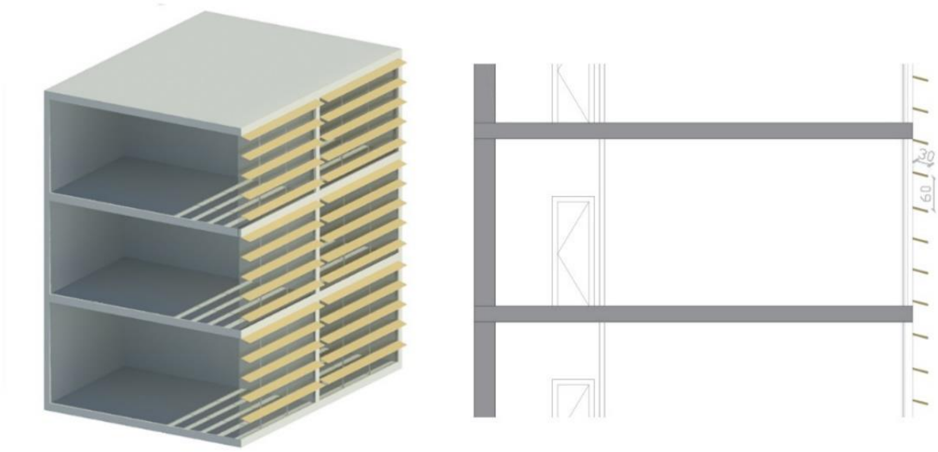

Figure 19. Section detail for H1 (horizontal louvers) scenario with depth (300 mm), spacing (600 mm) and angle (30°)

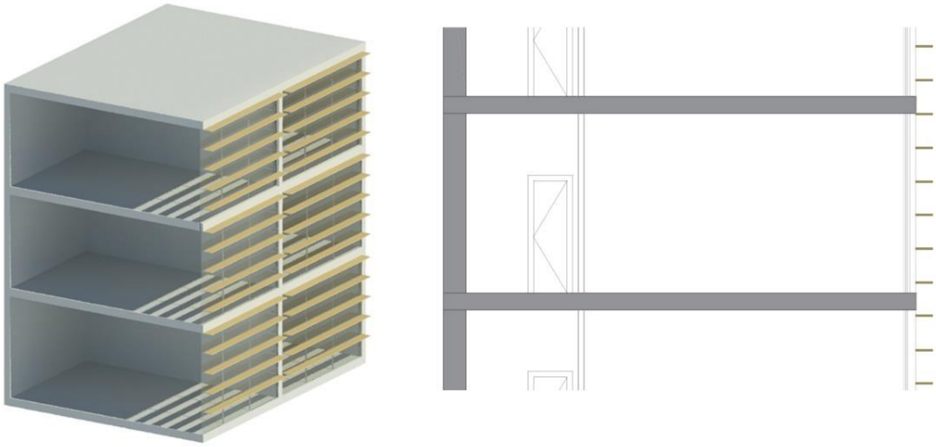

Figure 20. Section detail for H2 (horizontal louvers) scenario with depth (300 mm), spacing (600 mm) and angle (0°)

3.5.3. "III Category" Vertical (fins) shading design

"III Category" represents the base case with its respective scenarios according to the construction material properties as specified in Section 3.3. Specifically, V1, V2, V3 are the scenarios of "Category III" (see ***Figure 21***) Plans details are illustrated below in ***Figure 22*** for V1 scenario, ***Figure 23*** for V2 scenario and ***Figure 24*** for V3 scenario.

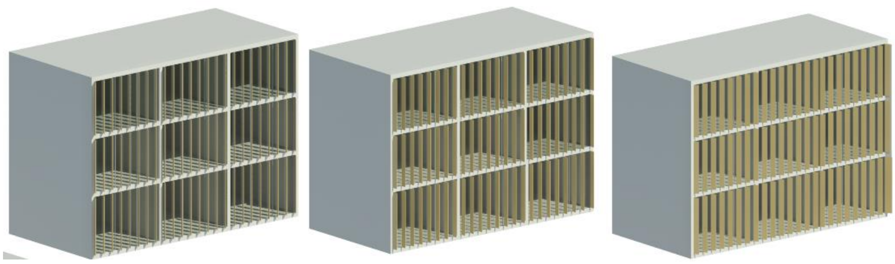

Figure 21. Scenarios of "Category III"

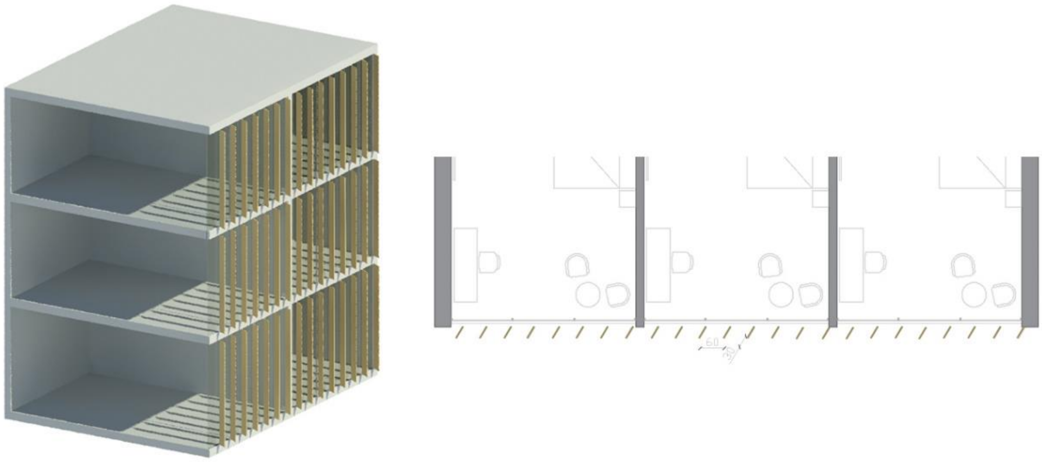

Figure 22. Plan detail for V1 (vertical fins) scenario with depth (300 mm), spacing (600 mm) and angle (-30°)

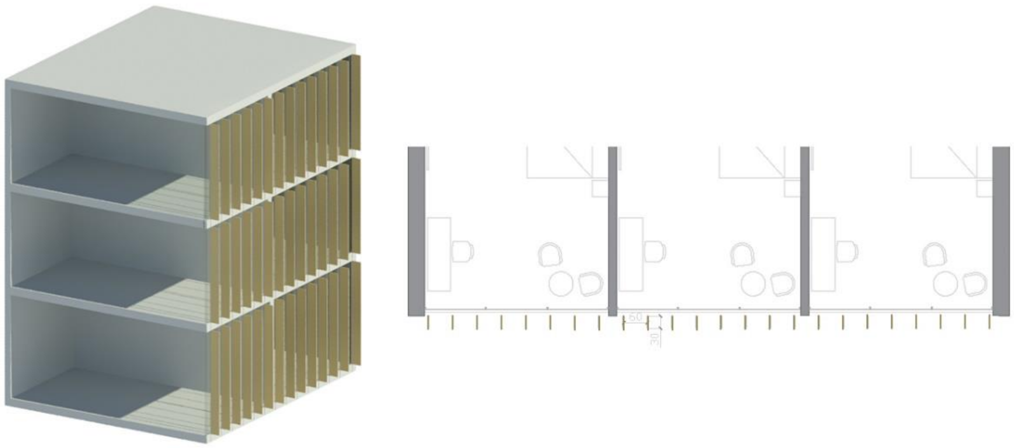

Figure 23. Plan detail for V2 (vertical fins) scenario with depth (300 mm), spacing (600 mm) and angle (0°)

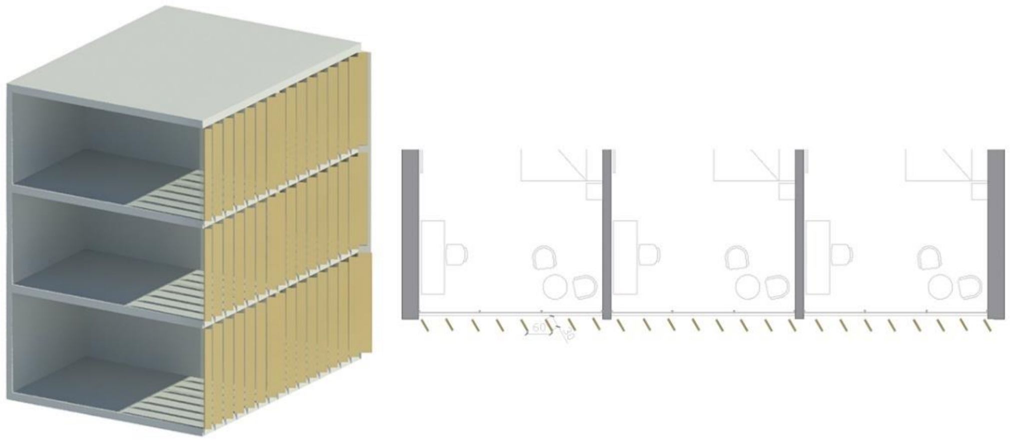

Figure 24. Plan detail for V3 (vertical fins) scenario with depth (300 mm), spacing (600 mm) and angle (30°)

3.6 Output variables

In order to evaluate the thermal performance of shading systems for different shading strategy applied for 100% window-to-wall ratio, the hourly indoor, (during two reference days in summer and winter period) is used on hotel room cells in three orientations east, south and west. In addition, hourly interior and exterior surface temperatures on facade (east, south, west) for a reference day in summer (3rd of August) are analyzed. The study also evaluates the cooling and heating energy use for all the selected scenarios. As an important part of the model development, the input parameters for the energy simulation process are used based on depth evaluation of the relevance of input parameters mentioned or applied in previous research studies.

CHAPTER 4

RESULTS

4.1 Overview

The proposed shading devices: “I Category” (egg-crate), “Category II” (horizontal) and “III Category” (vertical) simulations have successfully conducted for a typical summer and winter day. The data are reviewed and interpreted into charts. By using computer simulations, the proposed nine shading device designs in four Mediterranean climatic regions, show the relationship and interaction between shading devices and energy consumption of hotel building model.

4.2 Tirana, Albania

4.2.1 Indoor air temperature

Indoor air temperature results for “I Category”, “II Category”, and “III Category” in east, south and west orientation are analyzed by picking a typical summer and winter day. Beginning with the analysis of the “I Category’s”, followed by the "II Category" and "III Category" results. In conclusion, all of the scenarios are also compared for the Tirana climate.

“I Category”: ***Figure 25*** and ***Figure 26*** show the indoor air temperature results for the base case (BC) and EC1, EC2, HO and VO scenarios analyzed for both summer and winter period in east orientation. ***Figure 27*** and ***Figure 28*** show the indoor air temperature results for the base case (BC) and EC1, EC2, HO VO scenarios analyzed for both summer and winter period in south orientation. ***Figure 29*** and ***Figure 30*** show the indoor air temperature results for the base case (BC) and

EC1, EC2, HO and VO scenarios analyzed for both summer and winter period in west orientation.

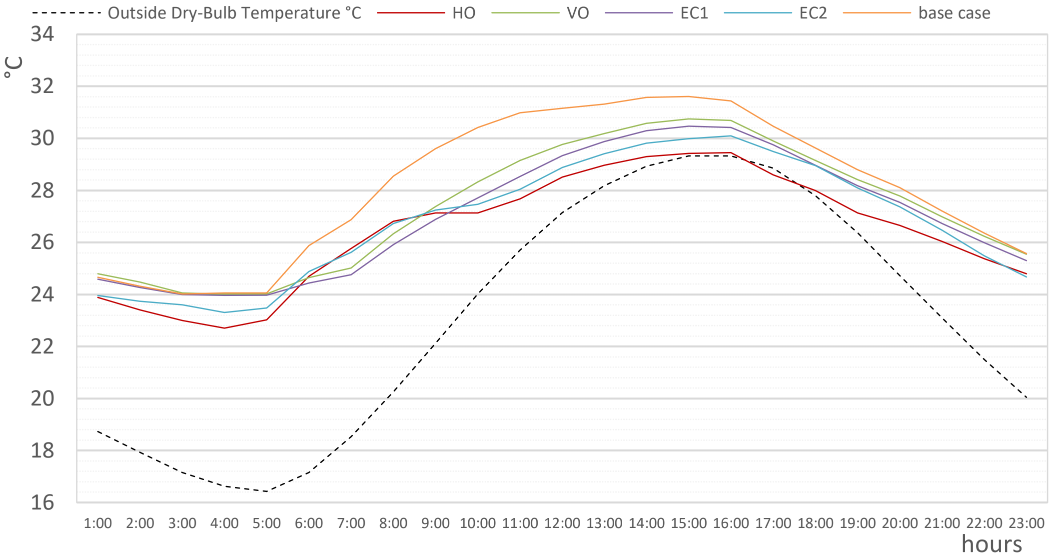

Figure 25. Simulated indoor air temperatures for the base case scenario BC and scenarios of "I Category": HO, VO, EC1 and EC2, together with the dry-bulb temperature from the weather file 3rd August in east direction

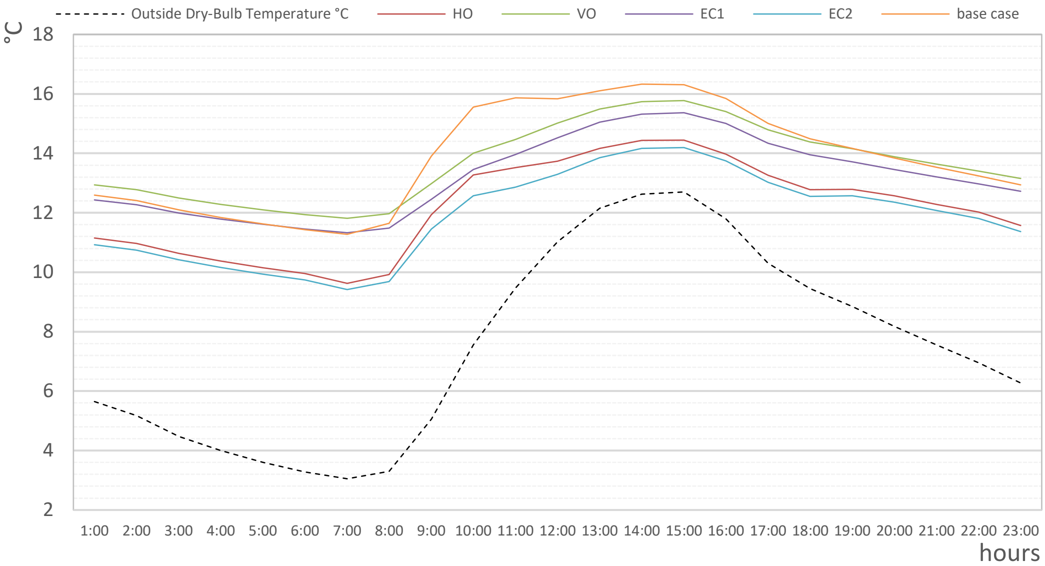

Figure 26. Simulated indoor air temperatures for the base case scenario BC and scenarios of "I Category": HO, VO, EC1 and EC2, together with the dry-bulb temperature from the weather file 4th January in east direction

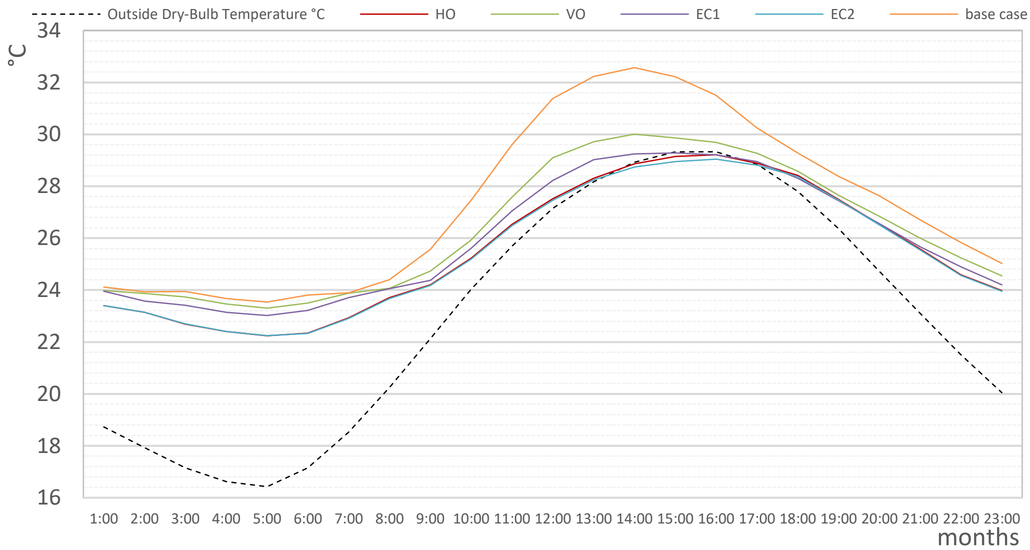

Figure 27. Simulated indoor air temperatures for the base case scenario BC and scenarios of "I Category": HO, VO, EC1 and EC2, together with the dry-bulb temperature from the weather file 3rd August in south direction

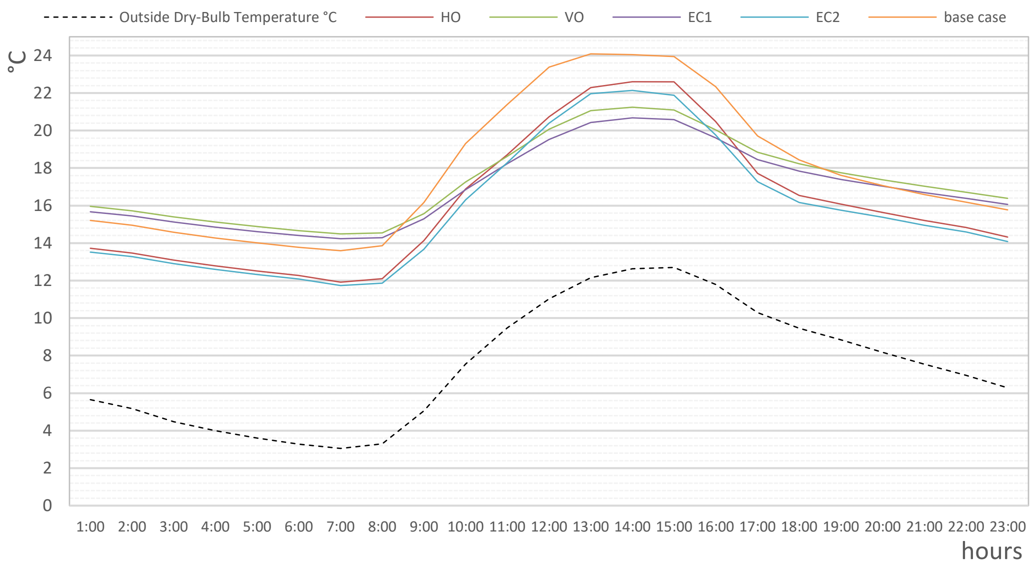

Figure 28. Simulated indoor air temperatures for the base case scenario BC and scenarios of “I Category”: HO, VO, EC1 and EC2, together with the dry-bulb temperature from the weather file 4th January in south direction

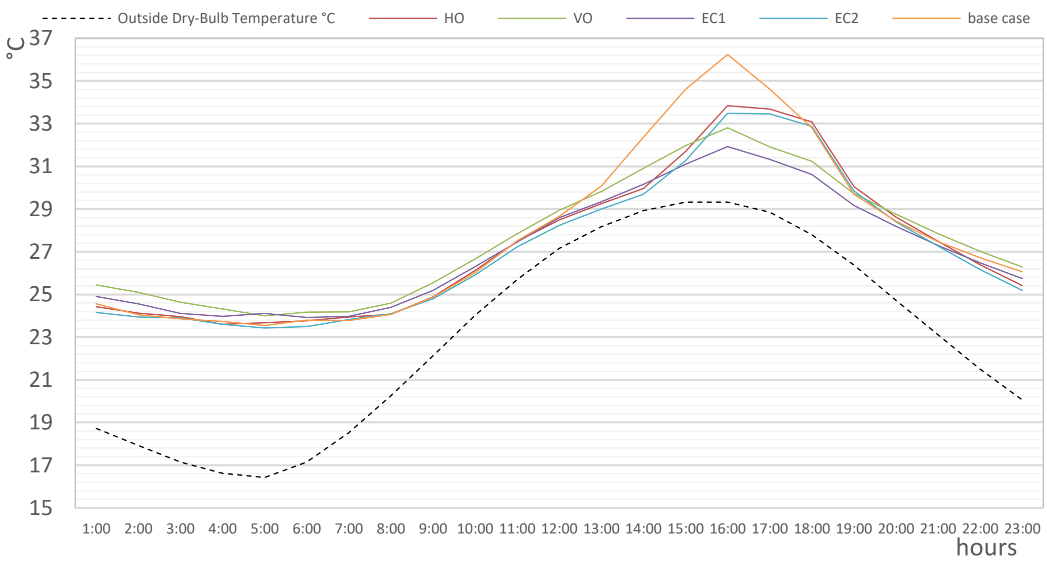

Figure 29. Simulated indoor air temperatures for the base case scenario BC and scenarios of “I Category”: HO, VO, EC1 and EC2, together with the dry-bulb temperature from the weather file 3rd August in west direction

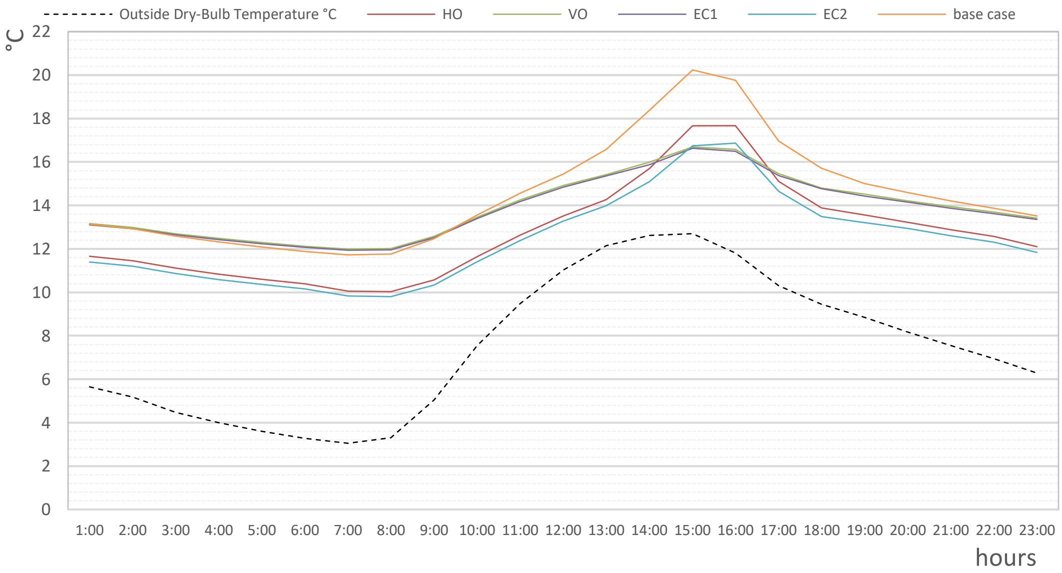

Figure 30. Simulated indoor air temperatures for the base case scenario BC and scenarios of "I Category": HO, VO, EC1 and EC2, together with the dry-bulb temperature from the weather file 4th January in west direction

"II Category": ***Figure 31*** and ***Figure 32*** show the indoor air temperature results for the base case (BC) and H1, H2 scenarios analyzed for both summer and winter period in east orientation. ***Figure 33*** and ***Figure 34*** show the indoor air temperature results for the base case (BC) and H1, H2 scenarios analyzed for both summer and winter period in south orientation. ***Figure 35*** and ***Figure 36*** show the indoor air temperature results for the base case (BC) and H1, H2 scenarios analyzed for both summer and winter period in west orientation.

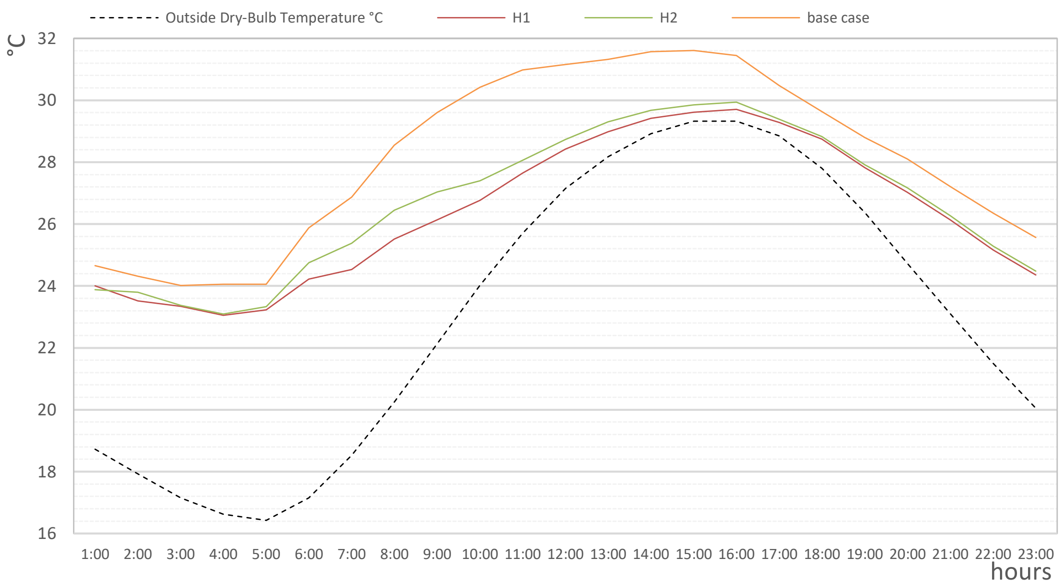

Figure 31. Simulated indoor air temperatures for the base case scenario BC and scenarios of "II Category": H1, and H2, together with the dry-bulb temperature from the weather file 3rd August in east direction

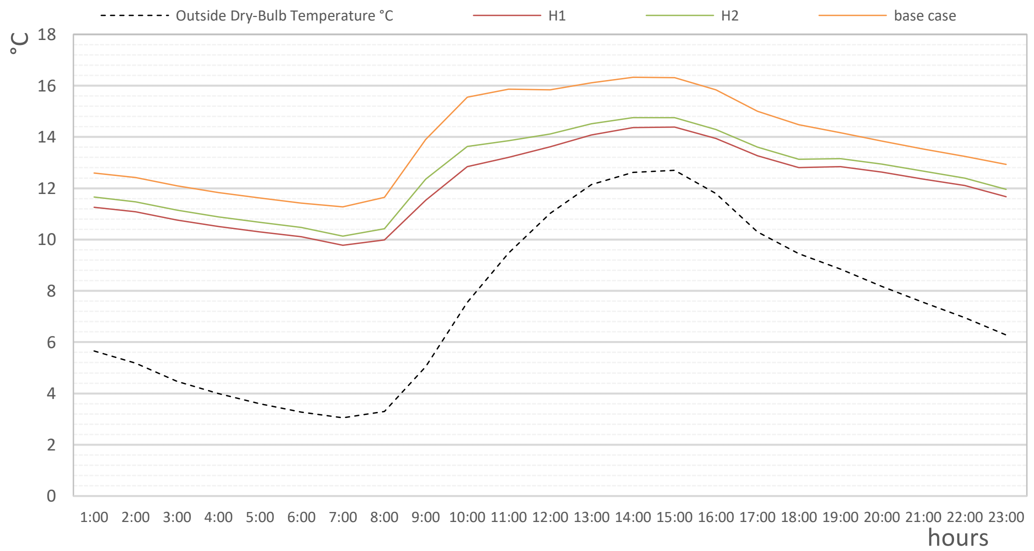

Figure 32. Simulated indoor air temperatures for the base case scenario BC and scenarios of "II Category": H1, and H2, together with the dry-bulb temperature from the weather file 4th January in east direction

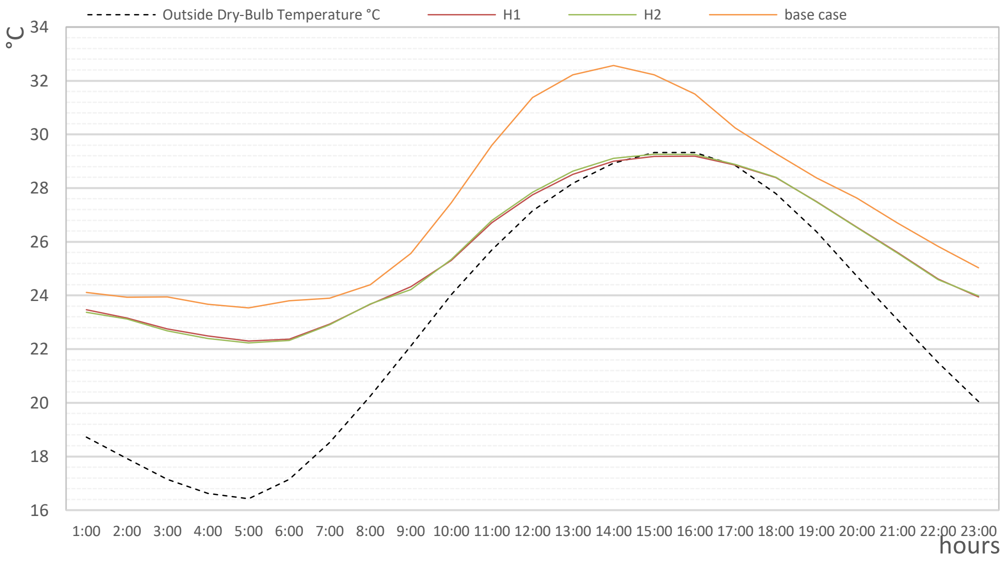

Figure 33. Simulated indoor air temperatures for the base case scenario BC and scenarios of "II Category": H1, and H2, together with the dry-bulb temperature from the weather file 3rd August in south direction

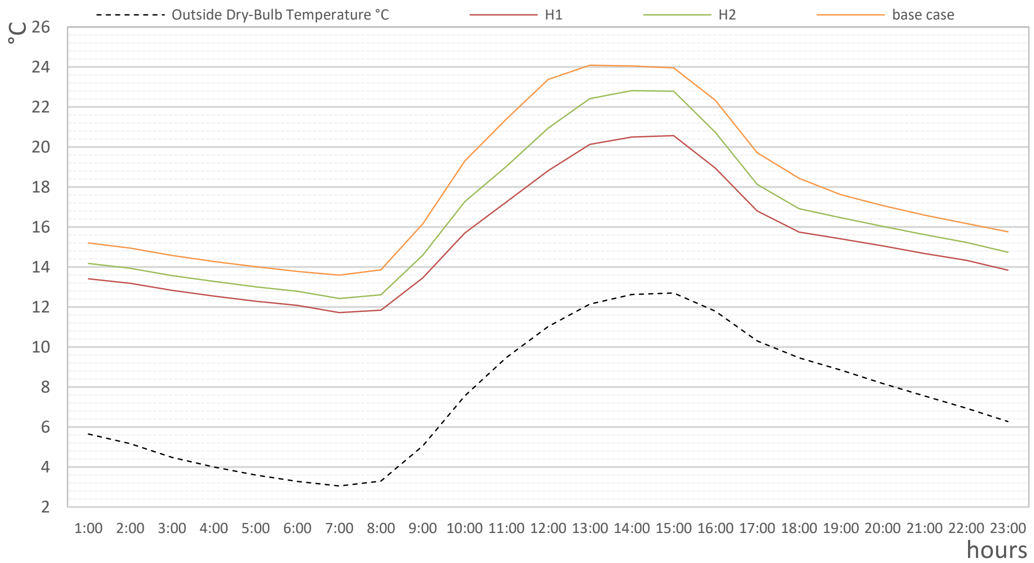

Figure 34. Simulated indoor air temperatures for the base case scenario BC and scenarios of "II Category": H1, and H2, together with the dry-bulb temperature from the weather file 4th January in south direction

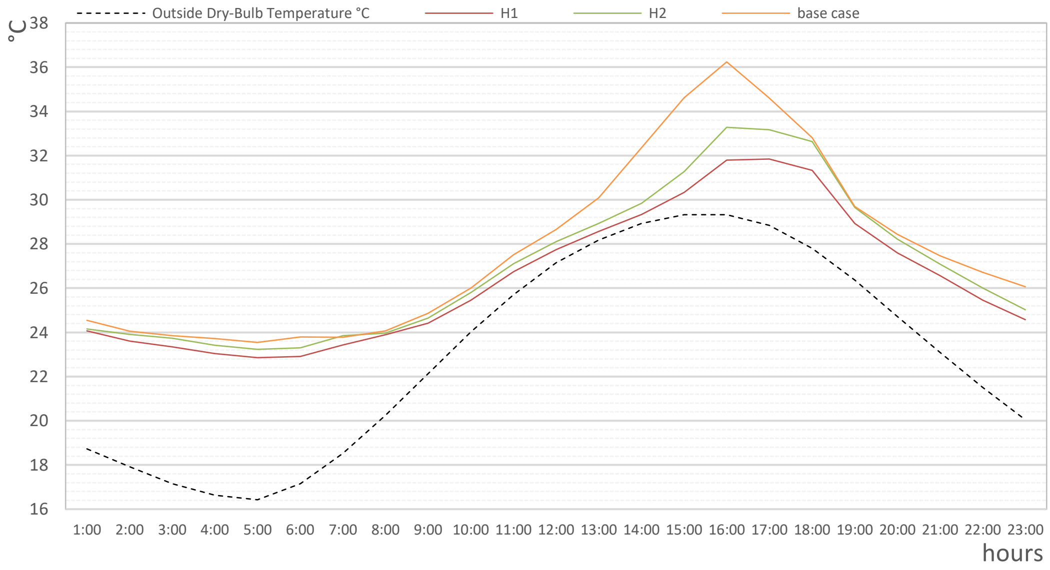

Figure 35. Simulated indoor air temperatures for the base case scenario BC and scenarios of "II Category": H1, and H2, together with the dry-bulb temperature from the weather file 3rd August in west direction

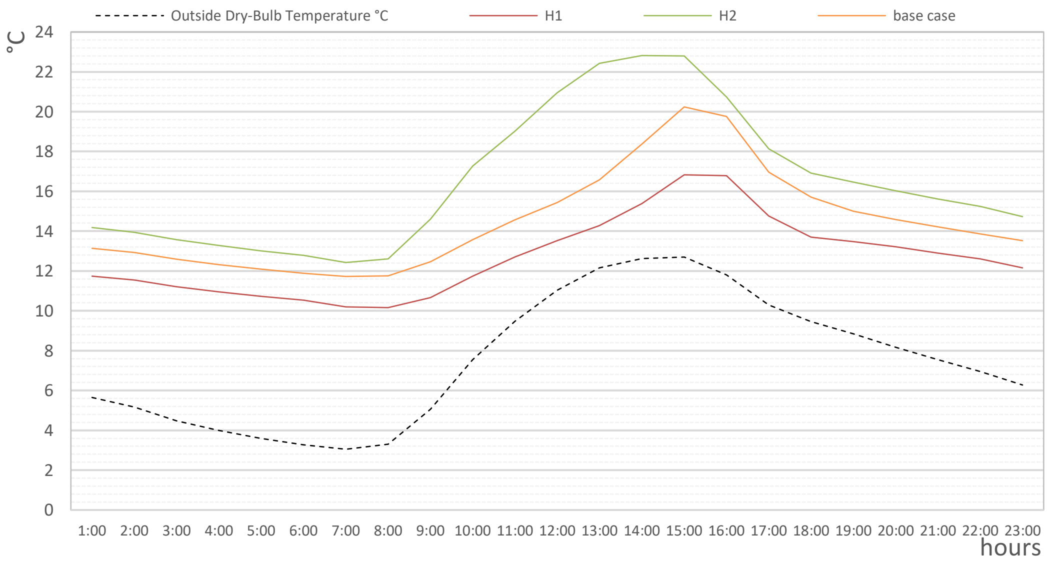

Figure 36. Simulated indoor air temperatures for the base case scenario BC and scenarios of "II Category": H1, and H2, together with the dry-bulb temperature from the weather file 4th January in west direction

“III Category”: ***Figure 37*** and ***Figure 38*** show the indoor air temperature results for the base case (BC) and V1, V2, V3 scenarios analyzed for both summer and winter period in east orientation. ***Figure 39*** and ***Figure 40*** show the indoor air temperature results for the base case (BC) and V1, V2, V3 scenarios analyzed for both summer and winter period in south orientation. ***Figure 41*** and ***Figure 42*** show the indoor air temperature results for the base case (BC) and V1, V2, V3 scenarios analyzed for both summer and winter period in west orientation.

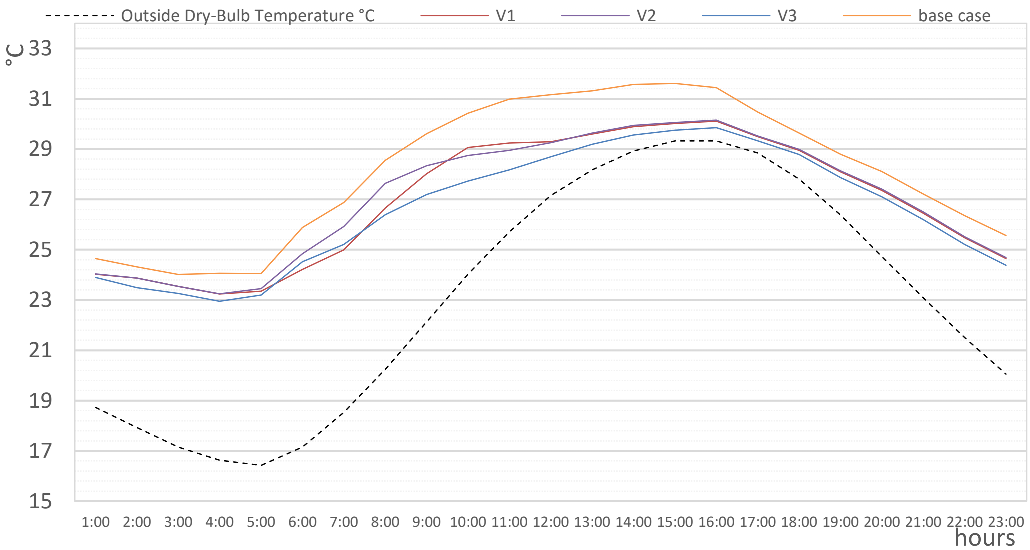

Figure 37. Simulated indoor air temperatures for the base case scenario BC and scenarios of “III Category”: V1, V2 and V3, together with the dry-bulb temperature from the weather file 3rd August in east direction

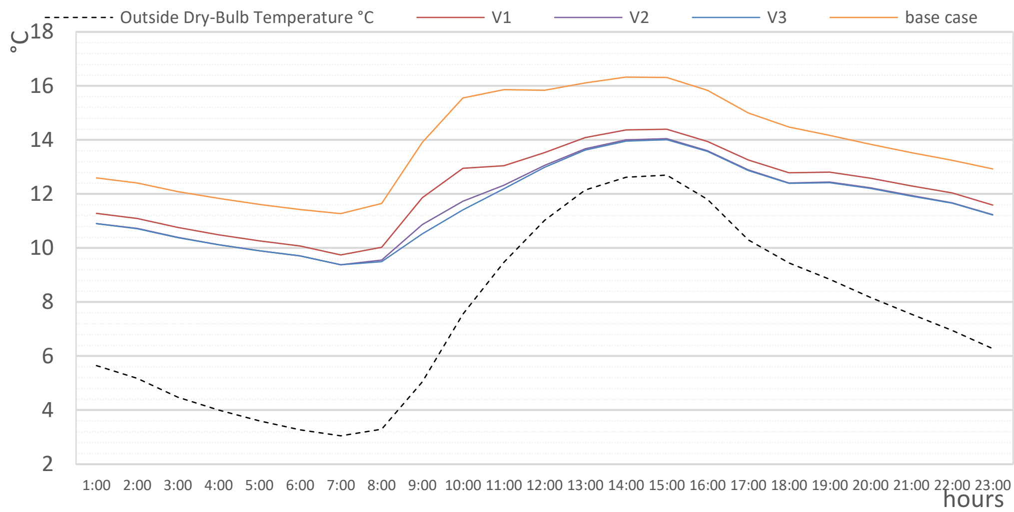

Figure 38. Simulated indoor air temperatures for the base case scenario BC and scenarios of "III Category": V1, V2 and V3, together with the dry-bulb temperature from the weather file 4th January in east direction

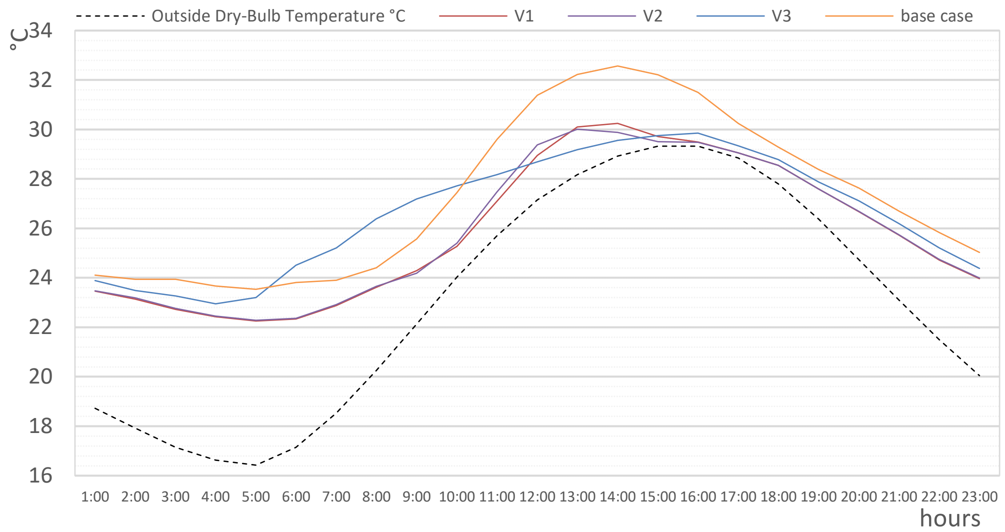

Figure 39. Simulated indoor air temperatures for the base case scenario BC and scenarios of "III Category": V1, V2 and V3, together with the dry-bulb temperature from the weather file 3rd August in south direction

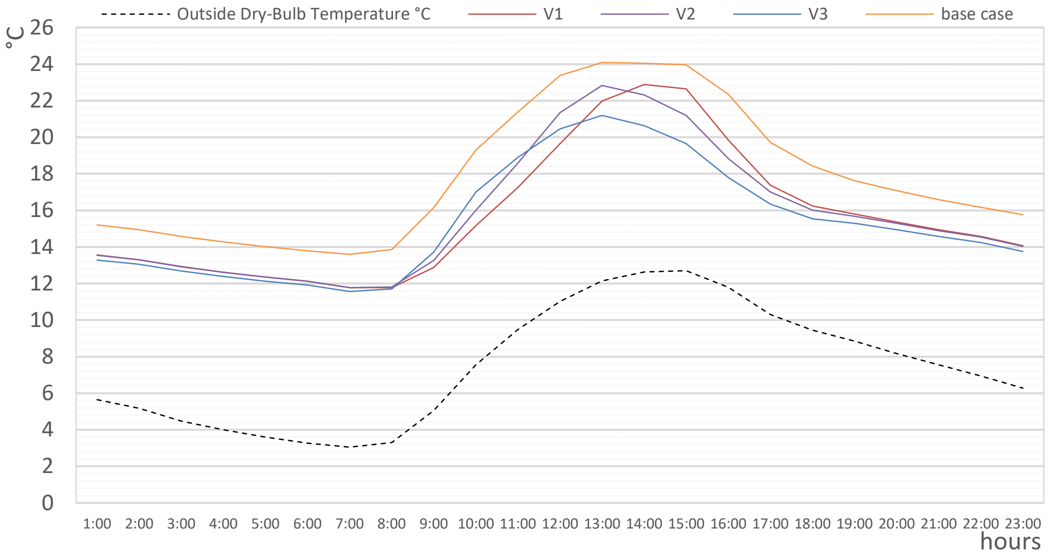

Figure 40. Simulated indoor air temperatures for the base case scenario BC and scenarios of "III Category": V1, V2 and V3, together with the dry-bulb temperature from the weather file 4th January in south direction

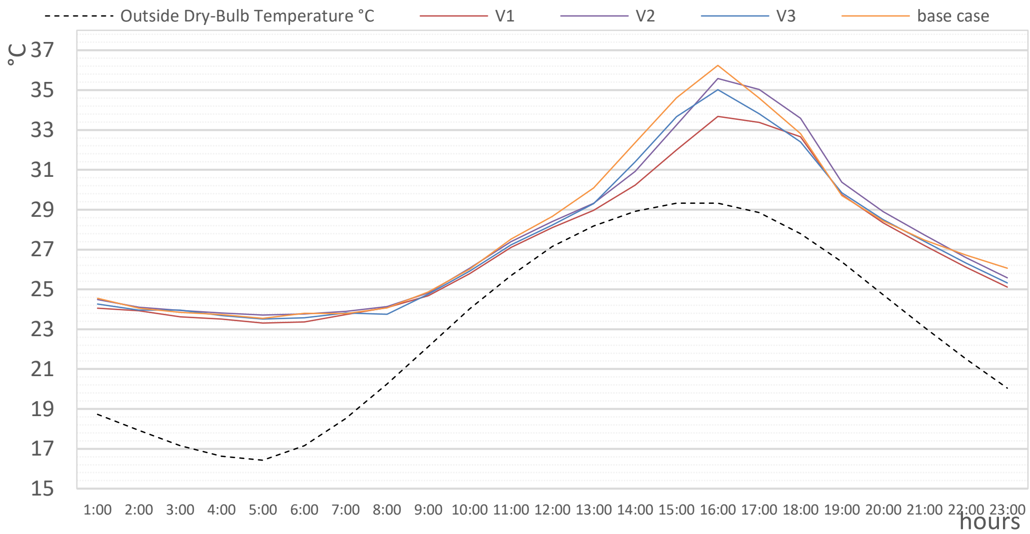

Figure 41. Simulated indoor air temperatures for the base case scenario BC and scenarios of "III Category": V1, V2 and V3, together with the dry-bulb temperature from the weather file 3rd August in west direction

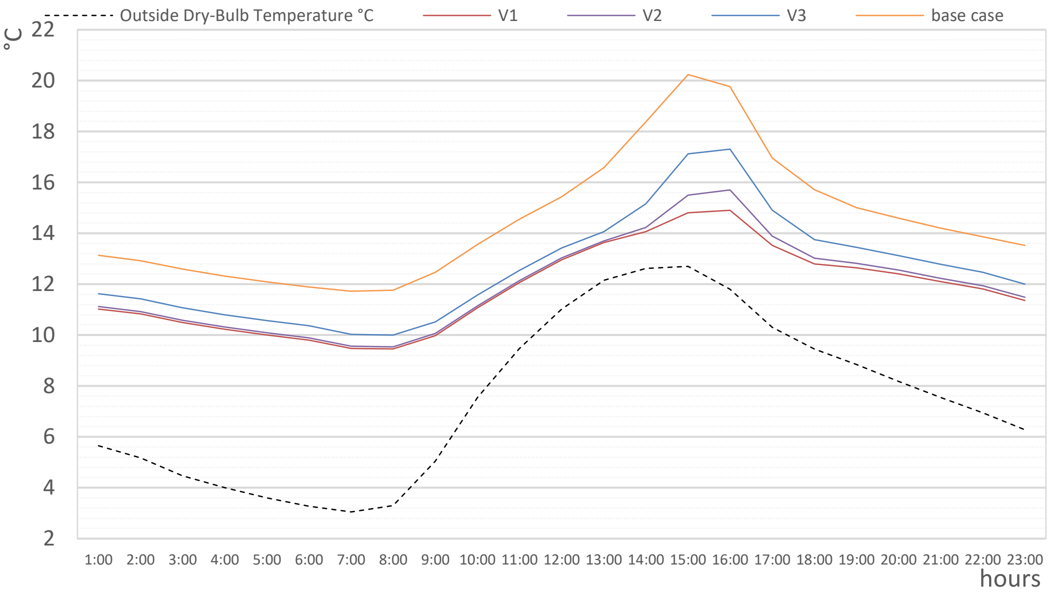

Figure 42. Simulated indoor air temperatures for the base case scenario BC and scenarios of “III Category”: V1, V2 and V3, together with the dry-bulb temperature from the weather file 4th January in west direction

Indoor air temperature results for “I Category”, “II Category” and “III Category” analyzed together. ***Figure 43*** and ***Figure 44*** show the indoor air temperature results for the base case (BC) and EC1, EC2, HO, VO, H1, H2, V1, V2, V3 scenarios analyzed for both summer and winter period in east orientation. ***Figure 45*** and ***Figure 46*** show the indoor air temperature results for the base case (BC) and EC1, EC2, HO, VO, H1, H2, V1, V2, V3 scenarios analyzed for both summer and winter period in south orientation. ***Figure 47*** and ***Figure 48*** show the indoor air temperature results for the base case (BC) and EC1, EC2, HO, VO, H1, H2, V1, V2, V3 scenarios analyzed for both summer and winter period in west orientation.

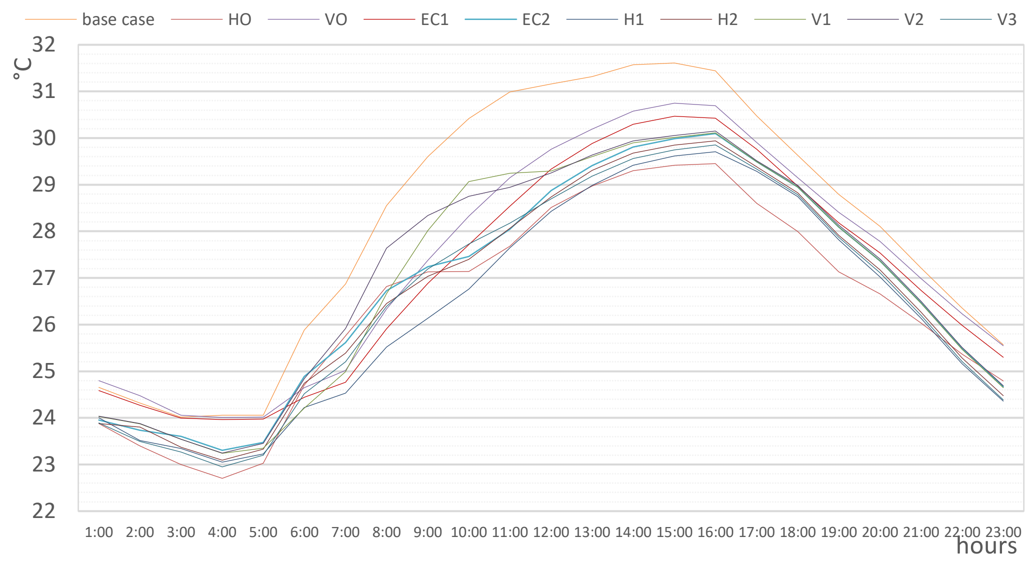

Figure 43. Simulated indoor air temperatures for the base case scenario BC and scenarios of "Catery I", "Category II" and "Category III" from the weather file 3rd August in east direction

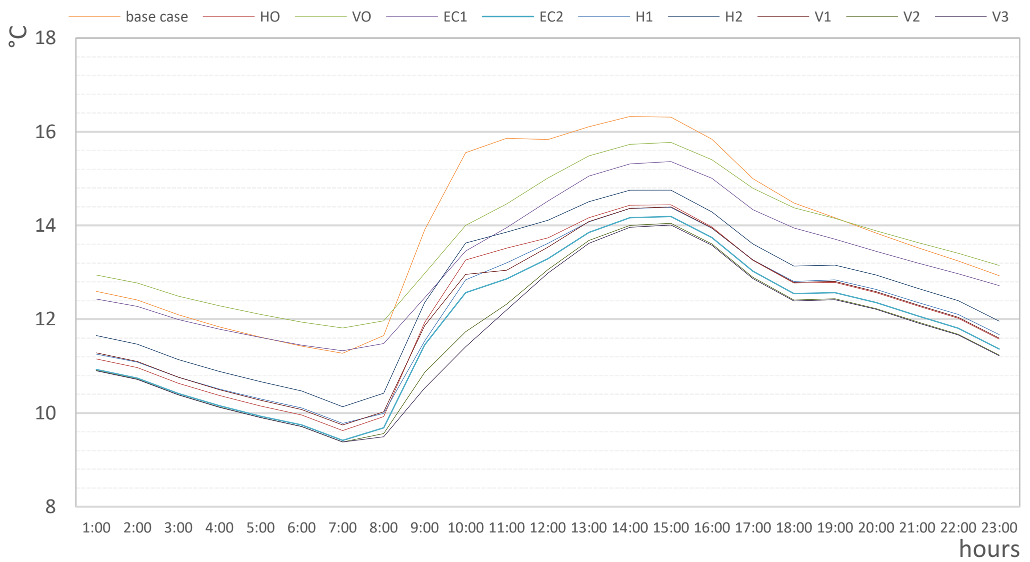

Figure 44. Simulated indoor air temperatures for the base case scenario BC and scenarios of "Catery I", "Category II" and "Category III" from the weather file 4th January in east direction

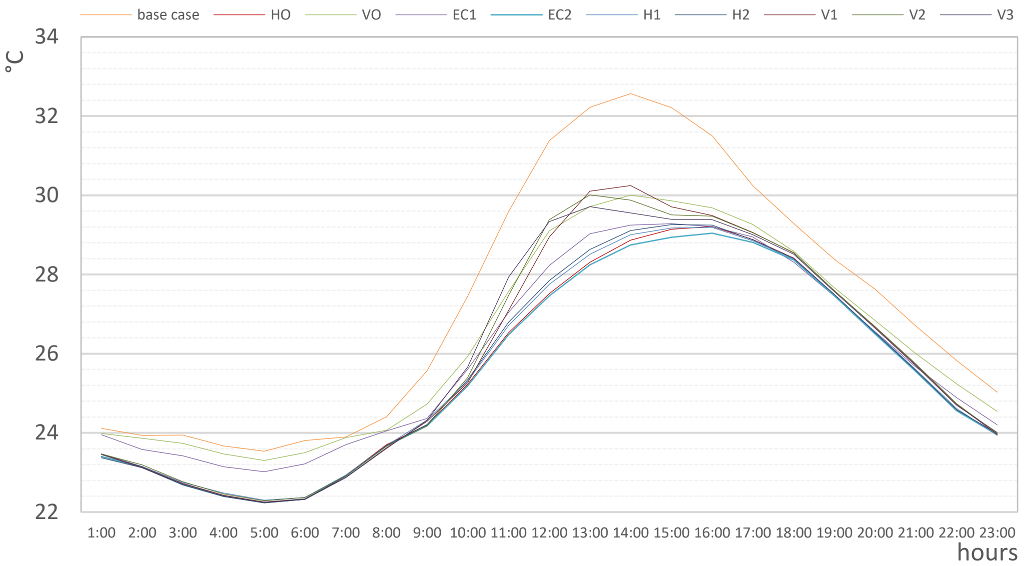

Figure 45. Simulated indoor air temperatures for the base case scenario BC and scenarios of "Catery I", "Category II" and "Category III" from the weather file 3rd August in south direction

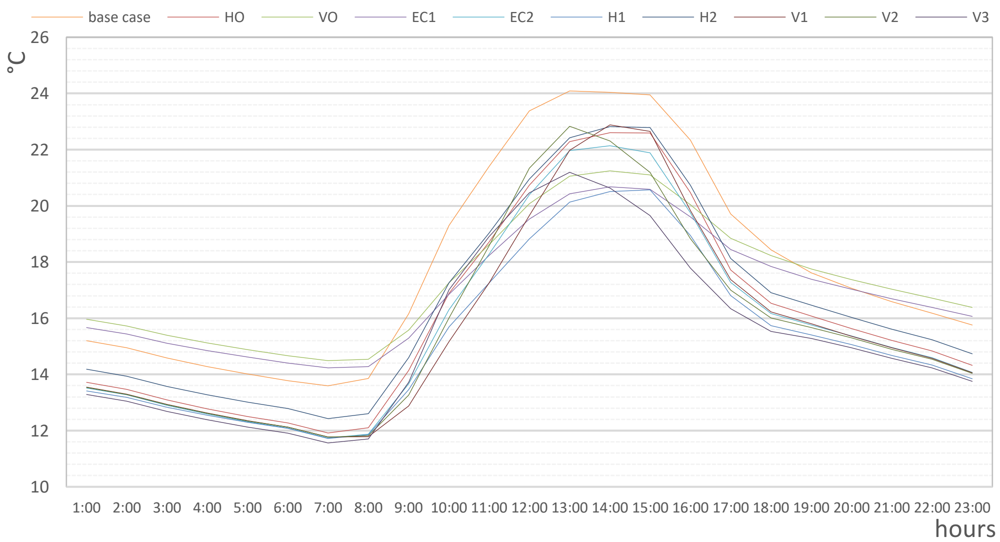

Figure 46. Simulated indoor air temperatures for the base case scenario BC and scenarios of "Catery I", "Category II" and "Category III" from the weather file 4th January in south direction

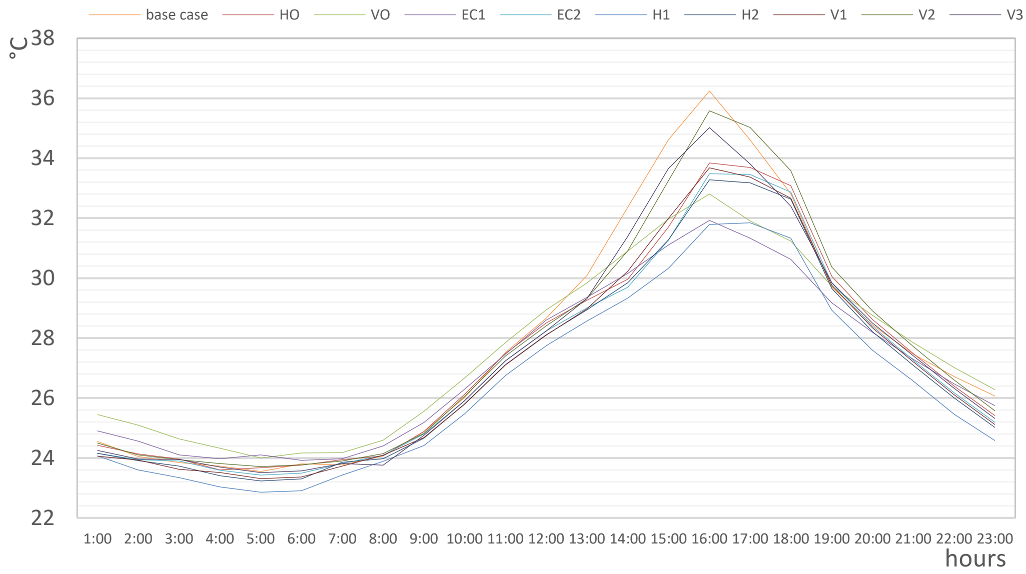

Figure 47. Simulated indoor air temperatures for the base case scenario BC and scenarios of "Catery I", "Category II" and "Category III" from the weather file 3rd August in west direction

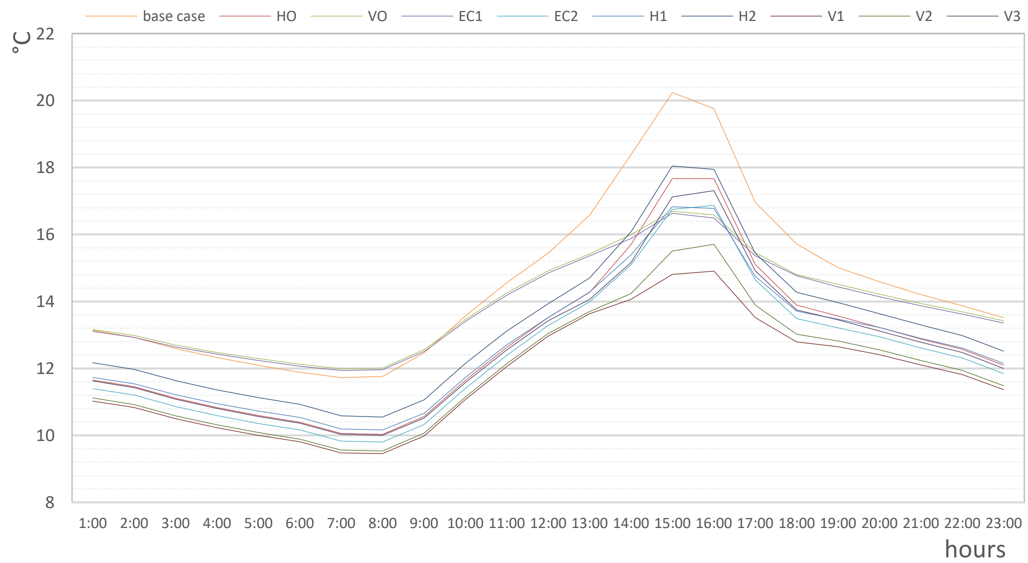

Figure 48. Simulated indoor air temperatures for the base case scenario BC and scenarios of "Catery I", "Category II" and "Category III" from the weather file 4th January in west direction

4.2.2 Energy performance

Simulated heating and cooling loads results, for “I Category”, “II Category”, and “III Category” in east, south and west orientation are analyzed. First, the "I Category" results are analyzed, followed by the "II Category" and "III Category" results. Finally, all of the scenarios together for the Tirana climate.

“I Category”: ***Figure 49*** and ***Figure 50*** shows the energy consumption for heating and cooling for the base case (BC) and EC1, EC2, HO and VO scenarios in east orientation. ***Figure 51*** and ***Figure 52*** shows the energy consumption for heating and cooling for the base case (BC) and EC1, EC2, HO and VO scenarios in south orientation. ***Figure 53*** and ***Figure 54*** shows the energy consumption for heating and cooling for the base case (BC) and EC1, EC2, HO and VO scenarios in west orientation.

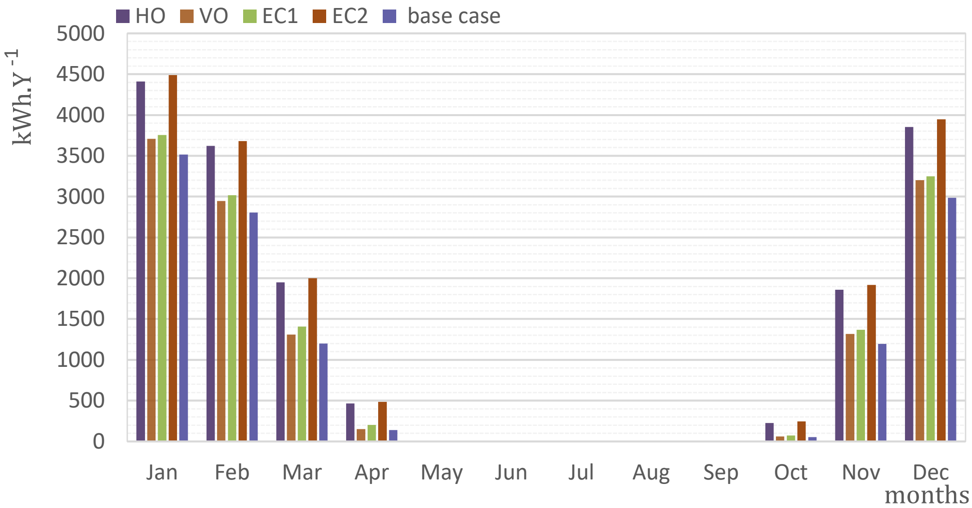

Figure 49. Comparision of simulated heating loads (kWh.Y^{-1}) of the base case scenario BC and scenarios of “I Category”: HO, VO, EC1 and EC2 in east orientation

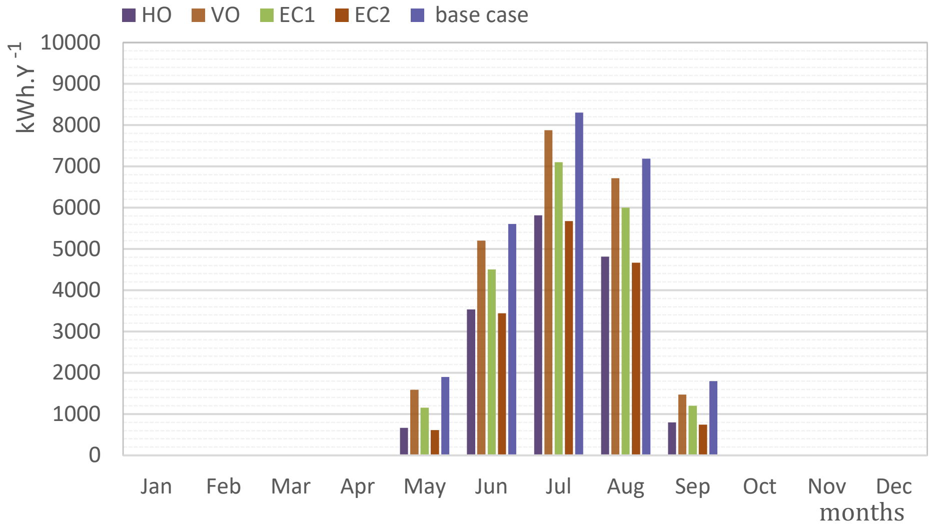

Figure 50. Comparision of simulated cooling loads (kWh.Y^{-1}) of the base case scenario BC and scenarios of “I Category”: HO, VO, EC1 and EC2 in east orientation

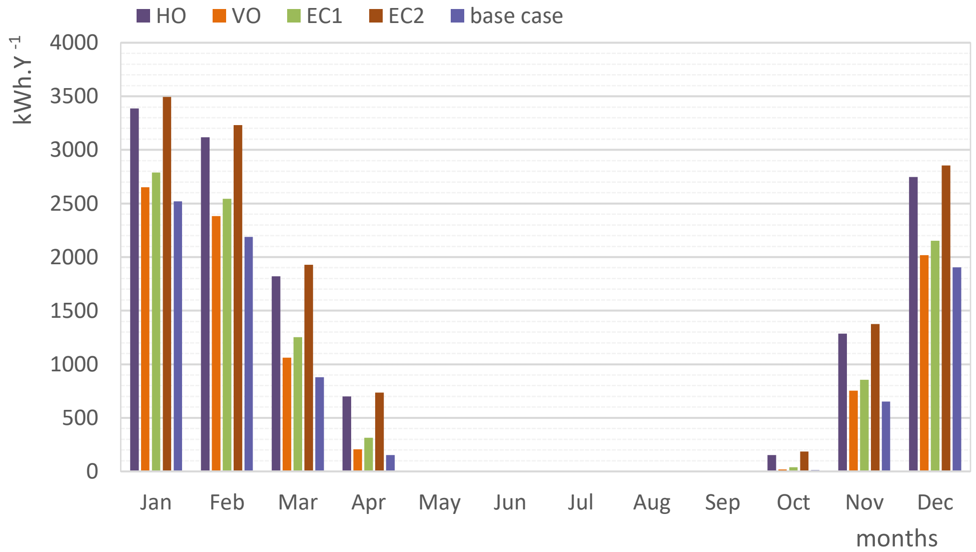

Figure 51. Comparision of simulated heating loads (kWh.Y^{-1}) of the base case scenario BC and scenarios of “I Category”: HO, VO, EC1 and EC2 in south orientation

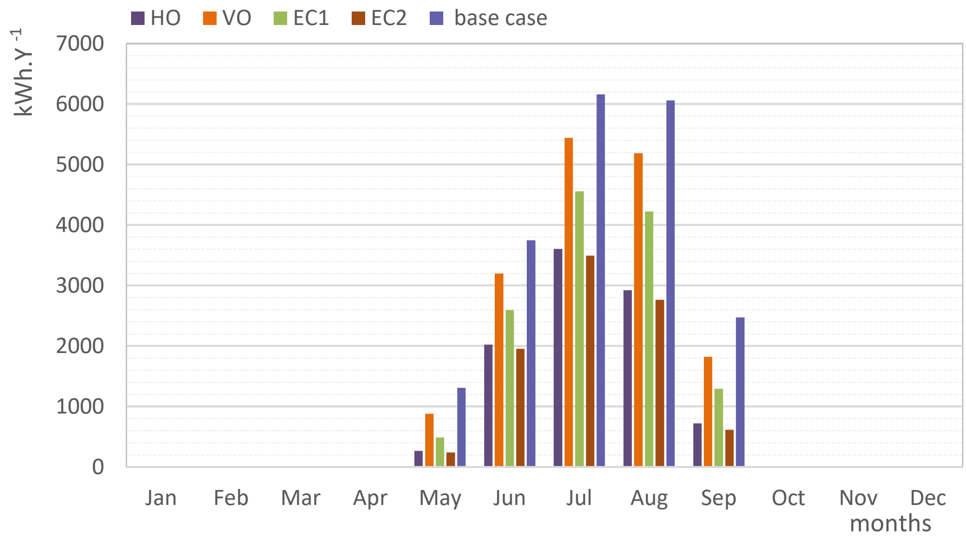

Figure 52. Comparision of simulated cooling loads (kWh.Y^{-1}) of the base case scenario BC and scenarios of "I Category": HO, VO, EC1 and EC2 in south orientation

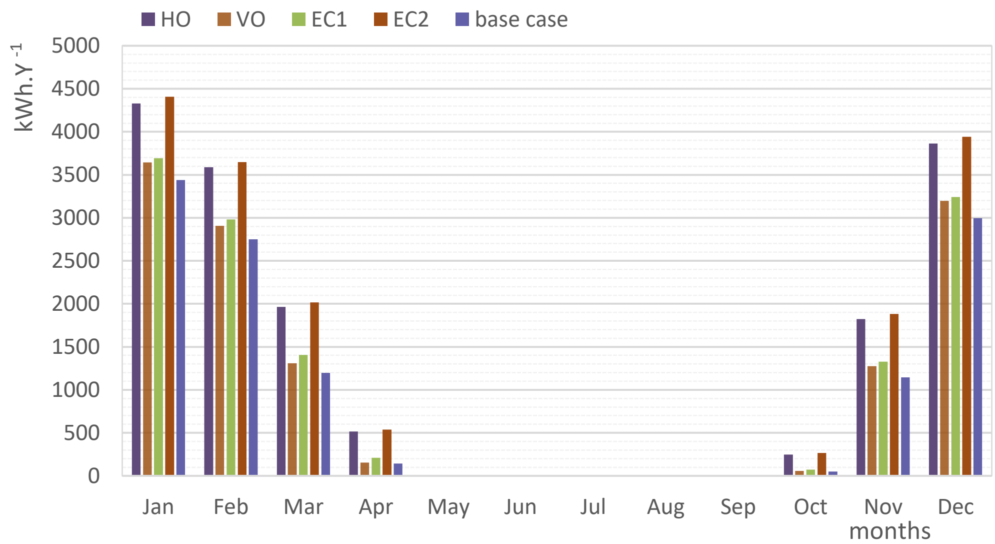

Figure 53. Comparision of simulated heating loads (kWh.Y^{-1}) of the base case scenario BC and scenarios of "I Category": HO, VO, EC1 and EC2 in west orientation

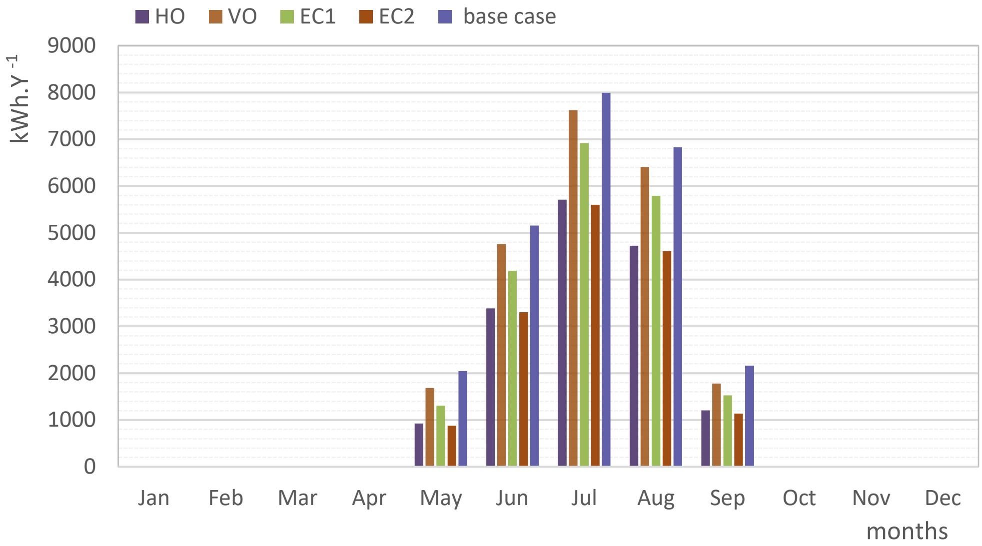

Figure 54. Comparision of simulated cooling loads (kWh.Y^{-1}) of the base case scenario BC and scenarios of "I Category": HO, VO, EC1 and EC2 in west orientation

"II Category": ***Figure 55*** and ***Figure 56*** shows the energy consumption for heating and cooling for the base case (BC) and H1, H2 scenarios in east orientation. ***Figure 57*** and ***Figure 58*** shows the energy consumption for heating and cooling for the base case (BC) and H1, H2 scenarios in south orientation. ***Figure 59*** and ***Figure 60*** shows the energy consumption for heating and cooling for the base case (BC) and H1, H2 scenarios in west orientation.

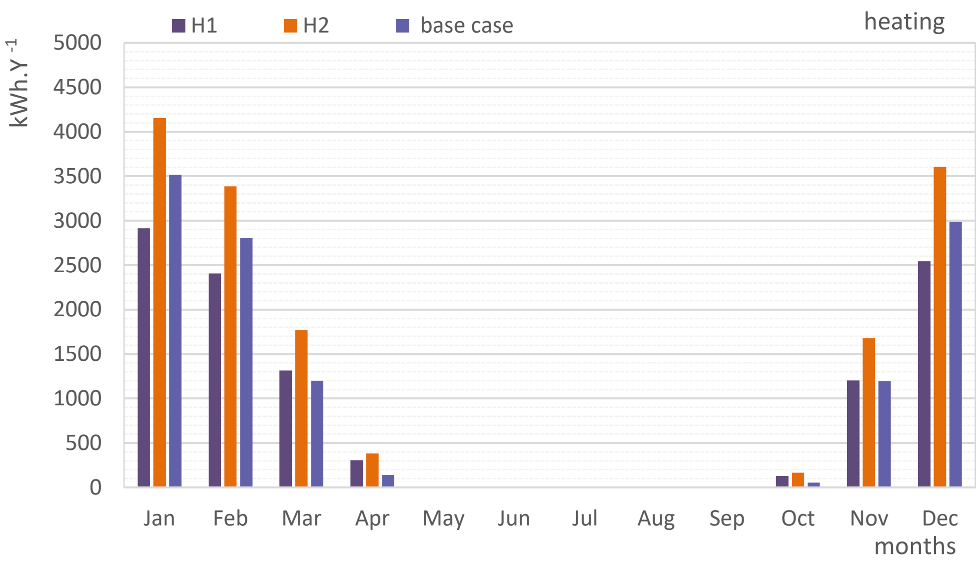

Figure 55. Comparision of simulated heating loads (kWh.Y^{-1}) of the base case scenario BC and scenarios of "II Category": H1 and H2 in east orientation

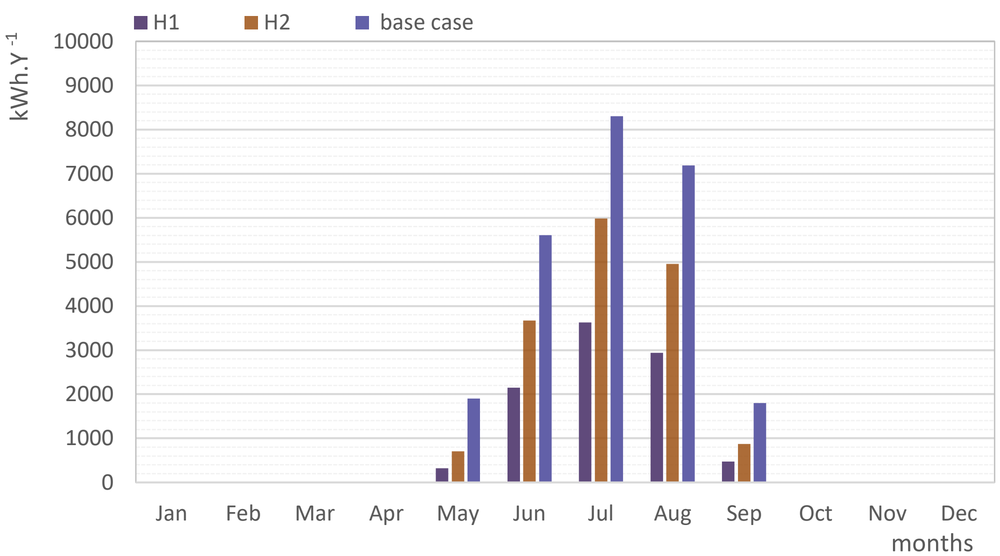

Figure 56. Comparision of simulated cooling loads (kWh.Y^{-1}) of the base case scenario BC and scenarios of "II Category": H1 and H2 in east orientation

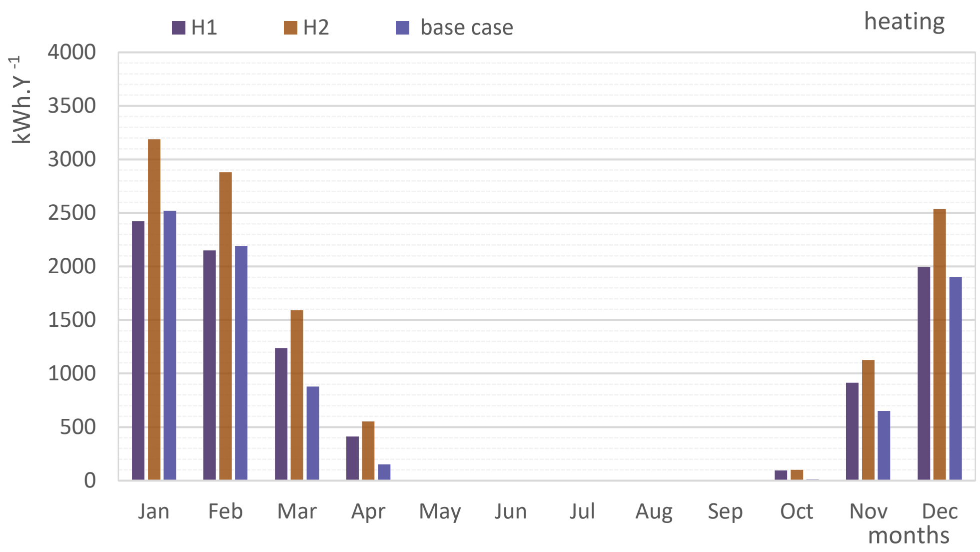

Figure 57. Comparision of simulated heating loads (kWh.Y^{-1}) of the base case scenario BC and scenarios of “II Category”: H1 and H2 in south orientation

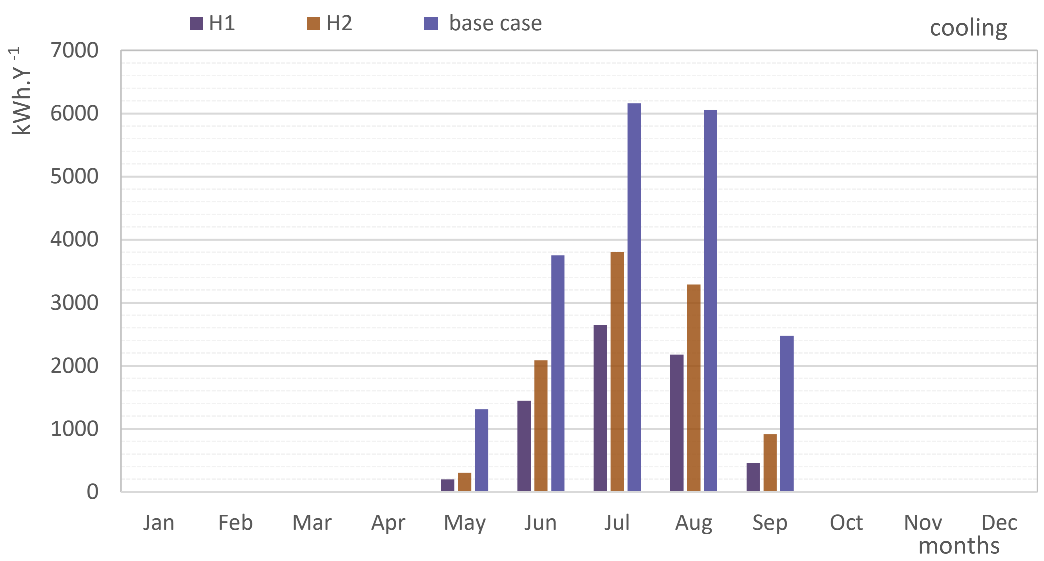

Figure 58. Comparision of simulated cooling loads (kWh.Y^{-1}) of the base case scenario BC and scenarios of “II Category”: H1 and H2 in south orientation

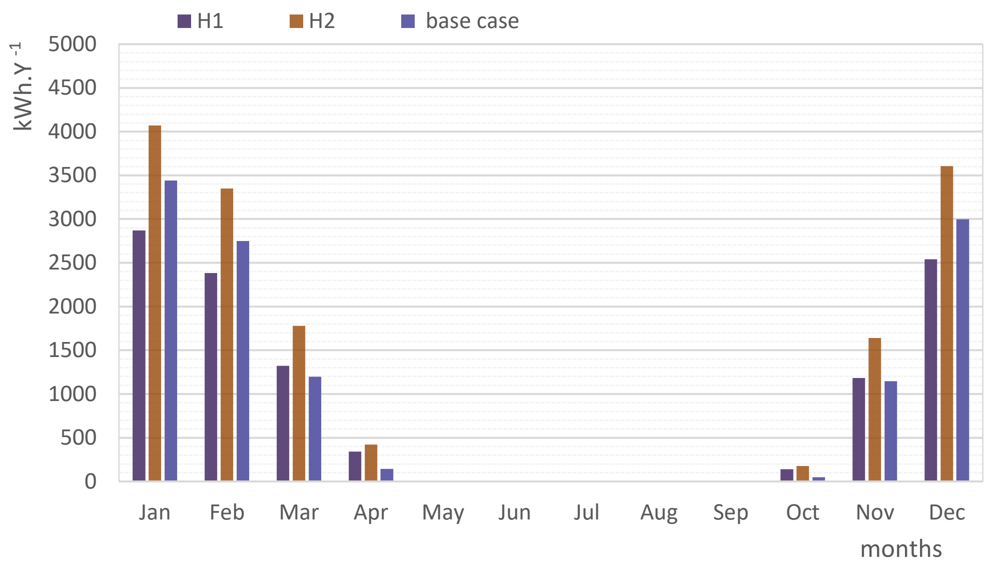

Figure 59. Comparision of simulated heating loads (kWh.Y^{-1}) of the base case scenario BC and scenarios of "II Category": H1 and H2 in west orientation

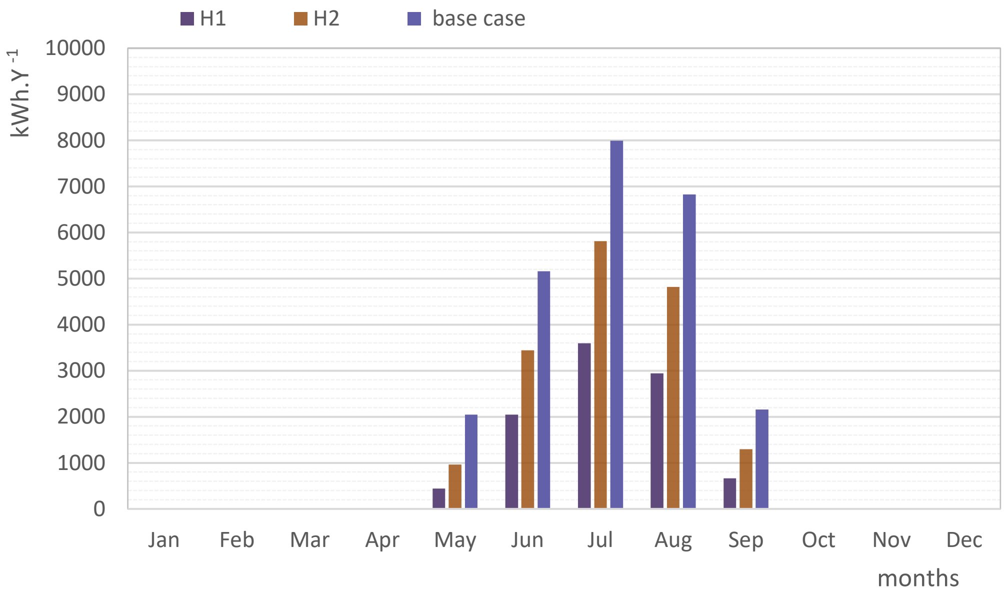

Figure 60. Comparision of simulated cooling loads (kWh.Y^{-1}) of the base case scenario BC and scenarios of "II Category": H1 and H2 in west orientation

“III Category”: ***Figure 61*** and ***Figure 62*** shows the energy consumption for heating and cooling for the base case (BC) and V1, V2, V3 scenarios in east orientation. ***Figure 63*** and ***Figure 64*** shows the energy consumption for heating and cooling for the base case (BC) and V1, V2, V3 scenarios in south orientation. ***Figure 65*** and ***Figure 66*** shows the energy consumption for heating and cooling for the base case (BC) and V1, V2, V3 scenarios in west orientation.

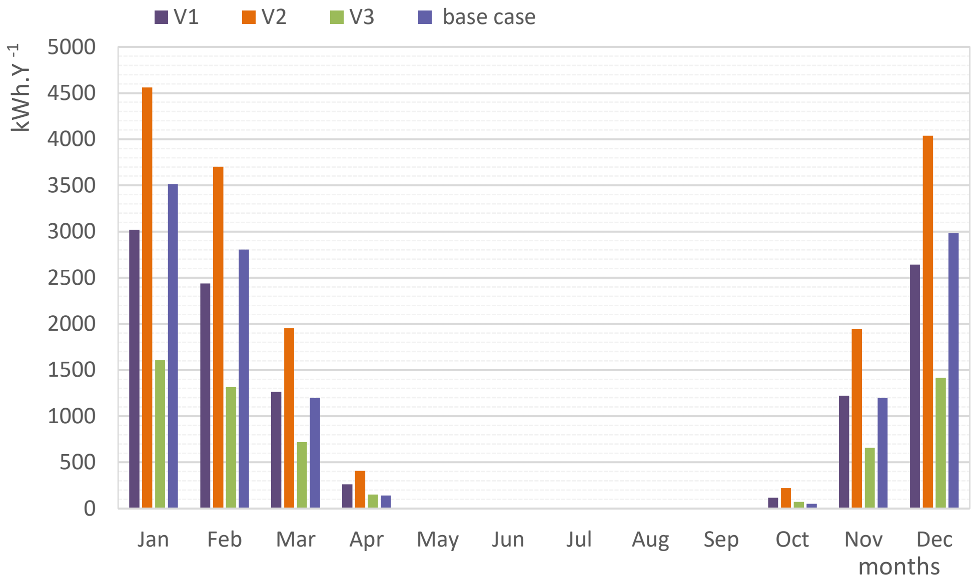

Figure 61. Comparision of simulated heating loads (kWh.Y^{-1}) of the base case scenario BC and scenarios of “III Category”: V1, V2 and V3 in east orientation

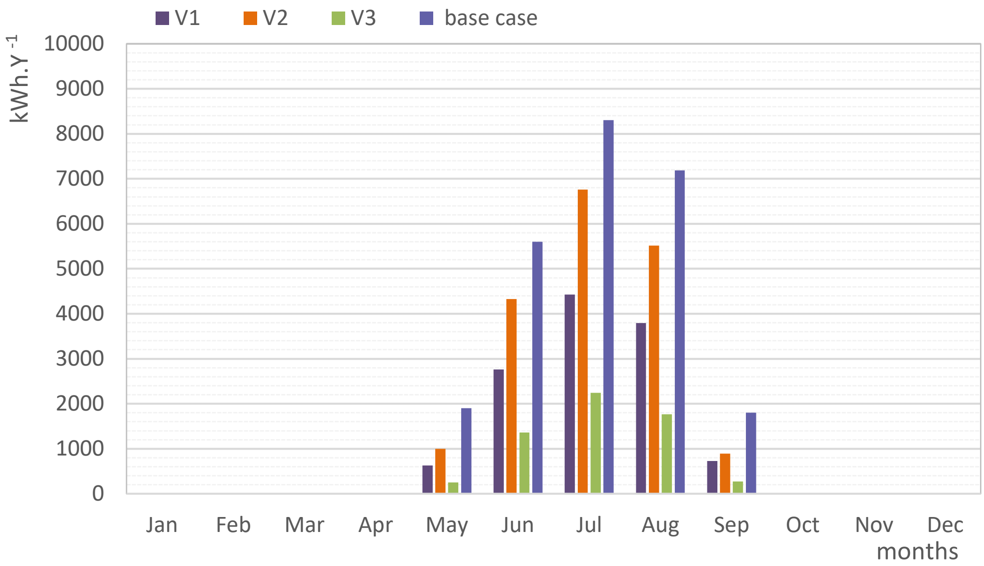

Figure 62. Comparision of simulated cooling loads (kWh.Y^{-1}) of the base case scenario BC and scenarios of “III Category”: V1, V2 and V3 in east orientation

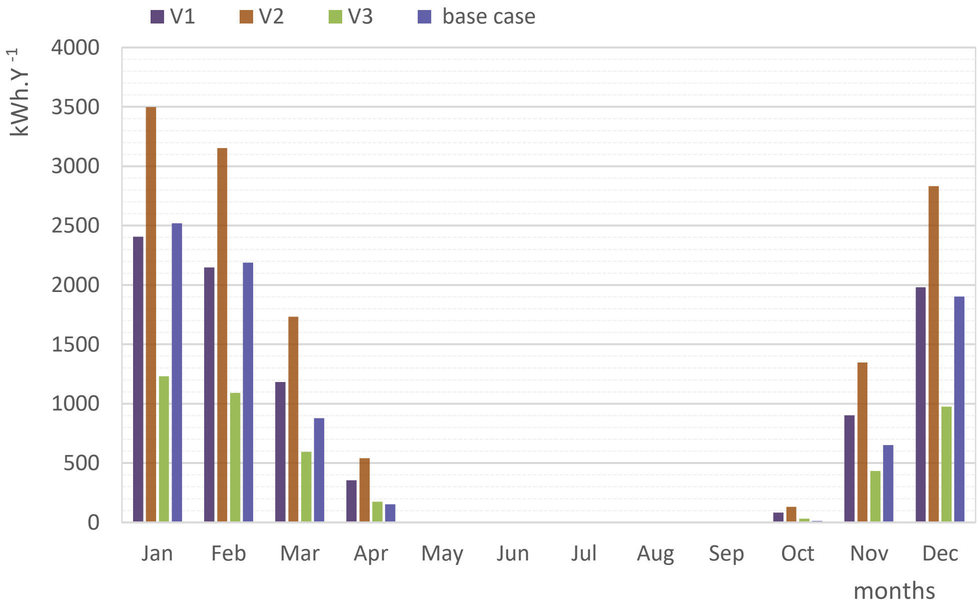

Figure 63. Comparision of simulated heating loads (kWh.Y^{-1}) of the base case scenario BC and scenarios of “III Category”: V1, V2 and V3 in south orientation

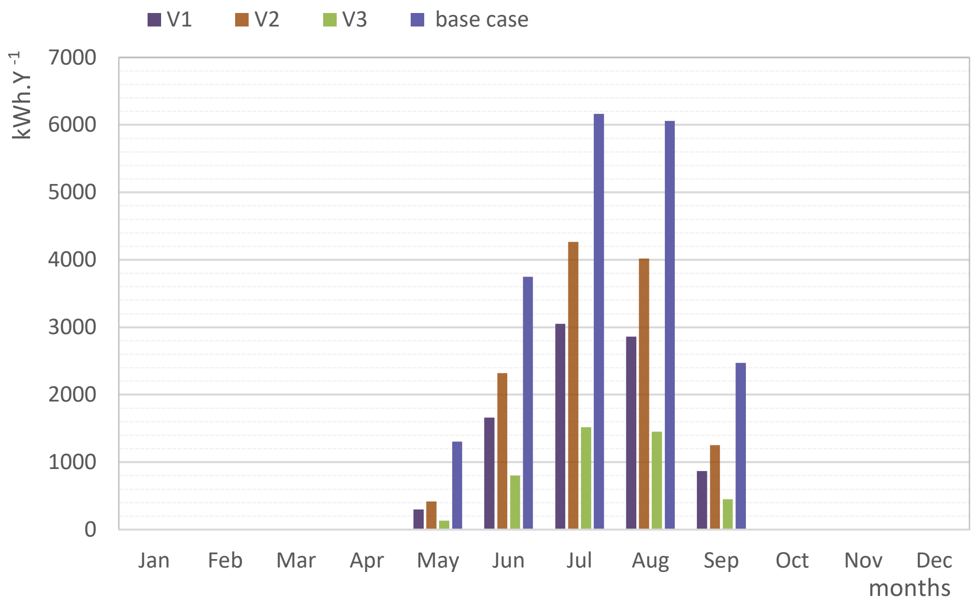

Figure 64. Comparision of simulated cooling loads (kWh.Y^{-1}) of the base case scenario BC and scenarios of “III Category”: V1, V2 and V3 in south orientation

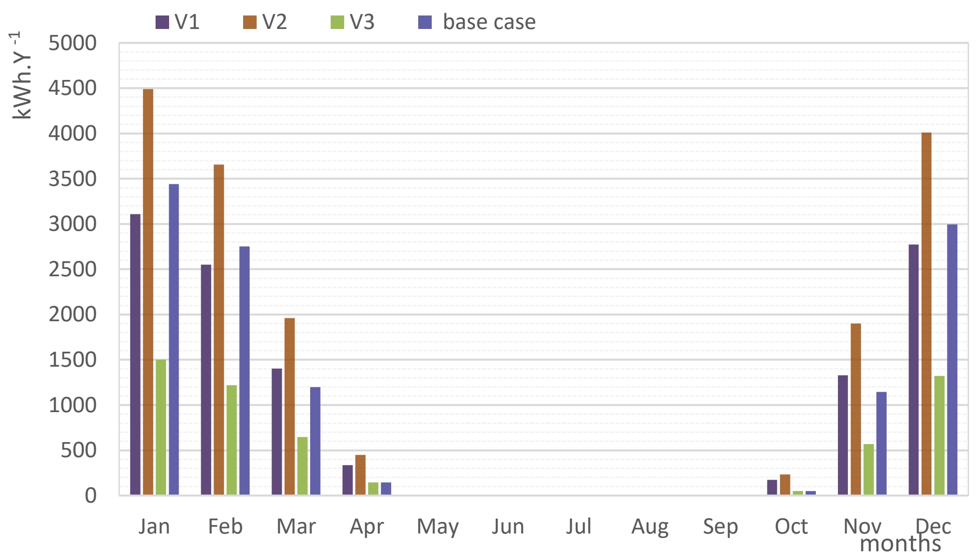

Figure 65. Comparision of simulated heating loads (kWh.Y^{-1}) of the base case scenario BC and scenarios of “III Category”: V1, V2 and V3 in west orientation

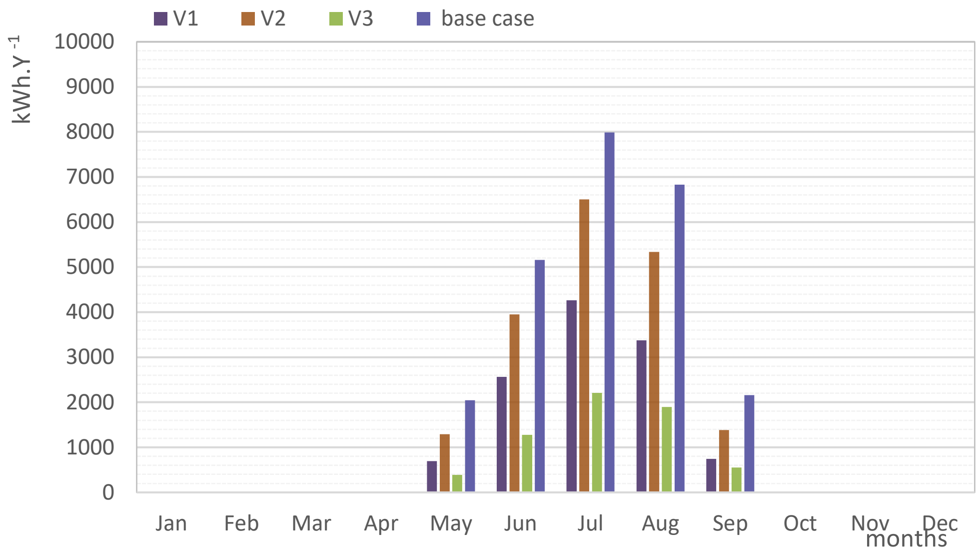

Figure 66. Comparision of simulated cooling loads (kWh.Y^{-1}) of the base case scenario BC and scenarios of "III Category": V1, V2 and V3 in west orientation

Energy consumption for heating and cooling loads for "I Category", "II Category" and "III Category" are analyzed together. ***Figure 67*** and ***Figure 68*** show heating and cooling loads results for the base case (BC) and EC1, EC2, HO, VO, H1, H2, V1, V2, V3 scenarios in east orientation. ***Figure 69*** and ***Figure 70*** show heating and cooling loads results for the base case (BC) and EC1, EC2, HO, VO, H1, H2, V1, V2, V3 scenarios in south orientation. ***Figure 71*** and ***Figure 72*** show heating and cooling loads results for the base case (BC) and EC1, EC2, HO, VO, H1, H2, V1, V2, V3 scenarios in west orientation.

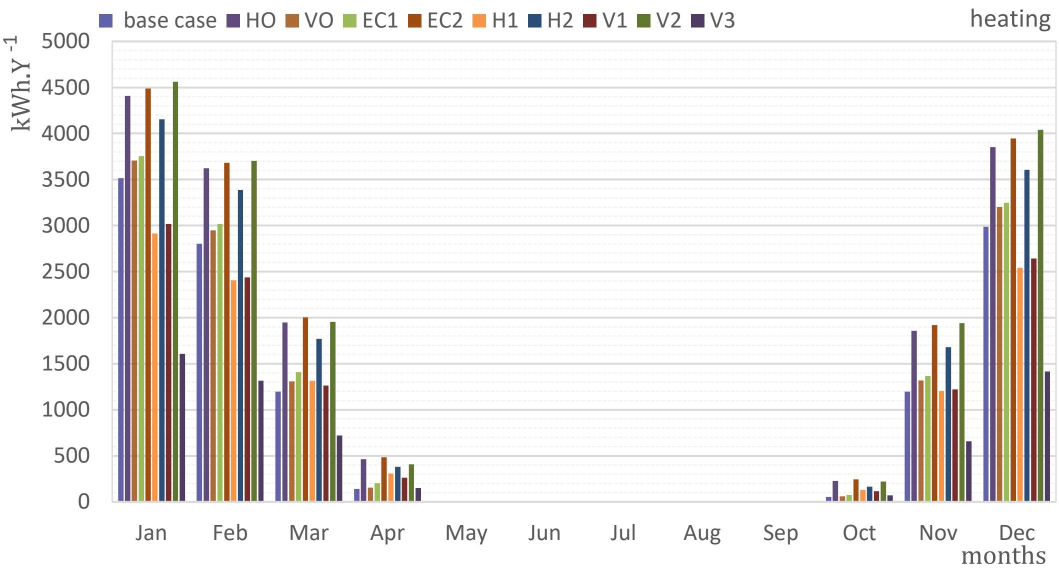

Figure 67. Comparision of simulated heating loads (kWh.Y^{-1}) of the base case scenario BC and scenarios of "I Category", "II Category" and "III Category" in east orientation

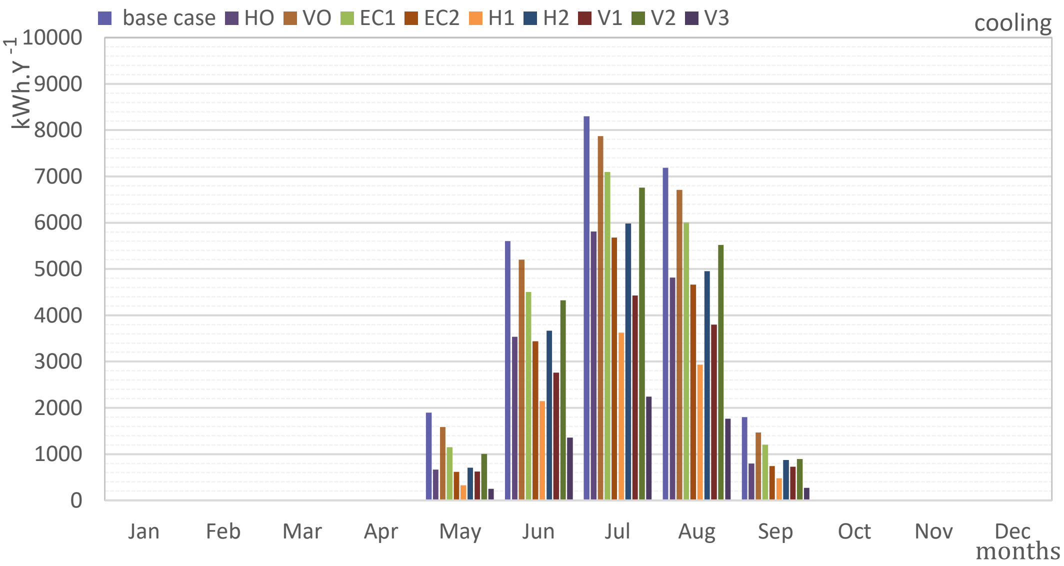

Figure 68. Comparision of simulated cooling loads (kWh.Y^{-1}) of the base case scenario BC and scenarios of "I Category", "II Category" and "III Category" in east orientation

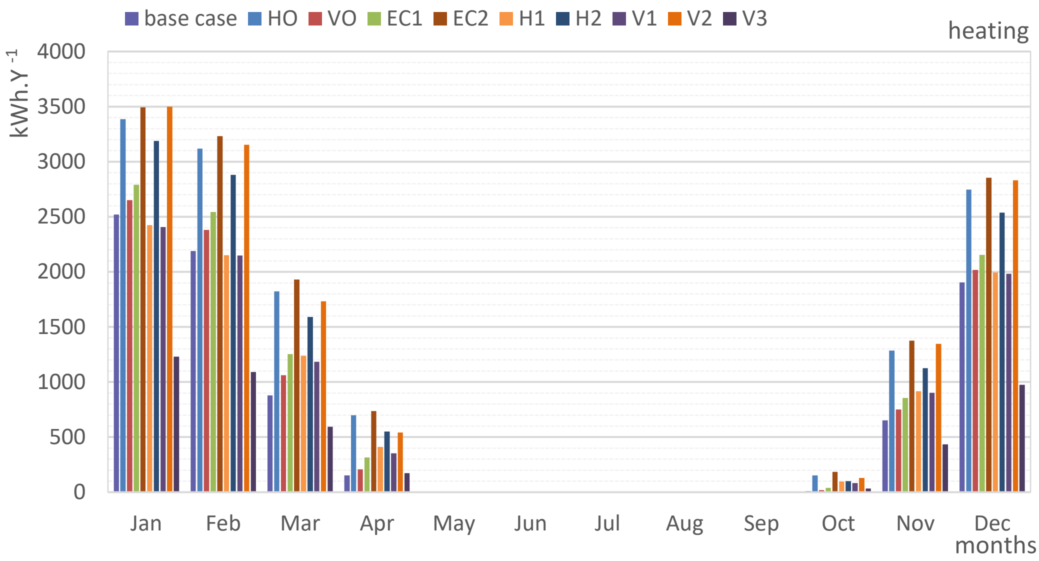

Figure 69. Comparision of simulated heating loads (kWh.Y^{-1}) of the base case scenario BC and scenarios of "I Category", "II Category" and "III Category" in south orientation

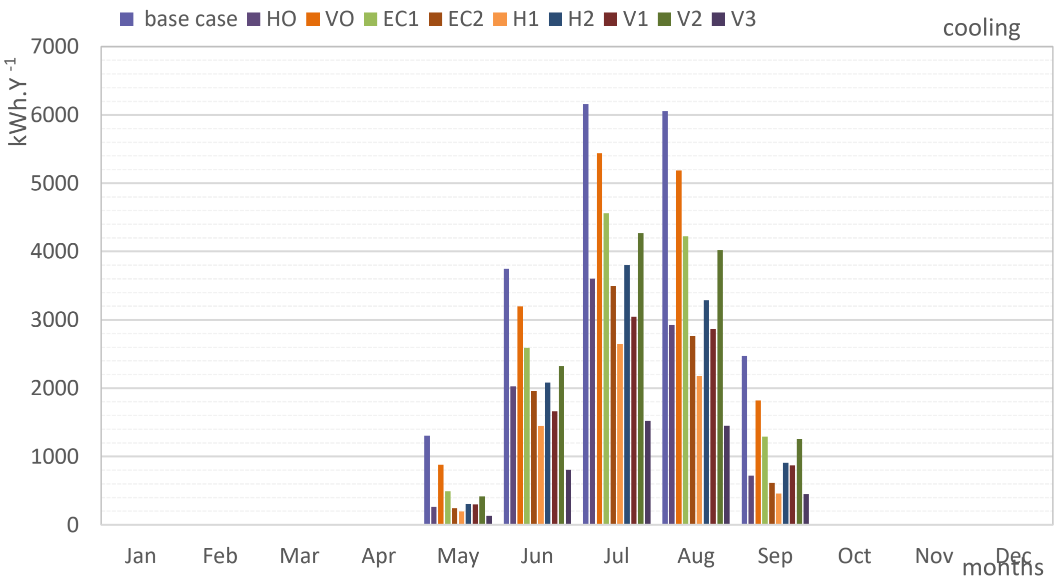

Figure 70. Comparision of simulated cooling loads (kWh.Y^{-1}) of the base case scenario BC and scenarios of "I Category", "II Category" and "III Category" in south orientation

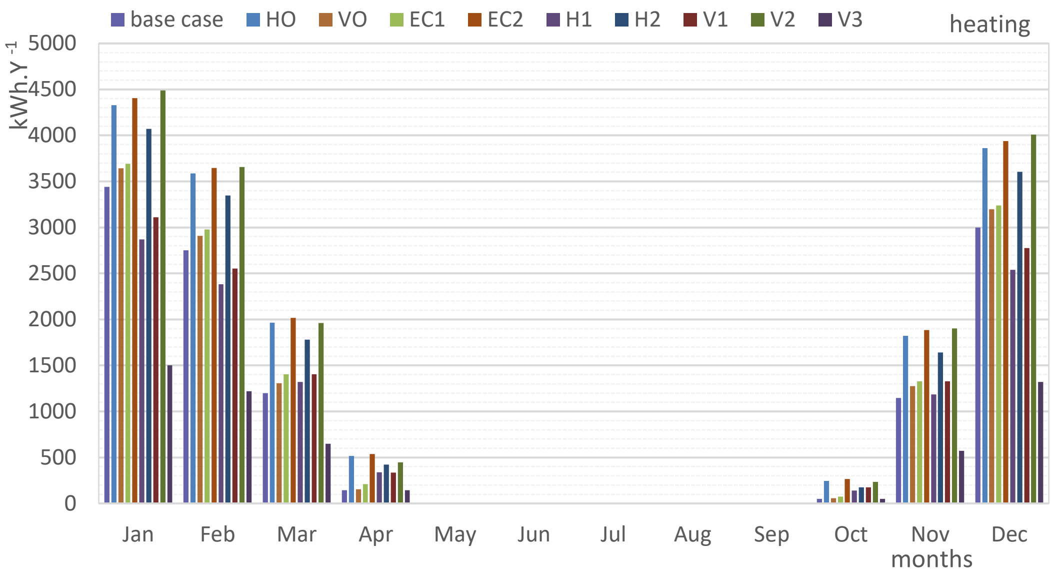

Figure 71. Comparision of simulated heating loads (kWh.Y^{-1}) of the base case scenario BC and scenarios of "I Category", "II Category" and "III Category" in west orientation

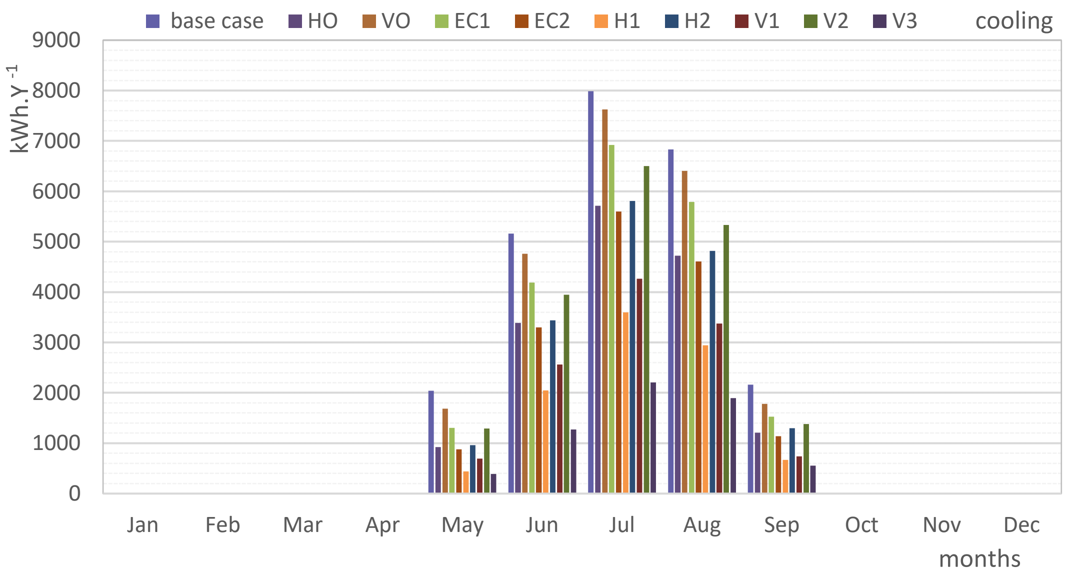

Figure 72. Comparision of simulated cooling loads (kWh.Y^{-1}) of the base case scenario BC and scenarios of "I Category", "II Category" and "III Category" in west orientation

4.3 Almeria, Spain

4.3.1 Indoor air temperature

Indoor air temperature results for “I Category”, “II Category”, and “III Category” in east, south and west orientation are analyzed by picking a typical summer and winter day. Beginning with the analysis of the “I Category’s”, followed by the "II Category" and "III Category" results. In conclusion, all of the scenarios are also compared for the Almeria climate.

“I Category”: ***Figure 73*** and ***Figure 74*** show the indoor air temperature results for the base case (BC) and EC1, EC2, HO and VO scenarios analyzed for both summer and winter period in east orientation. ***Figure 75*** and ***Figure 76*** show the indoor air temperature results for the base case (BC) and EC1, EC2, HO VO scenarios analyzed for both summer and winter period in south orientation. ***Figure 77*** and ***Figure 78*** show the indoor air temperature results for the base case (BC) and EC1, EC2, HO and VO scenarios analyzed for both summer and winter period in west orientation.

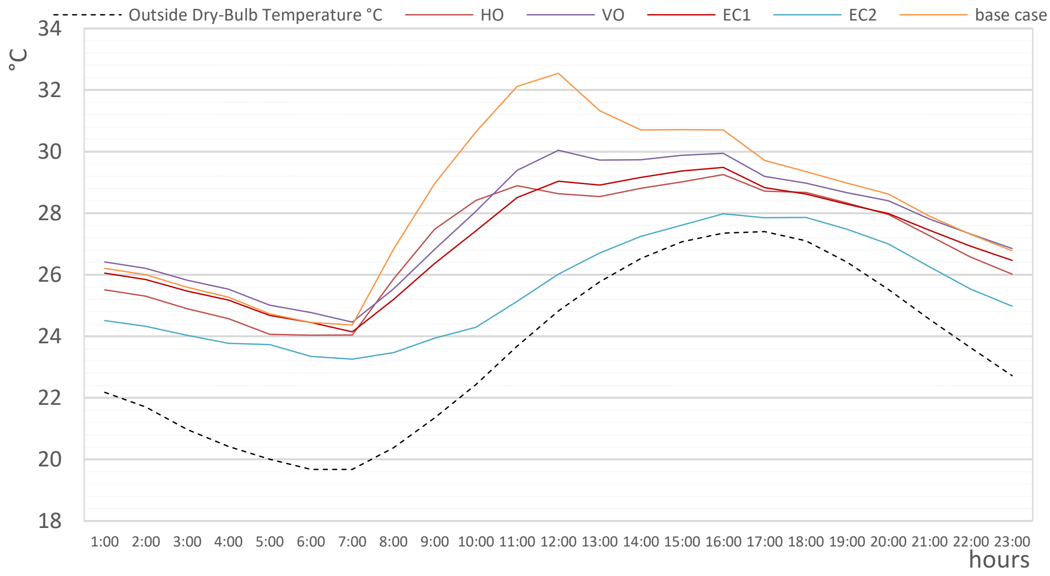

Figure 73. Simulated indoor air temperatures for the base case scenario BC and scenarios of "I Category": HO, VO, EC1 and EC2, together with the dry-bulb temperature from the weather file 3rd August in east direction

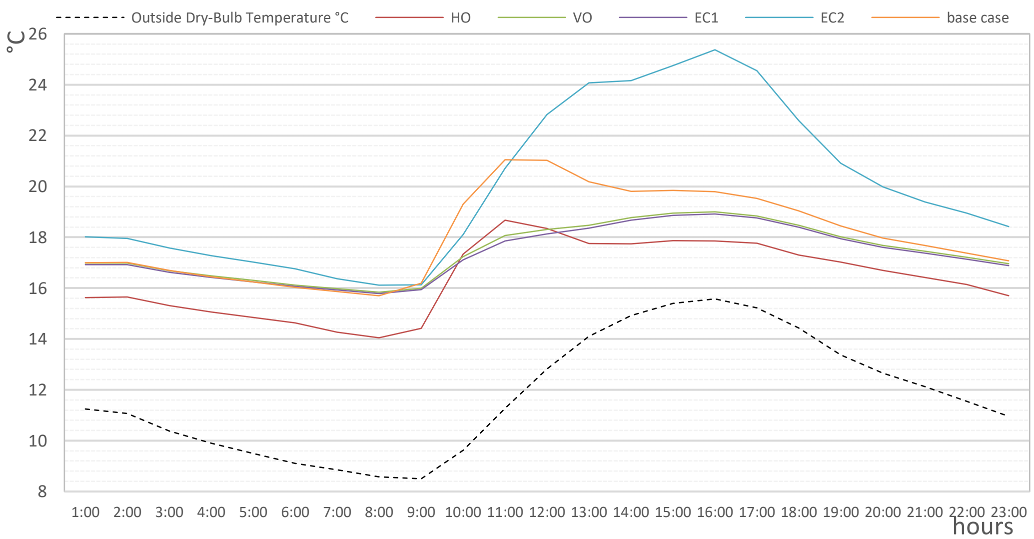

Figure 74. Simulated indoor air temperatures for the base case scenario BC and scenarios of "I Category": HO, VO, EC1 and EC2, together with the dry-bulb temperature from the weather file 4th January in east direction

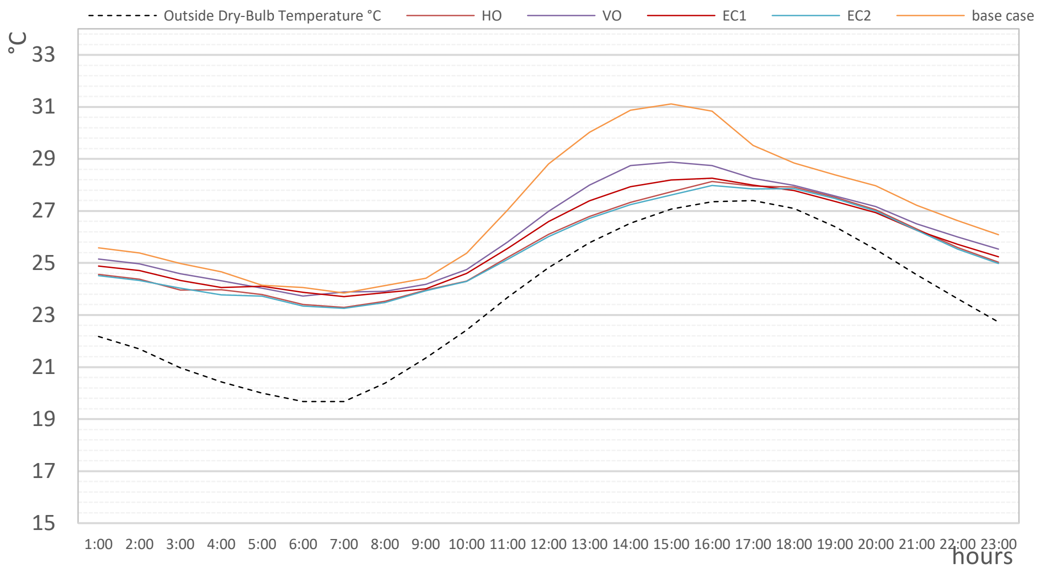

Figure 75. Simulated indoor air temperatures for the base case scenario BC and scenarios of "I Category": HO, VO, EC1 and EC2, together with the dry-bulb temperature from the weather file 3rd August in south direction

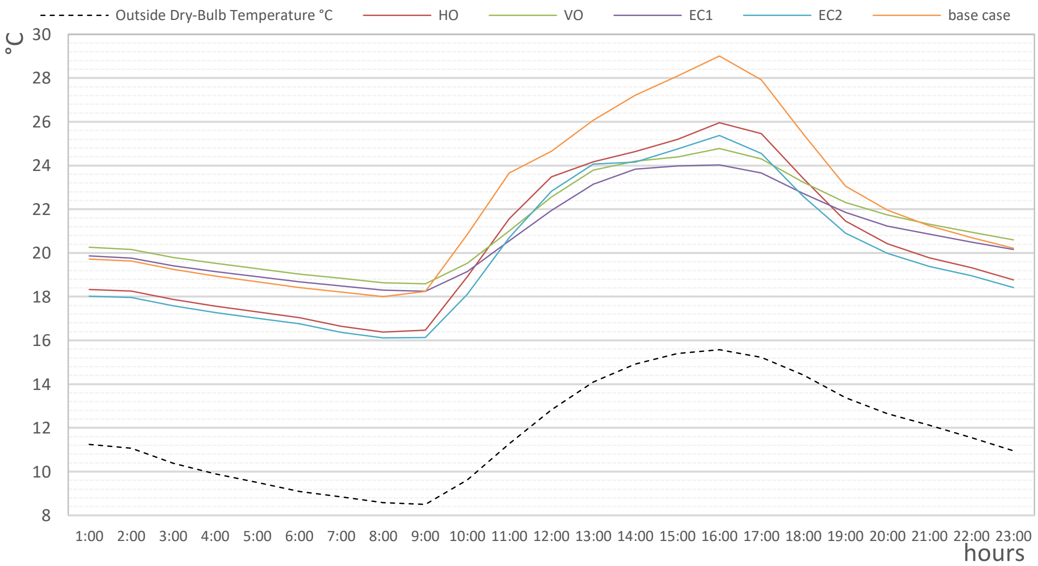

Figure 76. Simulated indoor air temperatures for the base case scenario BC and scenarios of "I Category": HO, VO, EC1 and EC2, together with the dry-bulb temperature from the weather file 4th January in south direction

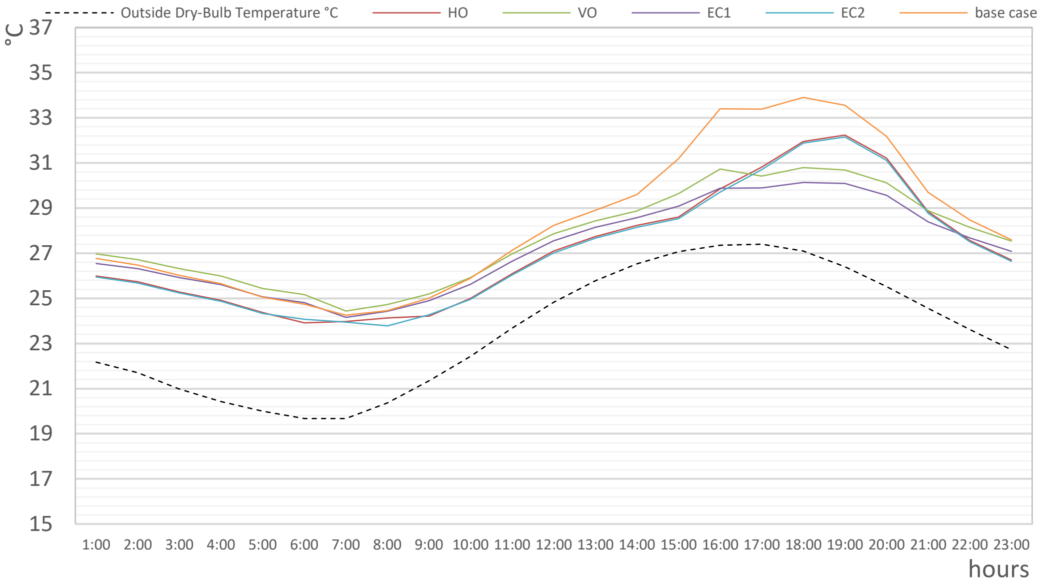

Figure 77. Simulated indoor air temperatures for the base case scenario BC and scenarios of "I Category": HO, VO, EC1 and EC2, together with the dry-bulb temperature from the weather file 3rd August in west direction

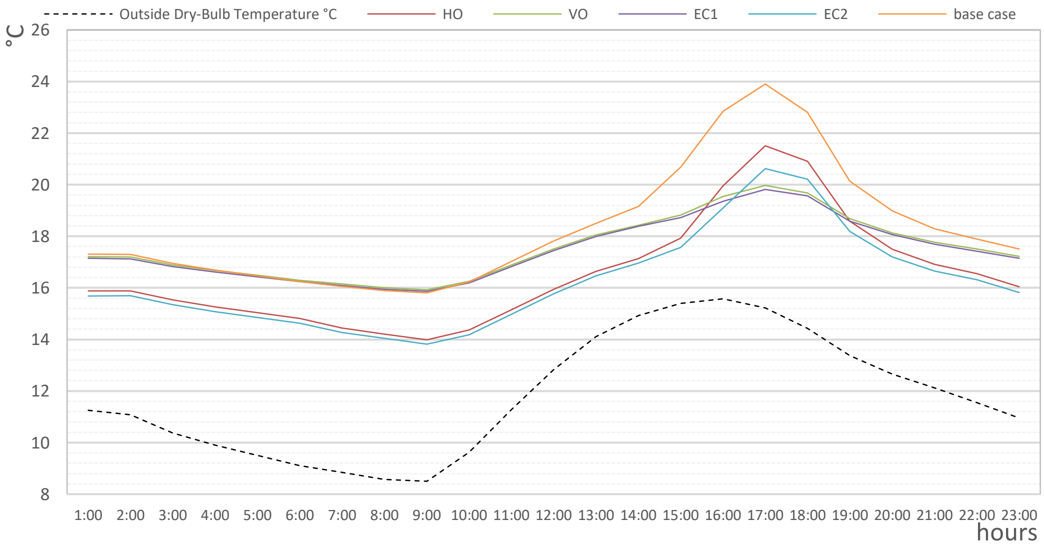

Figure 78. Simulated indoor air temperatures for the base case scenario BC and scenarios of "I Category": HO, VO, EC1 and EC2, together with the dry-bulb temperature from the weather file 4th January in west direction

“II Category”: ***Figure 79*** and ***Figure 80*** show the indoor air temperature results for the base case (BC) and H1, H2 scenarios analyzed for both summer and winter period in east orientation. ***Figure 81*** and ***Figure 82*** show the indoor air temperature results for the base case (BC) and H1, H2 scenarios analyzed for both summer and winter period in south orientation. ***Figure 83*** and ***Figure 84*** show the indoor air temperature results for the base case (BC) and H1, H2 scenarios analyzed for both summer and winter period in west orientation.

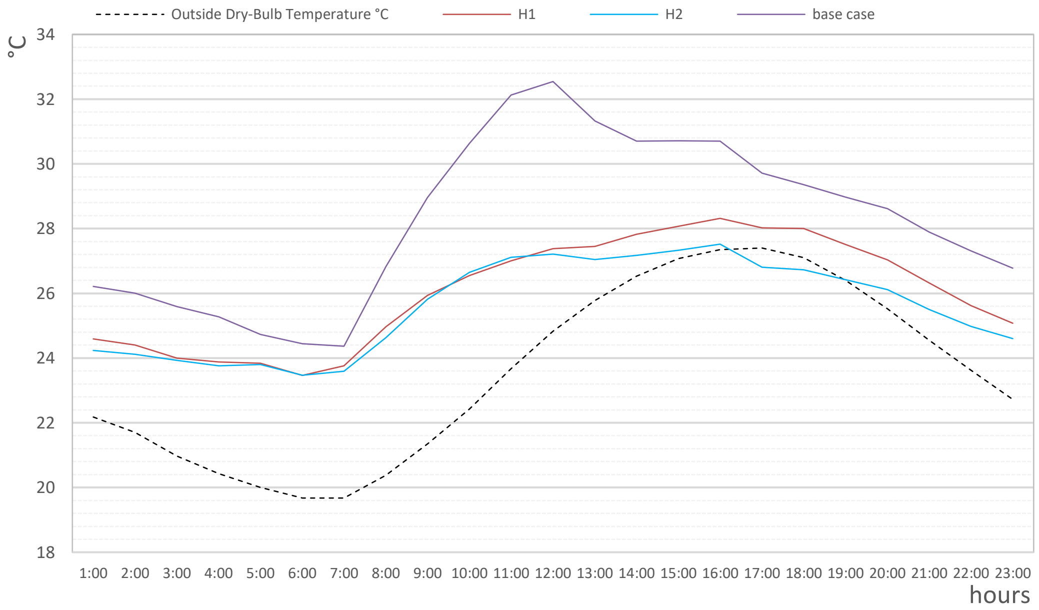

Figure 79. Simulated indoor air temperatures for the base case scenario BC and scenarios of “II Category”: H1, and H2, together with the dry-bulb temperature from the weather file 3rd August in east direction

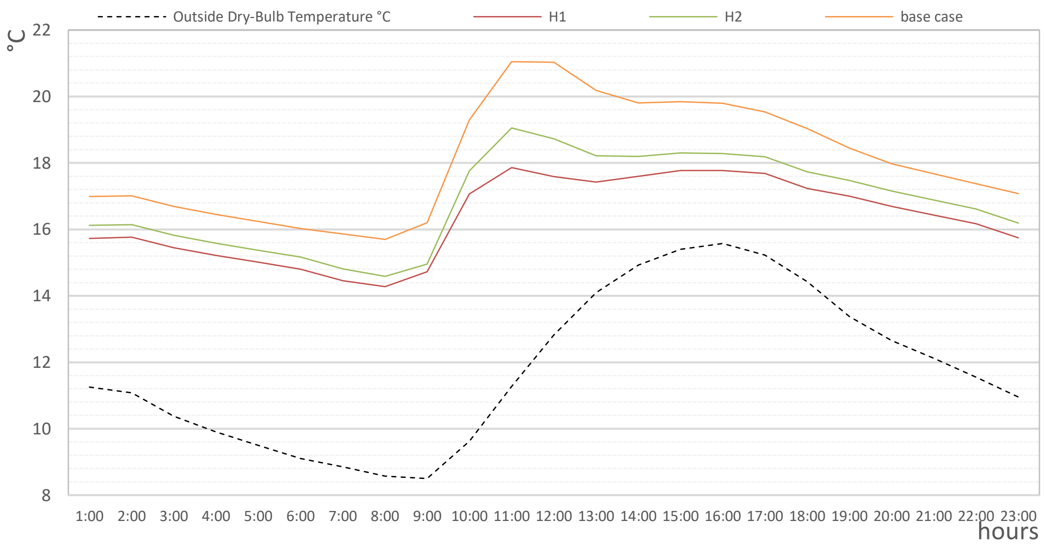

Figure 80. Simulated indoor air temperatures for the base case scenario BC and scenarios of "II Category": H1, and H2, together with the dry-bulb temperature from the weather file 4th January in east direction

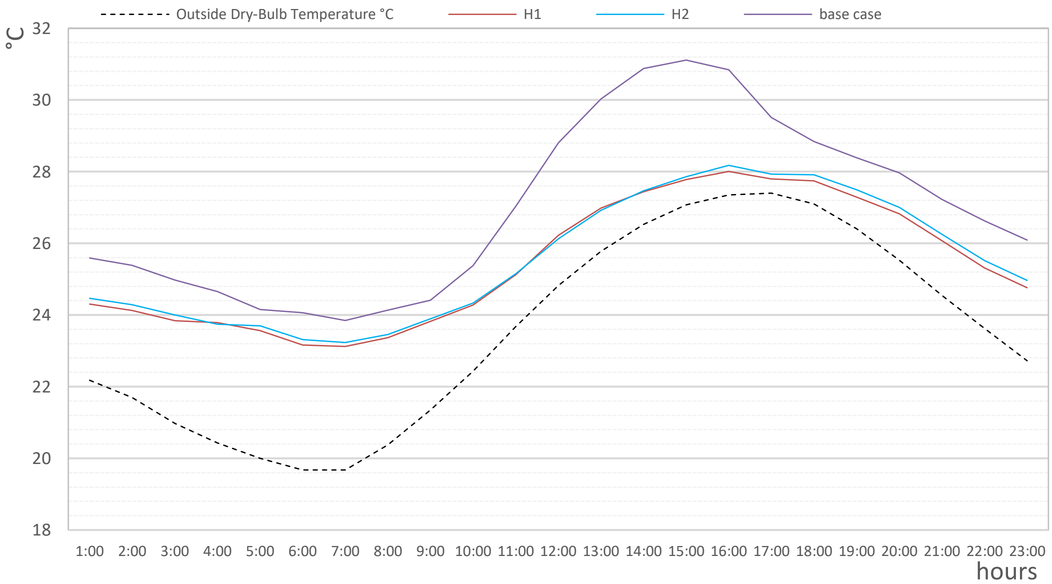

Figure 81. Simulated indoor air temperatures for the base case scenario BC and scenarios of "II Category": H1, and H2, together with the dry-bulb temperature from the weather file 3rd August in south direction

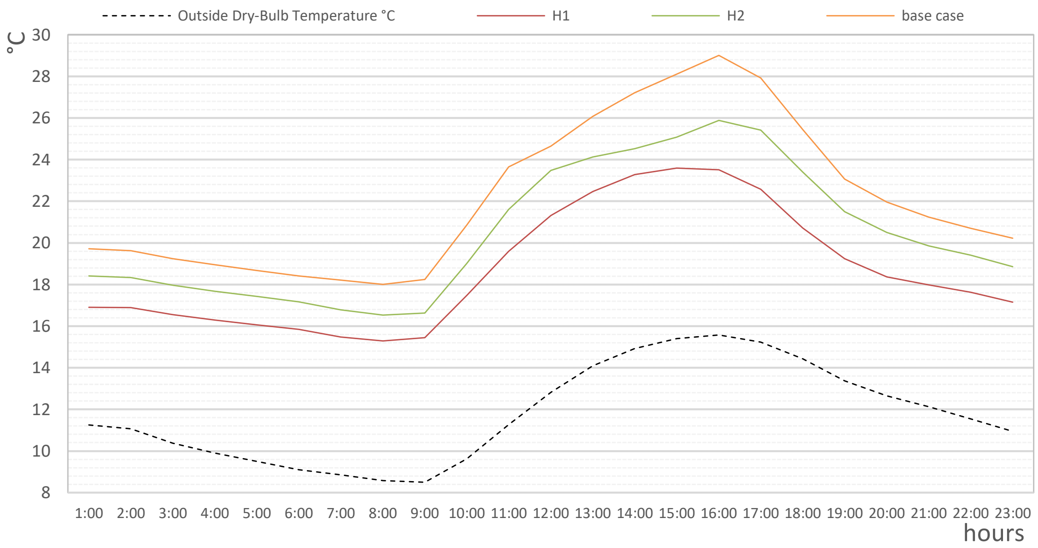

Figure 82. Simulated indoor air temperatures for the base case scenario BC and scenarios of "II Category": H1, and H2, together with the dry-bulb temperature from the weather file 4th January in south direction

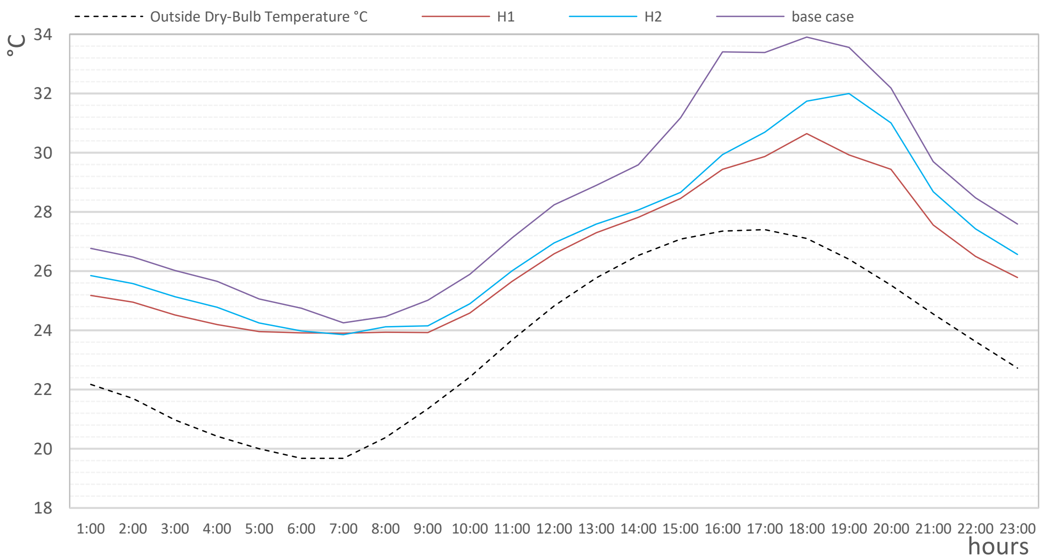

Figure 83. Simulated indoor air temperatures for the base case scenario BC and scenarios of "II Category": H1, and H2, together with the dry-bulb temperature from the weather file 3rd August in west direction

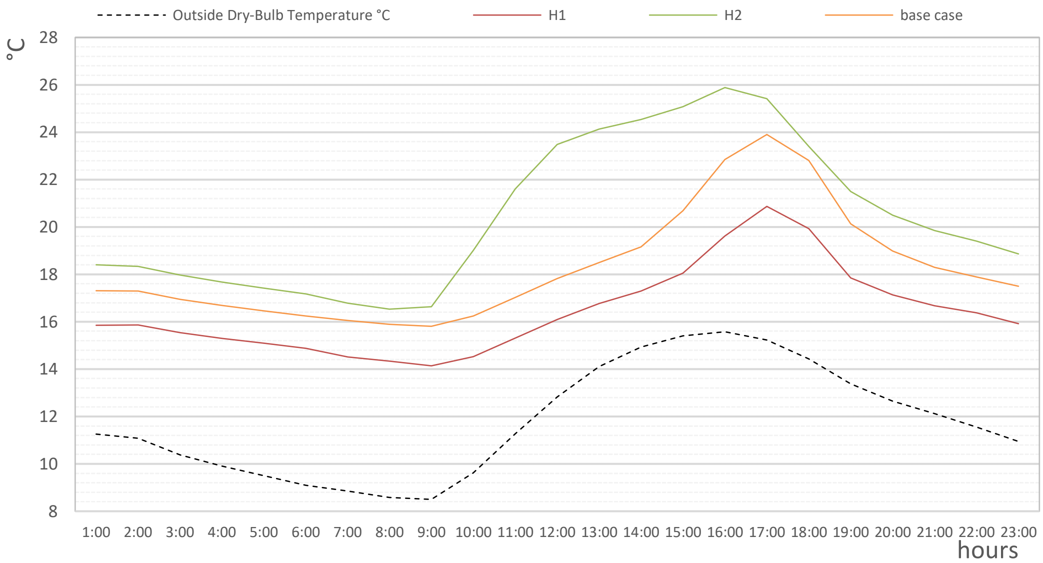

Figure 84. Simulated indoor air temperatures for the base case scenario BC and scenarios of "II Category": H1, and H2, together with the dry-bulb temperature from the weather file 4th January in west direction

"III Category": ***Figure 83*** and ***Figure 84*** show the indoor air temperature results for the base case (BC) and V1, V2, V3 scenarios analyzed for both summer and winter period in east orientation. ***Figure 85*** and ***Figure 86*** show the indoor air temperature results for the base case (BC) and V1, V2, V3 scenarios analyzed for both summer and winter period in south orientation. ***Figure 87*** and ***Figure 88*** show the indoor air temperature results for the base case (BC) and V1, V2, V3 scenarios analyzed for both summer and winter period in west orientation.

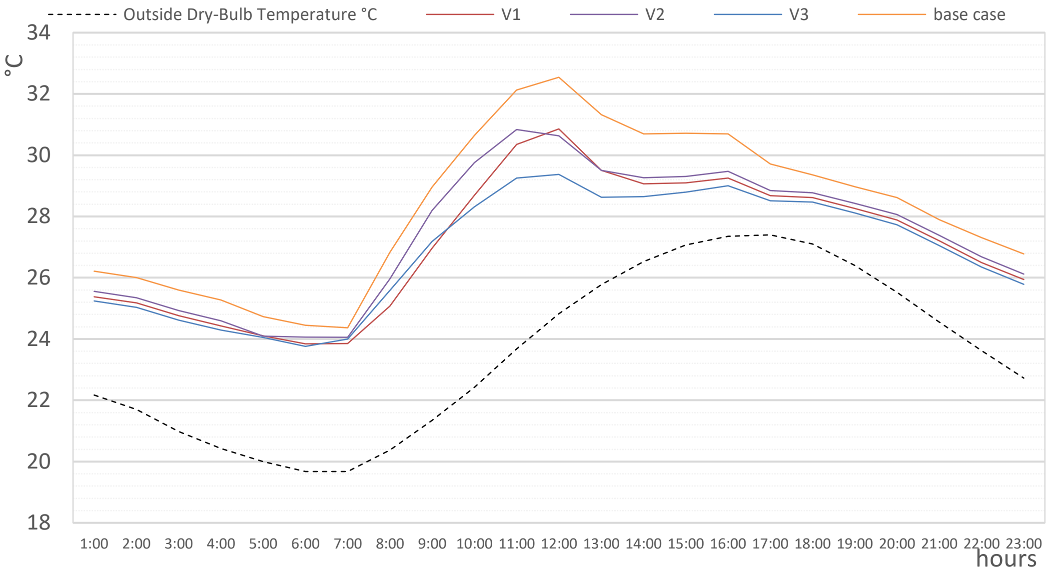

Figure 85. Simulated indoor air temperatures for the base case scenario BC and scenarios of "III Category": V1, V2 and V3 together with the dry-bulb temperature from the weather file 3rd August in east direction

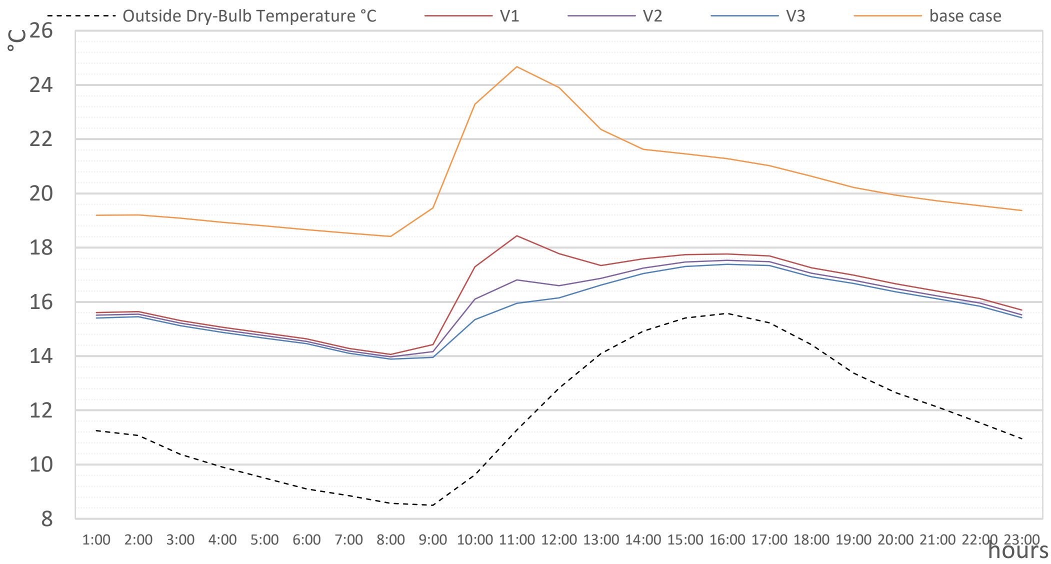

Figure 86. Simulated indoor air temperatures for the base case scenario BC and scenarios of "III Category": V1, V2 and V3 together with the dry-bulb temperature from the weather file 4th January in east direction

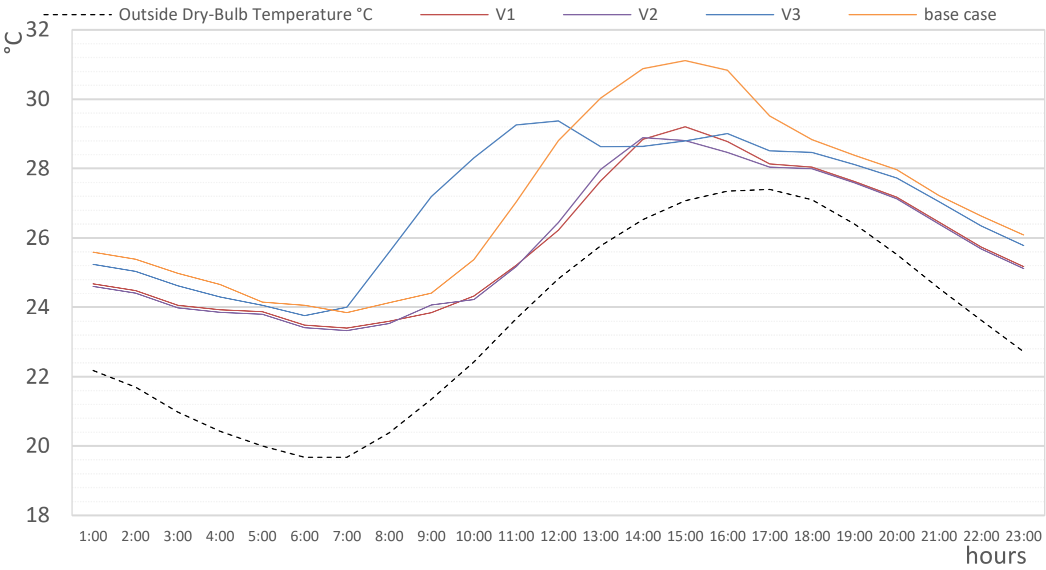

Figure 87. Simulated indoor air temperatures for the base case scenario BC and scenarios of "III Category": V1, V2 and V3 together with the dry-bulb temperature from the weather file 3rd August in south direction

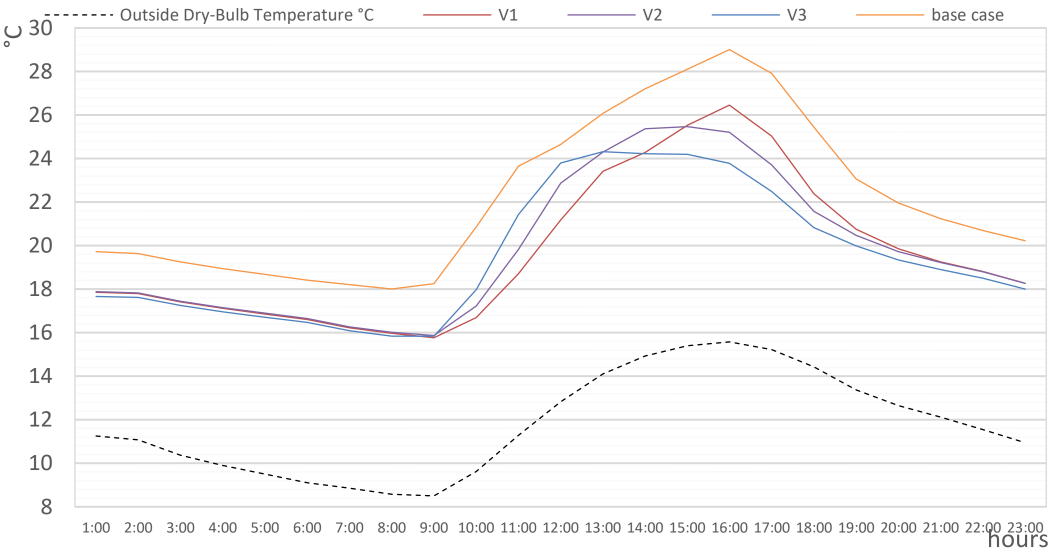

Figure 88. Simulated indoor air temperatures for the base case scenario BC and scenarios of "III Category": V1, V2 and V3 together with the dry-bulb temperature from the weather file 4th January in south direction

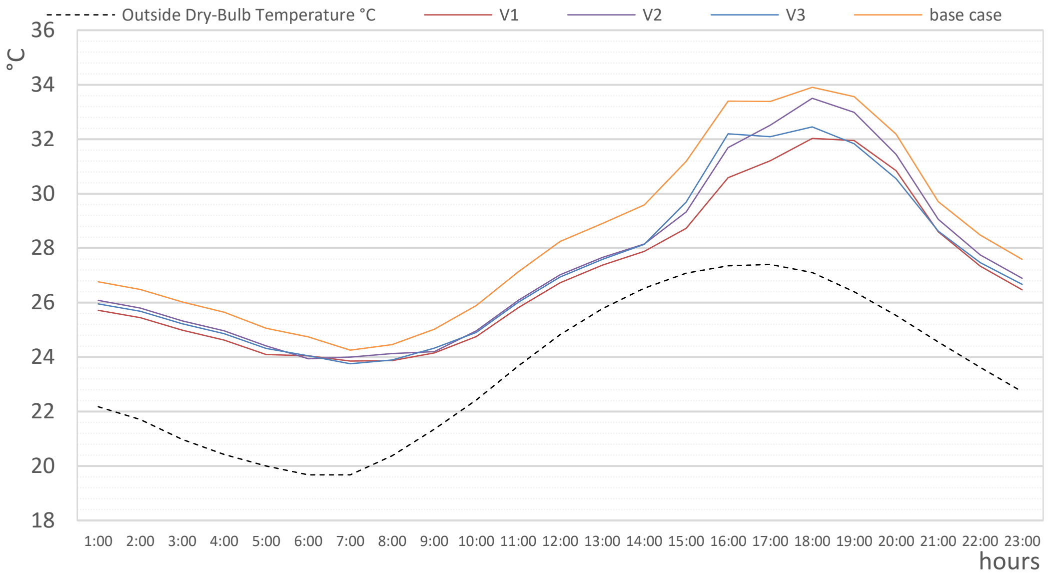

Figure 89. Simulated indoor air temperatures for the base case scenario BC and scenarios of "III Category": V1, V2 and V3 together with the dry-bulb temperature from the weather file 3rd August in west direction

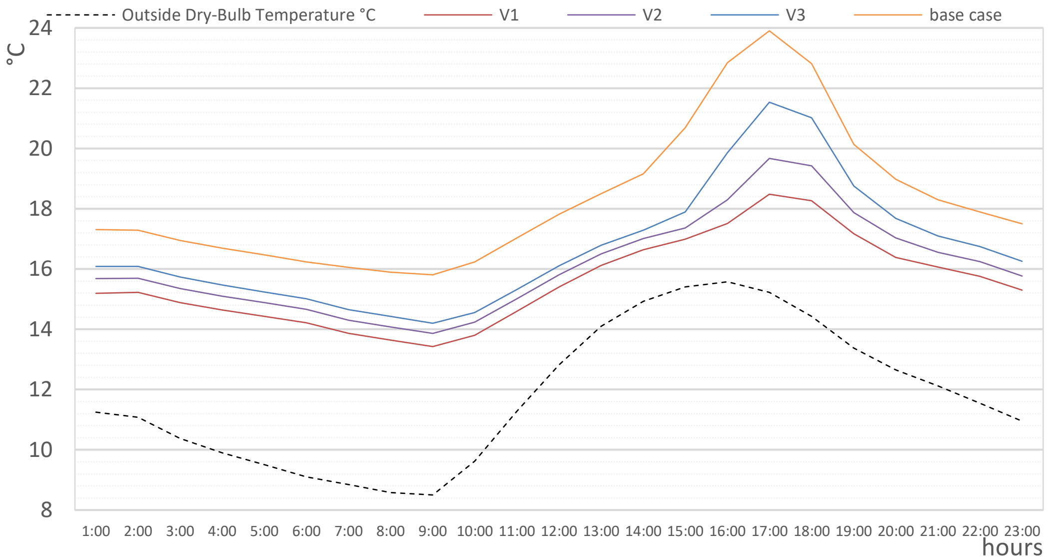

Figure 90. Simulated indoor air temperatures for the base case scenario BC and scenarios of "III Category": V1, V2 and V3 together with the dry-bulb temperature from the weather file 4th January in west direction

Indoor air temperature results for “I Category”, “II Category” and “III Category” analyzed together. ***Figure 91*** and ***Figure 92*** show the indoor air temperature results for the base case (BC) and EC1, EC2, HO, VO, H1, H2, V1, V2, V3 scenarios analyzed for both summer and winter period in east orientation. ***Figure 93*** and ***Figure 94*** show the indoor air temperature results for the base case (BC) and EC1, EC2, HO, VO, H1, H2, V1, V2, V3 scenarios analyzed for both summer and winter period in south orientation. ***Figure 95*** and ***Figure 96*** show the indoor air temperature results for the base case (BC) and EC1, EC2, HO, VO, H1, H2, V1, V2, V3 scenarios analyzed for both summer and winter period in west orientation.

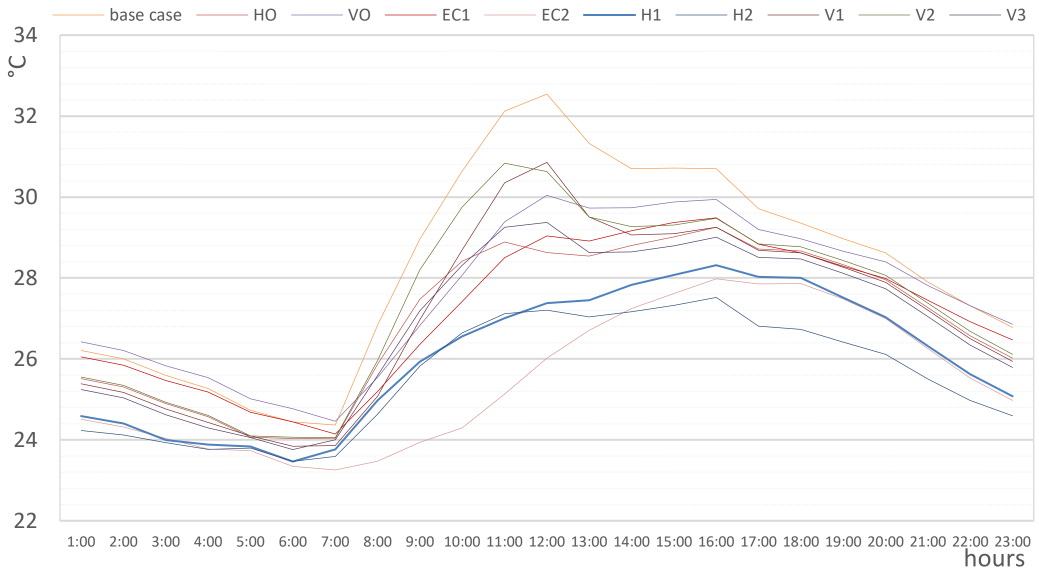

Figure 91. Simulated indoor air temperatures for the base case scenario BC and scenarios of "I Category", "II Category" and "III Category" from the weather file 3rd August in east direction

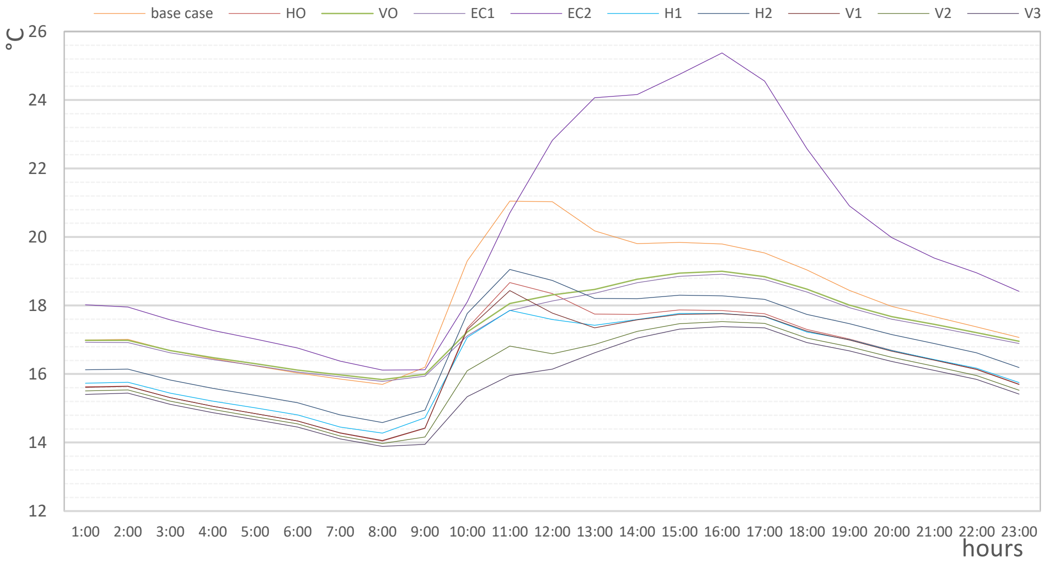

Figure 92. Simulated indoor air temperatures for the base case scenario BC and scenarios of "I Category", "II Category" and "III Category" from the weather file 4th January in east direction

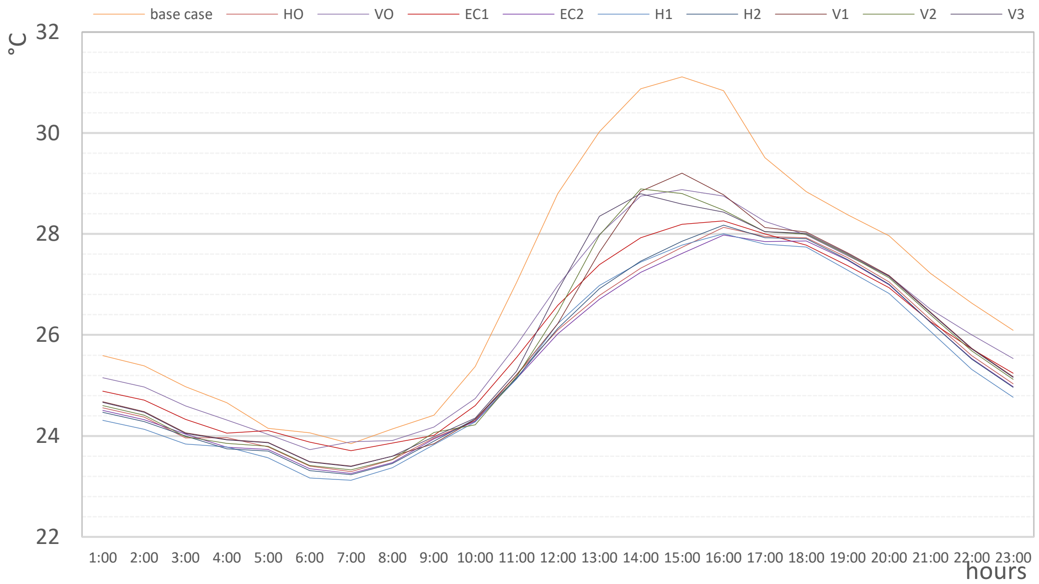

Figure 93. Simulated indoor air temperatures for the base case scenario BC and scenarios of "I Category", "II Category" and "III Category" from the weather file 3rd August in south direction

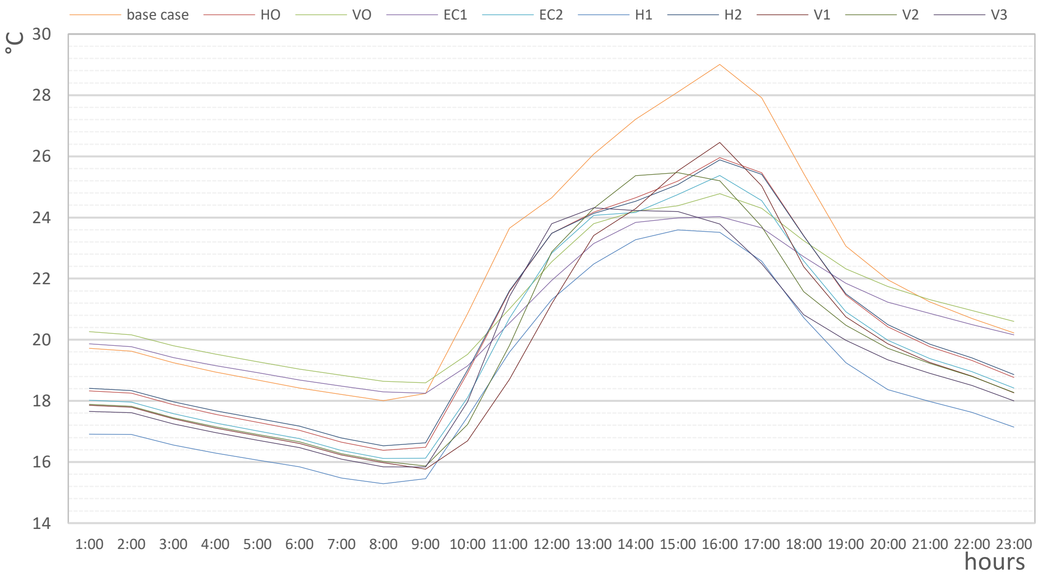

Figure 94. Simulated indoor air temperatures for the base case scenario BC and scenarios of "I Category", "II Category" and "III Category" from the weather file 4th January in south direction

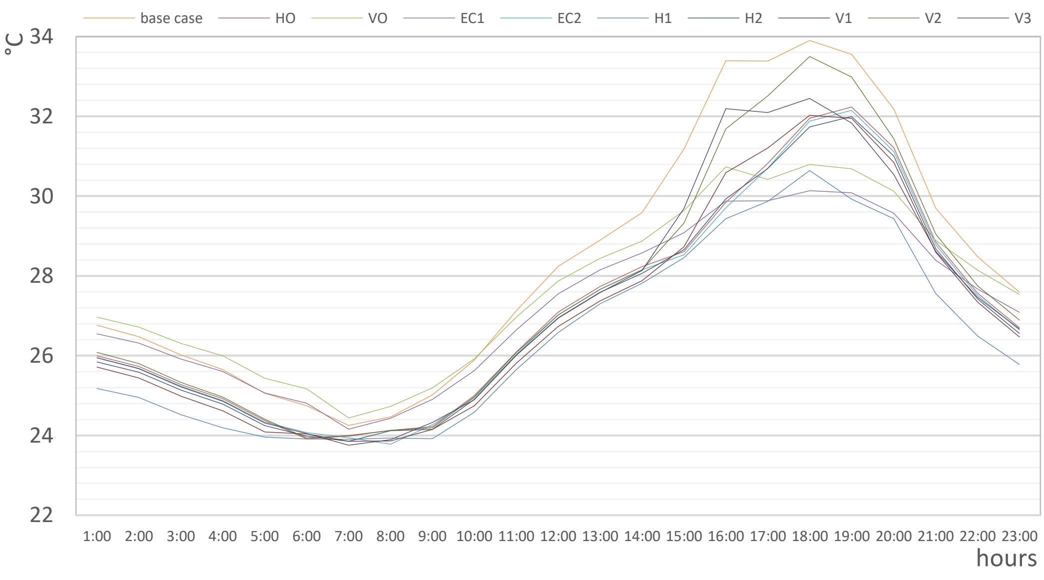

Figure 95. Simulated indoor air temperatures for the base case scenario BC and scenarios of "I Category", "II Category" and "III Category" from the weather file 3rd August in west direction

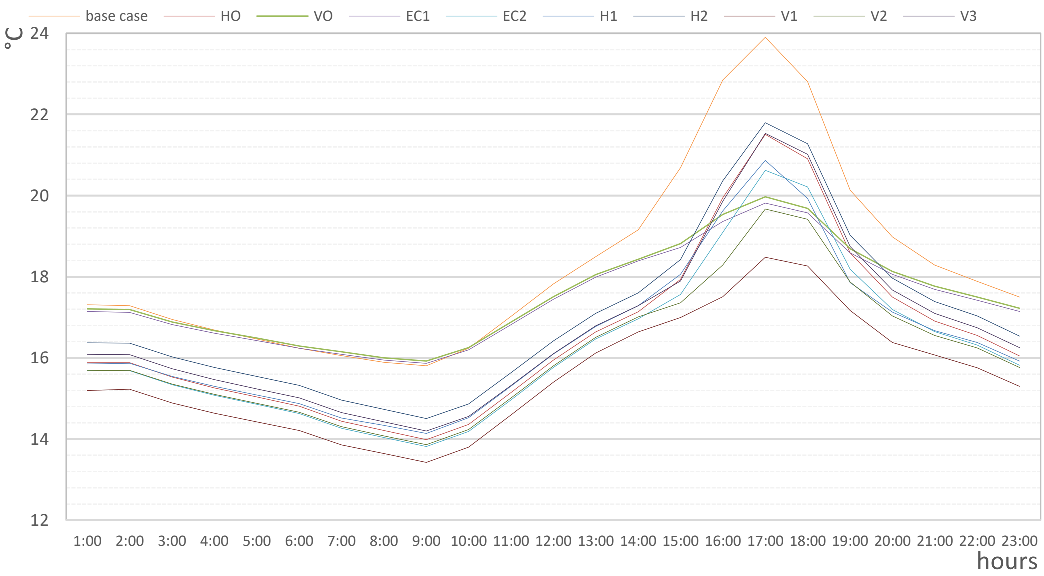

Figure 96. Simulated indoor air temperatures for the base case scenario BC and scenarios of "I Category", "II Category" and "III Category" from the weather file 4th January in west direction

4.3.2 Energy performance

Simulated heating and cooling loads results, for “I Category”, “II Category”, and “III Category” in east, south and west orientation are analyzed. First, the "I Category" results are analyzed, followed by the "II Category" and "III Category" results. Finally, all of the scenarios together for the Almeria climate.

“I Category”: ***Figure 97*** and ***Figure 98*** shows the energy consumption for heating and cooling for the base case (BC) and EC1, EC2, HO and VO scenarios in east orientation. ***Figure 99*** and ***Figure 100*** shows the energy consumption for heating and cooling for the base case (BC) and EC1, EC2, HO and VO scenarios in south orientation. ***Figure 101*** and ***Figure 102*** shows the energy consumption for heating and cooling for the base case (BC) and EC1, EC2, HO and VO scenarios in west orientation.

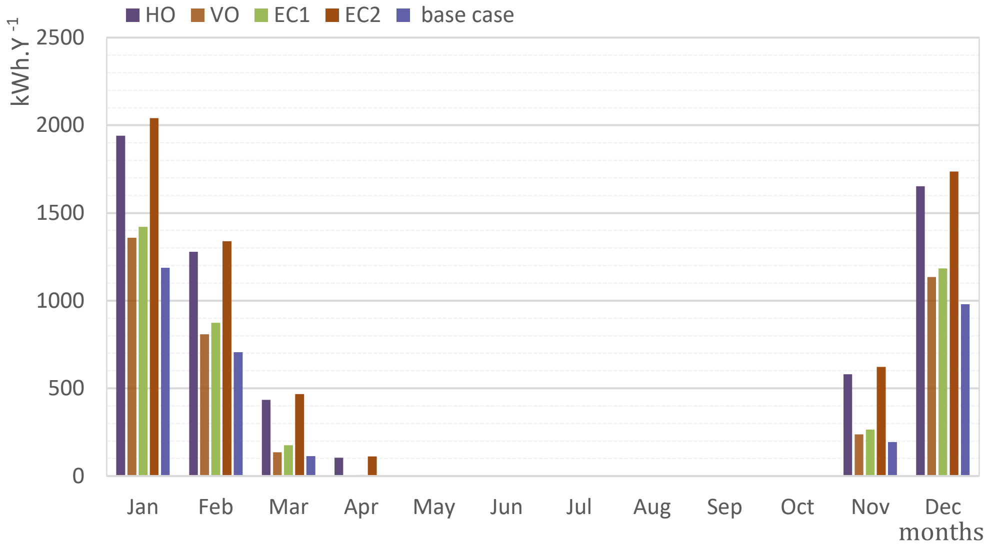

Figure 97. Comparision of simulated heating loads (kWh.Y^{-1}) of the base case scenario BC and scenarios of "I Category": HO, VO, EC1 and EC2 in east orientation

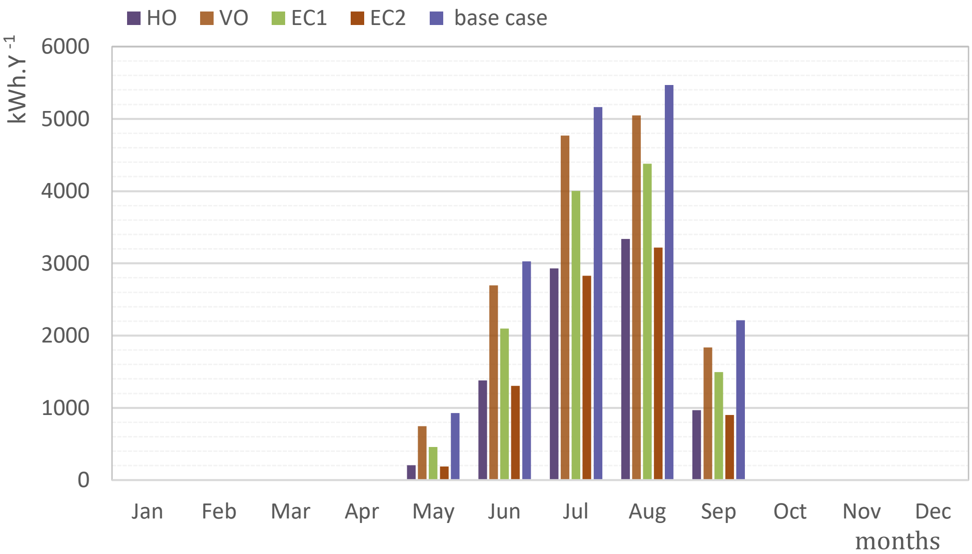

Figure 98. Comparision of simulated cooling loads (kWh.Y^{-1}) of the base case scenario BC and scenarios of "I Category": HO, VO, EC1 and EC2 in east orientation

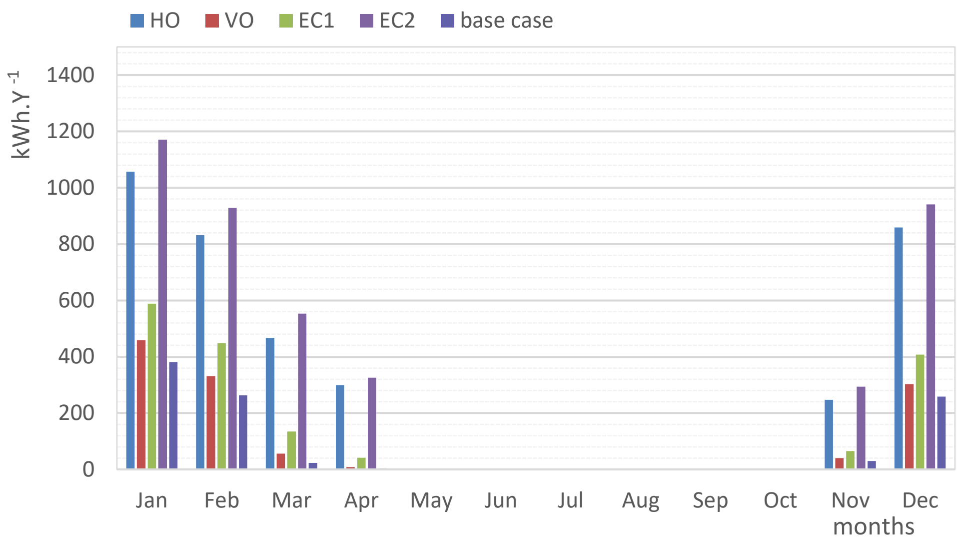

Figure 99. Comparision of simulated heating loads (kWh.Y^{-1}) of the base case scenario BC and scenarios of “I Category”: HO, VO, EC1 and EC2 in south orientation

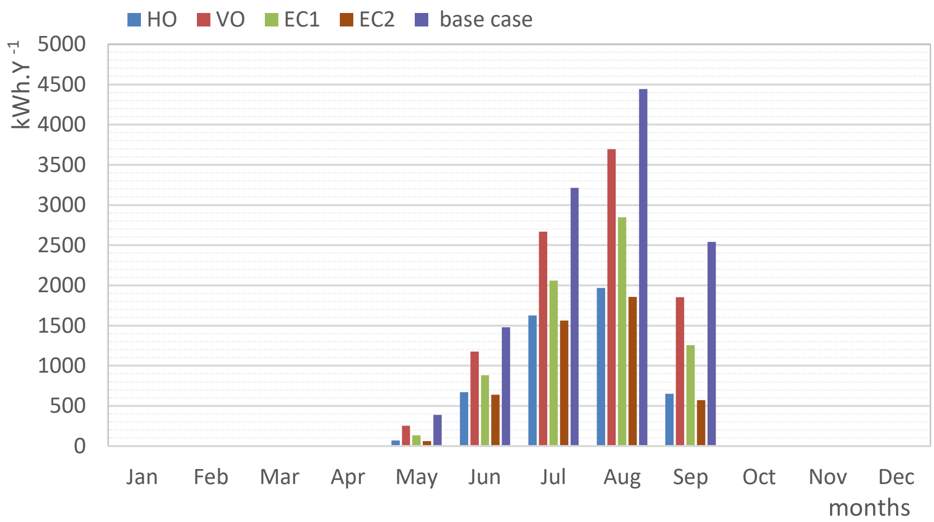

Figure 100. Comparision of simulated cooling loads (kWh.Y^{-1}) of the base case scenario BC and scenarios of “I Category”: HO, VO, EC1 and EC2 in south orientation

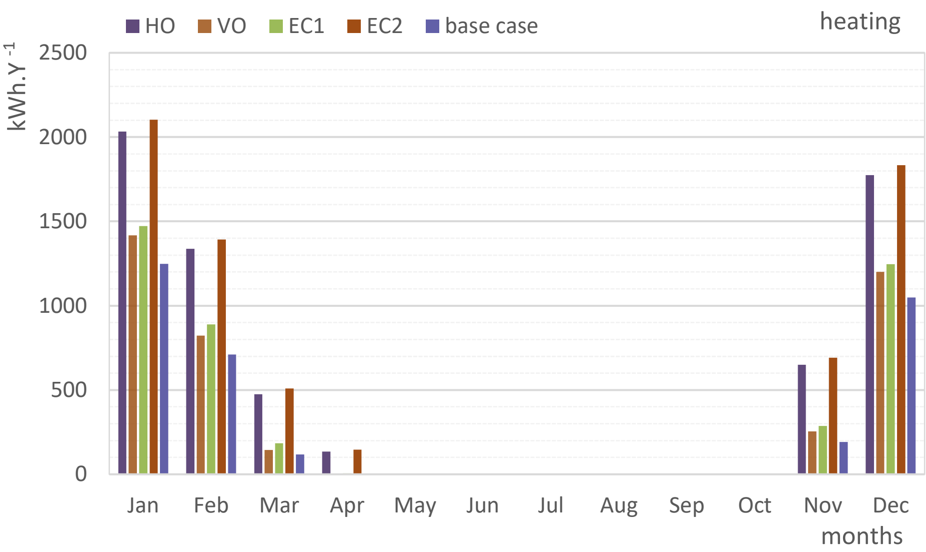

Figure 101. Comparision of simulated heating loads (kWh.Y^{-1}) of the base case scenario BC and scenarios of "I Category": HO, VO, EC1 and EC2 in west orientation

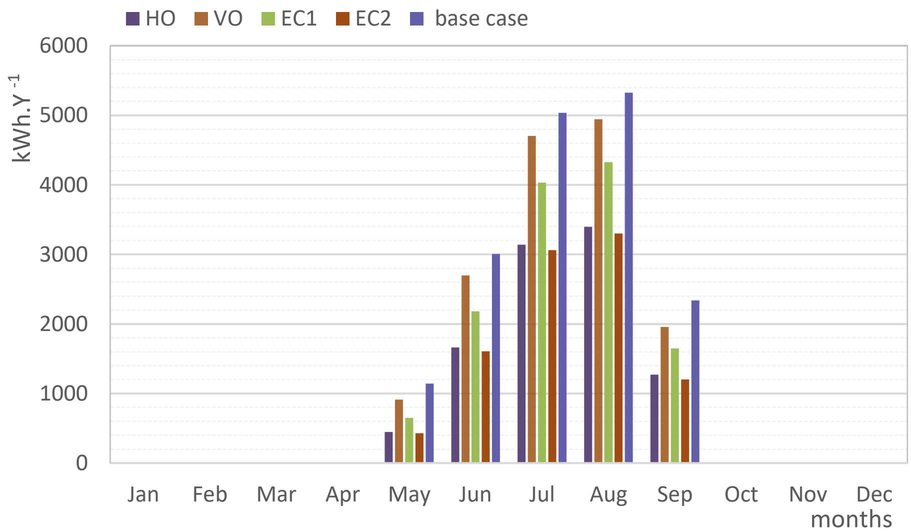

Figure 102. Comparision of simulated cooling loads (kWh.Y^{-1}) of the base case scenario BC and scenarios of "I Category": HO, VO, EC1 and EC2 in west orientation

"II Category": ***Figure 103*** and ***Figure 104*** shows the energy consumption for heating and cooling for the base case (BC) and H1, H2 scenarios in east orientation. ***Figure 105*** and ***Figure 106*** shows the energy consumption for heating and cooling for the base case (BC) and H1, H2 scenarios in south orientation. ***Figure 107*** and ***Figure 108*** shows the energy consumption for heating and cooling for the base case (BC) and H1, H2 scenarios in west orientation.

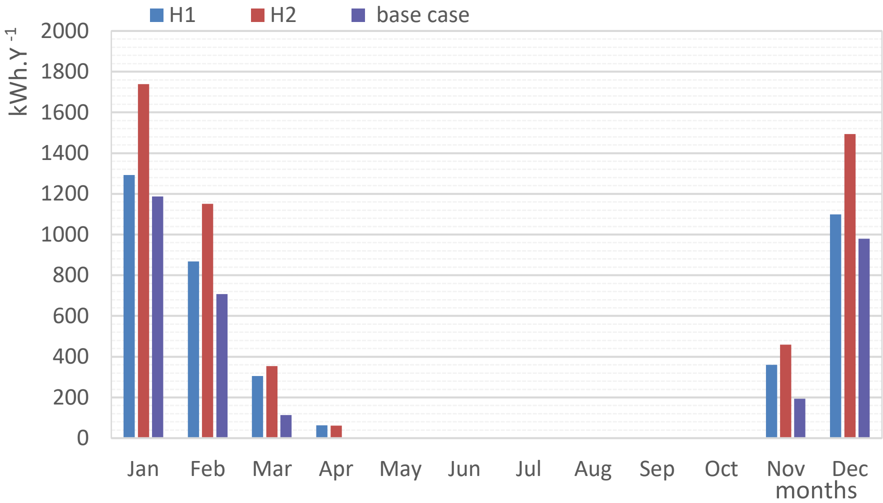

Figure 103. Comparision of simulated heating loads (kWh.Y^{-1}) of the base case scenario BC and scenarios of "II Category": H1, and H2 in east orientation

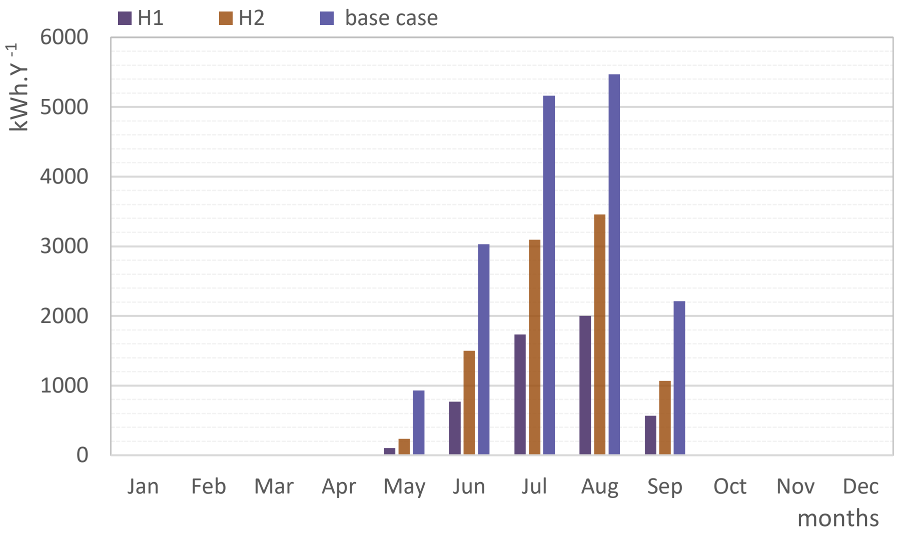

Figure 104. Comparision of simulated cooling loads (kWh.Y^{-1}) of the base case scenario BC and scenarios of "II Category": H1, and H2 in east orientation

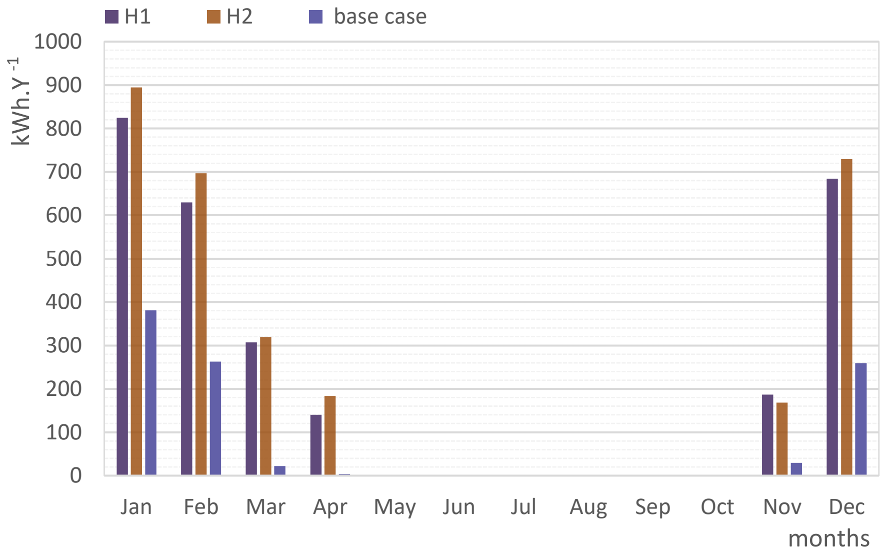

Figure 105. Comparision of simulated heating loads (kWh.Y^{-1}) of the base case scenario BC and scenarios of "II Category": H1, and H2 in south orientation

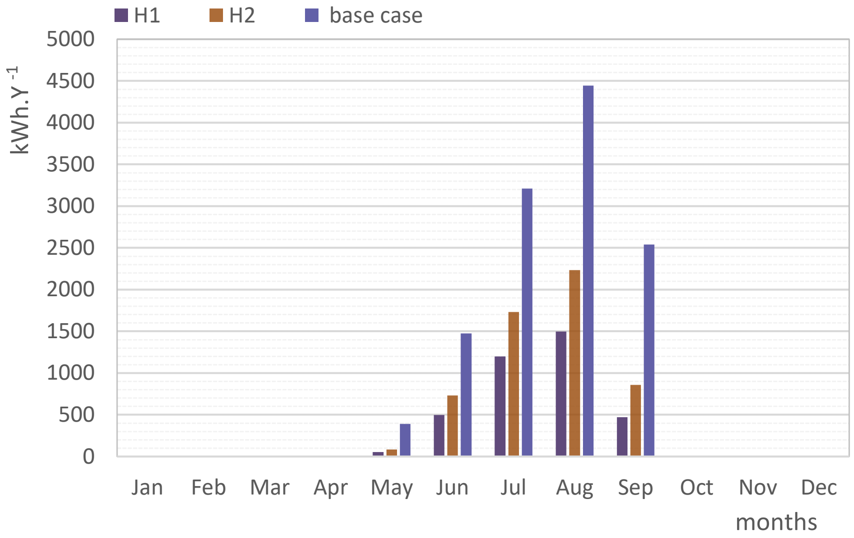

Figure 106. Comparision of simulated cooling loads (kWh.Y^{-1}) of the base case scenario BC and scenarios of “II Category”: H1, and H2 in south orientation

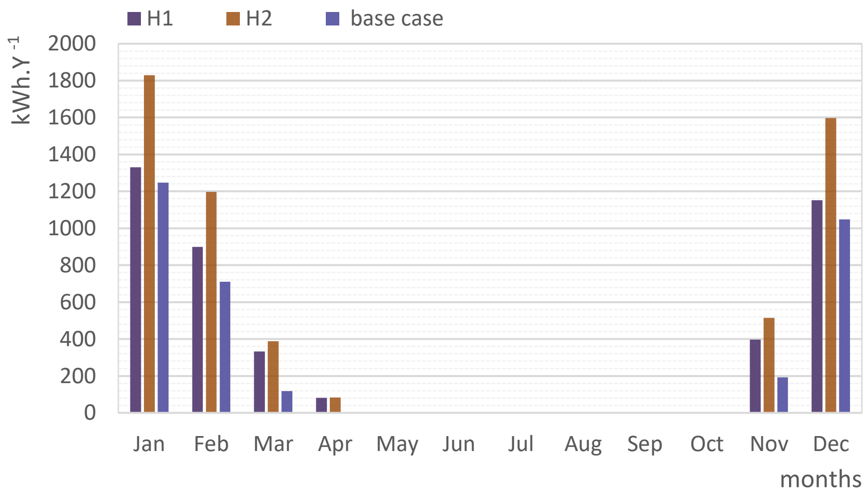

Figure 107. Comparision of simulated heating loads (kWh.Y^{-1}) of the base case scenario BC and scenarios of “II Category”: H1, and H2 in west orientation

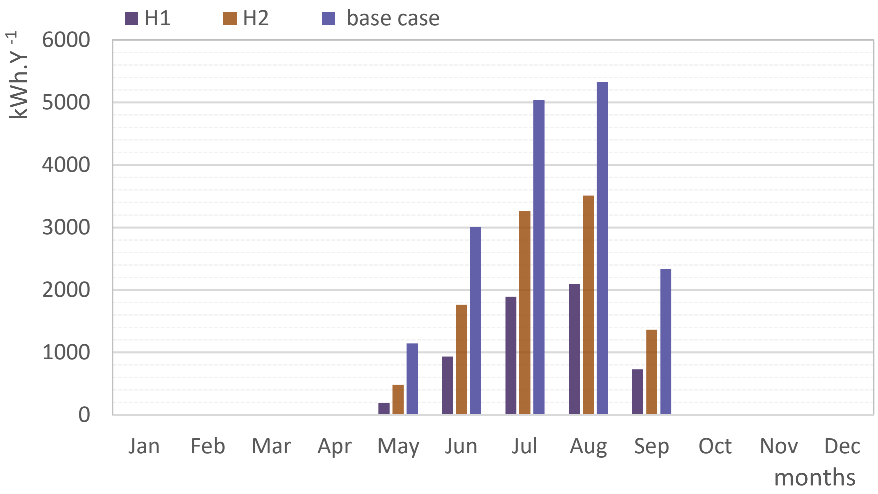

Figure 108. Comparision of simulated cooling loads (kWh.Y^{-1}) of the base case scenario BC and scenarios of "II Category": H1, and H2 in west orientation

"III Category": ***Figure 109*** and ***Figure 110*** shows the energy consumption for heating and cooling for the base case (BC) and V1, V2, V3 scenarios in east orientation. ***Figure 111*** and ***Figure 112*** shows the energy consumption for heating and cooling for the base case (BC) and V1, V2, V3 scenarios in south orientation. ***Figure 113*** and ***Figure 114*** shows the energy consumption for heating and cooling for the base case (BC) and V1, V2, V3 scenarios in west orientation.

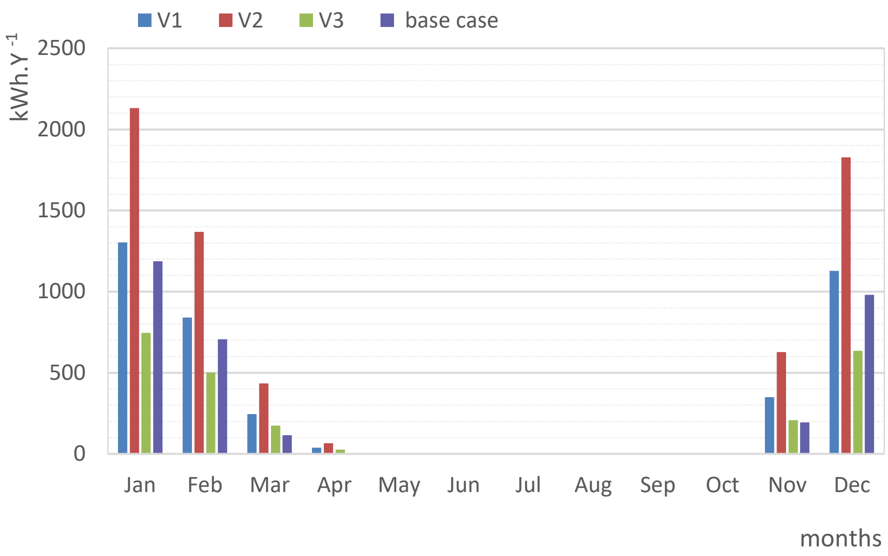

Figure 109. Comparision of simulated heating loads (kWh.Y^{-1}) of the base case scenario BC and scenarios of "III Category": V1, V2 and V3 in east orientation

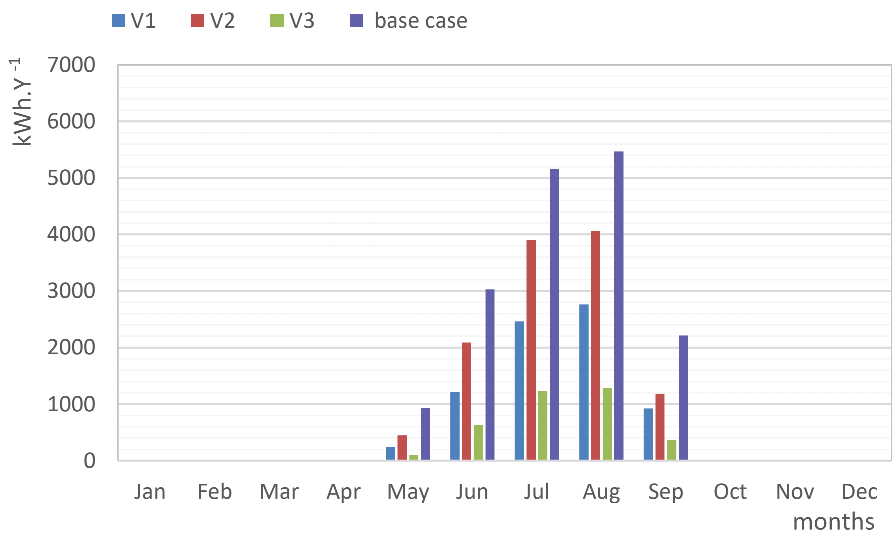

Figure 110. Comparision of simulated cooling loads (kWh.Y^{-1}) of the base case scenario BC and scenarios of "III Category": V1, V2 and V3 in east orientation

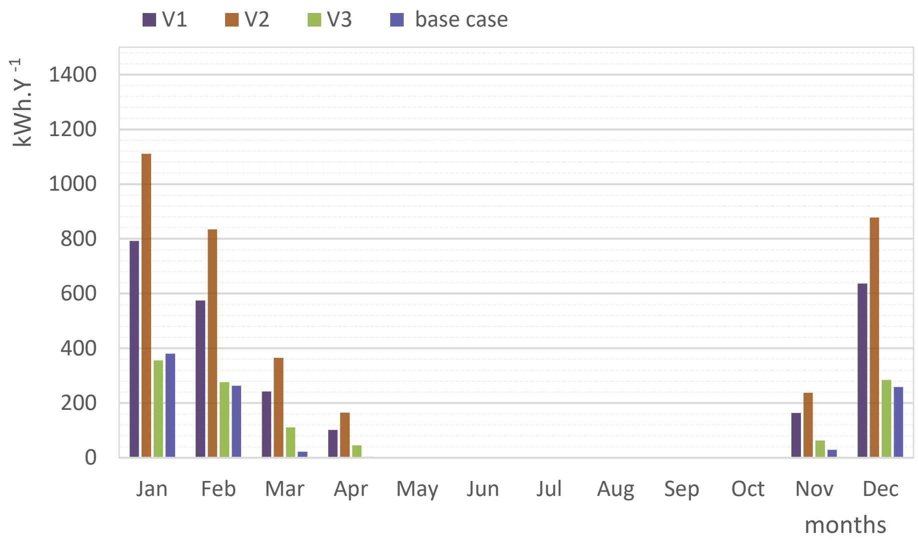

Figure 111. Comparision of simulated heating loads (kWh.Y^{-1}) of the base case scenario BC and scenarios of "III Category": V1, V2 and V3 in south orientation

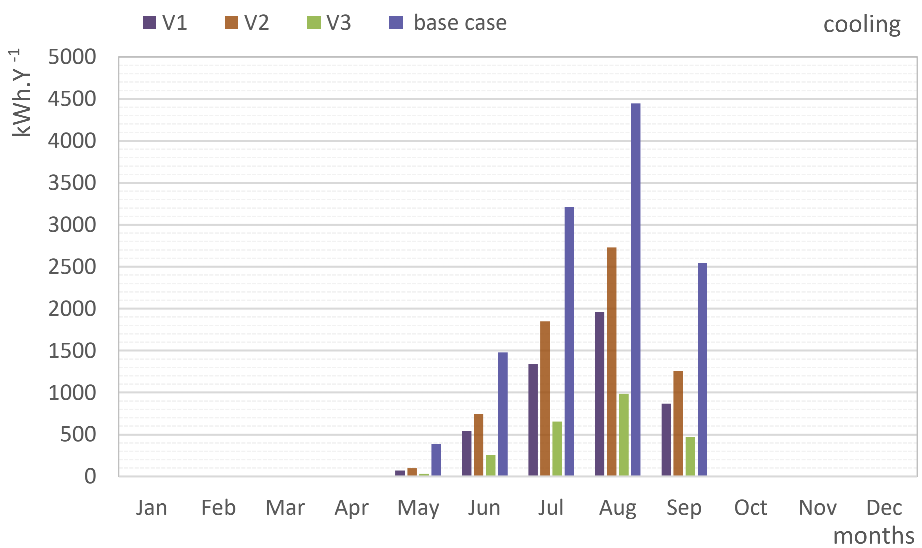

Figure 112. Comparision of simulated cooling loads (kWh.Y^{-1}) of the base case scenario BC and scenarios of "III Category": V1, V2 and V3 in south orientation

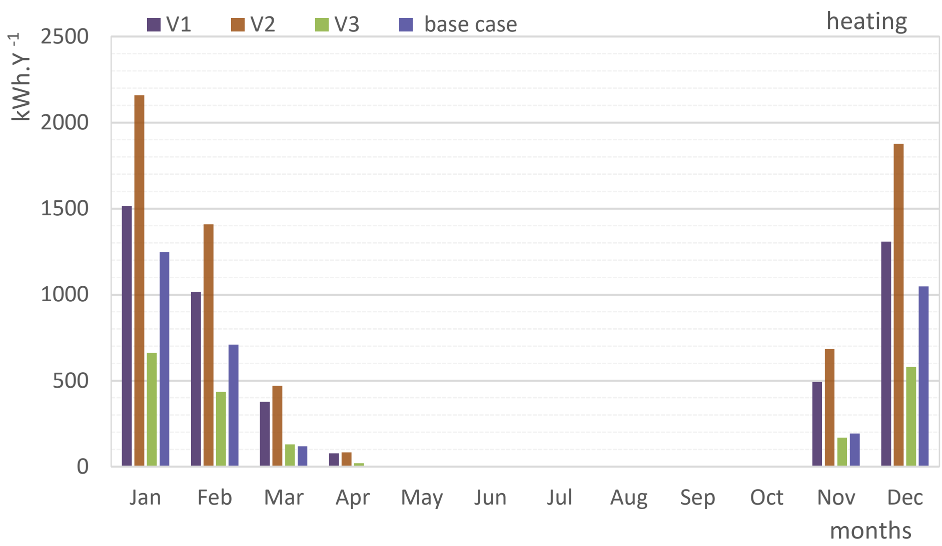

Figure 113. Comparision of simulated heating loads (kWh.Y^{-1}) of the base case scenario BC and scenarios of “III Category”: V1, V2 and V3 in west orientation

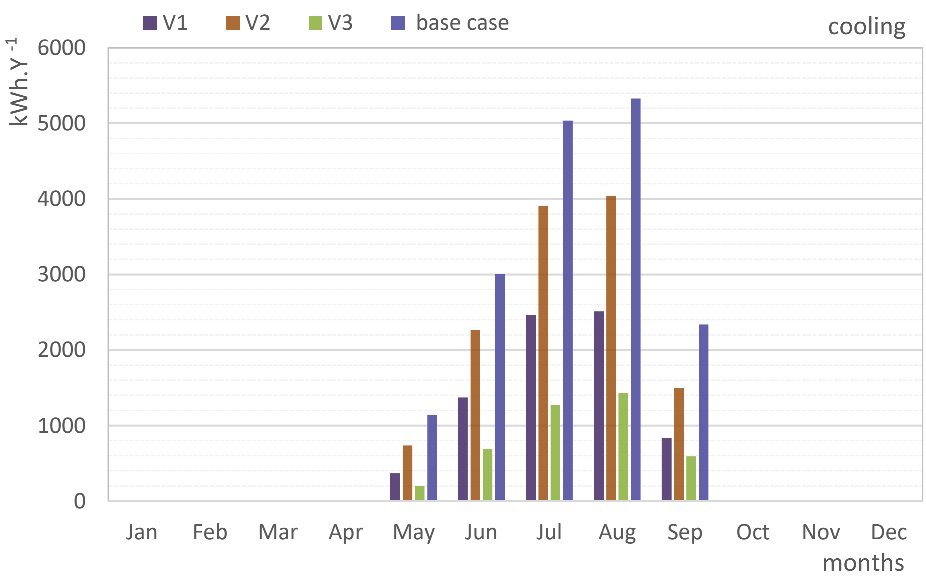

Figure 114. Comparision of simulated cooling loads (kWh.Y^{-1}) of the base case scenario BC and scenarios of “III Category”: V1, V2 and V3 in west orientation

Energy consumption for heating and cooling loads for “I Category”, “II Category” and “III Category” are analyzed together. ***Figure 115*** and ***Figure 116*** show heating and cooling loads results for the base case (BC) and EC1, EC2, HO, VO, H1, H2, V1, V2, V3 scenarios in east orientation. ***Figure 117*** and ***Figure 118*** show heating and cooling loads results for the base case (BC) and EC1, EC2, HO, VO, H1, H2, V1, V2, V3 scenarios in south orientation. ***Figure 119*** and ***Figure 120*** show heating and cooling loads results for the base case (BC) and EC1, EC2, HO, VO, H1, H2, V1, V2, V3 scenarios in west orientation.

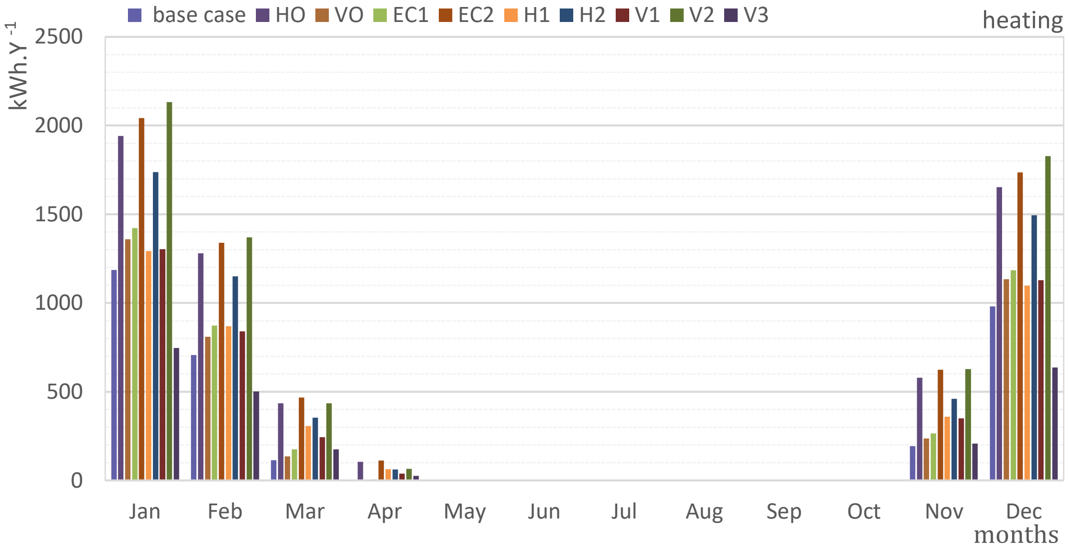

Figure 115. Comparision of simulated heating loads (kWh.Y^{-1}) of the base case scenario BC and scenarios of “I Category”, “II Category” and “III Category” in east orientation

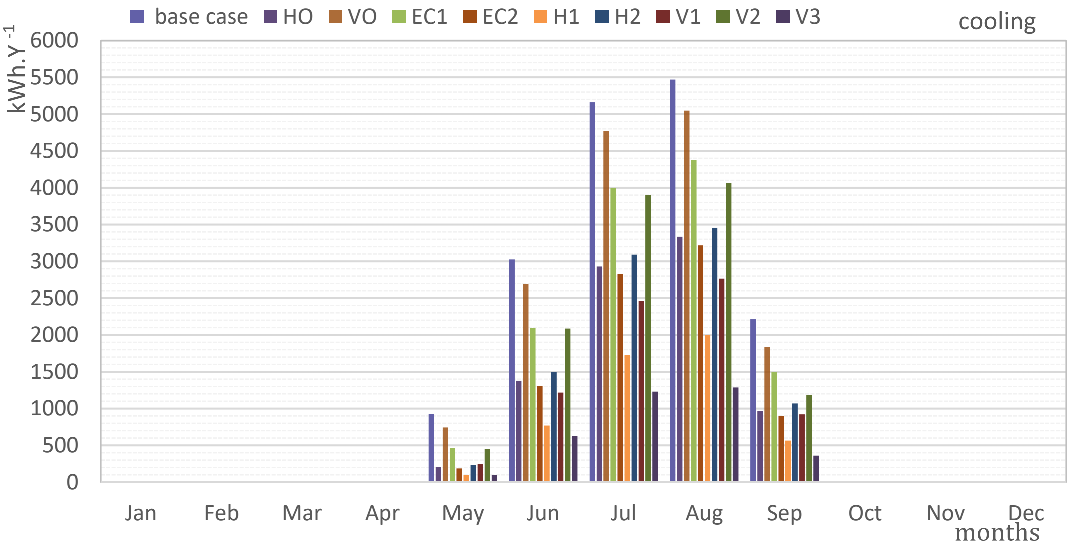

Figure 116. Comparision of simulated cooling loads (kWh.Y^{-1}) of the base case scenario BC and scenarios of "I Category", "II Category" and "III Category" in east orientation

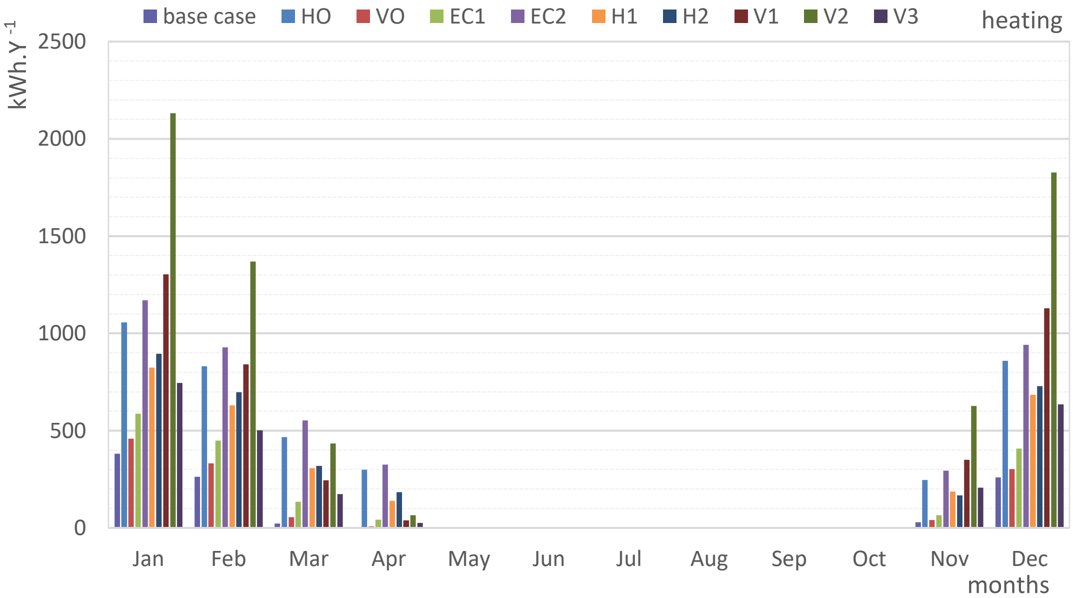

Figure 117. Comparision of simulated heating loads (kWh.Y^{-1}) of the base case scenario BC and scenarios of "I Category", "II Category" and "III Category" in south orientation

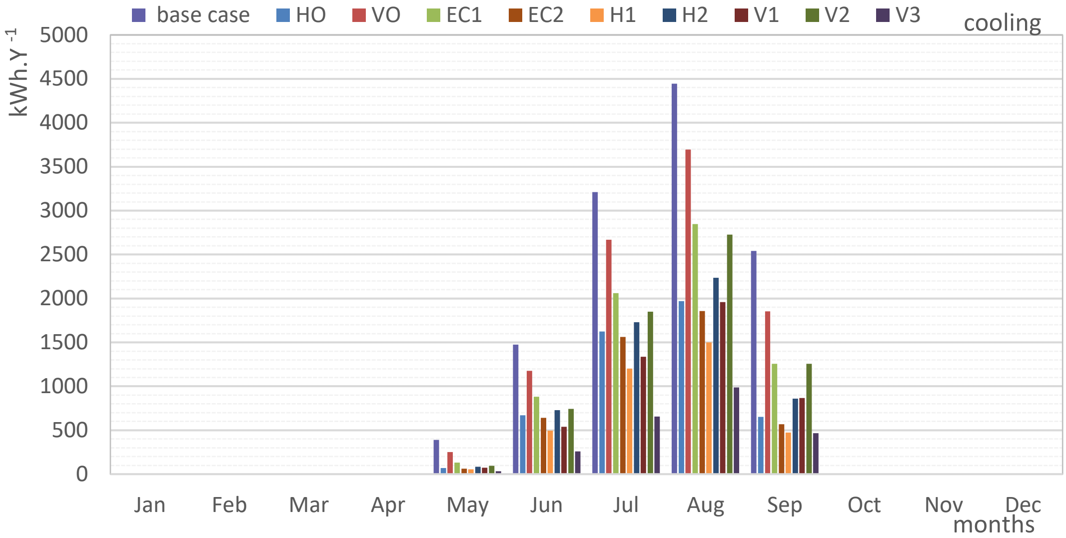

Figure 118. Comparision of simulated cooling loads (kWh.Y^{-1}) of the base case scenario BC and scenarios of “I Category”, “II Category” and “III Category” in south orientation

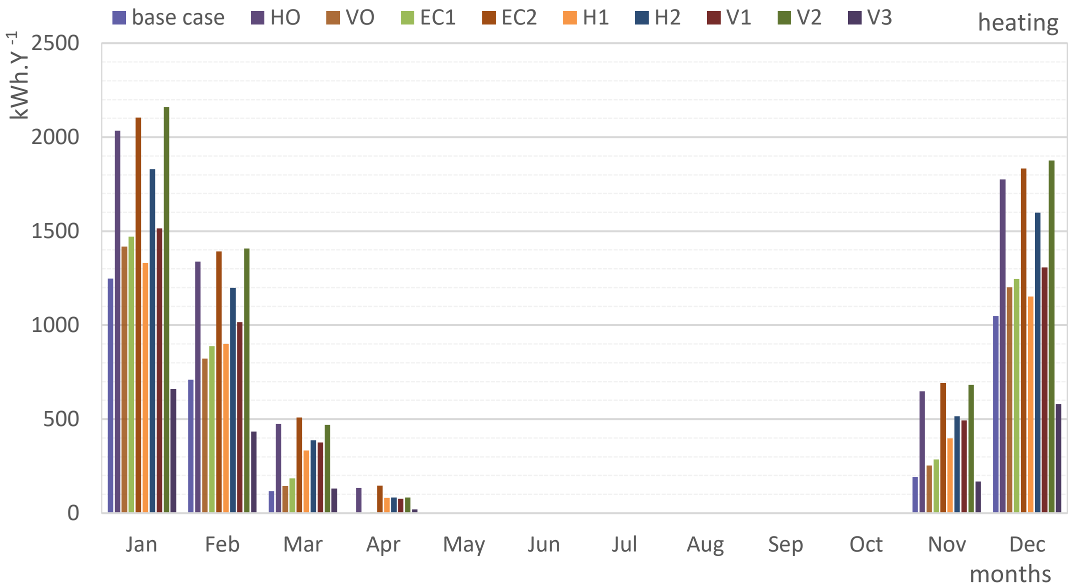

Figure 119. Comparision of simulated heating loads (kWh.Y^{-1}) of the base case scenario BC and scenarios of “I Category”, “II Category” and “III Category” in west orientation

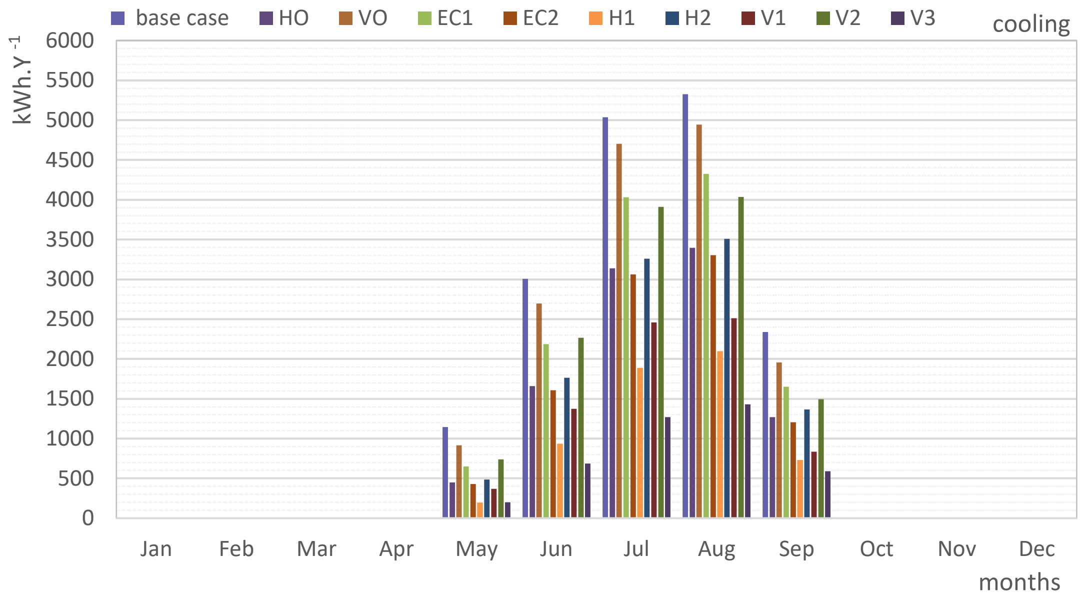

Figure 120. Comparision of simulated cooling loads (kWh.Y^{-1}) of the base case scenario BC and scenarios of "I Category", "II Category" and "III Category" in west orientation

4.4 Antalya, Turkey

4.4.1 Indoor air temperature

Indoor air temperature results for "I Category", "II Category", and "III Category" in east, south and west orientation are analyzed by picking a typical summer and winter day. Beginning with the analysis of the "I Category's", followed by the "II Category" and "III Category" results. In conclusion, all of the scenarios are also compared for the Antalya climate.

"I Category": ***Figure 121*** and ***Figure 122*** show the indoor air temperature results for the base case (BC) and EC1, EC2, HO and VO scenarios analyzed for both summer and winter period in east orientation. ***Figure 123*** and ***Figure 124*** show the indoor air temperature results for the base case (BC) and EC1, EC2, HO VO scenarios analyzed for both summer and winter period in south orientation. ***Figure***

125 and ***Figure 126*** show the indoor air temperature results for the base case (BC) and EC1, EC2, HO and VO scenarios analyzed for both summer and winter period in west orientation.

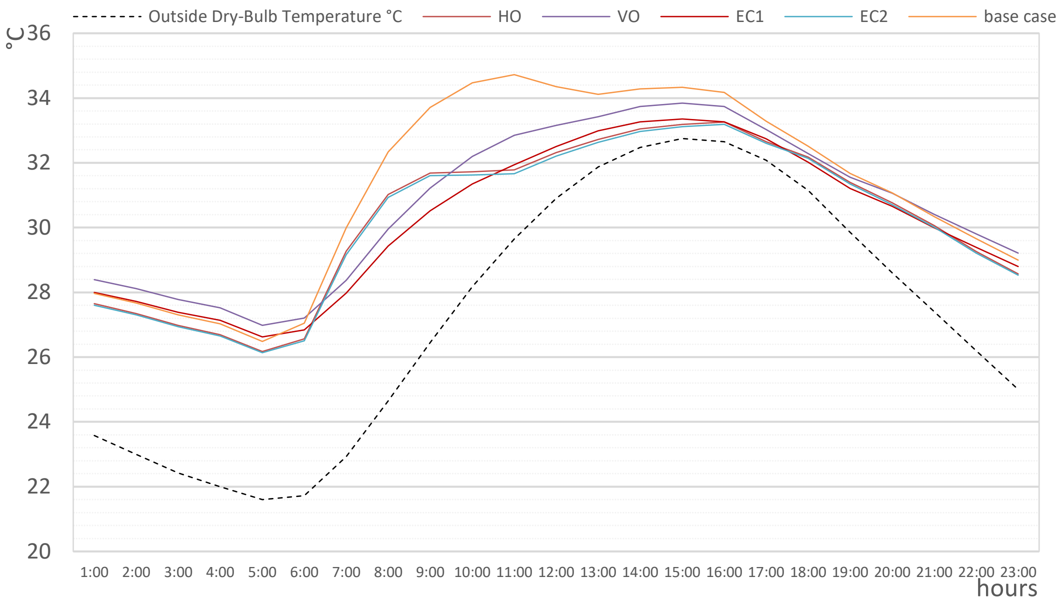

Figure 121. Simulated indoor air temperatures for the base case scenario BC and scenarios of “I Category”: HO, VO, EC1 and EC2, together with the dry-bulb temperature from the weather file 3rd August in east direction

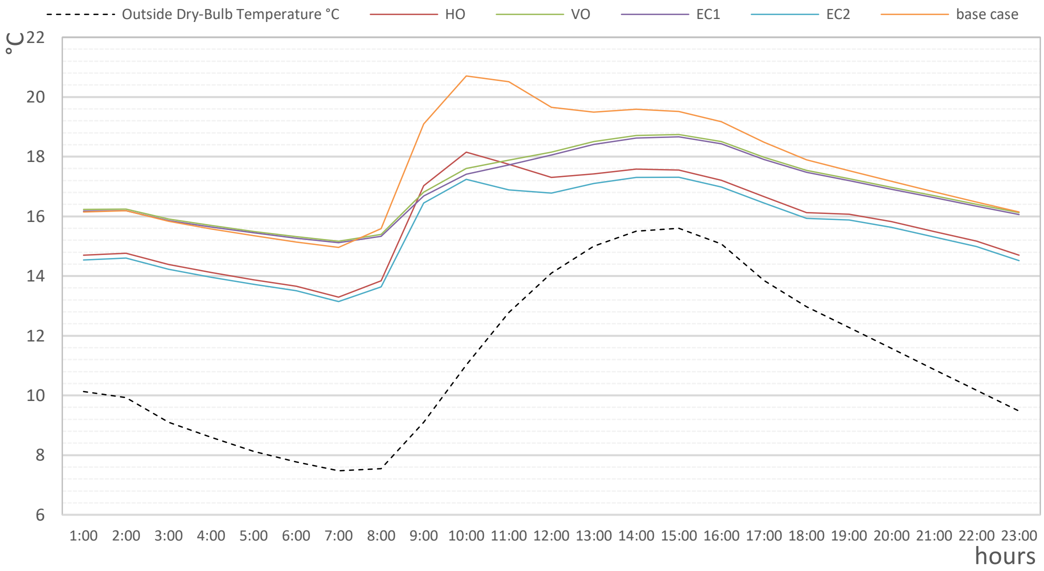

Figure 122. Simulated indoor air temperatures for the base case scenario BC and scenarios of "I Category": HO, VO, EC1 and EC2, together with the dry-bulb temperature from the weather file 4th January in east direction

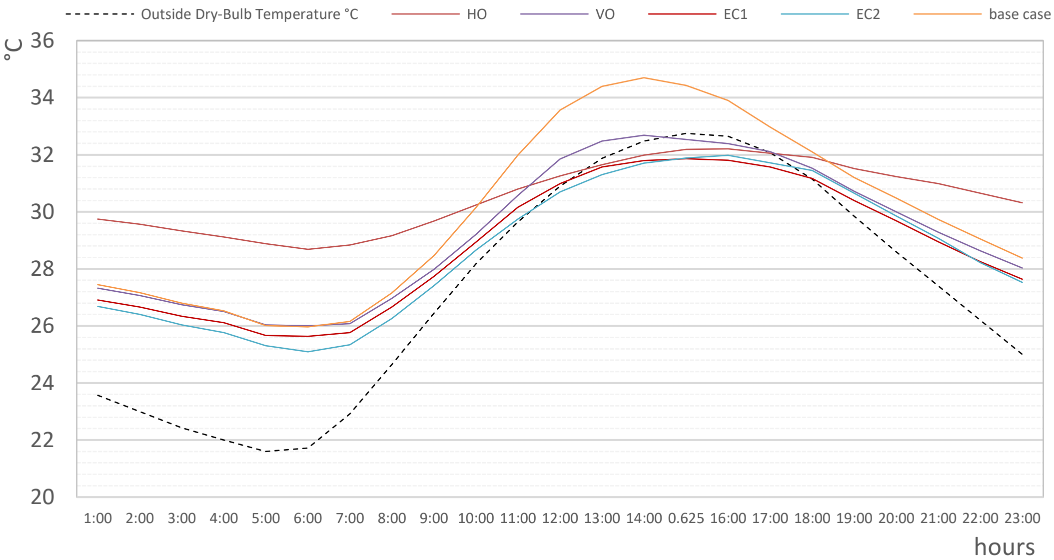

Figure 123. Simulated indoor air temperatures for the base case scenario BC and scenarios of "I Category": HO, VO, EC1 and EC2, together with the dry-bulb temperature from the weather file 3rd August in south direction

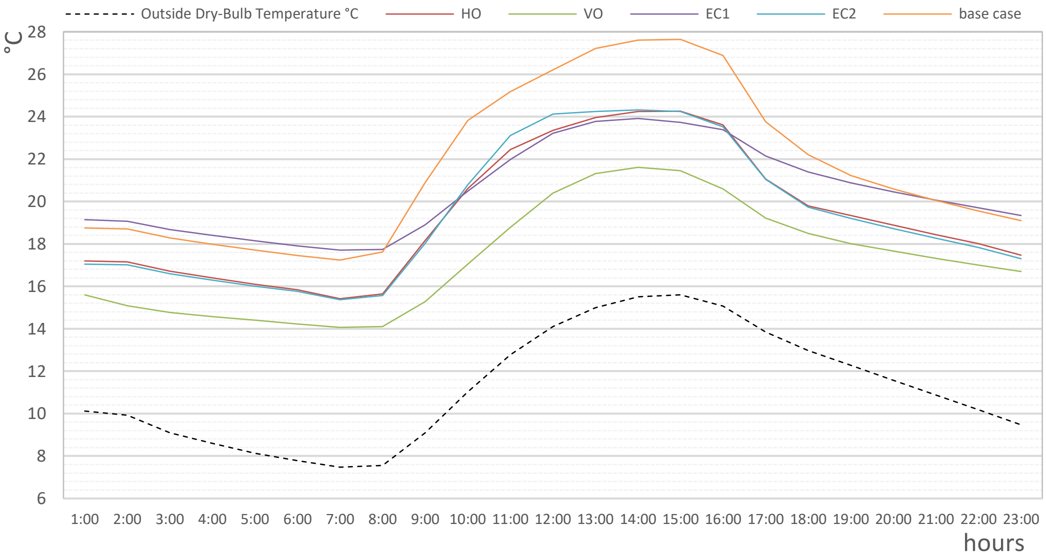

Figure 124. Simulated indoor air temperatures for the base case scenario BC and scenarios of "I Category": HO, VO, EC1 and EC2, together with the dry-bulb temperature from the weather file 4th January in south direction

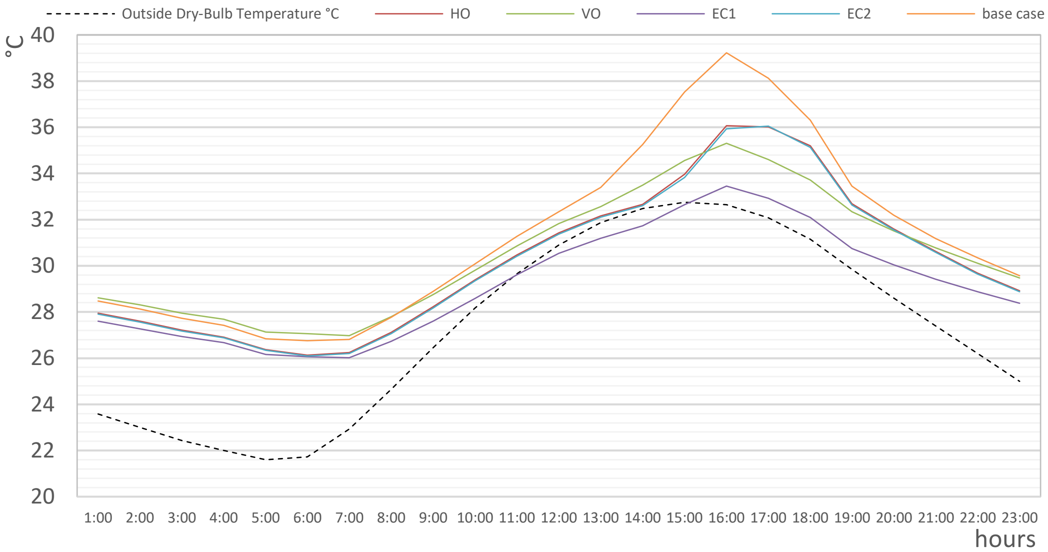

Figure 125. Simulated indoor air temperatures for the base case scenario BC and scenarios of "I Category": HO, VO, EC1 and EC2, together with the dry-bulb temperature from the weather file 3rd August in west direction

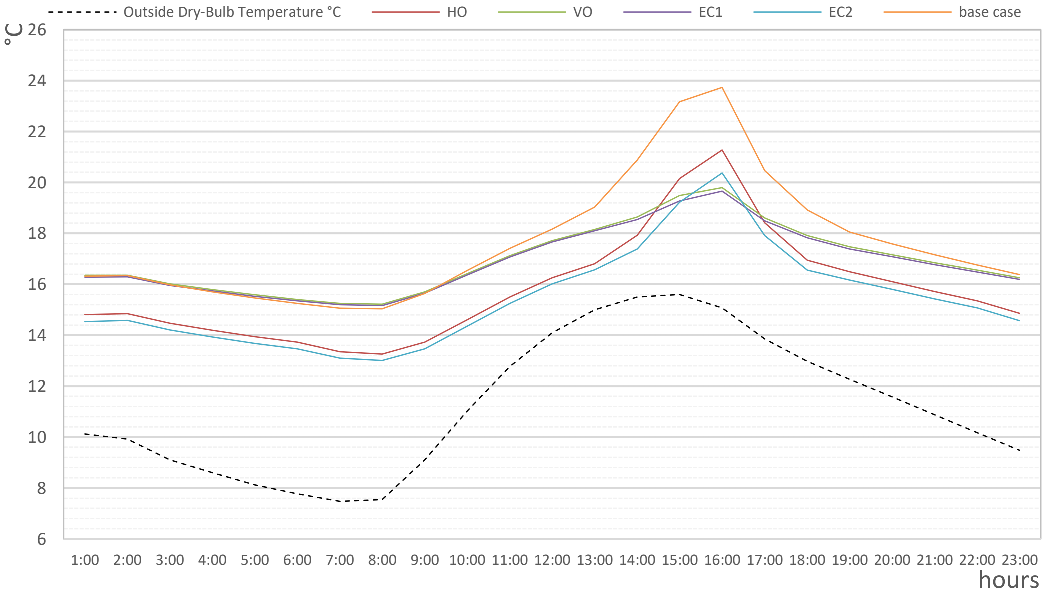

Figure 126. Simulated indoor air temperatures for the base case scenario BC and scenarios of "I Category": HO, VO, EC1 and EC2, together with the dry-bulb temperature from the weather file 4th January in west direction

"II Category": ***Figure 127*** and ***Figure 128*** show the indoor air temperature results for the base case (BC) and H1, H2 scenarios analyzed for both summer and winter period in east orientation. ***Figure 129*** and ***Figure 130*** show the indoor air temperature results for the base case (BC) and H1, H2 scenarios analyzed for both summer and winter period in south orientation. ***Figure 131*** and ***Figure 132*** show the indoor air temperature results for the base case (BC) and H1, H2 scenarios analyzed for both summer and winter period in west orientation.

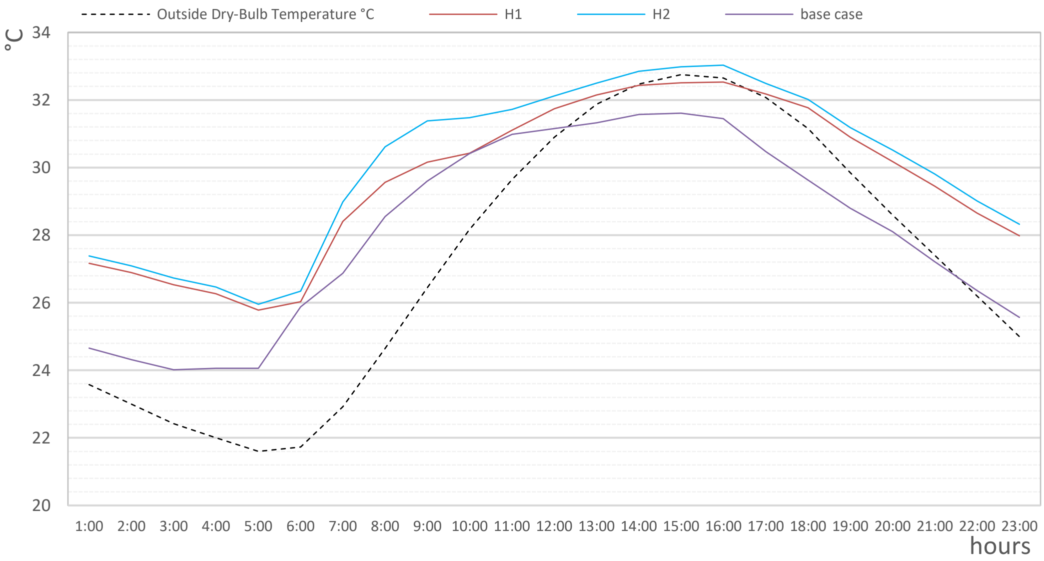

Figure 127. Simulated indoor air temperatures for the base case scenario BC and scenarios of “II Category”: H1, and H2, together with the dry-bulb temperature from the weather file 3rd August in east direction

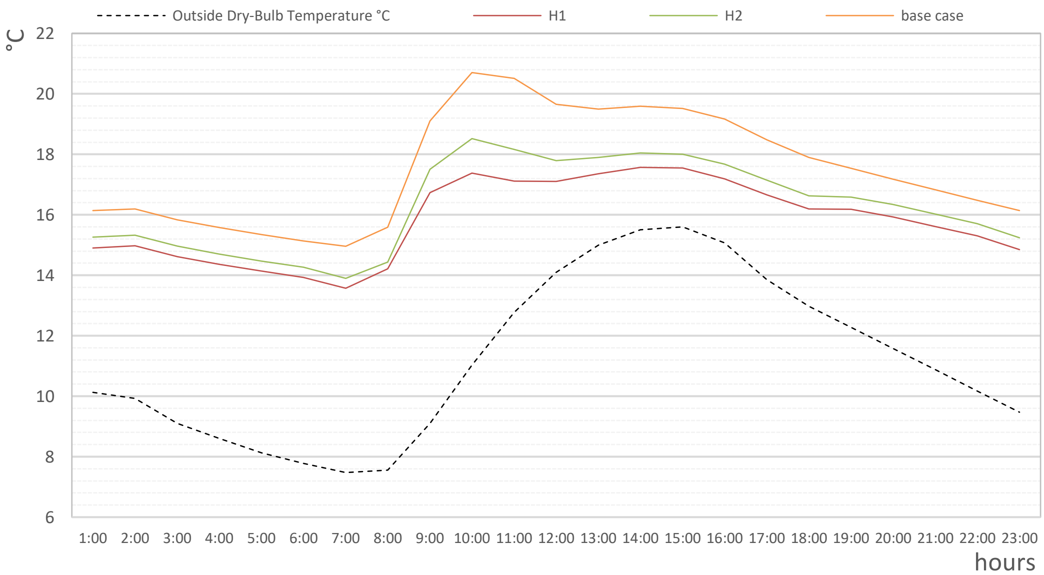

Figure 128. Simulated indoor air temperatures for the base case scenario BC and scenarios of “II Category”: H1, and H2, together with the dry-bulb temperature from the weather file 4th January in east direction

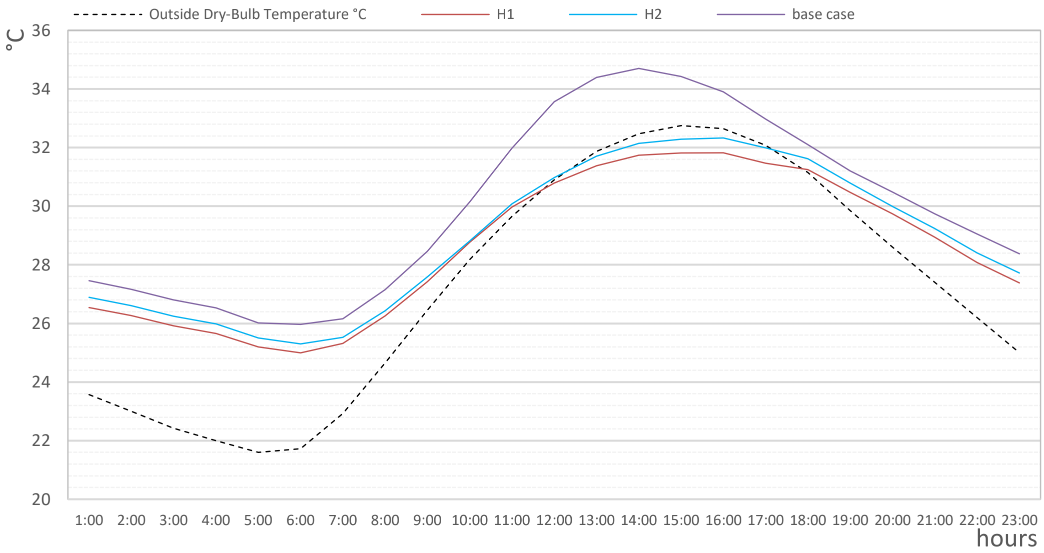

Figure 129. Simulated indoor air temperatures for the base case scenario BC and scenarios of "II Category": H1, and H2, together with the dry-bulb temperature from the weather file 3rd August in south direction

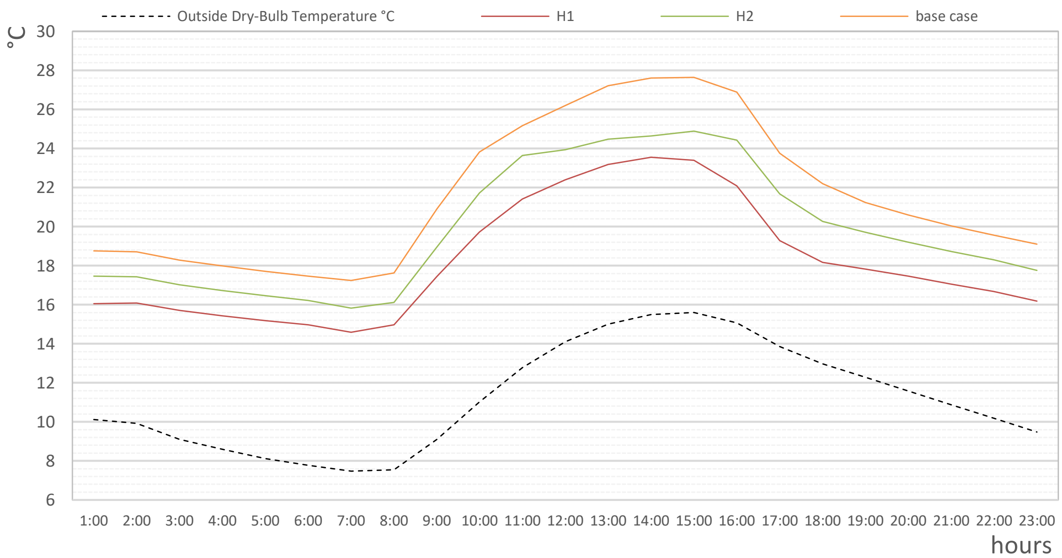

Figure 130. Simulated indoor air temperatures for the base case scenario BC and scenarios of "II Category": H1, and H2, together with the dry-bulb temperature from the weather file 4th January in south direction

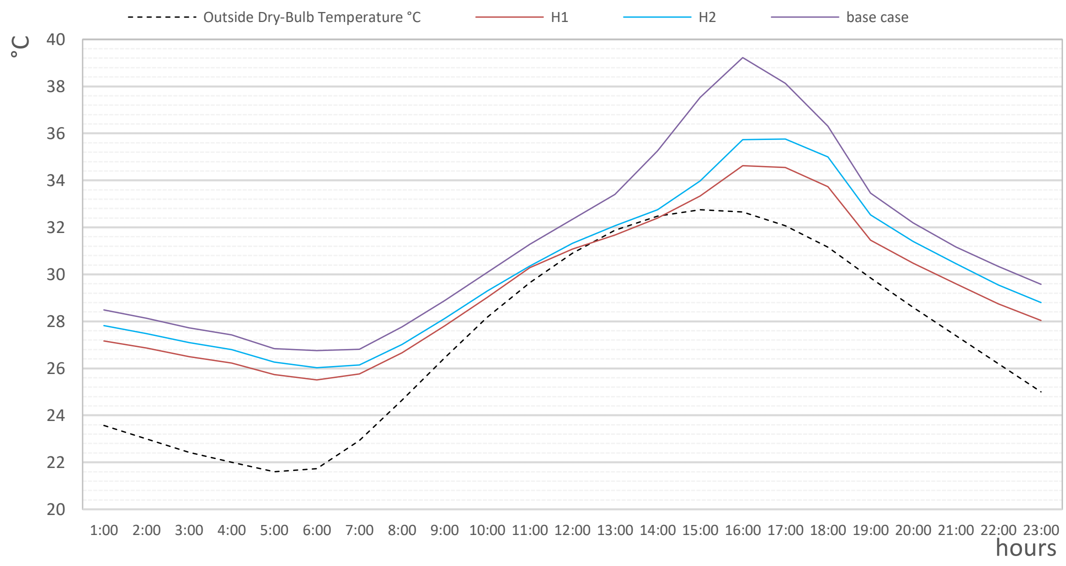

Figure 131. Simulated indoor air temperatures for the base case scenario BC and scenarios of "II Category": H1, and H2, together with the dry-bulb temperature from the weather file 3rd August in west direction

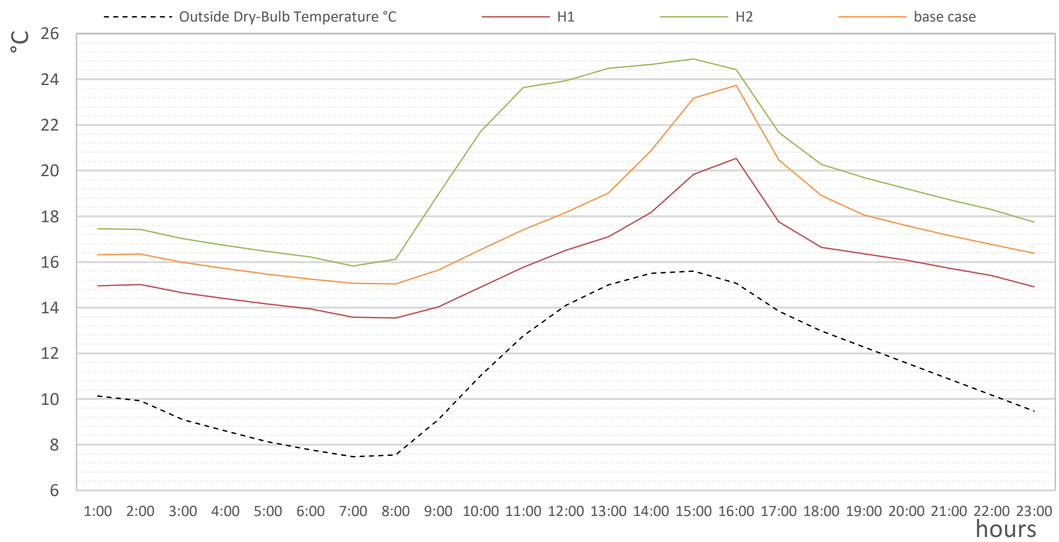

Figure 132. Simulated indoor air temperatures for the base case scenario BC and scenarios of "II Category": H1, and H2, together with the dry-bulb temperature from the weather file 4th January in west direction

“III Category”: ***Figure 133*** and ***Figure 134*** show the indoor air temperature results for the base case (BC) and V1, V2, V3 scenarios analyzed for both summer and winter period in east orientation. ***Figure 135*** and ***Figure 136*** show the indoor air temperature results for the base case (BC) and V1, V2, V3 scenarios analyzed for both summer and winter period in south orientation. ***Figure 137*** and ***Figure 138*** show the indoor air temperature results for the base case (BC) and V1, V2, V3 scenarios analyzed for both summer and winter period in west orientation.

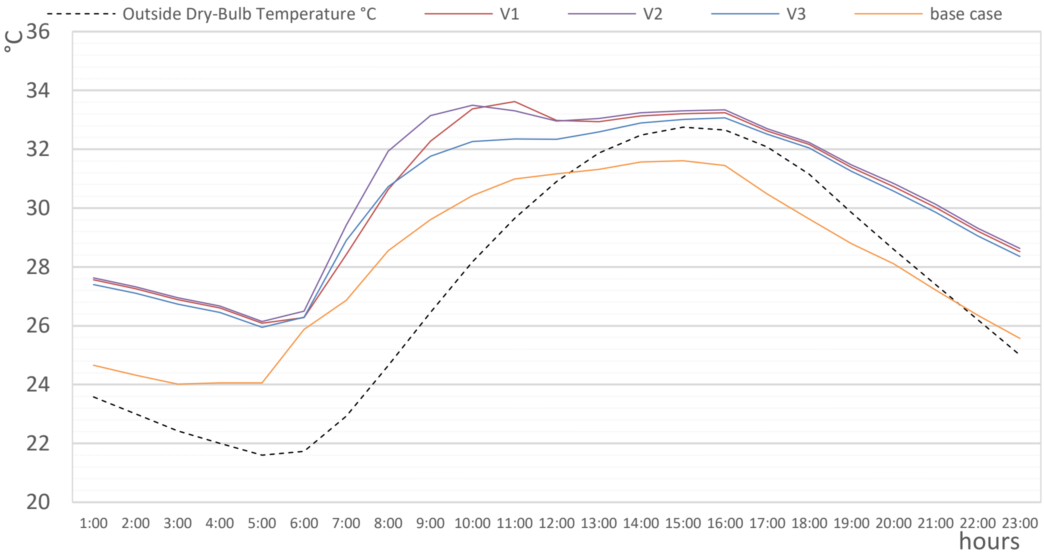

Figure 133. Simulated indoor air temperatures for the base case scenario BC and scenarios of “III Category”: V1, V2 and V3 together with the dry-bulb temperature from the weather file 3rd August in east direction

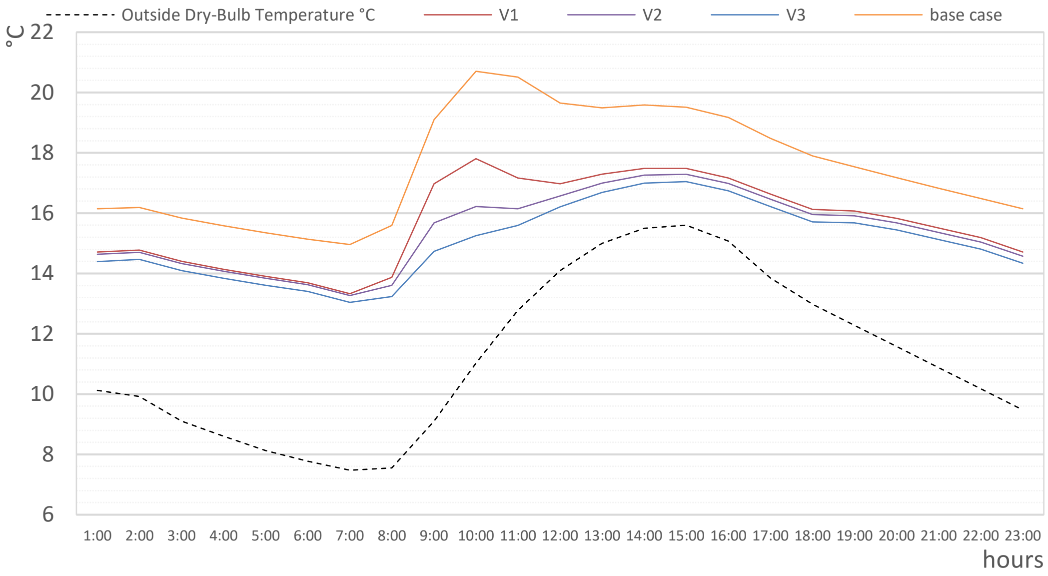

Figure 134. Simulated indoor air temperatures for the base case scenario BC and scenarios of "III Category": V1, V2 and V3 together with the dry-bulb temperature from the weather file 4th January in east direction

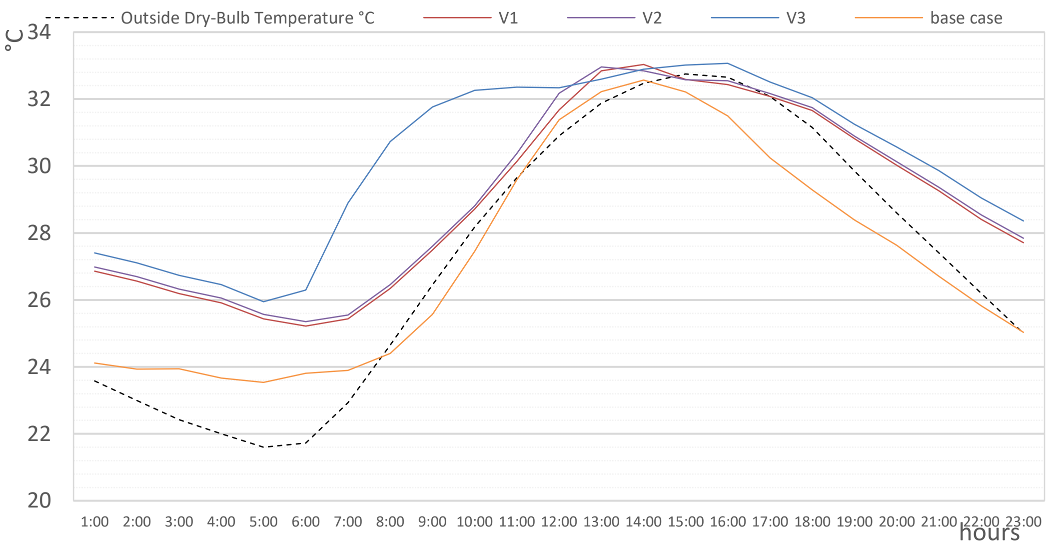

Figure 135. Simulated indoor air temperatures for the base case scenario BC and scenarios of "III Category": V1, V2 and V3 together with the dry-bulb temperature from the weather file 3rd August in south direction

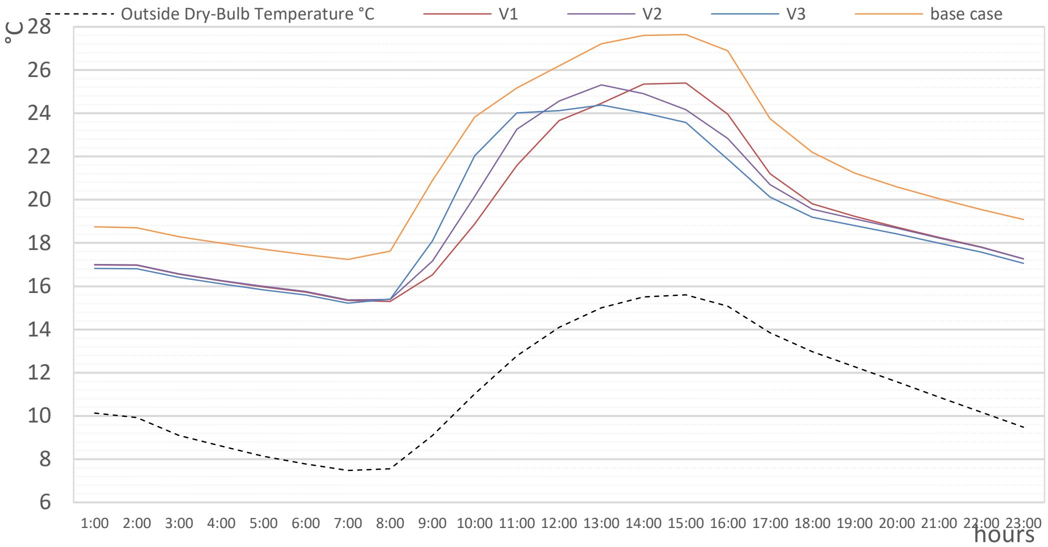

Figure 136. Simulated indoor air temperatures for the base case scenario BC and scenarios of “III Category”: V1, V2 and V3 together with the dry-bulb temperature from the weather file 4th January in south direction

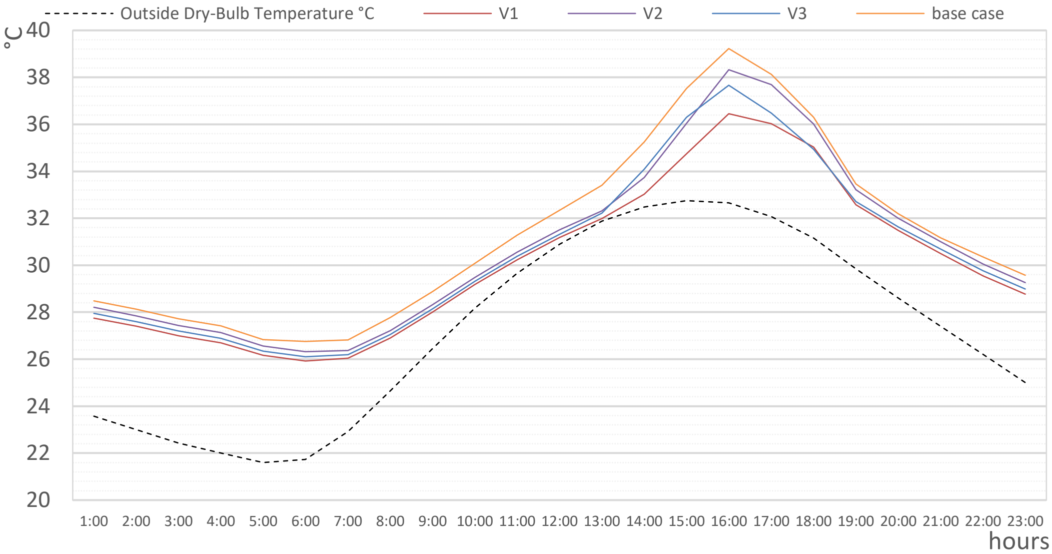

Figure 137. Simulated indoor air temperatures for the base case scenario BC and scenarios of “III Category”: V1, V2 and V3 together with the dry-bulb temperature from the weather file 3rd August in west direction

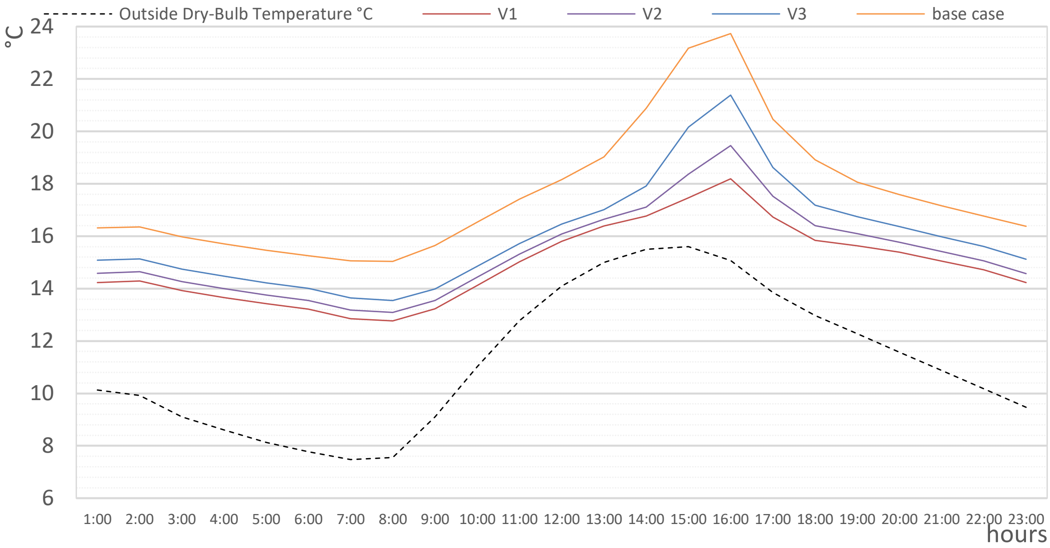

Figure 138. Simulated indoor air temperatures for the base case scenario BC and scenarios of “III Category”: V1, V2 and V3 together with the dry-bulb temperature from the weather file 4th January in west direction

Indoor air temperature results for “I Category”, “II Category” and “III Category” analyzed together. ***Figure 139*** and ***Figure 140*** show the indoor air temperature results for the base case (BC) and EC1, EC2, HO, VO, H1, H2, V1, V2, V3 scenarios analyzed for both summer and winter period in east orientation. ***Figure 141*** and ***Figure 142*** show the indoor air temperature results for the base case (BC) and EC1, EC2, HO, VO, H1, H2, V1, V2, V3 scenarios analyzed for both summer and winter period in south orientation. ***Figure 143*** and ***Figure 144*** show the indoor air temperature results for the base case (BC) and EC1, EC2, HO, VO, H1, H2, V1, V2, V3 scenarios analyzed for both summer and winter period in west orientation.

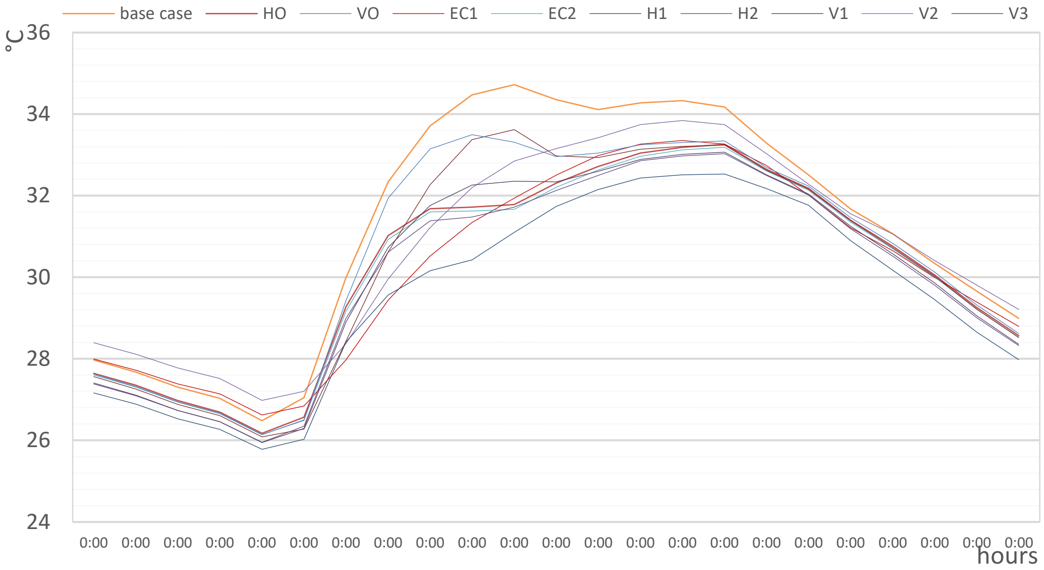

Figure 139. Simulated indoor air temperatures for the base case scenario BC and scenarios of "I Category", "II Category" and "III Category" from the weather file 3rd August in east direction

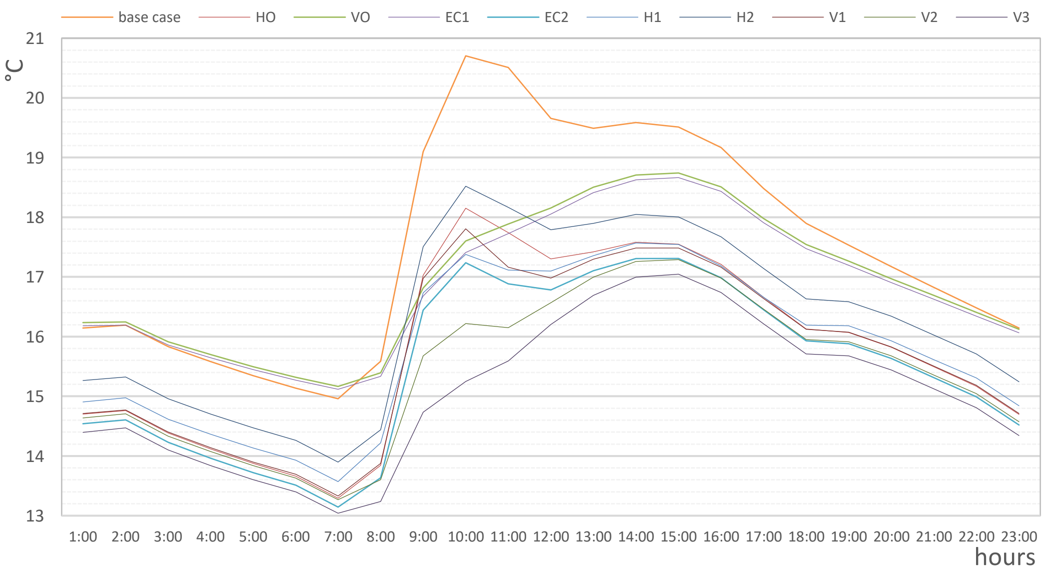

Figure 140. Simulated indoor air temperatures for the base case scenario BC and scenarios of "I Category", "II Category" and "III Category" from the weather file 4th January in east direction

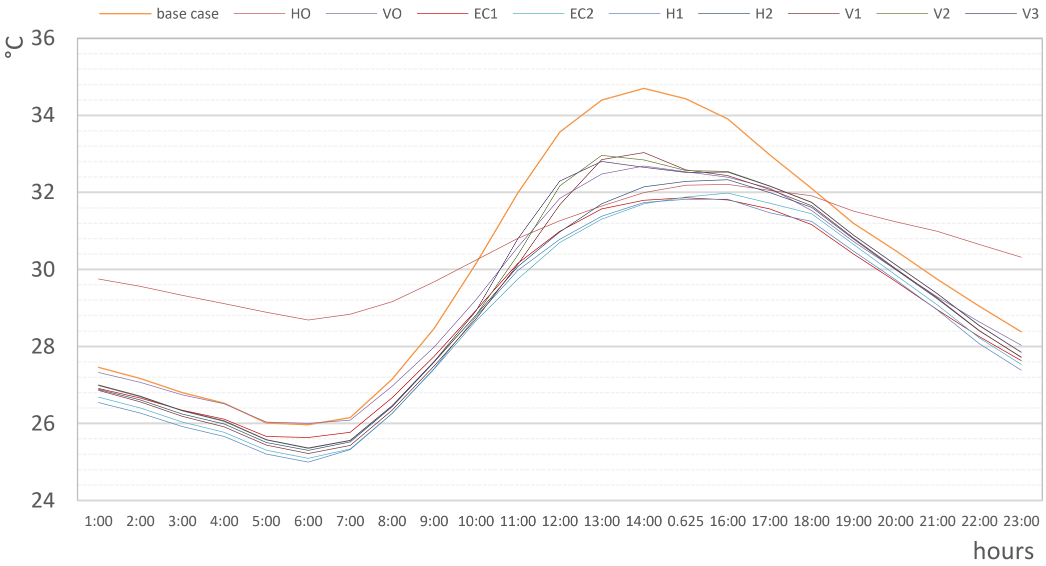

Figure 141. Simulated indoor air temperatures for the base case scenario BC and scenarios of "I Category", "II Category" and "III Category" from the weather file 3rd August in south direction

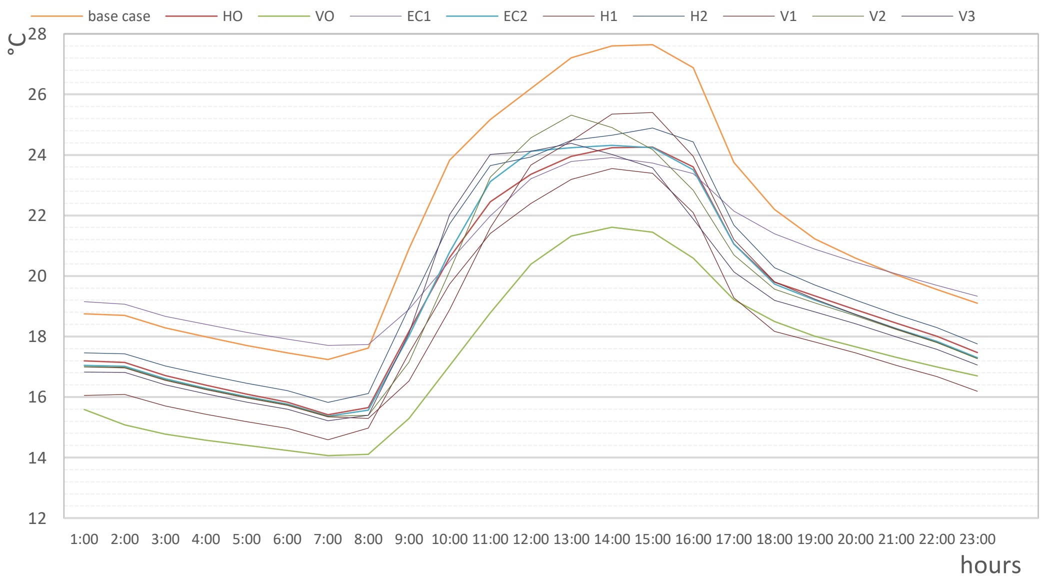

Figure 142. Simulated indoor air temperatures for the base case scenario BC and scenarios of "I Category", "II Category" and "III Category" from the weather file 4th January in south direction

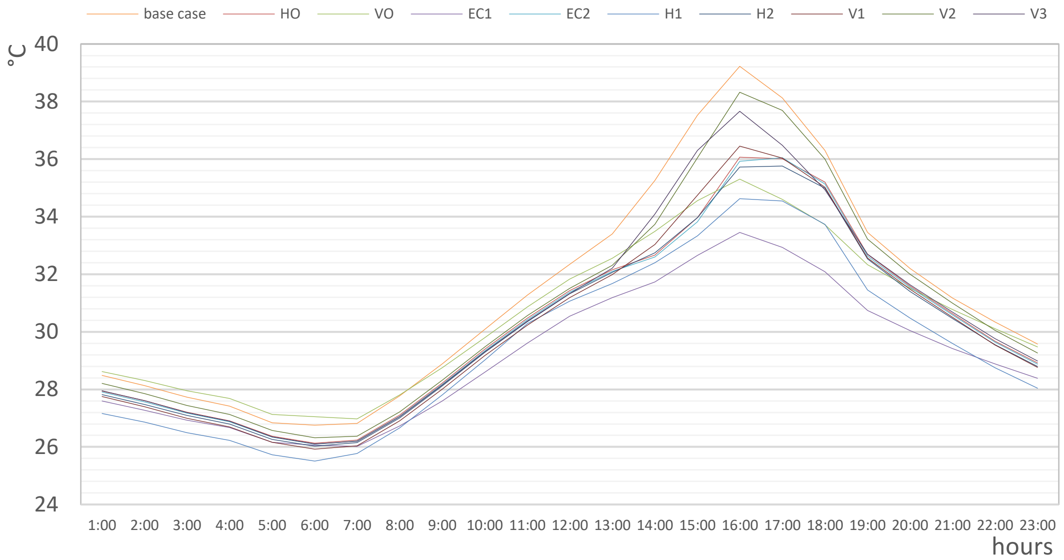

Figure 143. Simulated indoor air temperatures for the base case scenario BC and scenarios of "I Category", "II Category" and "III Category" from the weather file 3rd August in west direction

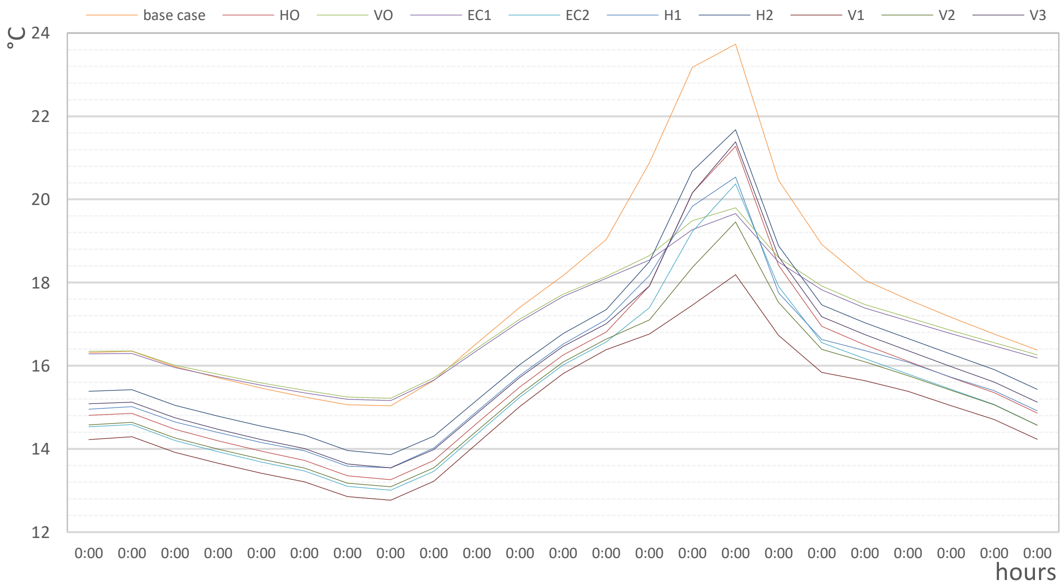

Figure 144. Simulated indoor air temperatures for the base case scenario BC and scenarios of "I Category", "II Category" and "III Category" from the weather file 4th January in west direction

4.4.2 Energy performance

Simulated heating and cooling loads results, for “I Category”, “II Category”, and “III Category” in east, south and west orientation are analyzed. First, the "I Category" results are analyzed, followed by the "II Category" and "III Category" results. Finally, all of the scenarios together for the Antalya climate.

“I Category”: ***Figure 145*** and ***Figure 146*** shows the energy consumption for heating and cooling for the base case (BC) and EC1, EC2, HO and VO scenarios in east orientation. ***Figure 147*** and ***Figure 148*** shows the energy consumption for heating and cooling for the base case (BC) and EC1, EC2, HO and VO scenarios in south orientation. ***Figure 149*** and ***Figure 150*** shows the energy consumption for heating and cooling for the base case (BC) and EC1, EC2, HO and VO scenarios in west orientation.

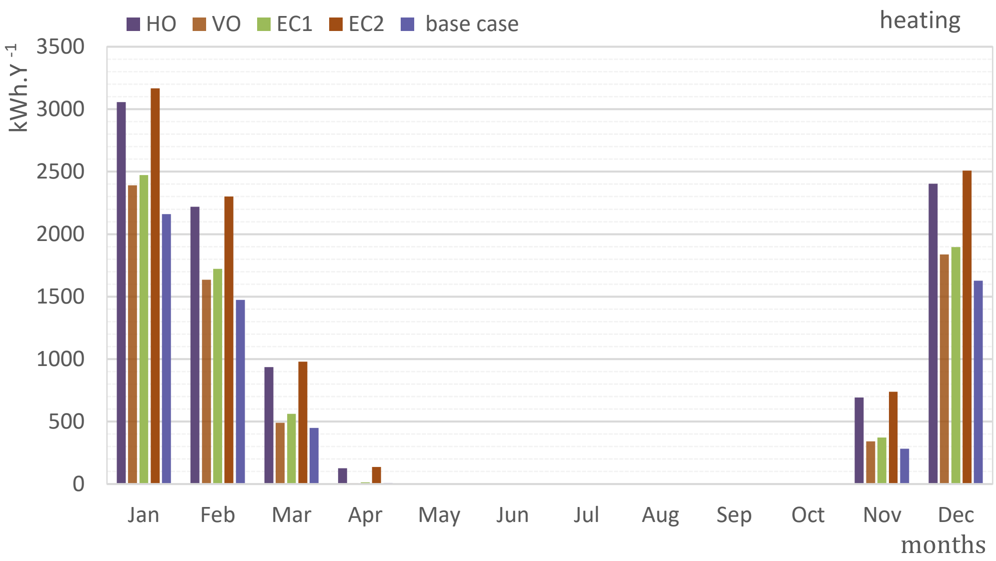

Figure 145. Comparision of simulated heating loads (kWh.Y^{-1}) of the base case scenario BC and scenarios of “I Category”: HO, VO, EC1 and EC2 in east orientation

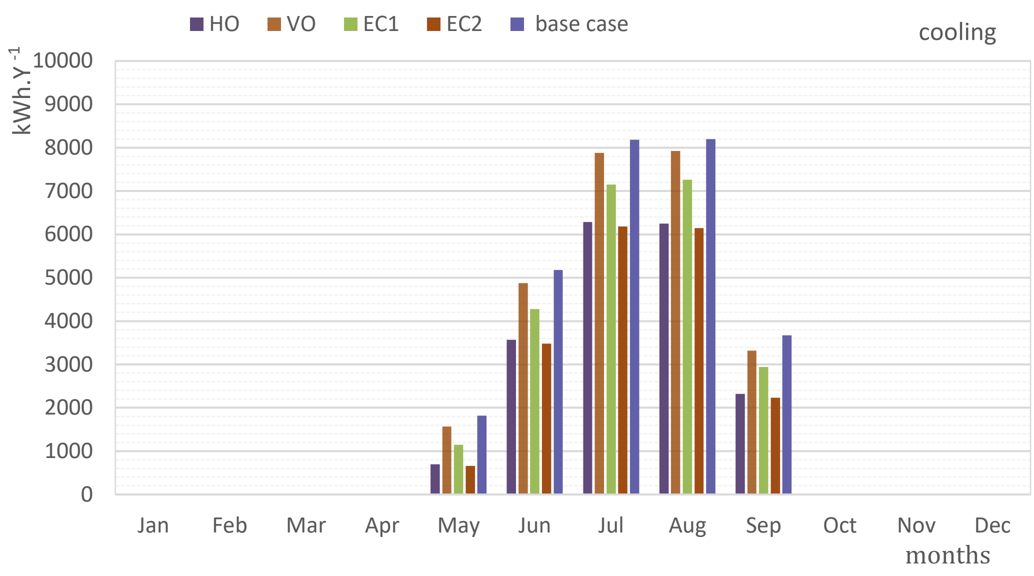

Figure 146. Comparision of simulated cooling loads (kWh.Y^{-1}) of the base case scenario BC and scenarios of "I Category": HO, VO, EC1 and EC2 in east orientation

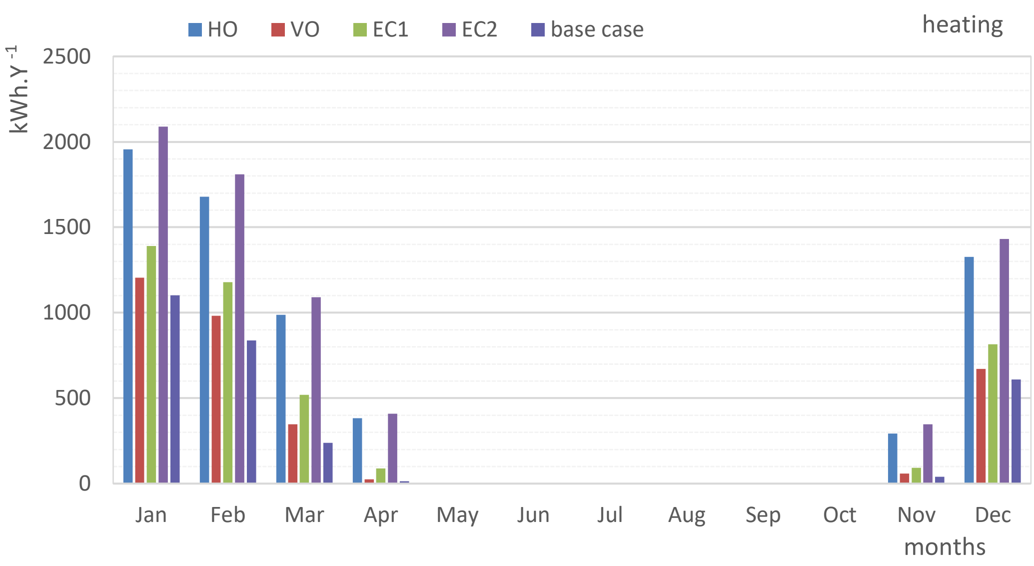

Figure 147. Comparision of simulated heating loads (kWh.Y^{-1}) of the base case scenario BC and scenarios of "I Category": HO, VO, EC1 and EC2 in south orientation

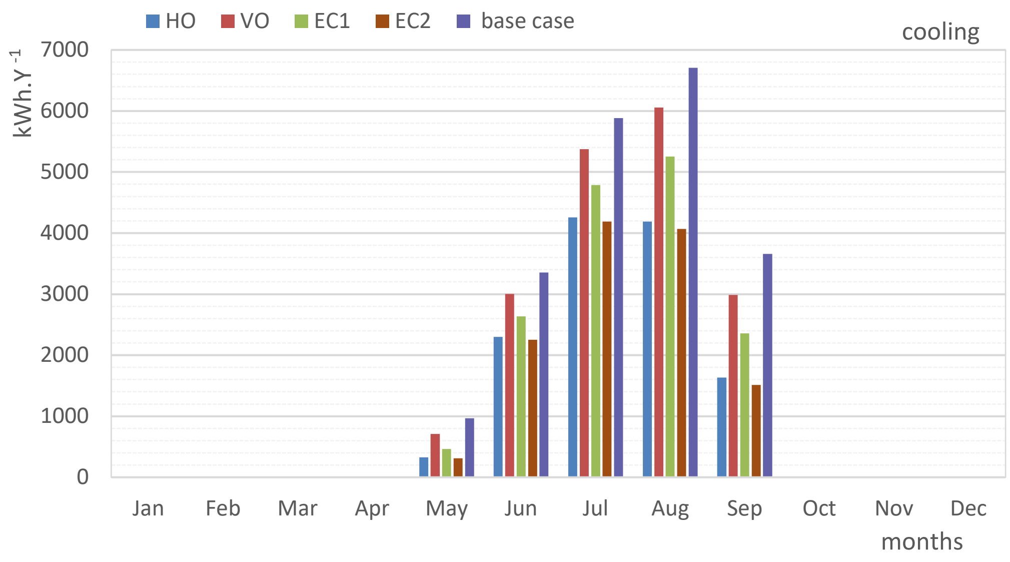

Figure 148. Comparision of simulated cooling loads (kWh.Y^{-1}) of the base case scenario BC and scenarios of "I Category": HO, VO, EC1 and EC2 in south orientation

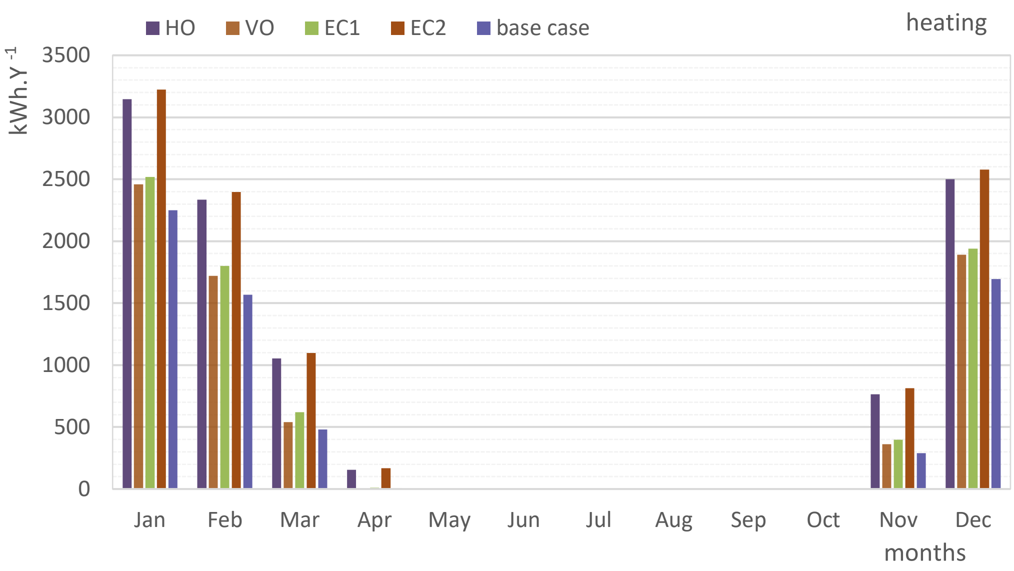

Figure 149. Comparision of simulated heating loads (kWh.Y^{-1}) of the base case scenario BC and scenarios of "I Category": HO, VO, EC1 and EC2 in west orientation

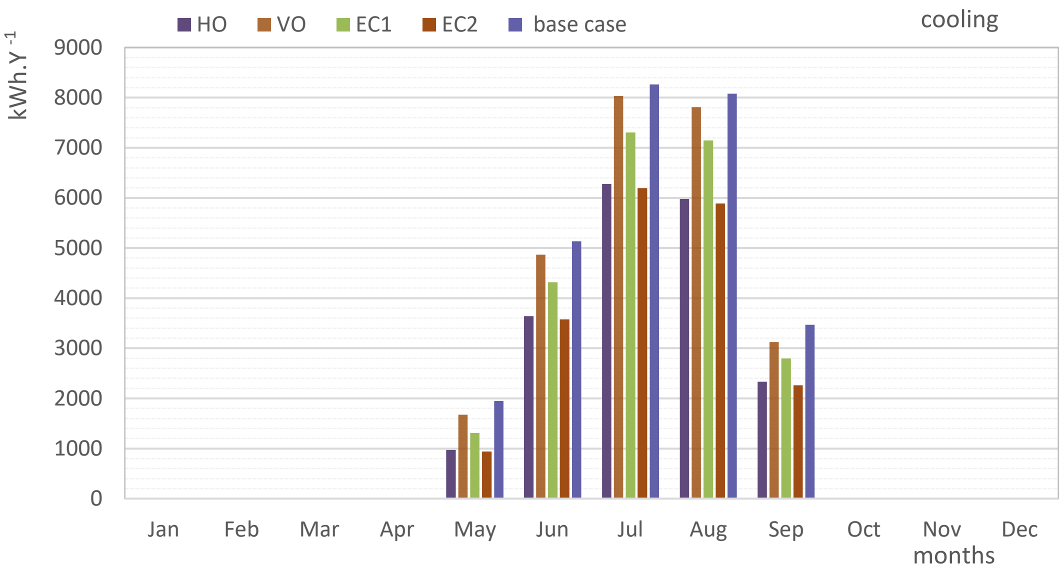

Figure 150. Comparision of simulated cooling loads (kWh.Y^{-1}) of the base case scenario BC and scenarios of "I Category": HO, VO, EC1 and EC2 in west orientation

"II Category": ***Figure 151*** and ***Figure 152*** shows the energy consumption for heating and cooling for the base case (BC) and H1, H2 scenarios in east orientation. ***Figure 153*** and ***Figure 154*** shows the energy consumption for heating and cooling for the base case (BC) and H1, H2 scenarios in south orientation. ***Figure 155*** and ***Figure 156*** shows the energy consumption for heating and cooling for the base case (BC) and H1, H2 scenarios in west orientation.

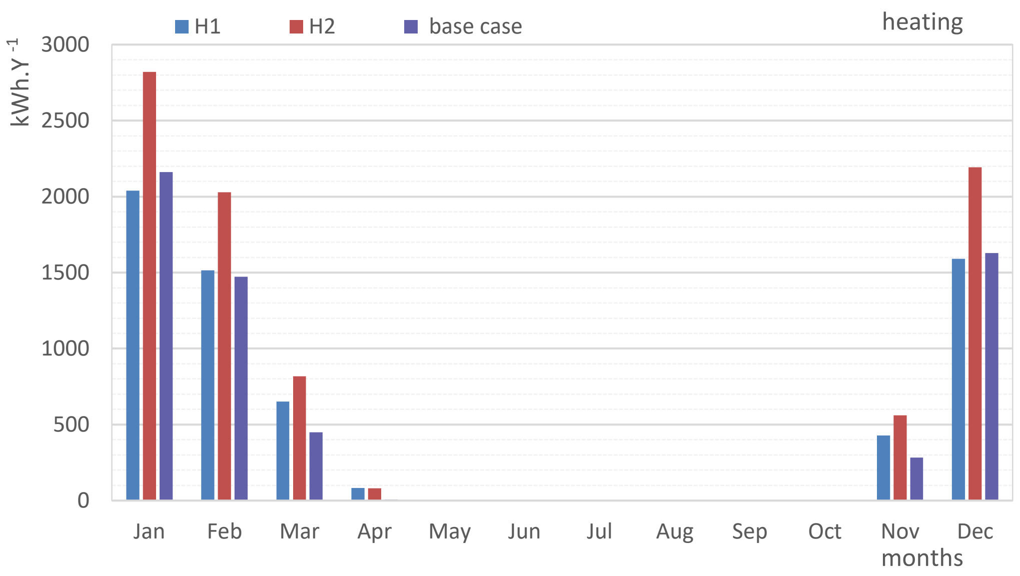

Figure 151. Comparision of simulated heating loads (kWh.Y^{-1}) of the base case scenario BC and scenarios of "II Category": H1, and H2 in east orientation

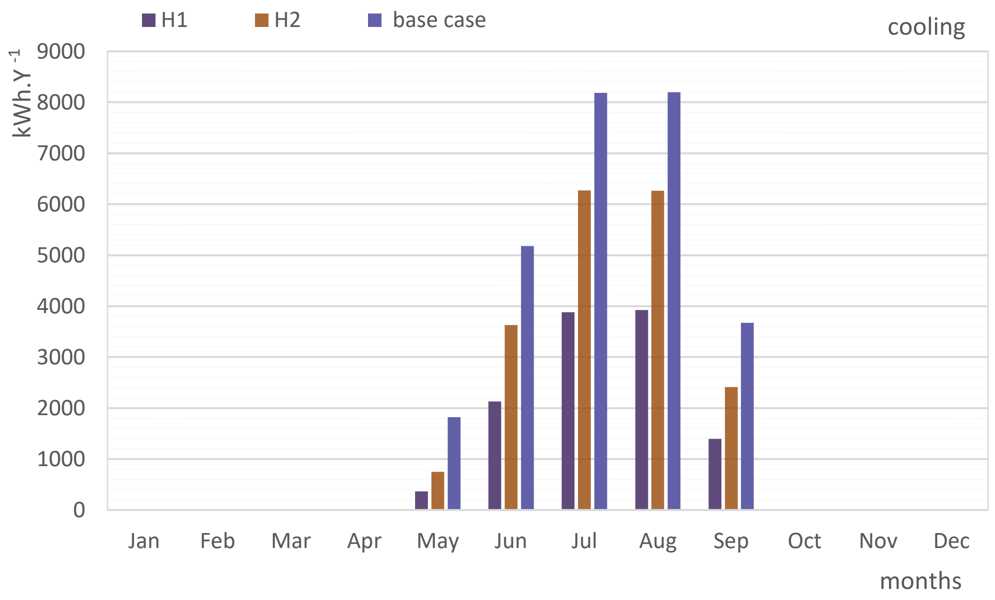

Figure 152. Comparision of simulated cooling loads (kWh.Y^{-1}) of the base case scenario BC and scenarios of "II Category": H1, and H2 in east orientation

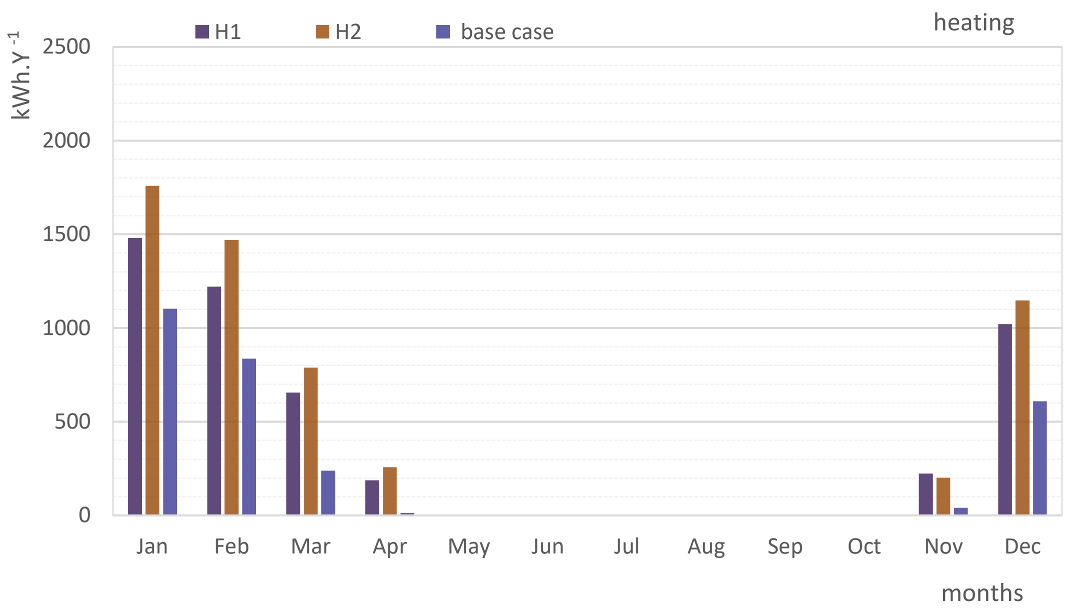

Figure 153. Comparision of simulated heating loads (kWh.Y^{-1}) of the base case scenario BC and scenarios of "II Category": H1, and H2 in south orientation

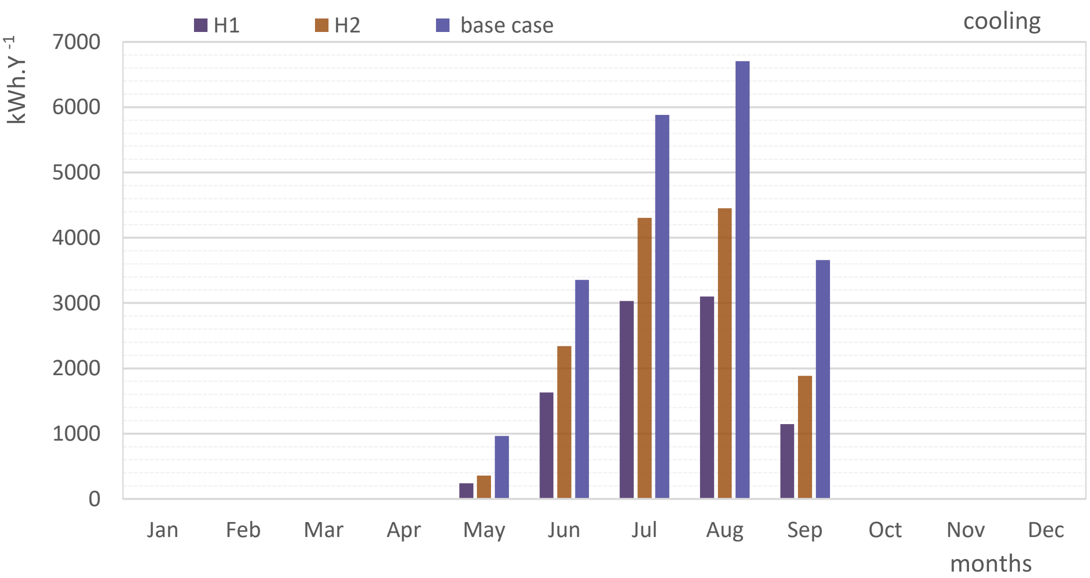

Figure 154. Comparision of simulated cooling loads (kWh.Y^{-1}) of the base case scenario BC and scenarios of "II Category": H1, and H2 in south orientation

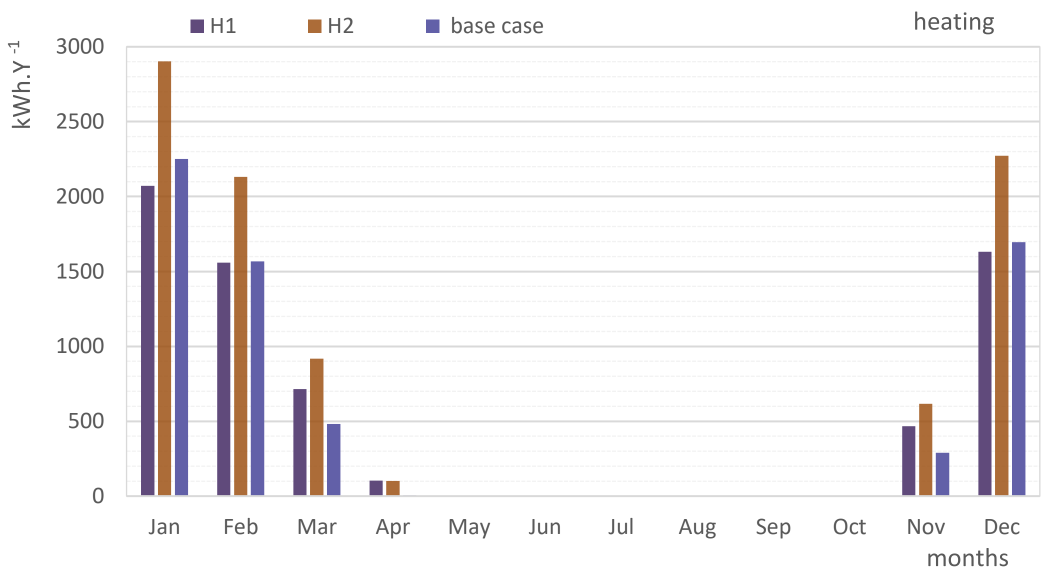

Figure 155. Comparision of simulated heating loads (kWh.Y^{-1}) of the base case scenario BC and scenarios of "II Category": H1, and H2 in west orientation

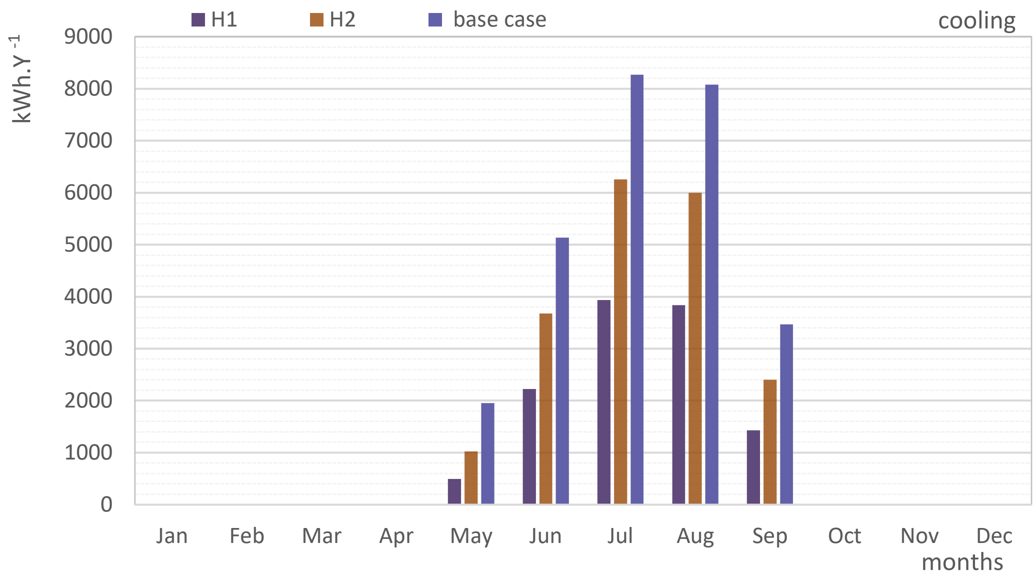

Figure 156. Comparision of simulated cooling loads (kWh.Y^{-1}) of the base case scenario BC and scenarios of "II Category": H1, and H2 in west orientation

“III Category”: ***Figure 157*** and ***Figure 158*** shows the energy consumption for heating and cooling for the base case (BC) and V1, V2, V3 scenarios in east orientation. ***Figure 159*** and ***Figure 160*** shows the energy consumption for heating and cooling for the base case (BC) and V1, V2, V3 scenarios in south orientation. ***Figure 161*** and ***Figure 162*** shows the energy consumption for heating and cooling for the base case (BC) and V1, V2, V3 scenarios in west orientation.

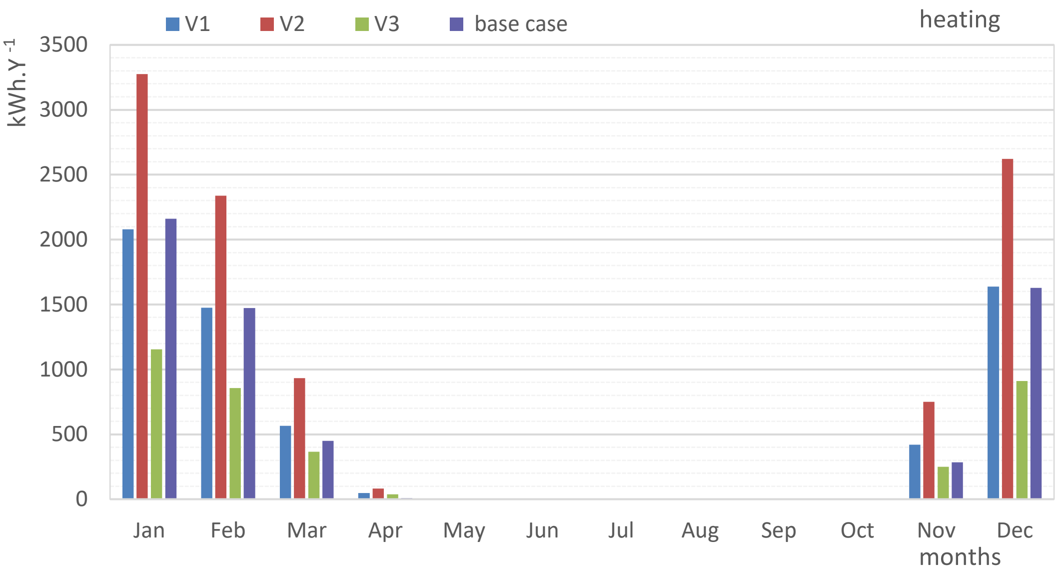

Figure 157. Comparision of simulated heating loads (kWh.Y^{-1}) of the base case scenario BC and scenarios of “III Category”: V1, V2 and V3 in east orientation

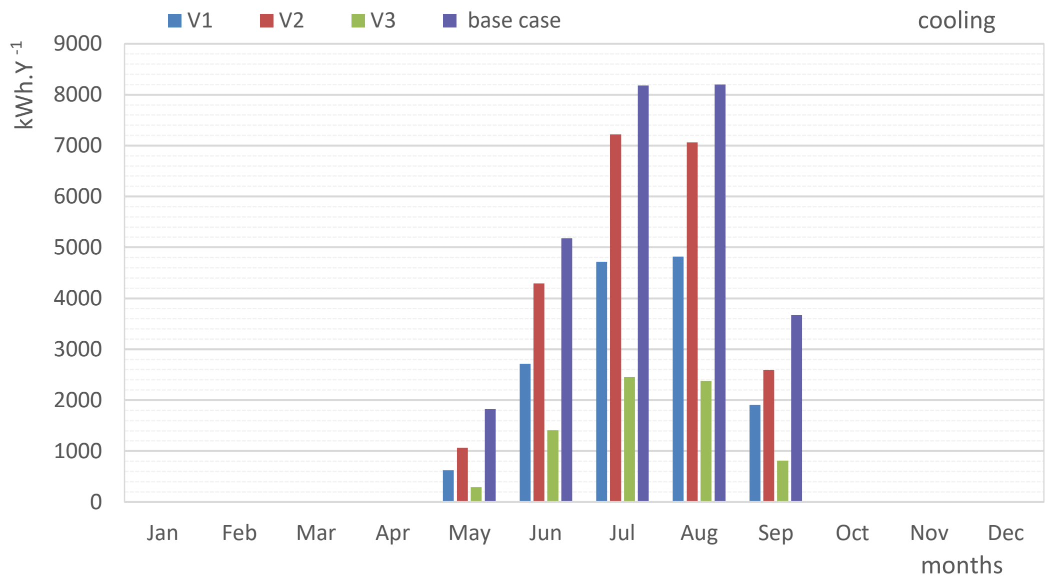

Figure 158. Comparision of simulated cooling loads (kWh.Y^{-1}) of the base case scenario BC and scenarios of “III Category”: V1, V2 and V3 in east orientation

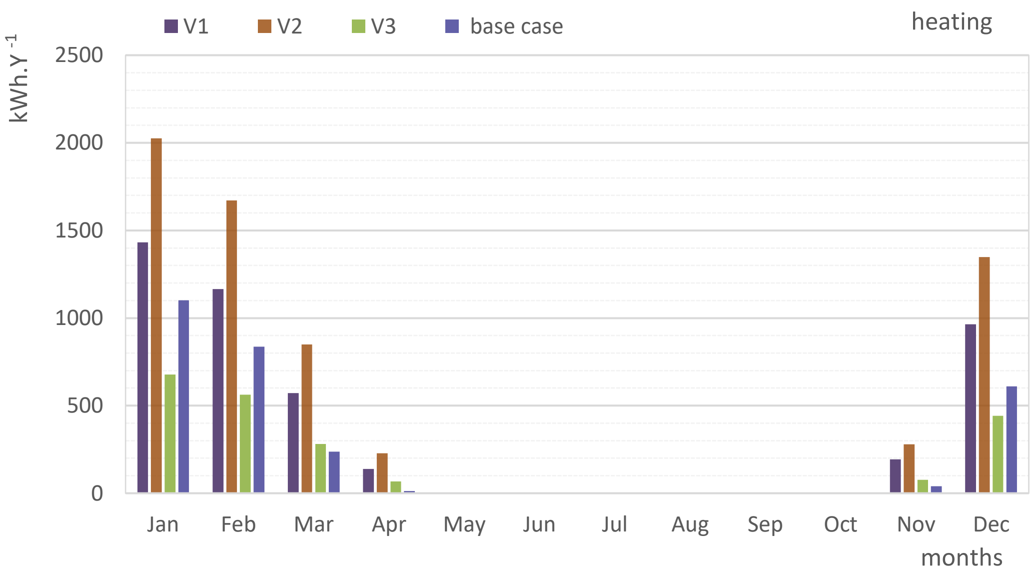

Figure 159. Comparision of simulated heating loads (kWh.Y^{-1}) of the base case scenario BC and scenarios of “III Category”: V1, V2 and V3 in south orientation

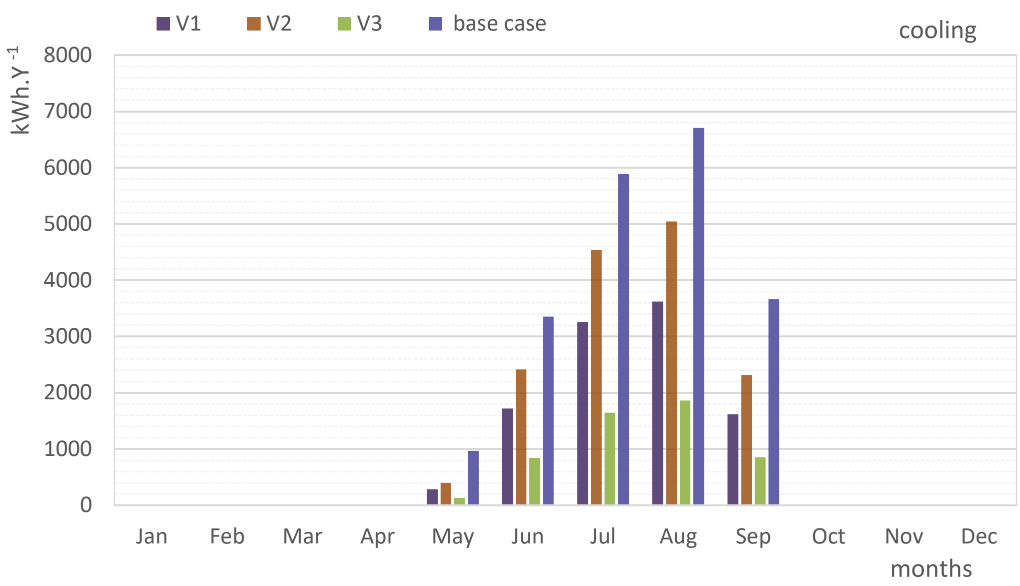

Figure 160. Comparision of simulated cooling loads (kWh.Y^{-1}) of the base case scenario BC and scenarios of "III Category": V1, V2 and V3 in south orientation

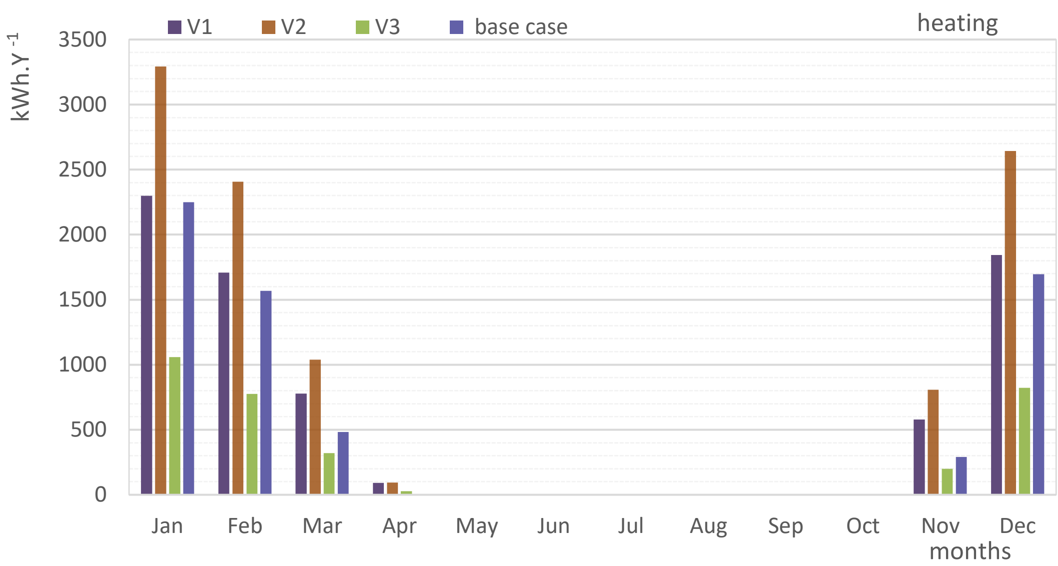

Figure 161. Comparision of simulated heating loads (kWh.Y^{-1}) of the base case scenario BC and scenarios of "III Category": V1, V2 and V3 in west orientation

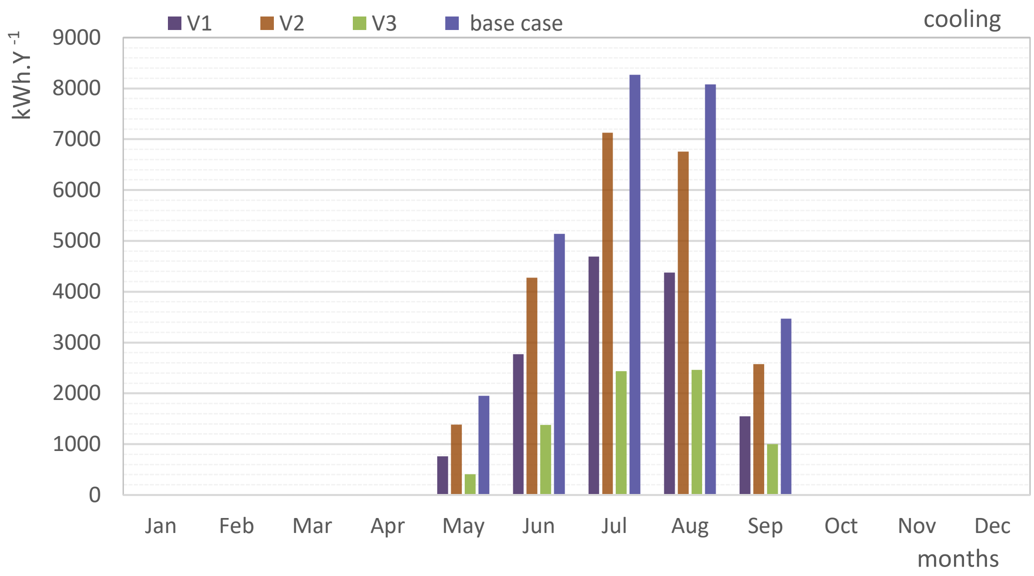

Figure 162. Comparision of simulated cooling loads (kWh.Y^{-1}) of the base case scenario BC and scenarios of "III Category": V1, V2 and V3 in west orientation

Energy consumption for heating and cooling loads for "I Category", "II Category" and "III Category" are analyzed together. ***Figure 163*** and ***Figure 164*** show heating and cooling loads results for the base case (BC) and EC1, EC2, HO, VO, H1, H2, V1, V2, V3 scenarios in east orientation. ***Figure 165*** and ***Figure 166*** show heating and cooling loads results for the base case (BC) and EC1, EC2, HO, VO, H1, H2, V1, V2, V3 scenarios in south orientation. ***Figure 167*** and ***Figure 168*** show heating and cooling loads results for the base case (BC) and EC1, EC2, HO, VO, H1, H2, V1, V2, V3 scenarios in west orientation.

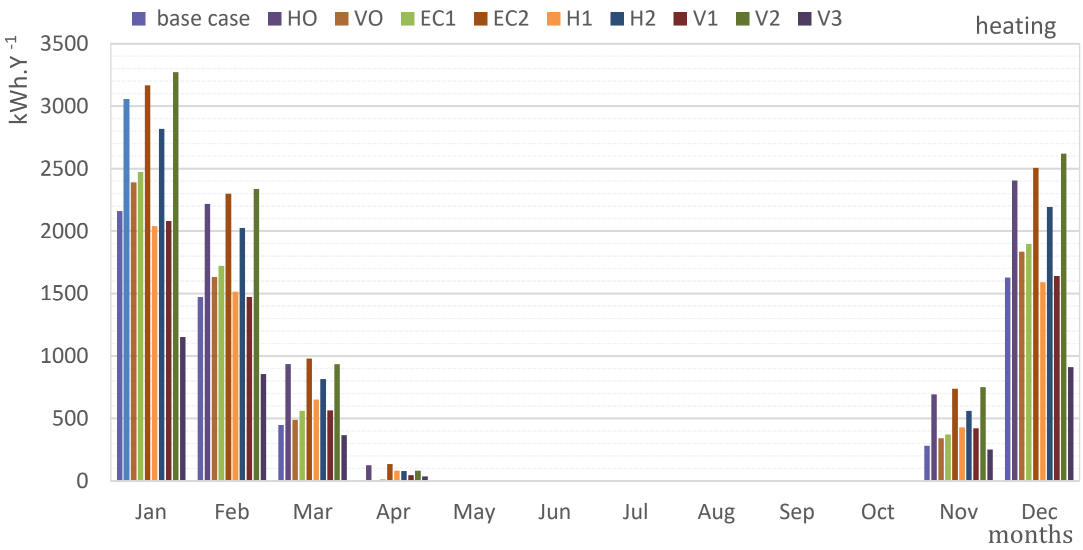

Figure 163. Comparison of simulated heating loads (kWh.Y^{-1}) of the base case scenario BC and scenarios of "I Category", "II Category" and "III Category" in east orientation

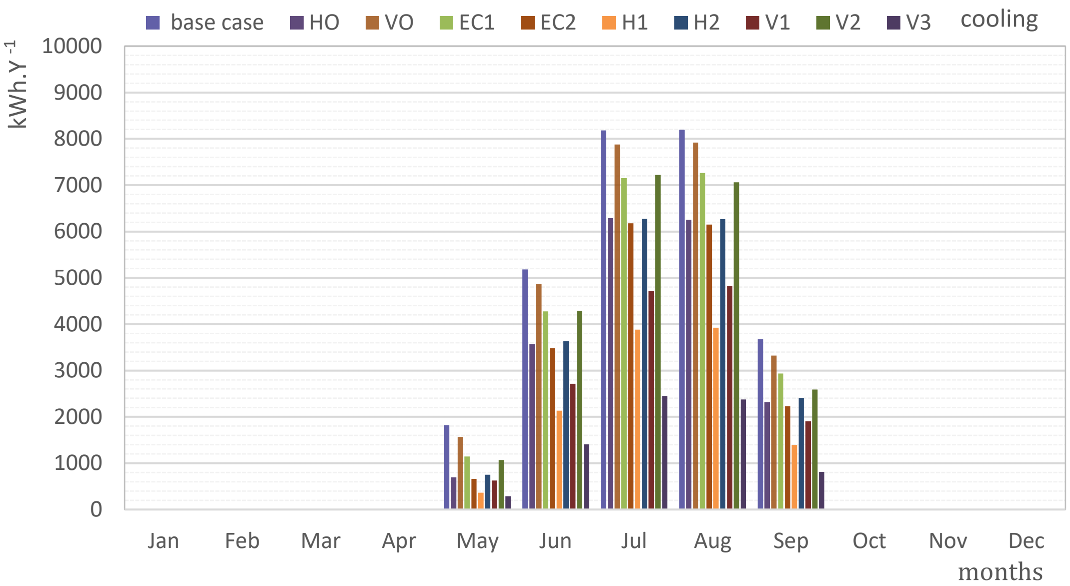

Figure 164. Comparison of simulated cooling loads (kWh.Y^{-1}) of the base case scenario BC and scenarios of "I Category", "II Category" and "III Category" in east orientation

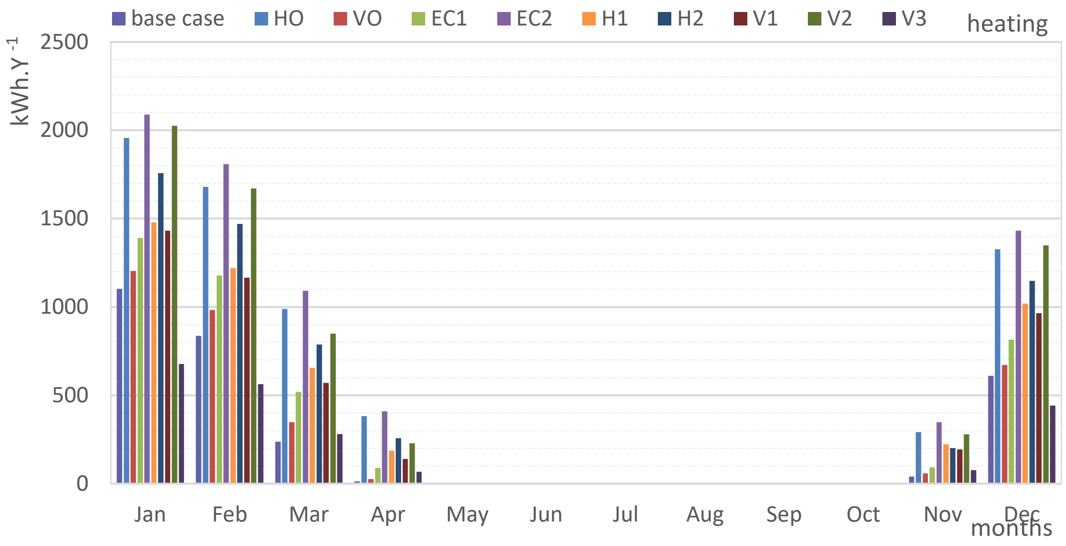

Figure 165. Comparison of simulated heating loads (kWh.Y^{-1}) of the base case scenario BC and scenarios of "I Category", "II Category" and "III Category" in south orientation

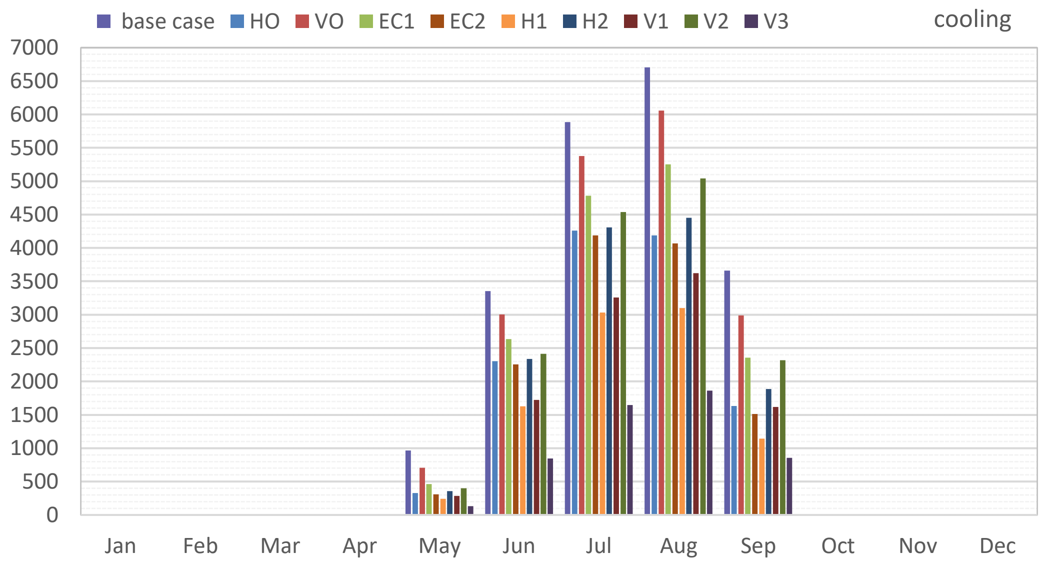

Figure 166. Comparison of simulated cooling loads (kWh.Y^{-1}) of the base case scenario BC and scenarios of "I Category", "II Category" and "III Category" in south orientation

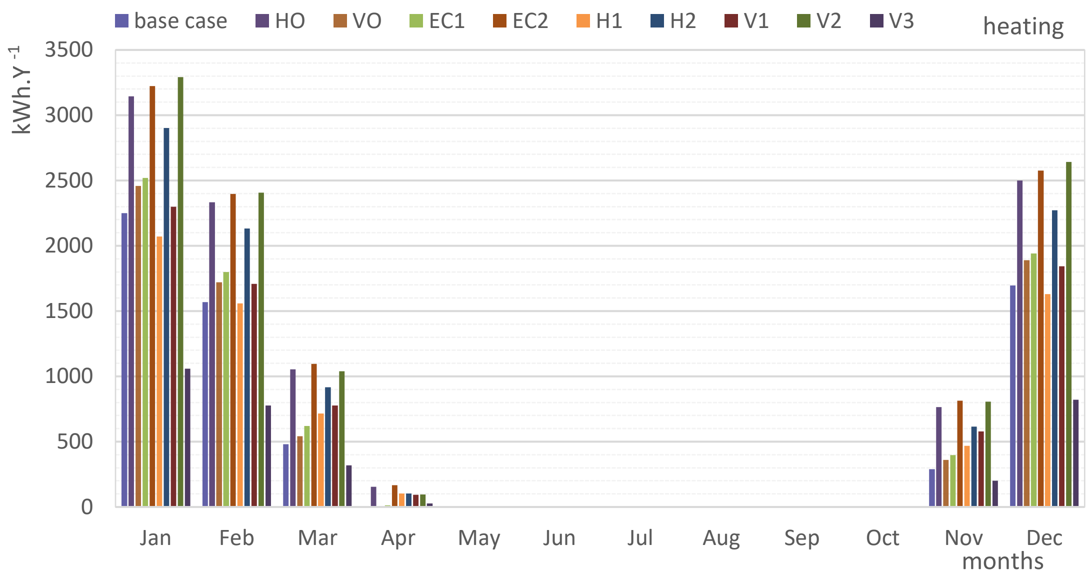

Figure 167. Comparison of simulated heating loads (kWh.Y^{-1}) of the base case scenario BC and scenarios of "I Category", "II Category" and "III Category" in west orientation

4.5 Naples, Italy

4.5.1 Indoor air temperature

Indoor air temperature results for "I Category", "II Category", and "III Category" in east, south and west orientation are analyzed by picking a typical summer and winter day. Beginning with the analysis of the "I Category's", followed by the "II Category" and "III Category" results. In conclusion, all of the scenarios are also compared for the Naples climate.

"I Category": ***Figure 168*** and ***Figure 169*** show the indoor air temperature results for the base case (BC) and EC1, EC2, HO and VO scenarios analyzed for both summer and winter period in east orientation. ***Figure 170*** and ***Figure 169*** show the indoor air temperature results for the base case (BC) and EC1, EC2, HO VO scenarios analyzed for both summer and winter period in south orientation. ***Figure 171*** and ***Figure 172*** show the indoor air temperature results for the base case (BC) and EC1, EC2, HO and VO scenarios analyzed for both summer and winter period in west orientation.

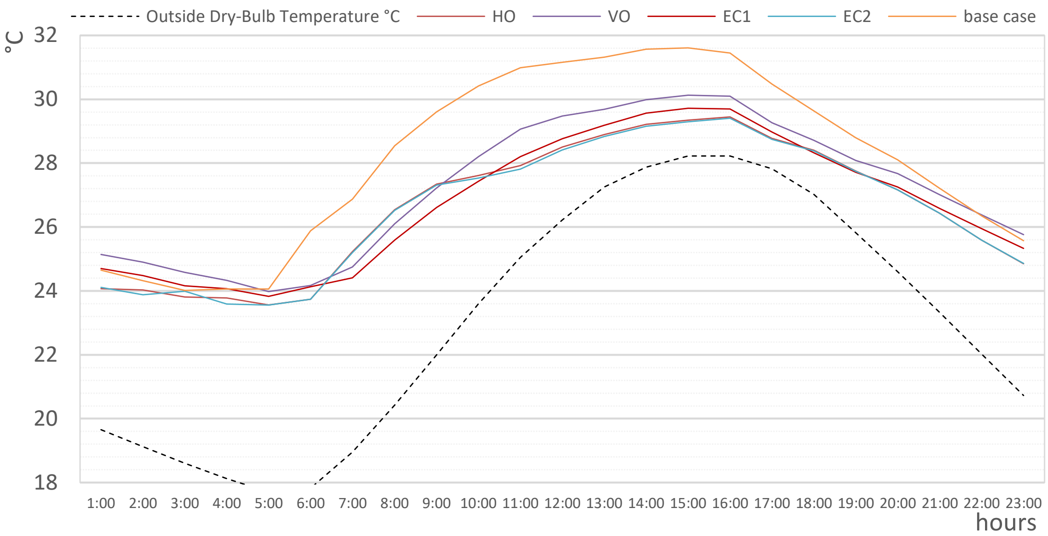

Figure 168. Simulated indoor air temperatures for the base case scenario BC and scenarios of “I Category”: HO, VO, EC1 and EC2, together with the dry-bulb temperature from the weather file 3rd August in east direction

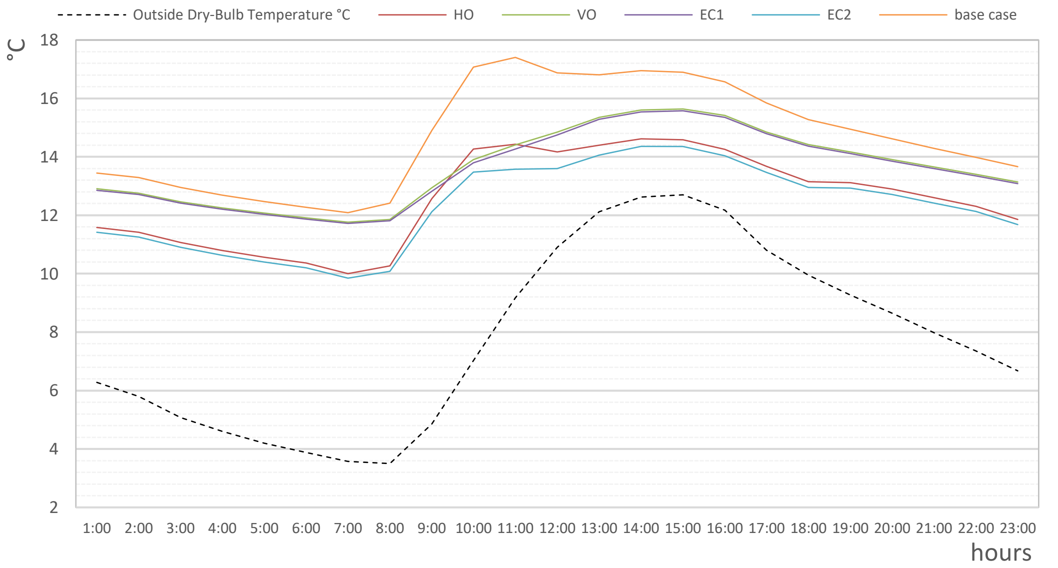

Figure 169. Simulated indoor air temperatures for the base case scenario BC and scenarios of "I Category": HO, VO, EC1 and EC2, together with the dry-bulb temperature from the weather file 4th January in east direction

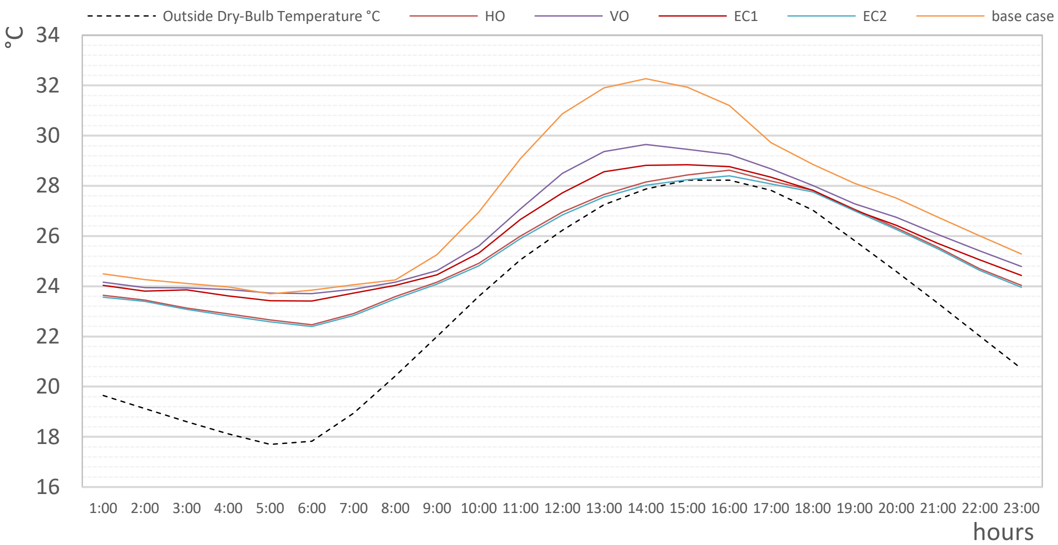

Figure 170. Simulated indoor air temperatures for the base case scenario BC and scenarios of "I Category": HO, VO, EC1 and EC2, together with the dry-bulb temperature from the weather file 3rd August in south direction

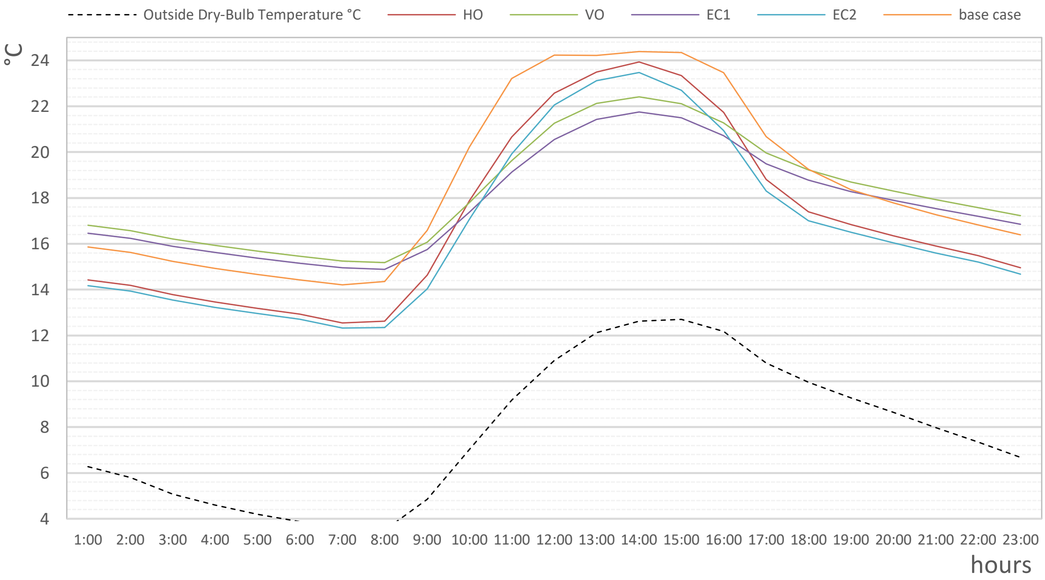

Figure 171. Simulated indoor air temperatures for the base case scenario BC and scenarios of "I Category": HO, VO, EC1 and EC2, together with the dry-bulb temperature from the weather file 4th January in south direction

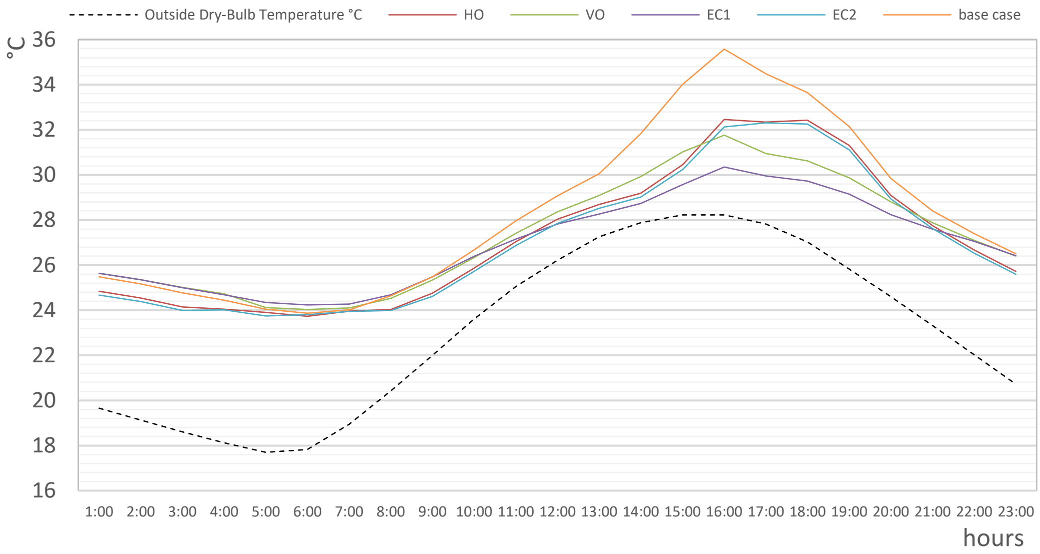

Figure 172. Simulated indoor air temperatures for the base case scenario BC and scenarios of "I Category": HO, VO, EC1 and EC2, together with the dry-bulb temperature from the weather file 3rd August in west direction

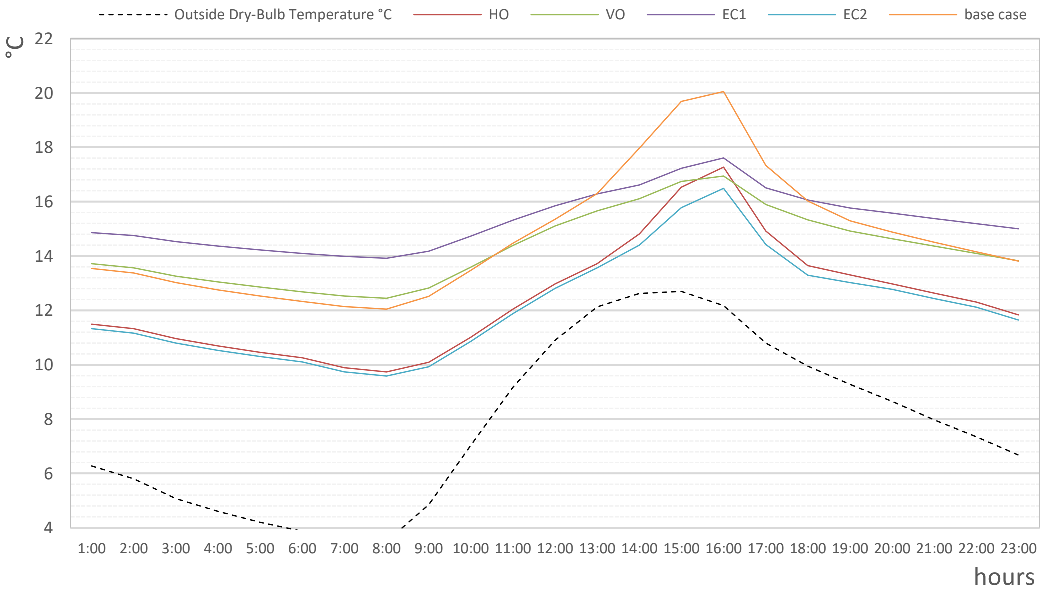

Figure 173. Simulated indoor air temperatures for the base case scenario BC and scenarios of "I Category": HO, VO, EC1 and EC2, together with the dry-bulb temperature from the weather file 4th January in west direction

"II Category": ***Figure 174*** and ***Figure 175*** show the indoor air temperature results for the base case (BC) and H1, H2 scenarios analyzed for both summer and winter period in east orientation. ***Figure 176*** and ***Figure 177*** show the indoor air temperature results for the base case (BC) and H1, H2 scenarios analyzed for both summer and winter period in south orientation. ***Figure 178*** and ***Figure 179*** show the indoor air temperature results for the base case (BC) and H1, H2 scenarios analyzed for both summer and winter period in west orientation.

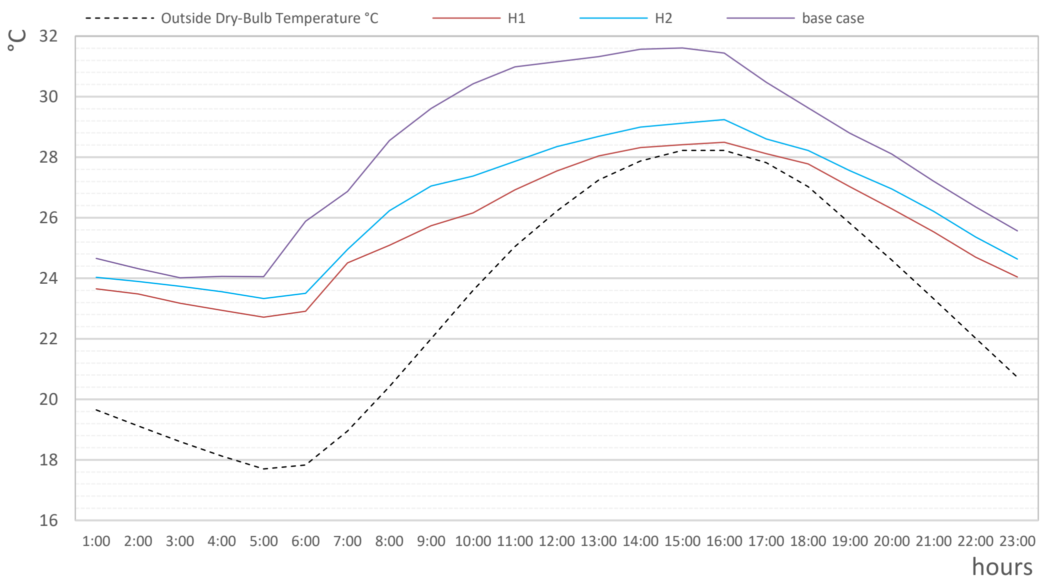

Figure 174. Simulated indoor air temperatures for the base case scenario BC and scenarios of “II Category”: H1, and H2, together with the dry-bulb temperature from the weather file 3rd August in east direction

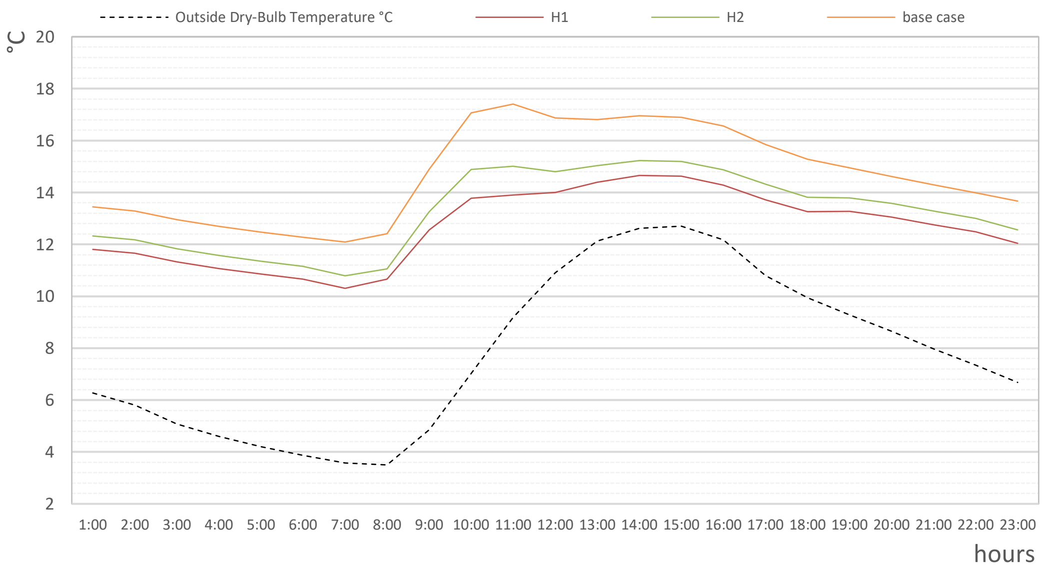

Figure 175. Simulated indoor air temperatures for the base case scenario BC and scenarios of “II Category”: H1, and H2, together with the dry-bulb temperature from the weather file 4th January in east direction

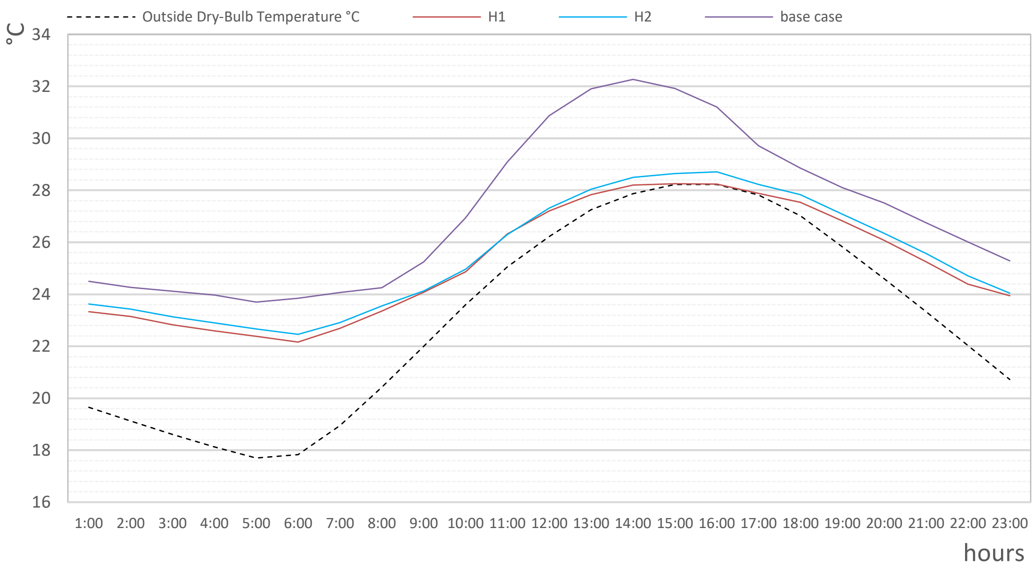

Figure 176. Simulated indoor air temperatures for the base case scenario BC and scenarios of "II Category": H1, and H2, together with the dry-bulb temperature from the weather file 3rd August in south direction

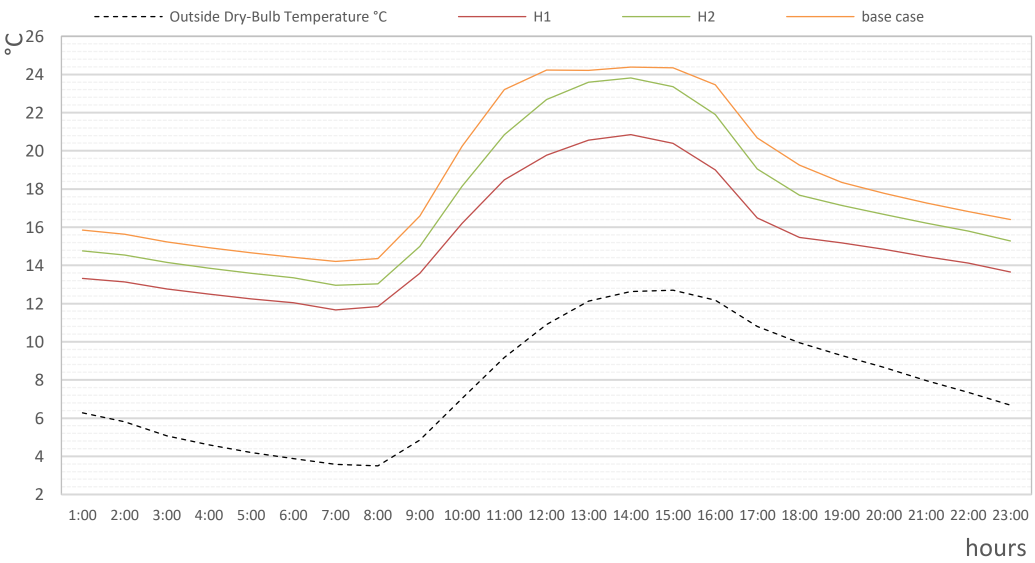

Figure 177. Simulated indoor air temperatures for the base case scenario BC and scenarios of "II Category": H1, and H2, together with the dry-bulb temperature from the weather file 4th January in south direction

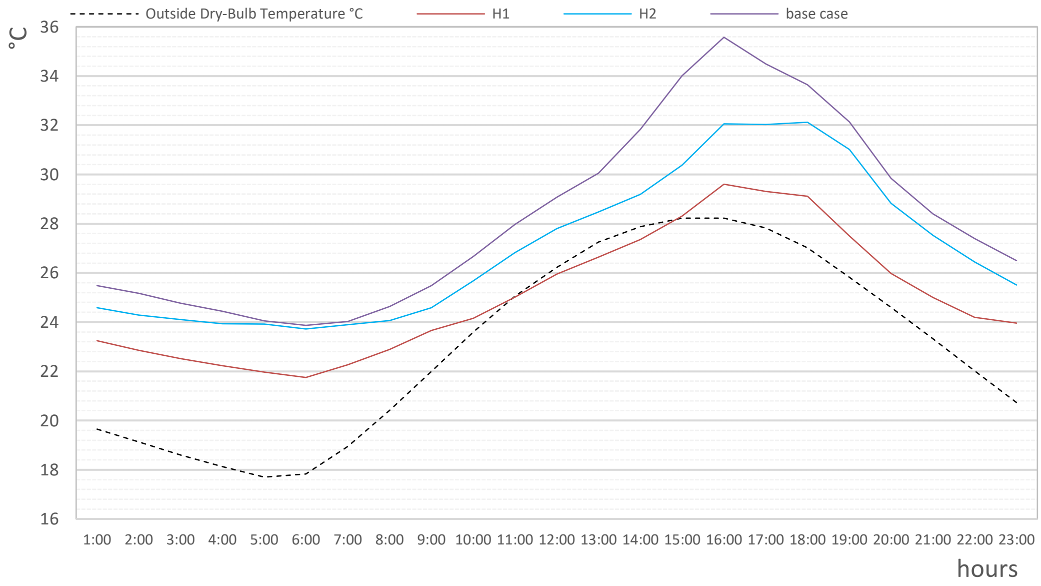

Figure 178. Simulated indoor air temperatures for the base case scenario BC and scenarios of "II Category": H1, and H2, together with the dry-bulb temperature from the weather file 3rd August in west direction

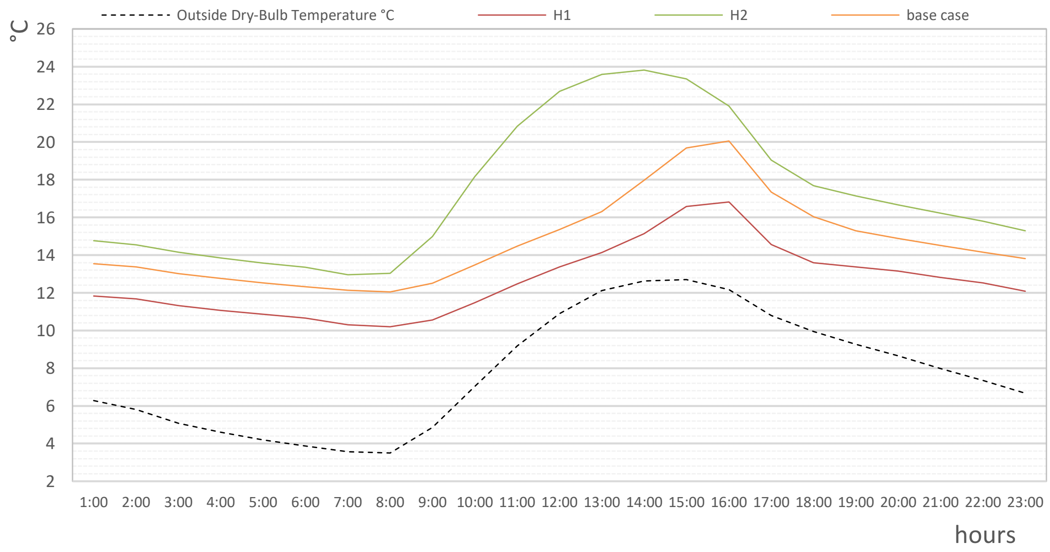

Figure 179. Simulated indoor air temperatures for the base case scenario BC and scenarios of "II Category": H1, and H2, together with the dry-bulb temperature from the weather file 4th January in west direction

"III Category": ***Figure 180*** and ***Figure 181*** show the indoor air temperature results for the base case (BC) and V1, V2, V3 scenarios analyzed for both summer and winter period in east orientation. ***Figure 182*** and ***Figure 183*** show the indoor air temperature results for the base case (BC) and V1, V2, V3 scenarios analyzed for both summer and winter period in south orientation. ***Figure 184*** and ***Figure 185*** show the indoor air temperature results for the base case (BC) and V1, V2, V3 scenarios analyzed for both summer and winter period in west orientation.

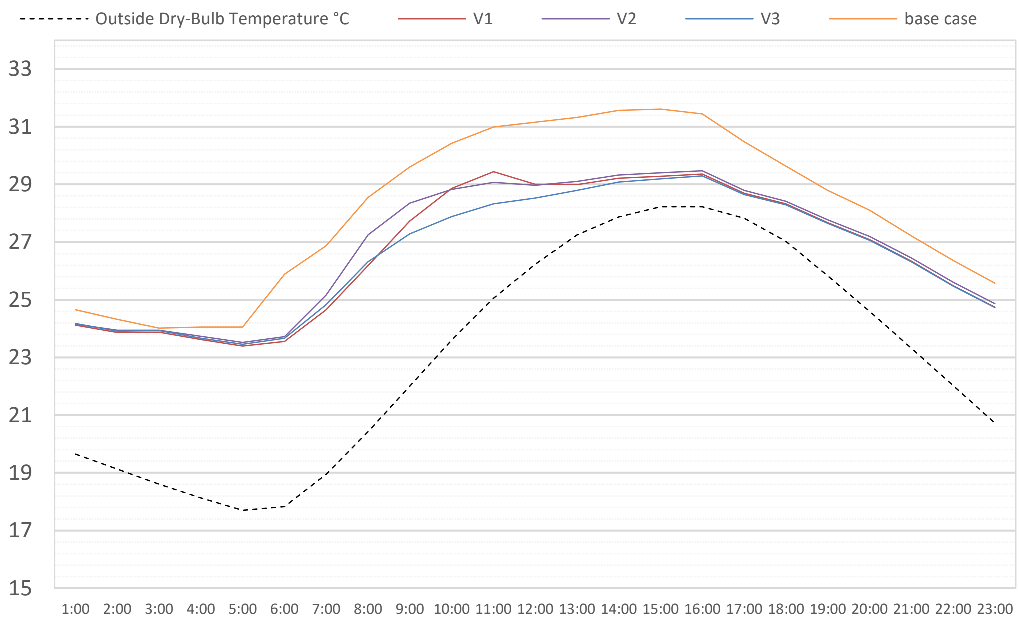

Figure 180. Simulated indoor air temperatures for the base case scenario BC and scenarios of "III Category": V1, V2 and V3 together with the dry-bulb temperature from the weather file 3rd August in east direction

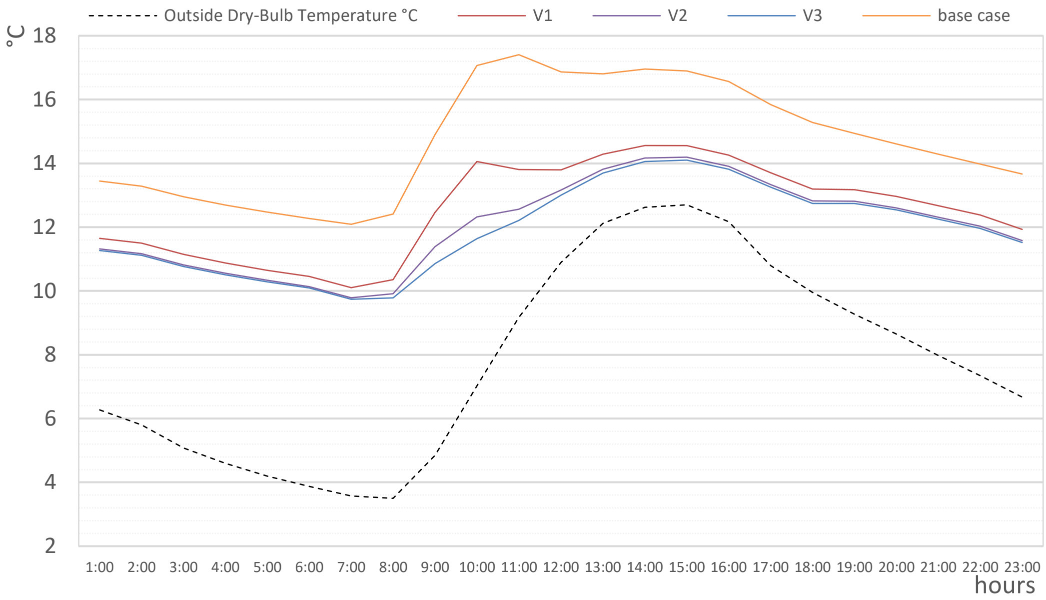

Figure 181. Simulated indoor air temperatures for the base case scenario BC and scenarios of "III Category": V1, V2 and V3 together with the dry-bulb temperature from the weather file 4th January in east direction

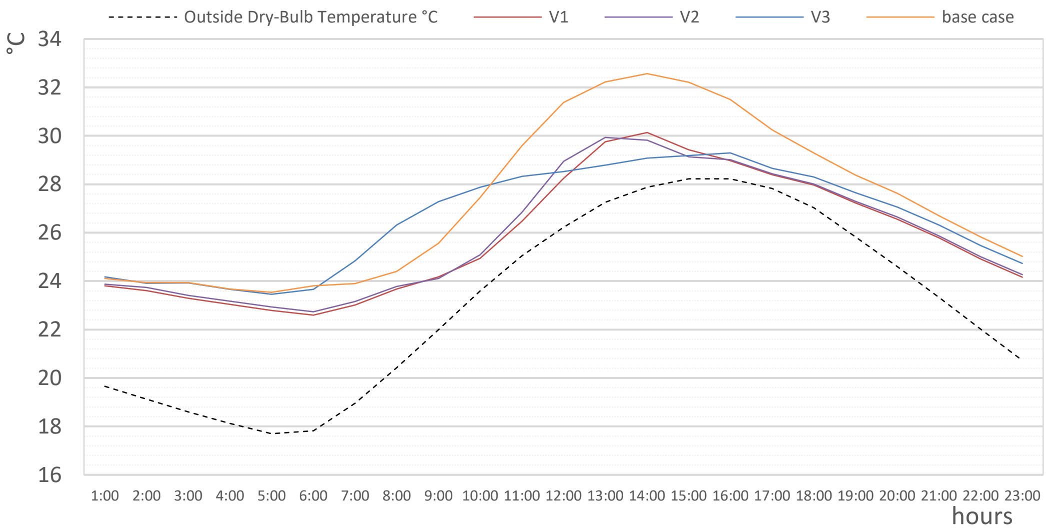

Figure 182. Simulated indoor air temperatures for the base case scenario BC and scenarios of "III Category": V1, V2 and V3 together with the dry-bulb temperature from the weather file 3rd August in south direction

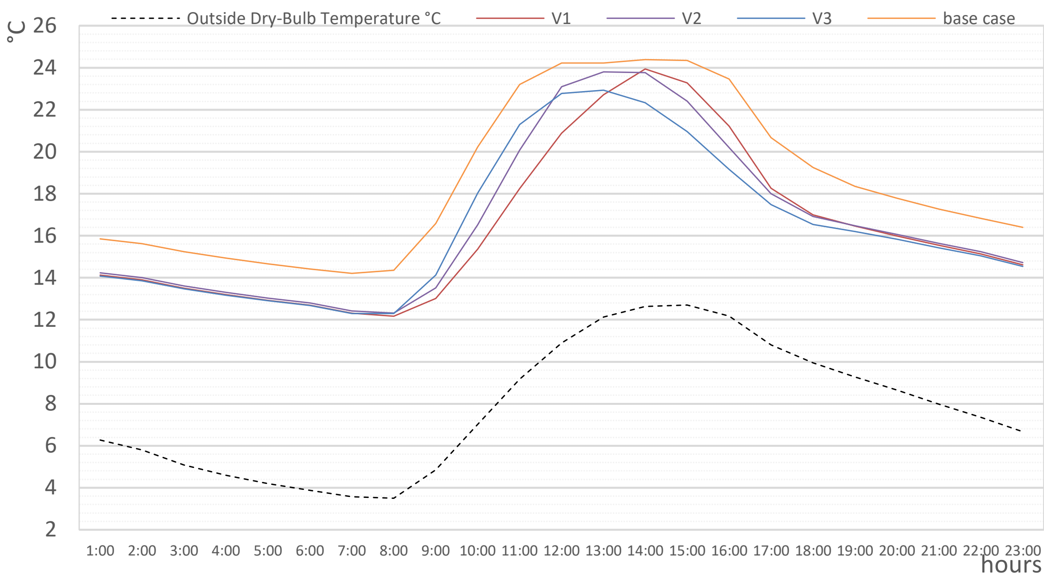

Figure 183. Simulated indoor air temperatures for the base case scenario BC and scenarios of "III Category": V1, V2 and V3 together with the dry-bulb temperature from the weather file 4th January in south direction

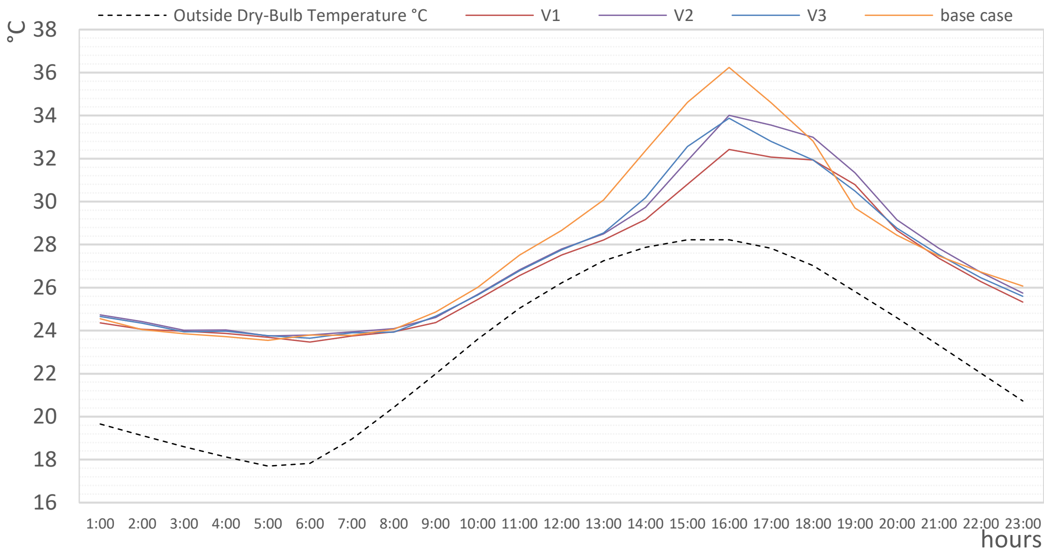

Figure 184. Simulated indoor air temperatures for the base case scenario BC and scenarios of "III Category": V1, V2 and V3 together with the dry-bulb temperature from the weather file 3rd August in west direction

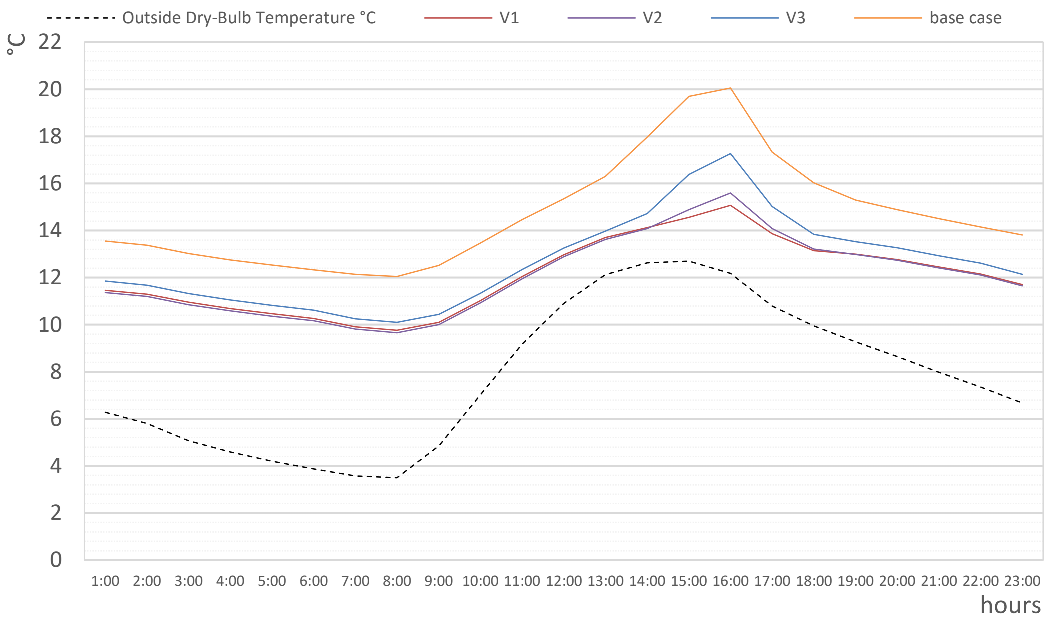

Figure 185. Simulated indoor air temperatures for the base case scenario BC and scenarios of "III Category": V1, V2 and V3 together with the dry-bulb temperature from the weather file 4th January in west direction

Indoor air temperature results for "I Category", "II Category" and "III Category" analyzed together. ***Figure 186*** and ***Figure 187*** show the indoor air temperature results for the base case (BC) and EC1, EC2, HO, VO, H1, H2, V1, V2, V3 scenarios analyzed for both summer and winter period in east orientation. ***Figure 188*** and ***Figure 189*** show the indoor air temperature results for the base case (BC) and EC1, EC2, HO, VO, H1, H2, V1, V2, V3 scenarios analyzed for both summer and winter period in south orientation. ***Figure 190*** and ***Figure 191*** show the indoor air temperature results for the base case (BC) and EC1, EC2, HO, VO, H1, H2, V1, V2, V3 scenarios analyzed for both summer and winter period in west orientation.

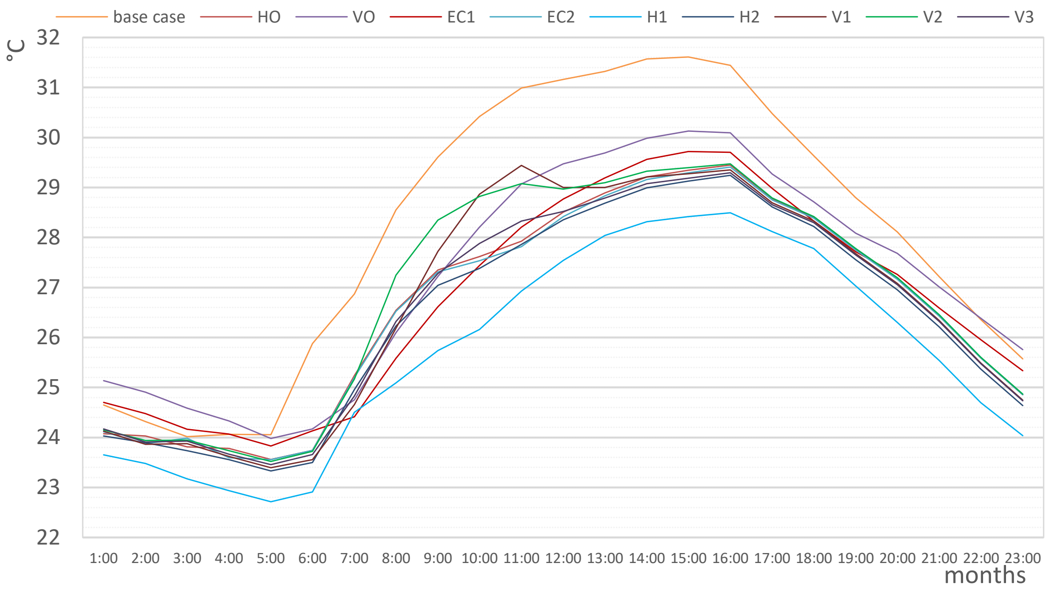

Figure 186. Simulated indoor air temperatures for the base case scenario BC and scenarios of "I Category", "II Category" and "III Category" from the weather file 3rd August in east direction

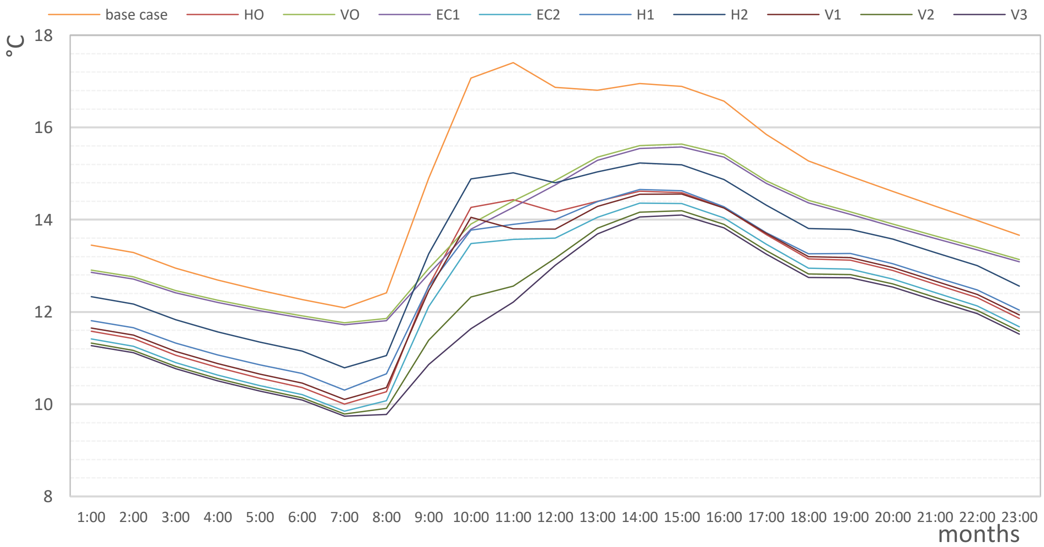

Figure 187. Simulated indoor air temperatures for the base case scenario BC and scenarios of "I Category", "II Category" and "III Category" from the weather file 4th January in east direction

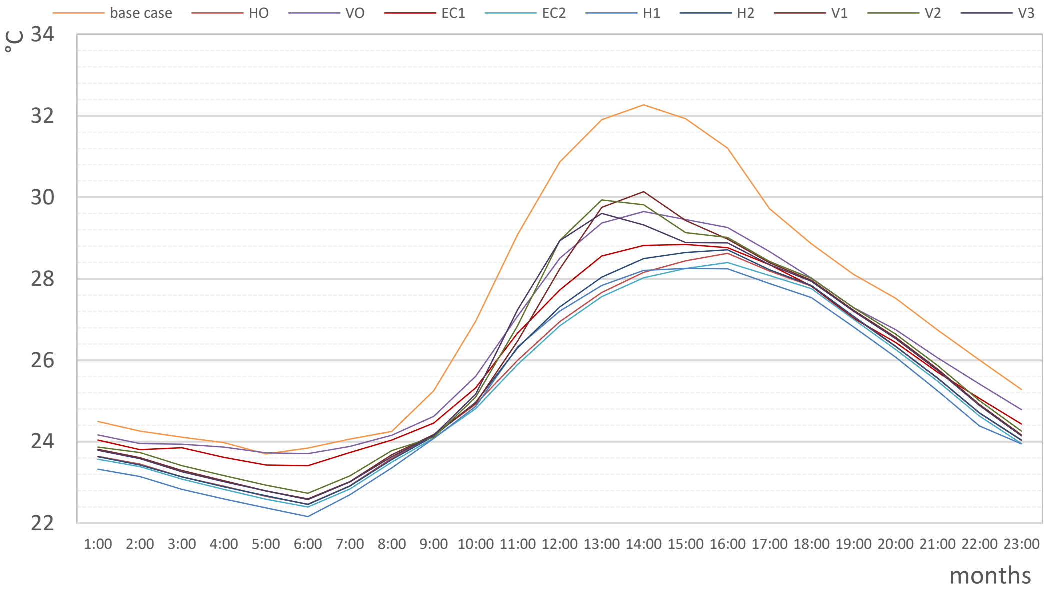

Figure 188. Simulated indoor air temperatures for the base case scenario BC and scenarios of "I Category", "II Category" and "III Category" from the weather file 3rd August in south direction

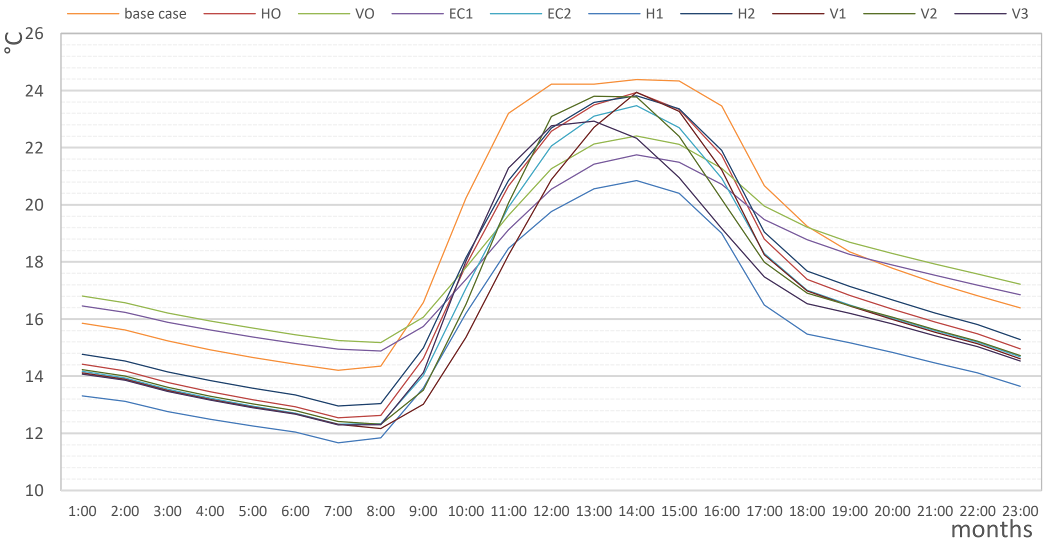

Figure 189. Simulated indoor air temperatures for the base case scenario BC and scenarios of "I Category", "II Category" and "III Category" from the weather file 4th January in south direction

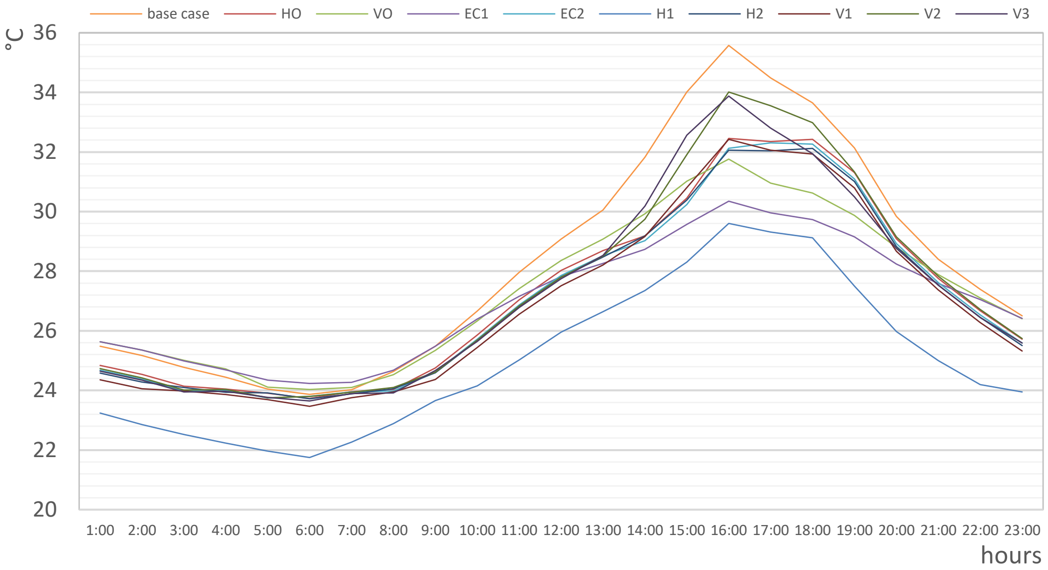

Figure 190. Simulated indoor air temperatures for the base case scenario BC and scenarios of "I Category", "II Category" and "III Category" from the weather file 3rd August in west direction

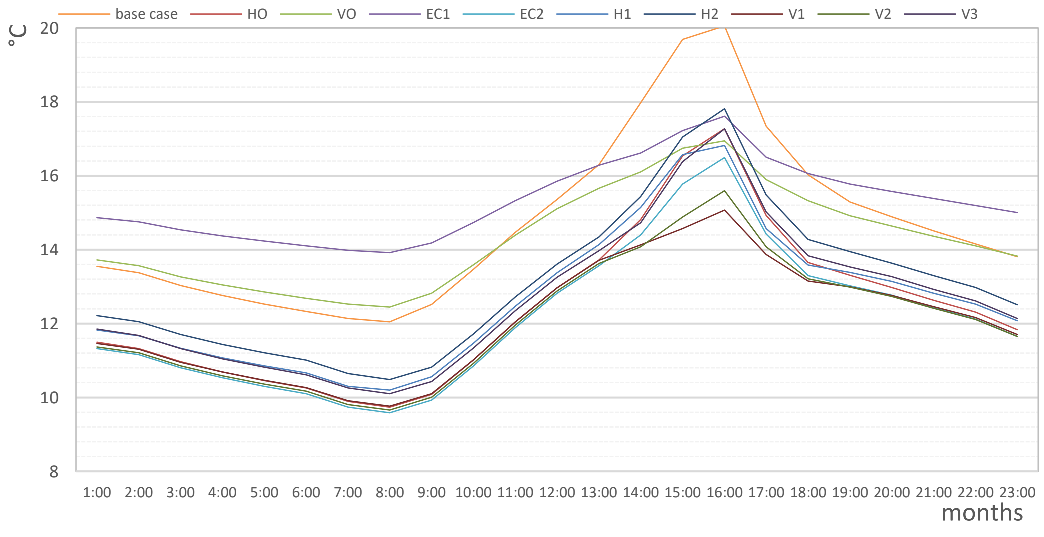

Figure 191. Simulated indoor air temperatures for the base case scenario BC and scenarios of "I Category", "II Category" and "III Category" from the weather file 4th January in west direction

4.5.2 Energy performance

Simulated heating and cooling loads results, for “I Category”, “II Category”, and “III Category” in east, south and west orientation are analyzed. First, the "I Category" results are analyzed, followed by the "II Category" and "III Category" results. Finally, all of the scenarios together for the Naples climate.

“I Category”: ***Figure 192*** and ***Figure 193*** shows the energy consumption for heating and cooling for the base case (BC) and EC1, EC2, HO and VO scenarios in east orientation. ***Figure 194*** and ***Figure 195*** shows the energy consumption for heating and cooling for the base case (BC) and EC1, EC2, HO and VO scenarios in south orientation. ***Figure 196*** and ***Figure 197*** shows the energy consumption for heating and cooling for the base case (BC) and EC1, EC2, HO and VO scenarios in west orientation.

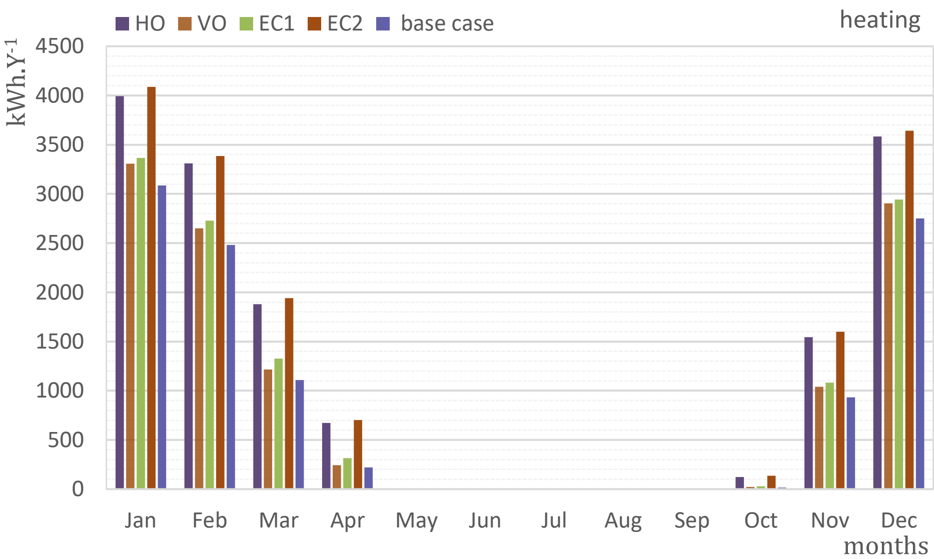

Figure 192. Comparision of simulated heating loads (kWh.Y^{-1}) of the base case scenario BC and scenarios of “I Category”: HO, VO, EC1 and EC2 in east orientation

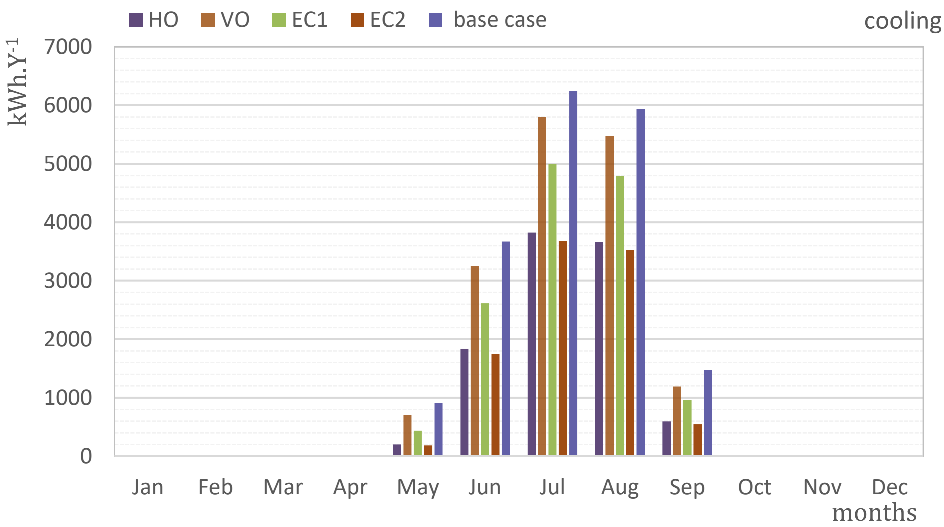

Figure 193. Comparision of simulated cooling loads (kWh.Y^{-1}) of the base case scenario BC and scenarios of "I Category": HO, VO, EC1 and EC2 in east orientation

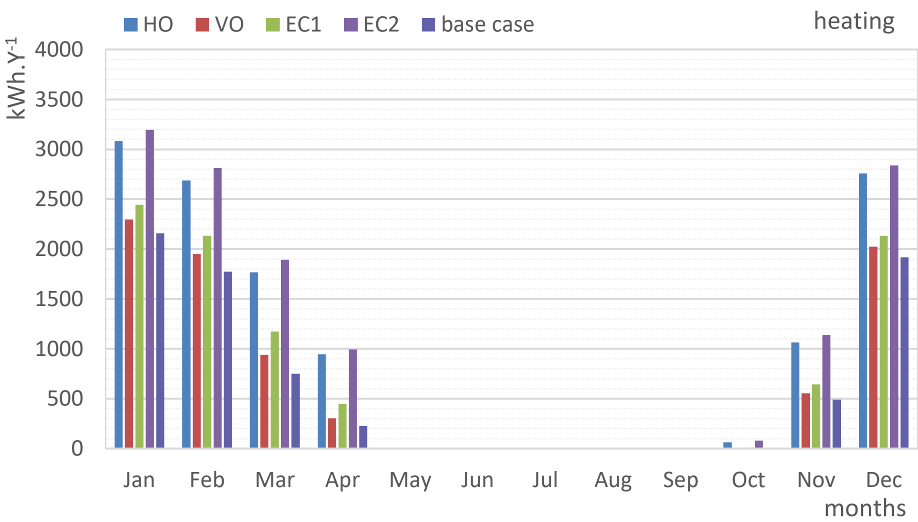

Figure 194. Comparision of simulated heating loads (kWh.Y^{-1}) of the base case scenario BC and scenarios of "I Category": HO, VO, EC1 and EC2 in south orientation

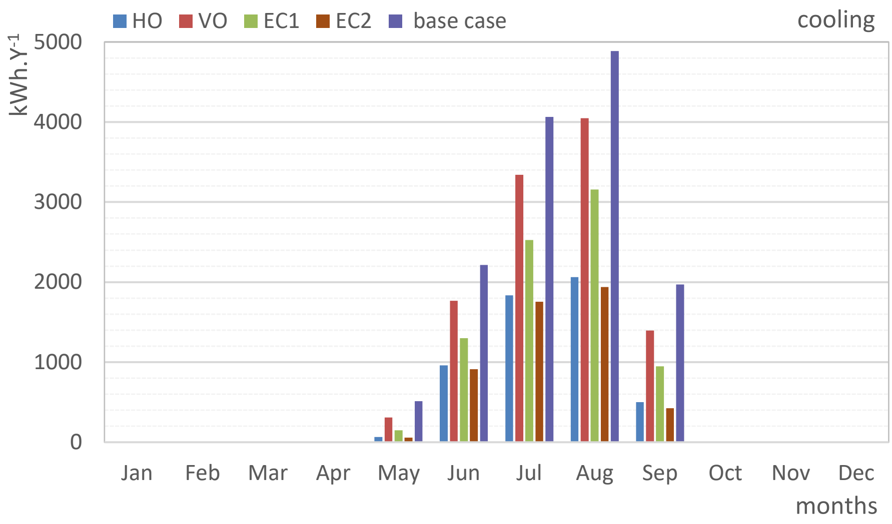

Figure 195. Comparision of simulated cooling loads (kWh.Y^{-1}) of the base case scenario BC and scenarios of "I Category": HO, VO, EC1 and EC2 in south orientation

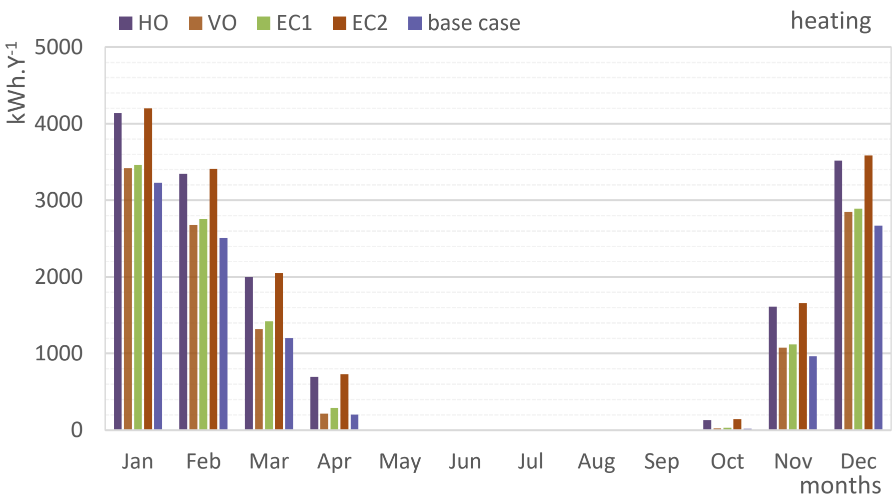

Figure 196. Comparision of simulated heating loads (kWh.Y^{-1}) of the base case scenario BC and scenarios of "I Category": HO, VO, EC1 and EC2 in west orientation

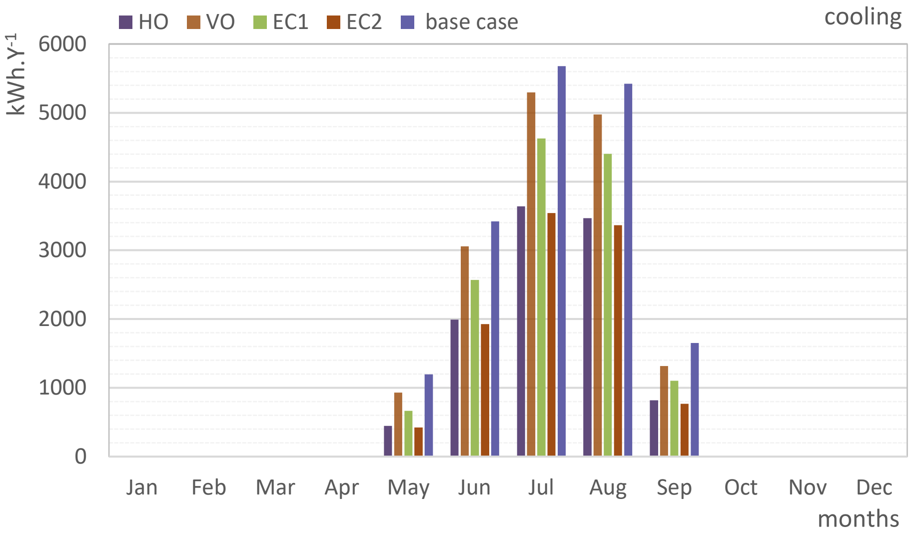

Figure 197. Comparision of simulated cooling loads (kWh.Y^{-1}) of the base case scenario BC and scenarios of "I Category": HO, VO, EC1 and EC2 in west orientation

"II Category": ***Figure 198*** and ***Figure 199*** shows the energy consumption for heating and cooling for the base case (BC) and H1, H2 scenarios in east orientation. ***Figure 200*** and ***Figure 201*** shows the energy consumption for heating and cooling for the base case (BC) and H1, H2 scenarios in south orientation. ***Figure 202*** and ***Figure 203*** shows the energy consumption for heating and cooling for the base case (BC) and H1, H2 scenarios in west orientation.

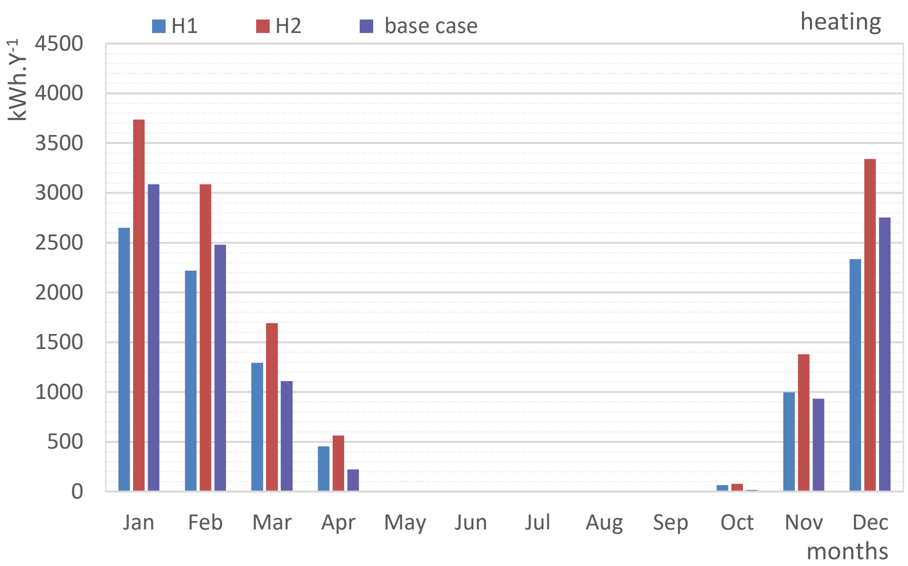

Figure 198. Comparision of simulated heating loads (kWh.Y^{-1}) of the base case scenario BC and scenarios of "II Category": H1 and H2 in east orientation

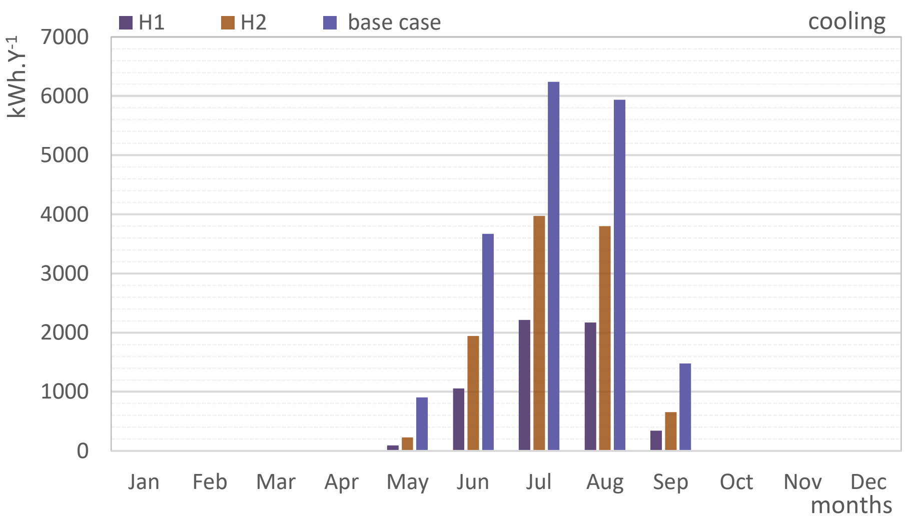

Figure 199. Comparision of simulated cooling loads (kWh.Y^{-1}) of the base case scenario BC and scenarios of "II Category": H1 and H2 in east orientation

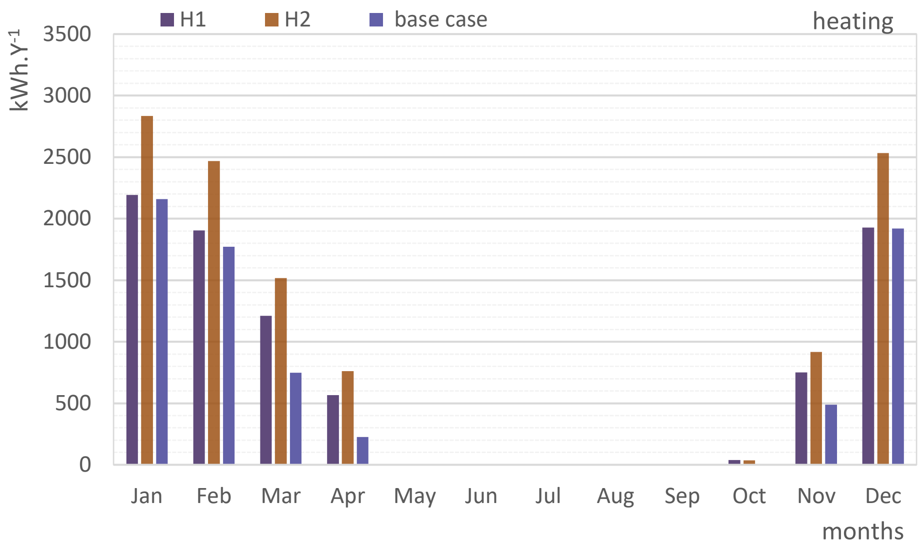

Figure 200. Comparision of simulated heating loads (kWh.Y^{-1}) of the base case scenario BC and scenarios of “II Category”: H1 and H2 in south orientation

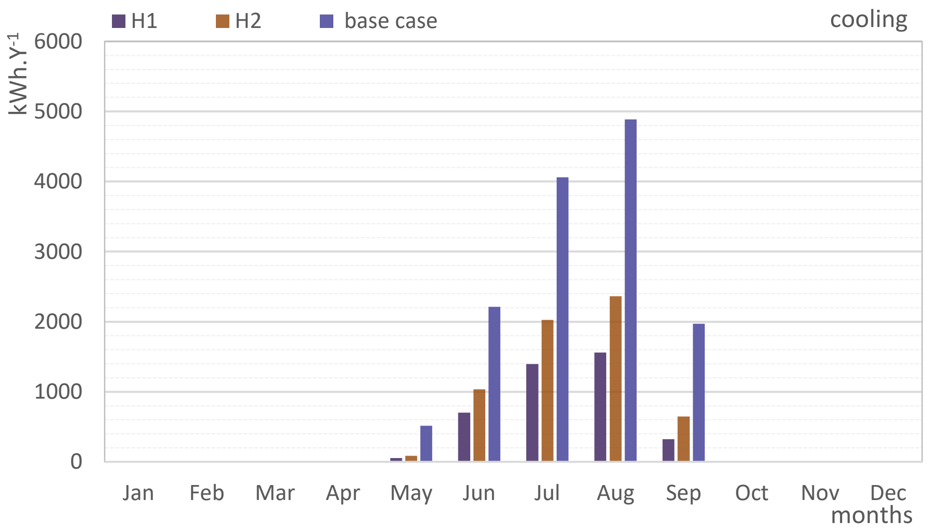

Figure 201. Comparision of simulated cooling loads (kWh.Y^{-1}) of the base case scenario BC and scenarios of “II Category”: H1 and H2 in south orientation

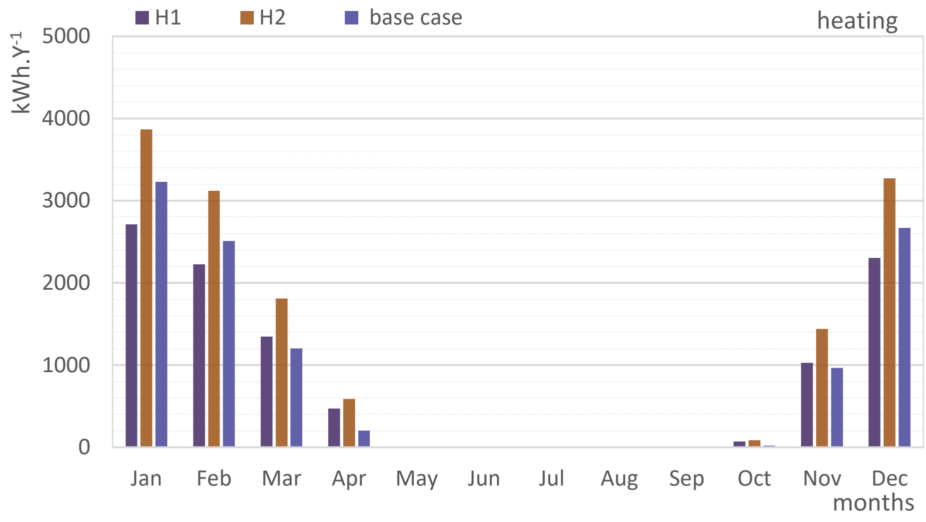

Figure 202. Comparision of simulated heating loads (kWh.Y^{-1}) of the base case scenario BC and scenarios of “II Category”: H1 and H2 in west orientation

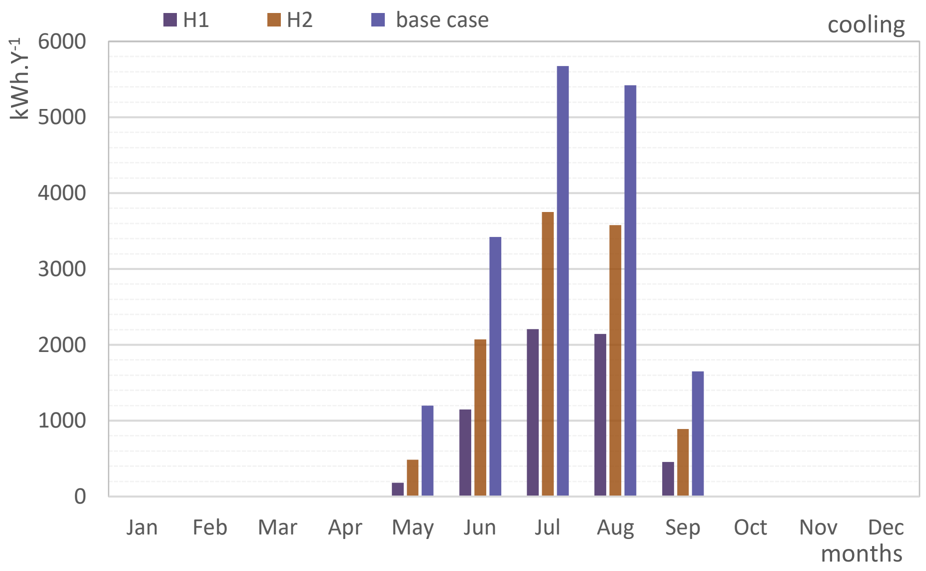

Figure 203. Comparision of simulated cooling loads (kWh.Y^{-1}) of the base case scenario BC and scenarios of “II Category”: H1 and H2 in west orientation

“III Category”: ***Figure 204*** and ***Figure 205*** shows the energy consumption for heating and cooling for the base case (BC) and V1, V2, V3 scenarios in east orientation. ***Figure 206*** and ***Figure 207*** shows the energy consumption for heating and cooling for the base case (BC) and V1, V2, V3 scenarios in south orientation. ***Figure 208*** and ***Figure 209*** shows the energy consumption for heating and cooling for the base case (BC) and V1, V2, V3 scenarios in west orientation.

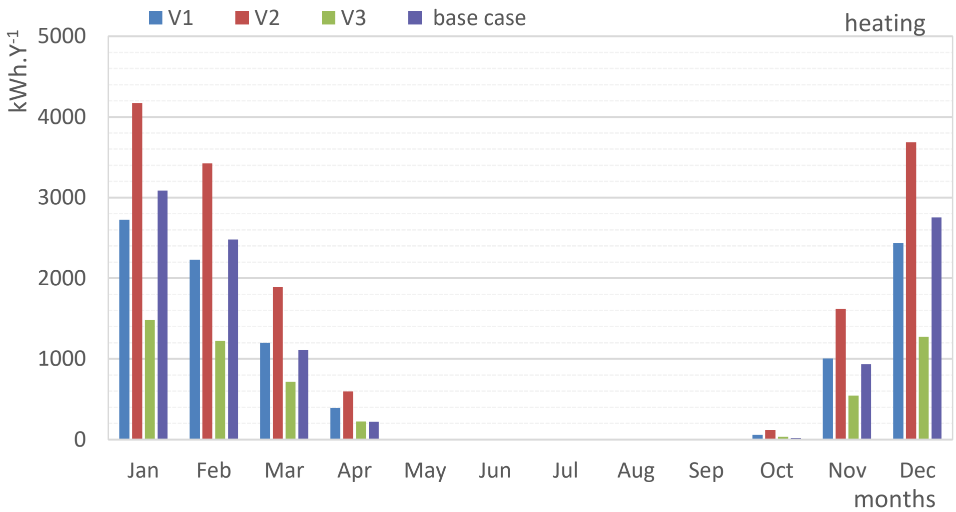

Figure 204. Comparision of simulated heating loads (kWh.Y^{-1}) of the base case scenario BC and scenarios of “III Category”: V1, V2 and V3 in east orientation

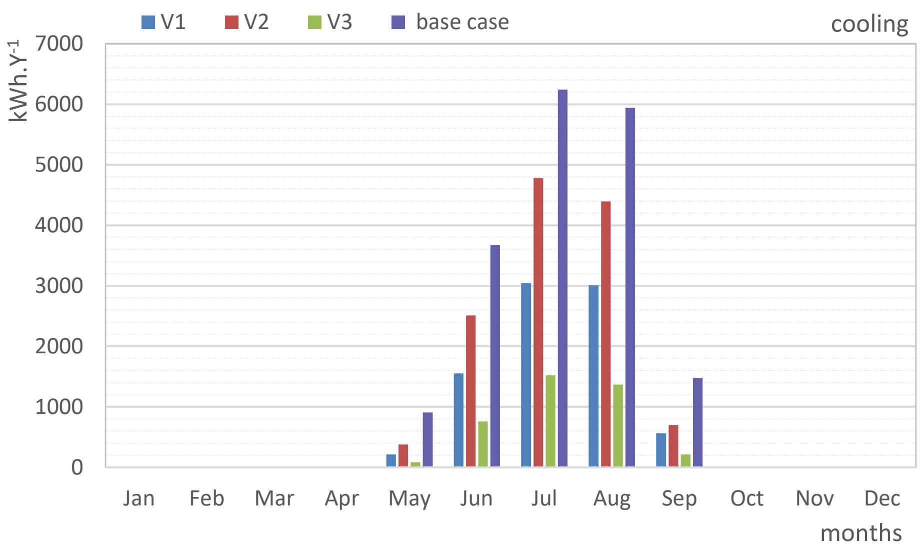

Figure 205. Comparision of simulated cooling loads (kWh.Y^{-1}) of the base case scenario BC and scenarios of "III Category": V1, V2 and V3 in east orientation

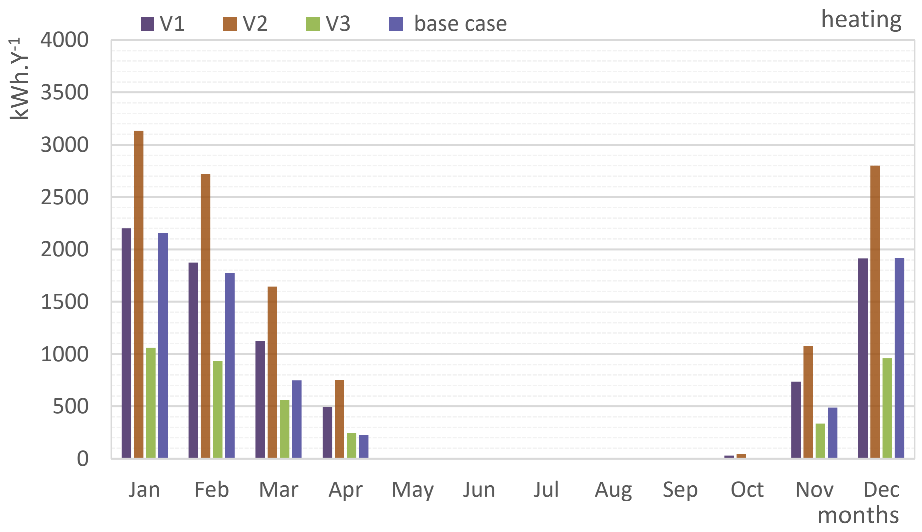

Figure 206. Comparision of simulated heating loads (kWh.Y^{-1}) of the base case scenario BC and scenarios of "III Category": V1, V2 and V3 in south orientation

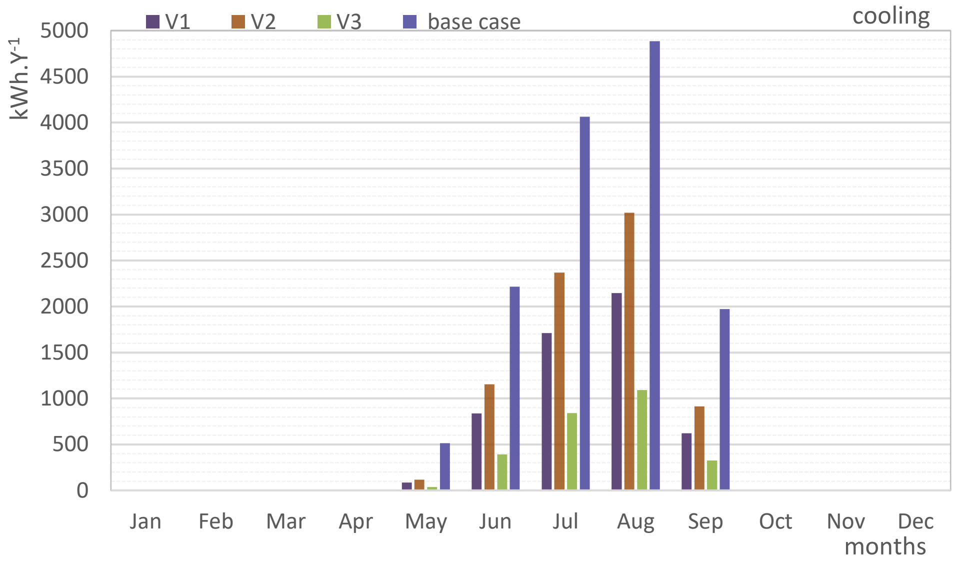

Figure 207. Comparision of simulated cooling loads (kWh.Y^{-1}) of the base case scenario BC and scenarios of “III Category”: V1, V2 and V3 in south orientation

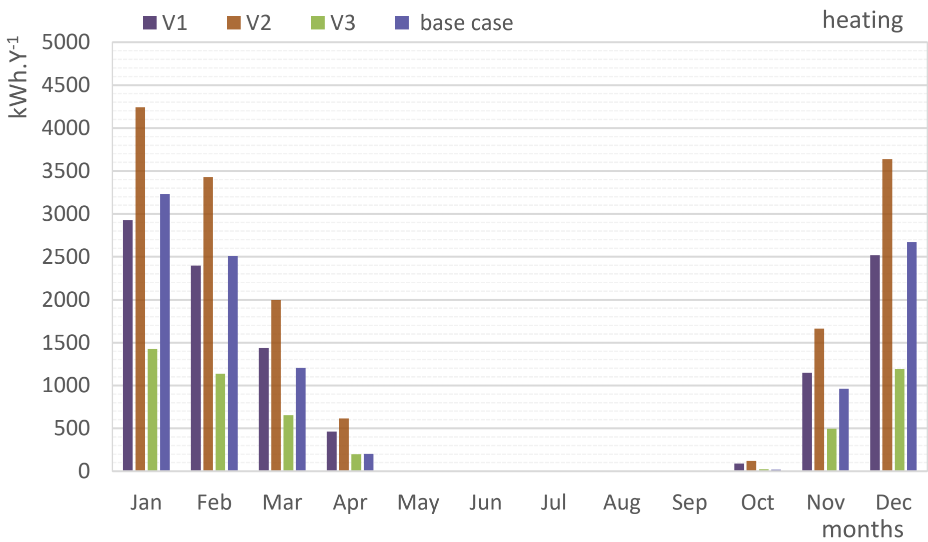

Figure 208. Comparision of simulated heating loads (kWh.Y^{-1}) of the base case scenario BC and scenarios of “III Category”: V1, V2 and V3 in west orientation

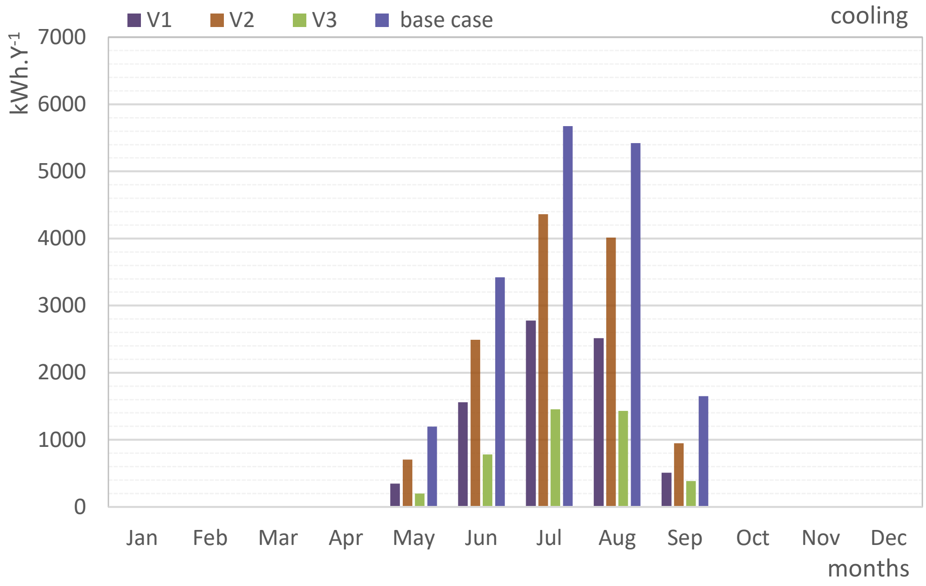

Figure 209. Comparision of simulated cooling loads (kWh.Y^{-1}) of the base case scenario BC and scenarios of "III Category": V1, V2 and V3 in west orientation

Energy consumption for heating and cooling loads for "I Category", "II Category" and "III Category" are analyzed together. ***Figure 210*** and ***Figure 211*** show heating and cooling loads results for the base case (BC) and EC1, EC2, HO, VO, H1, H2, V1, V2, V3 scenarios in east orientation. ***Figure 212*** and ***Figure 213*** show heating and cooling loads results for the base case (BC) and EC1, EC2, HO, VO, H1, H2, V1, V2, V3 scenarios in south orientation. ***Figure 214*** and ***Figure 215*** show heating and cooling loads results for the base case (BC) and EC1, EC2, HO, VO, H1, H2, V1, V2, V3 scenarios in west orientation.

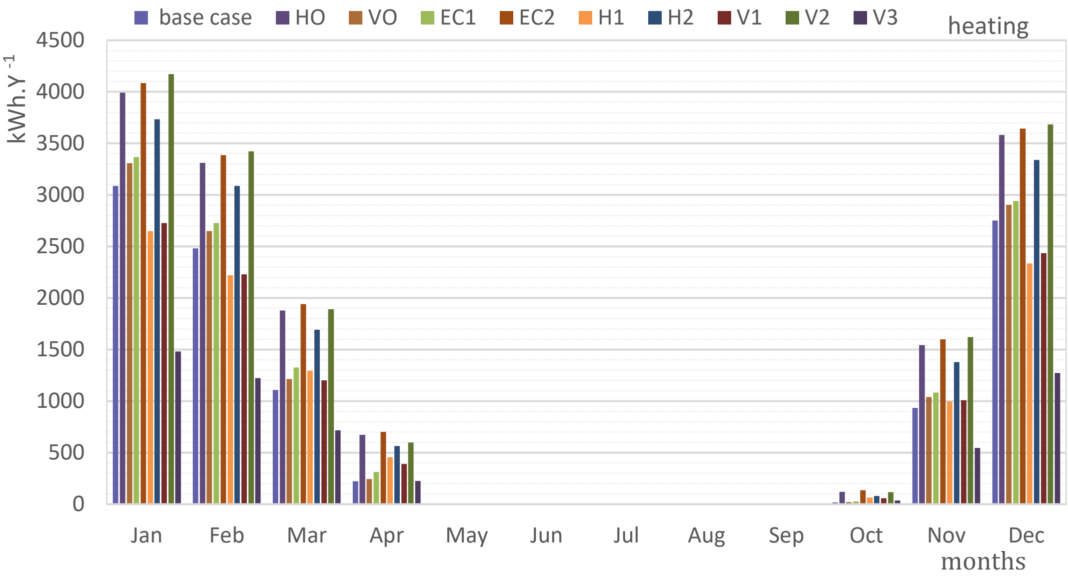

Figure 210. Comparison of simulated heating loads (kWh.Y^{-1}) of the base case scenario BC and scenarios of "I Category", "II Category" and "III Category" in east orientation

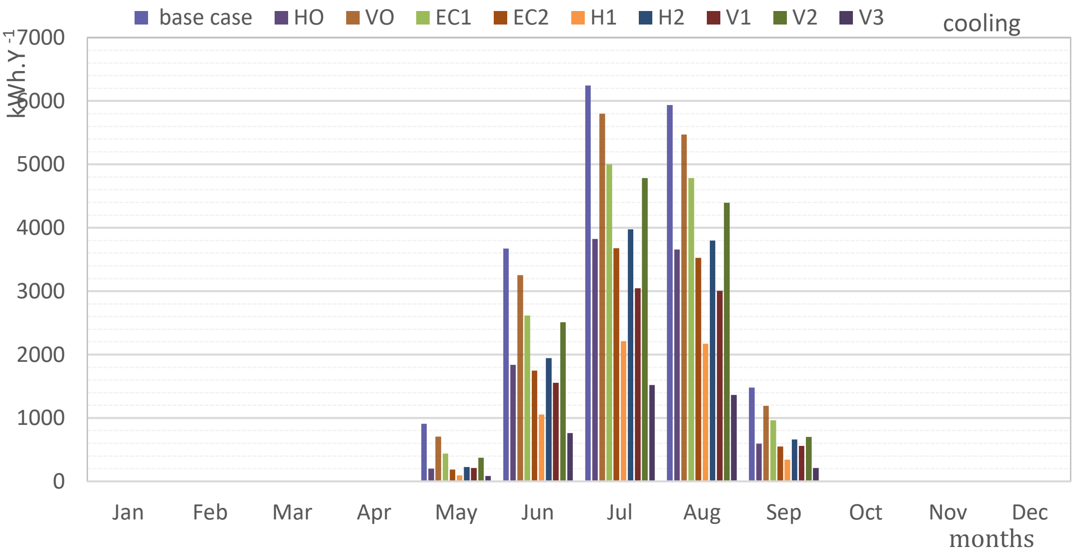

Figure 211. Comparison of simulated cooling loads (kWh.Y^{-1}) of the base case scenario BC and scenarios of "I Category", "II Category" and "III Category" in east orientation

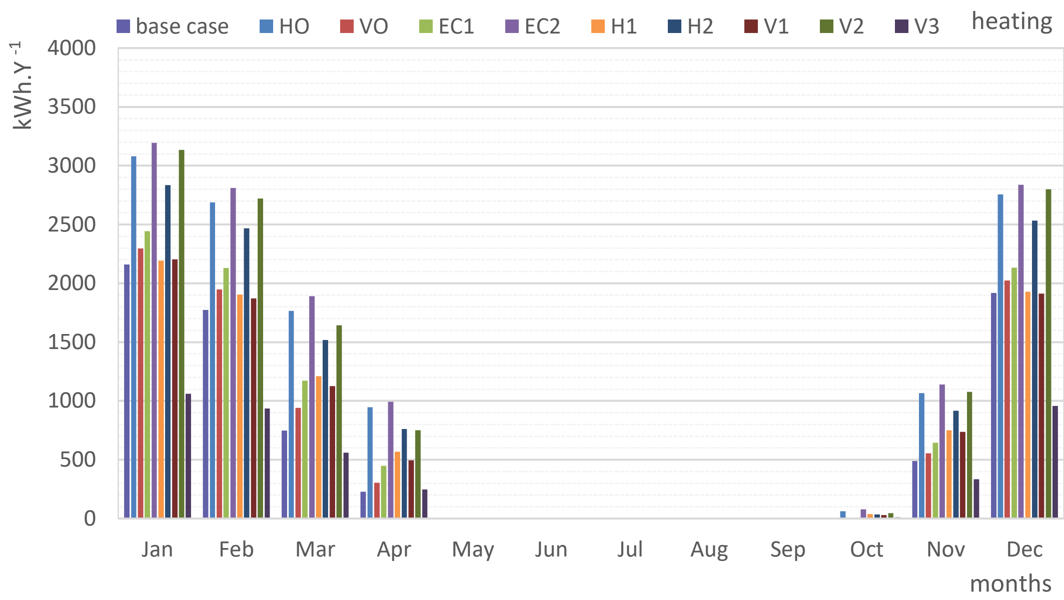

Figure 212. Comparison of simulated heating loads (kWh.Y^{-1}) of the base case scenario BC and scenarios of "I Category", "II Category" and "III Category" in south orientation

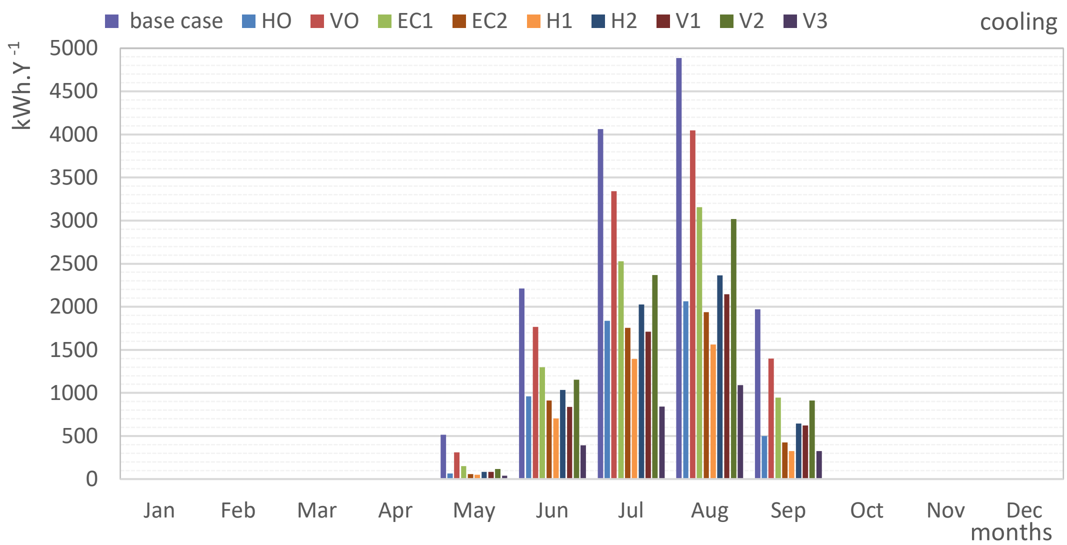

Figure 213. Comparison of simulated cooling loads (kWh.Y^{-1}) of the base case scenario BC and scenarios of "I Category", "II Category" and "III Category" in south orientation

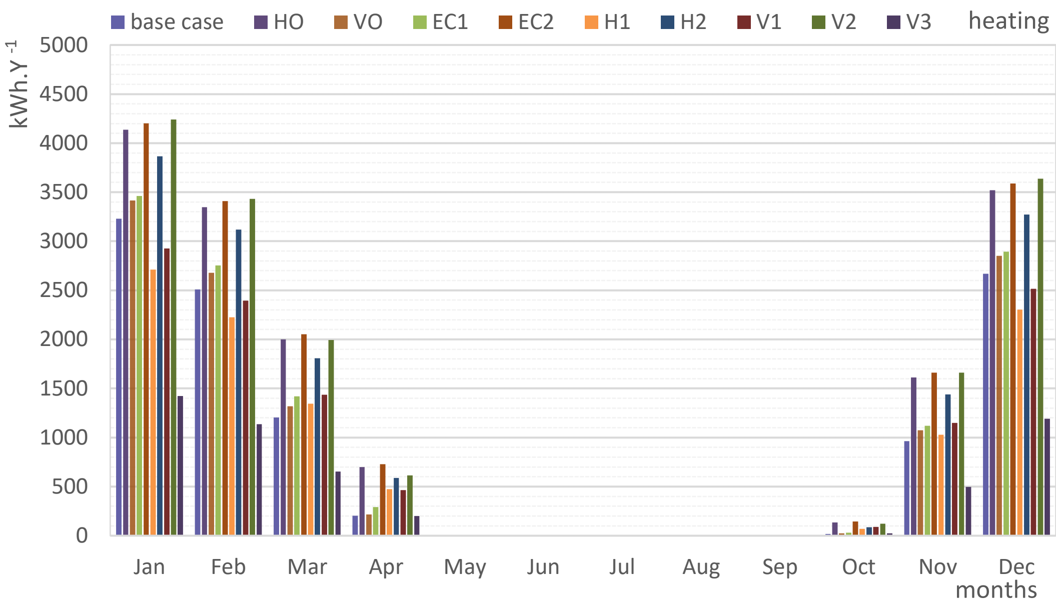

Figure 214. Comparison of simulated heating loads (kWh.Y^{-1}) of the base case scenario BC and scenarios of "I Category", "II Category" and "III Category" in west orientation

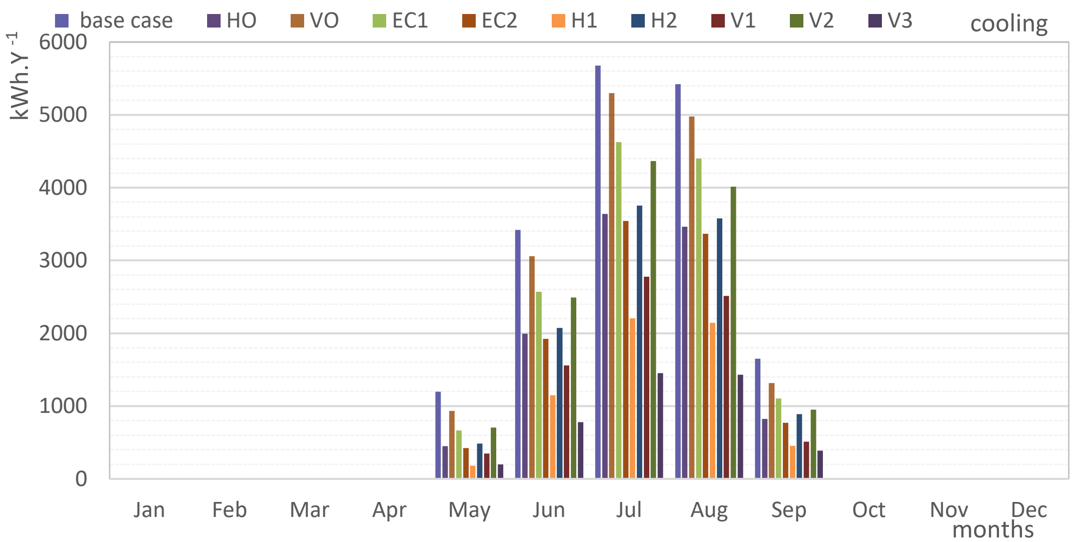

Figure 215. Comparison of simulated cooling loads (kWh.Y^{-1}) of the base case scenario BC and scenarios of "I Category", "II Category" and "III Category" in west orientation

CHAPTER 5

DISCUSSIONS

5.1 Tirana, Albania

5.1.1. Indoor air temperature

The proposed scenarios belong to three different categories of shading design. To begin with, an analysis of the results within each category is conducted, followed by a ranking of all proposed scenarios. The simulation results show that within the "I Category" scenarios (HO, VO, EC1 and EC2) have different impact depending on the east south or west orientation for a typical summer day (refer to ***Figure 21***, ***Figure 23*** and ***Figure 25***). In the east and west orientation, a decrease in air temperature up to 2.72 °C and 3.51 °C with the impact of EC1 scenario. While in the south a decrease up to 3.86 degrees with the HO scenario (see ***Table 9***).

The simulation results show that within the scenarios of "II Category" (H1 and H2) the one that has a better performance is H1 with a decrease in air temperature up to 3.47 °C (see ***Table 9***).

The simulation results show that the "III Category" scenarios (V1, V2 and V3) have different impact depending on the east south or west orientation for a selected summer day (refer to ***Figure 29***, ***Figure 31*** and ***Figure 33***). In the east orientation what performs better is V3 with an air temperature decrease up to 2.41 °C while in the south and west orientation the scenario that performs better is V1 with an air temperature decrease up to 2.44 °C south and 2.62 °C west (see ***Table 9***).

A comparison of simulation results within categories was made. What also interests us in further studies is which of all these scenarios performs best and which is most appropriate for a particular orientation making that and within a given situation in future proposals may have a combination of them depending on the orientation.

According to the above detailed analysis for each category we can make a selection of the best scenario and the one which has less impact for a selected summer day. In the east and west orientation, the one that has the greatest impact in lowering the temperature is H1 with 3.47 °C and in the south direction it is EC2 4.17 °C (refer to ***Table 9***). However, for all scenarios no significant change in temperature is registered in east, south and east orientation for a typical winter day.

Table 9. Simulation results of air temperature for a typical summer day (3rd August)

	East, Peak hour; 9:00			**South, Peak hour; 12:00**			**West, Peak hour; 15:00**		
T[°C]	Exterior	Interior	ΔT	Exterior	Interior	ΔT	Exterior	Interior	ΔT
BC	22.12	29.60	**-7.48**	27.15	31.38	**-4.23**	29.33	34.62	**-5.29**
HO	22.12	27.13	**-5.01**	27.15	27.52	**-0.37**	29.33	31.71	**-2.38**
VO	22.12	27.37	**-5.25**	27.15	29.10	**-1.95**	29.33	31.97	**-2.65**
EC1	22.12	26.88	**-4.76**	27.15	28.23	**-1.08**	29.33	31.10	**-1.78**
EC2	22.12	27.24	**-5.12**	27.15	27.46	**-0.31**	29.33	31.27	**-1.94**
H1	22.12	26.13	**-4.01**	27.15	27.75	**-0.60**	29.33	30.33	**-1.01**
H2	22.12	27.03	**-4.91**	27.15	27.85	**-0.70**	29.33	31.27	**-1.95**
V1	22.12	28.01	**-5.89**	27.15	28.94	**-1.79**	29.33	32.00	**-2.67**
V2	22.12	28.33	**-6.21**	27.15	29.38	**-2.23**	29.33	33.25	**-3.92**
V3	22.12	27.19	**-5.07**	27.15	29.33	**-2.18**	29.33	33.66	**-4.34**

5.1.2. Energy performance

An overall comparative analysis of monthly heating, cooling and total loads for three categories is carried out as follows. As illustrated in ***Figure 216*** no significant improvement in heating performance during cold months (January, February, March, April, October, November, December) is noted with the use of HO, VO, EC1, EC2, and V2 scenarios in east, south and west orientation. However, a significant decrease in heating energy consumption with 8% up to 53% is registered with H1, V1, and V3 scenario (refer to ***Table 10***). The position and angle of H1, V1, and V3 shading devices design bring more heat gain into the building during cold months.

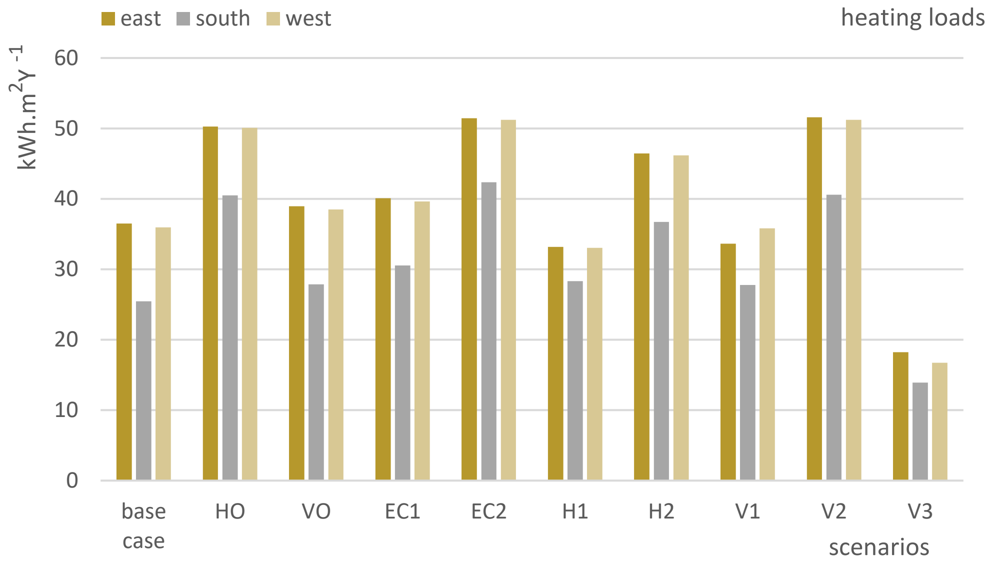

Figure 216. Comparison of simulated yearly heating loads (kWh.m^2.Y^{-1}) of the base case scenario all scenarios

Table 10. Shading effectiveness [%] for heating loads in east, south and west direction.

Scenarios	EAST	SOUTH	WEST
BC	-	-	-
HO	37.73	59.05	39.26
VO	6.77	9.43	7.02
EC1	9.92	19.82	10.25
EC2	40.97	66.24	17.76
H1	-9.01	11.15	-8.10
H2	27.32	44.19	28.34
V1	-7.80	9.06	-0.40
V2	41.44	59.33	42.43
V3	-50.06	-45.44	-53.50

0%; -20%	-20%; -40%	-40%; -60%	-60%; -80%
0%; +20%	+20%; +40%	+40%; +60%	+60%; +80%

The benefit of shade was proven during the peak summer months from May to September. As illustrated in ***Figure 217*** significant improvement in cooling performance during warm months (May, June, July, August, September) is noted with the use of all shading design scenarios in east, south and west orientation. However, a significant decrease in cooling energy consumption with 77.9% is registered V3 scenario (refer to ***Table 11***). Vertical fins provide privacy, which is a necessary characteristic in a hotel's bedrooms. A combination of vertical fins and horizontal overhangs also contributes to a self-shading envelope, which may be easily integrated early in the design process (Alhuwayil et. al., 2018).

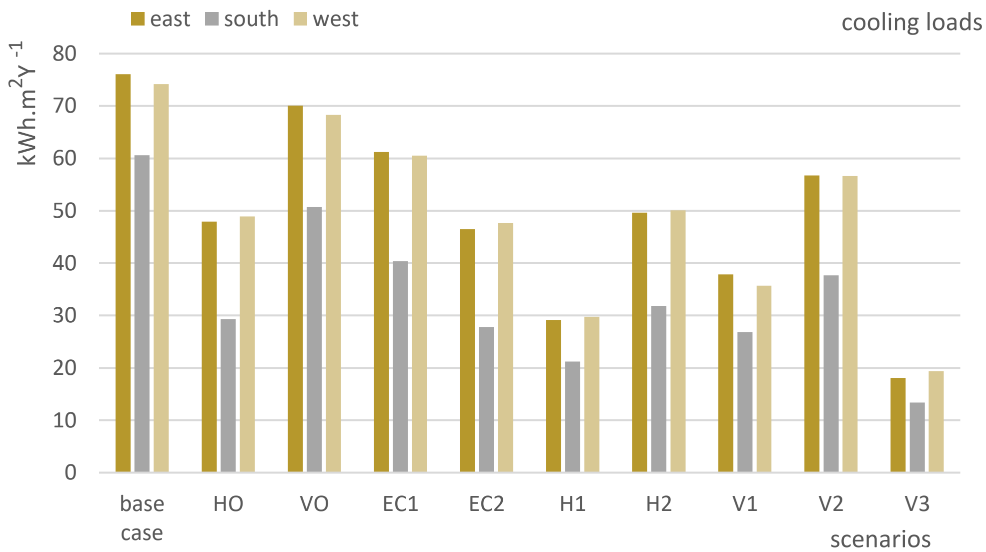

Figure 217. Comparison of simulated yearly cooling loads (kWh.m^2.Y^{-1}) of the base case scenario all scenarios

Table 11. Shading effectiveness [%] for cooling loads in east, south and west direction.

Scenarios	EAST	SOUTH	WEST
BC	-	-	-
HO	-33.93	-51.70	-34.04
VO	-7.85	-16.31	-7.97
EC1	-19.49	-33.38	-18.43
EC2	-32.37	-54.07	-62.49
H1	-61.67	-64.95	-59.90
H2	-34.73	-47.40	-32.50
V1	-50.23	-55.73	-51.89
V2	-25.39	-37.83	-23.66
V3	-76.23	-77.95	-73.87

0%; -20%	-20%; -40%	-40%; -60%	-60%; -80%

Furthermore, a panoramic comparison of annual heating load, cooling load, total energy consumption, and savings in cooling load and total energy consumption with respect to the base case for all shading devices, in east south and west orientation is presented in ***Table 12*** and ***Figure 218***. There is dramatic increase in heating load of the base case in all cases, but this did not affect the saving in the total energy consumption. This is attributed to the fact that, as per the prevailing climate of the study area, the heating load of the building is low (6-59%) compared to the cooling load (76-80%) (see ***Table 13***). Therefore, the impact of external shading devices on cooling load is highly significant compared to the heating load. This ascertains the fact that the choice of proper shading strategy of a building depends mainly on the climatic location. For instance, in a cooling dominated climate, attention should be given to reducing the cooling load, and vice versa in a heating dominated climate (Alhuwayil et. al., 2018). The reduction in heat loss from the building (higher heat retention rate) can also be seen attributable to the significantly reduced U-values of the external wall and roof (due to improved insulation).

Table 12. Annual simulation results obtained for all the scenarios

	Annual heating demand			**Annual cooling demand**			**Annual energy demand**		
	Total heating [kWh]	Heating/ conditioned area [kWh/m2]	Shading effective-ness [%]	Total cooling [kWh]	Cooling/ conditioned area [kWh/m2]	Shading effective-ness [%]	Total energy demand [kWh]	Total energy/ conditioned area [kWh/m2]	Total Shading effectiveness [%]
BC_E	11893.38	36.48	-	24793.00	76.05	-	36686.38	112.54	-
HO_E	16380.87	50.25	**37.73**	16380.87	50.25	**-33.93**	32005.56	98.18	**-12.76**
VO_E	12698.93	38.95	**6.77**	22847.95	70.09	**-7.85**	35546.89	109.04	**-3.11**
EC1_E	13072.84	40.10	**9.92**	19960.09	61.23	**-19.49**	33032.92	101.33	**-9.96**
EC2_E	16766.47	51.43	**40.97**	15140.66	51.43	**-32.37**	31907.13	97.88	**-13.03**
H1_E	10822.34	33.20	**-9.01**	9503.93	29.15	**-61.67**	20326.27	62.35	**-44.59**
H2_E	15142.54	46.45	**27.32**	16183.10	49.64	**-34.73**	31325.64	96.09	**-14.61**
V1_E	10965.71	33.64	**-7.80**	12340.38	37.86	**-50.23**	23306.09	71.49	**-36.47**
V2_E	16822.53	51.60	**41.44**	18498.34	56.75	**-25.39**	35320.87	108.35	**-3.72**
V3_E	5939.72	18.22	**-50.06**	5893.82	18.08	**-76.23**	11833.54	36.30	**-67.74**
BC_S	8305.01	25.48	-	19747.66	60.58	-	28052.67	86.05	-
HO_S	13208.90	40.52	**59.05**	9537.65	29.26	**-51.70**	22746.55	69.78	**-18.91**
VO_S	9088.39	27.88	**9.43**	16527.11	50.70	**-16.31**	25615.50	78.58	**-8.69**
EC1_S	9951.32	30.53	**19.82**	13155.03	40.35	**-33.38**	23106.36	70.88	**-17.63**
EC2_S	13806.26	42.35	**66.24**	9069.26	27.82	**-54.07**	22875.51	70.17	**-18.46**
H1_S	9230.92	28.32	**11.15**	6920.88	21.23	**-64.95**	16151.80	49.55	**-42.42**
H2_S	11974.70	36.73	**44.19**	10387.09	31.86	**-47.40**	22361.78	68.60	**-20.29**
V1_S	9057.42	27.78	**9.06**	8742.29	26.82	**-55.73**	17799.71	54.60	**-36.55**
V2_S	13232.73	40.59	**59.33**	12276.80	37.66	**-37.83**	25509.53	78.25	**-9.07**
V3_S	4531.48	13.90	**-45.44**	4354.95	13.36	**-77.95**	8886.43	27.26	**-68.32**
BC_W	11724.50	35.97	-	24181.16	74.18	-	35905.66	110.14	-
HO_W	16328.09	50.09	**39.26**	15949.01	48.92	**-34.04**	32277.10	99.01	**-10.11**
VO_W	12547.71	38.49	**7.02**	22254.44	68.27	**-7.97**	34802.15	106.76	**-3.07**
EC1_W	12925.71	39.65	**10.25**	19725.31	60.51	**-18.43**	19725.31	60.51	**-45.06**
EC2_W	13806.26	42.35	**17.76**	9069.26	27.82	**-62.49**	22875.51	70.17	**-36.29**
H1_W	10774.92	33.05	**-8.10**	9697.07	29.75	**-59.90**	20471.99	62.80	**-42.98**
H2_W	15047.16	46.16	**28.34**	16323.17	50.07	**-32.50**	31370.33	96.23	**-12.63**
V1_W	11677.18	35.82	**-0.40**	11633.64	35.69	**-51.89**	23310.82	71.51	**-35.08**
V2_W	16699.29	51.23	**42.43**	18460.38	56.63	**-23.66**	35159.67	107.86	**-2.08**
V3_W	5451.58	16.72	**-53.50**	6319.19	19.38	**-73.87**	11770.77	36.11	**-67.22**

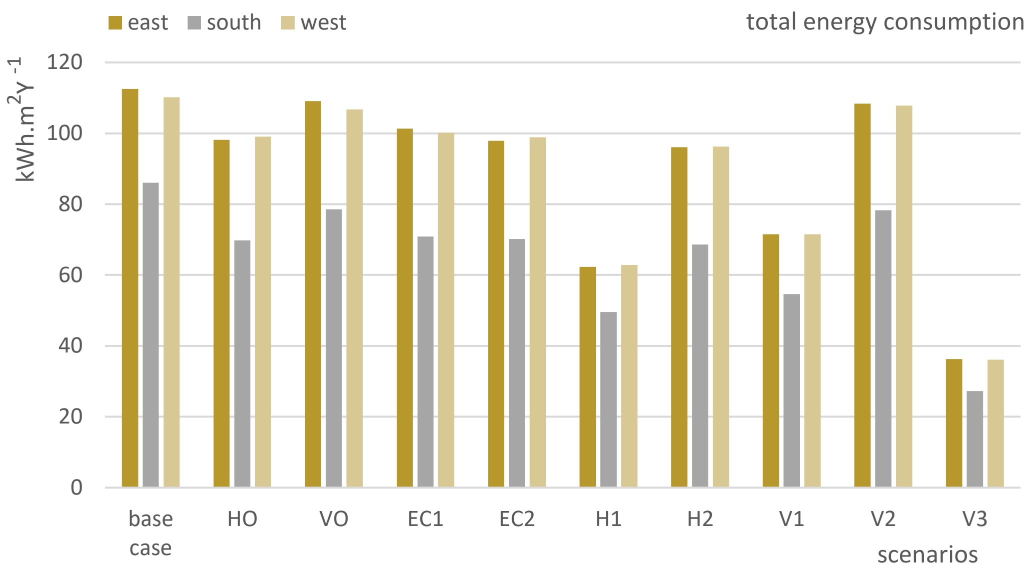

Figure 218. Comparison of simulated yearly total energy consumption (kWh.m^2.Y^{-1}) of the base case scenario all scenarios

Table 13. Total shading effectiveness [%] for total energy/conditioned area [kWh/m^2] in east, south and west direction.

Scenarios	EAST	SOUTH	WEST
BC	-	-	-
HO	-12.76	-18.91	-10.11
VO	-3.11	-8.69	-3.07
EC1	-9.96	-17.63	-45.06
EC2	-13.03	-18.46	-36.29
H1	-44.59	-42.42	-42.98
H2	-14.61	-20.29	-12.63
V1	-36.47	-36.55	-35.08
V2	-3.72	-9.07	-2.08
V3	-67.74	-68.32	-67.22
0%; -20%	-20%; -40%	-40%; -60%	-60%; -80%

5.2 Almeria, Spain

5.2.1. Indoor air temperature

The proposed scenarios belong to three different categories of shading design. To begin with, an analysis of the results within each category is conducted, followed by a ranking of all proposed scenarios. The simulation results show that within the "I Category" scenarios (HO, VO, EC1 and EC2) have different impact depending on the east south or west orientation for a typical summer day (refer to ***Figure 71***, ***Figure 73*** and ***Figure 75***). From the results we observe that the EC2 scenario performed better in all orientations for the first category. In the east, south and west orientation, a decrease in air temperature up to 5 °C, 2.75 °C and 2.66 °C with the impact of EC2 scenario (see ***Table 14***).

The simulation results show that within the "II Category", scenario H2 has the same impact in east and south direction for a selected summer day but in the west orientation the one that has a better performance is H1 with a decrease in air temperature up to 2.72 °C (see ***Table 14***).

The simulation results show that the "III Category" scenarios (V1, V2 and V3) have almost the same impact depending on the east south or west orientation for a selected summer day (refer to ***Figure 83***, ***Figure 84*** and ***Figure 85***). Different from other scenarios V1 has a better performance within this category in all directions with a decrease in temperature up to 2.58 °C (see ***Table 14***).

According to the above detailed analysis for each category we can make a selection of the best scenario and the one which has less impact for a selected summer day. In the east and south orientation, the one that has the greatest impact in lowering the temperature is EC2 with 5 °C and in the west direction it is H1 2.72 °C (see ***Table 14***). However, for all scenarios no significant change in temperature is registered in east, south and east orientation for a typical winter day.

Table 14. Simulation results of air temperature for a typical summer day (3rd August)

	East, Peak hour; 9:00			**South, Peak hour; 12:00**			**West, Peak hour; 15:00**		
T[°C]	Exterior	Interior	ΔT	Exterior	Interior	ΔT	Exterior	Interior	ΔT
BC	21.35	28.96	**-7.61**	24.83	28.80	**-3.98**	27.08	31.18	**-4.11**
HO	21.35	27.48	**-6.13**	24.83	26.10	**-1.28**	27.08	28.61	**-1.53**
VO	21.35	26.82	**-5.47**	24.83	26.98	**-2.16**	27.08	29.63	**-2.56**
EC1	21.35	26.36	**-5.01**	24.83	26.59	**-1.76**	27.08	29.08	**-2.01**
EC2	21.35	23.94	**-2.59**	24.83	26.02	**-1.19**	27.08	28.52	**-1.45**
H1	21.35	25.93	**-4.58**	24.83	26.23	**-1.40**	27.08	28.46	**-1.38**
H2	21.35	25.82	**-4.47**	24.83	26.13	**-1.30**	27.08	28.66	**-1.58**
V1	21.35	26.97	**-5.62**	24.83	26.22	**-1.40**	27.08	28.73	**-1.65**
V2	21.35	28.20	**-6.85**	24.83	26.44	**-1.62**	27.08	29.32	**-2.25**
V3	21.35	27.19	**-5.84**	24.83	26.88	**-2.05**	27.08	29.69	**-2.62**

5.2.2. Energy performance

An overall comparative analysis of monthly heating, cooling and total loads for three categories is carried out as follows. As illustrated in ***Figure 219*** no significant improvement in heating performance during cold months (January, February, March, April, October, November, December) is noted with the use of HO, VO, EC1, EC2, H1, H2, V1 and V2 scenarios in east, south and west orientation. However, a significant decrease in heating energy consumption with 28% up to 40% is registered with V3 scenario in east and west orientations (refer to ***Table 15***).

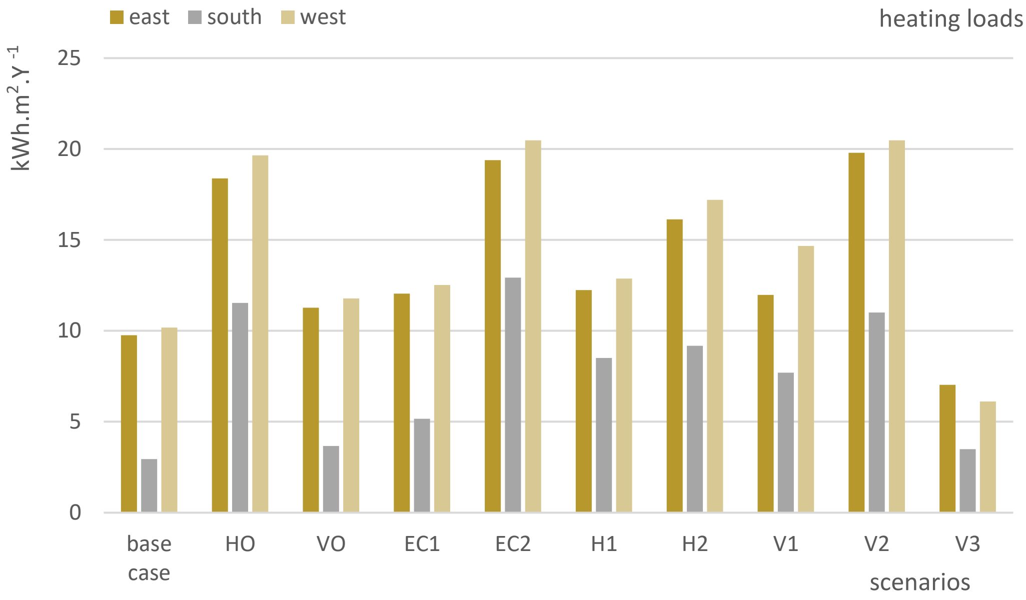

Figure 219. Comparison of simulated yearly heating loads (kWh.m^2.Y^{-1}) of the base case scenario all scenarios

Table 15. Shading effectiveness [%] for heating loads in east, south and west direction.

Scenarios	EAST	SOUTH	WEST
BC	-	-	-
HO	88.26	292.50	93.13
VO	15.49	24.81	15.78
EC1	23.32	75.84	23.08
EC2	98.54	339.81	101.26
H1	25.32	189.45	26.52
H2	65.15	212.32	69.17
V1	22.73	162.24	44.27
V2	102.80	274.67	101.35
V3	-28.05	18.75	-39.91

0%; -20%	-20%; -40%	-40%; -60%	-60%; -80%
0%; +100%	+100%; +200%	+200%; +300%	+300%; +400%

The benefit of shade was proven during the peak summer months from May to September. As illustrated in ***Figure 220*** significant improvement in cooling performance during warm months (May, June, July, August, September) is noted with the use of all shading design scenarios in east, south and west orientation. However, a significant decrease in cooling energy consumption with 80.12% is registered V3 scenario (refer to ***Table 16***).

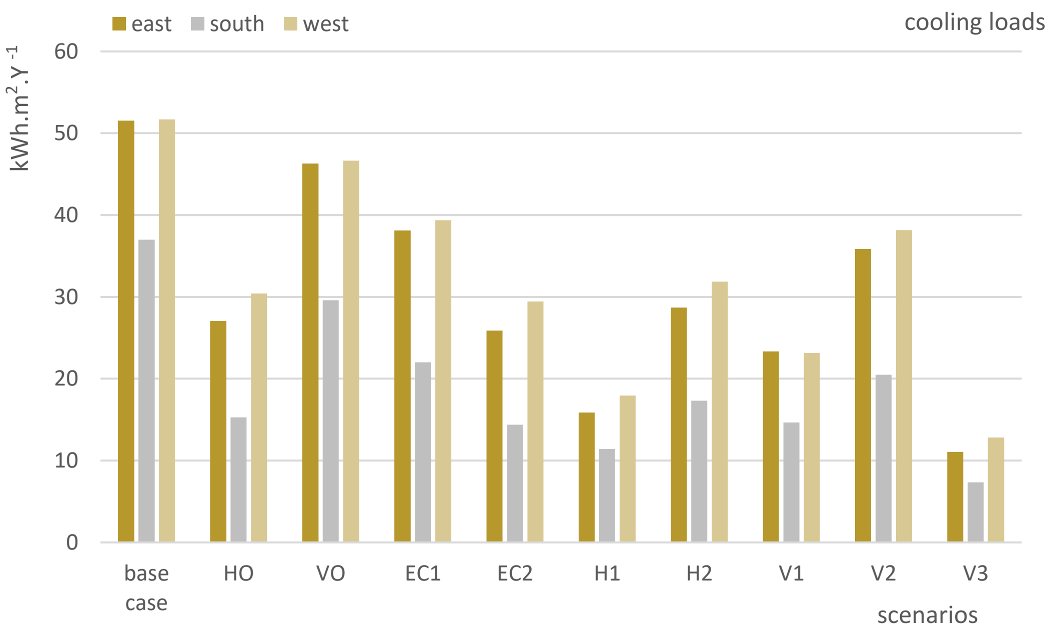

Figure 220. Comparison of simulated yearly cooling loads (kWh.m2.Y^{-1}) of the base case scenario all scenarios

Table 16. Shading effectiveness [%] for cooling loads in east, south and west direction.

Scenarios	EAST	SOUTH	WEST
BC	-	-	-
HO	-47.52	-58.67	-41.17
VO	-10.18	-20.03	-9.74
EC1	-26.00	-40.49	-23.80
EC2	-49.76	-61.09	-43.01
H1	-69.22	-69.14	-65.31
H2	-44.28	-53.25	-38.38
V1	-54.71	-60.42	-55.21
V2	-30.44	-44.68	-26.14
V3	-78.51	-80.12	-75.20

0%; -20%	-20%; -40%	-40%; -60%	-60%; -80%

Furthermore, a panoramic comparison of annual heating load, cooling load, total energy consumption, and savings in cooling load and total energy consumption with respect to the base case for all shading devices, in east south and west orientation is presented in ***Table 17*** and ***Figure 221***. There is dramatic increase in heating load of the base case in all cases, but this did not affect the saving in the total energy consumption. This is attributed to the fact that, as per the prevailing climate of the study area, the heating load of the building is low (28-40%) compared to the cooling load (60-80%) (see ***Table 18***).

Table 17. Annual simulation results obtained for all the scenario

	Annual heating demand			**Annual cooling demand**			**Annual energy demand**		
	Total heating [kWh]	Heating/ conditioned area [kWh/m2]	Shading effective-ness [%]	Total cooling [kWh]	Cooling/ conditioned area [kWh/m2]	Shading effective-ness [%]	Total energy demand [kWh]	Total energy/ conditioned area [kWh/m2]	Total Shading effectiveness [%]
BC_E	3183.12	9.76	-	16800.65	51.54	-	19983.77	61.30	-
HO_E	5992.62	18.38	**88.26**	8816.86	27.05	**-47.52**	14809.48	45.43	**-25.89**
VO_E	3676.31	11.28	**15.49**	15091.08	46.29	**-10.18**	18767.39	57.57	**-6.09**
EC1_E	3925.35	12.04	**23.32**	12432.80	38.14	**-26.00**	16358.15	50.18	**-18.14**
EC2_E	6319.83	19.39	**98.54**	8439.83	25.89	**-49.76**	14759.66	45.28	**-26.14**
H1_E	3988.97	12.24	**25.32**	5170.69	15.86	**-69.22**	9159.66	28.10	**-54.16**
H2_E	5257.03	16.13	**65.15**	9360.51	28.71	**-44.28**	14617.53	44.84	**-26.85**
V1_E	3906.59	11.98	**22.73**	7609.18	23.34	**-54.71**	11515.77	35.33	**-42.37**
V2_E	6455.40	19.80	**102.80**	11687.35	35.85	**-30.44**	18142.75	55.65	**-9.21**
V3_E	2290.36	7.03	**-28.05**	3609.62	11.07	**-78.51**	5899.98	18.10	**-70.48**
BC_S	958.10	2.94	-	12062.62	37.00	-	13020.72	39.94	-
HO_S	3760.57	11.54	**292.50**	4985.28	15.29	**-58.67**	8745.85	26.83	**-32.83**
VO_S	1195.84	3.67	**24.81**	9647.00	29.59	**-20.03**	10842.84	33.26	**-16.73**
EC1_S	1684.75	5.17	**75.84**	7178.12	22.02	**-40.49**	8862.87	27.19	**-31.93**
EC2_S	4213.83	12.93	**339.81**	4693.14	14.40	**-61.09**	8906.97	27.32	**-31.59**
H1_S	2773.20	8.51	**189.45**	3722.69	11.42	**-69.14**	6495.89	19.93	**-50.11**
H2_S	2992.31	9.18	**212.32**	5639.51	17.30	**-53.25**	8631.82	26.48	**-33.71**
V1_S	2512.53	7.71	**162.24**	4774.61	14.65	**-60.42**	7287.15	22.35	**-44.03**
V2_S	3589.75	11.01	**274.67**	6672.99	20.47	**-44.68**	10262.75	31.48	**-21.18**
V3_S	1137.71	3.49	**18.75**	2398.55	7.36	**-80.12**	3536.26	10.85	**-72.84**
BC_W	3316.62	10.17	-	16852.51	51.70	-	20169.13	61.87	-
HO_W	6405.36	19.65	**93.13**	9915.05	30.42	**-41.17**	16320.40	50.06	**-19.08**
VO_W	3839.89	11.78	**15.78**	15210.55	46.66	**-9.74**	19050.44	58.44	**-5.55**
EC1_W	4082.04	12.52	**23.08**	12840.80	39.39	**-23.80**	16922.85	51.91	**-16.10**
EC2_W	6675.19	20.48	**101.26**	9603.82	29.46	**-43.01**	16279.01	49.94	**-19.29**
H1_W	4196.15	12.87	**26.52**	5845.71	17.93	**-65.31**	10041.86	30.80	**-50.21**
H2_W	5610.70	17.21	**69.17**	10385.13	31.86	**-38.38**	15995.83	49.07	**-20.69**
V1_W	4784.95	14.68	**44.27**	7548.72	23.16	**-55.21**	12333.68	37.83	**-38.85**
V2_W	6677.91	20.49	**101.35**	12446.45	38.18	**-26.14**	19124.36	58.67	**-5.18**
V3_W	1992.80	6.11	**-39.91**	4179.75	12.82	**-75.20**	6172.55	18.93	**-69.40**

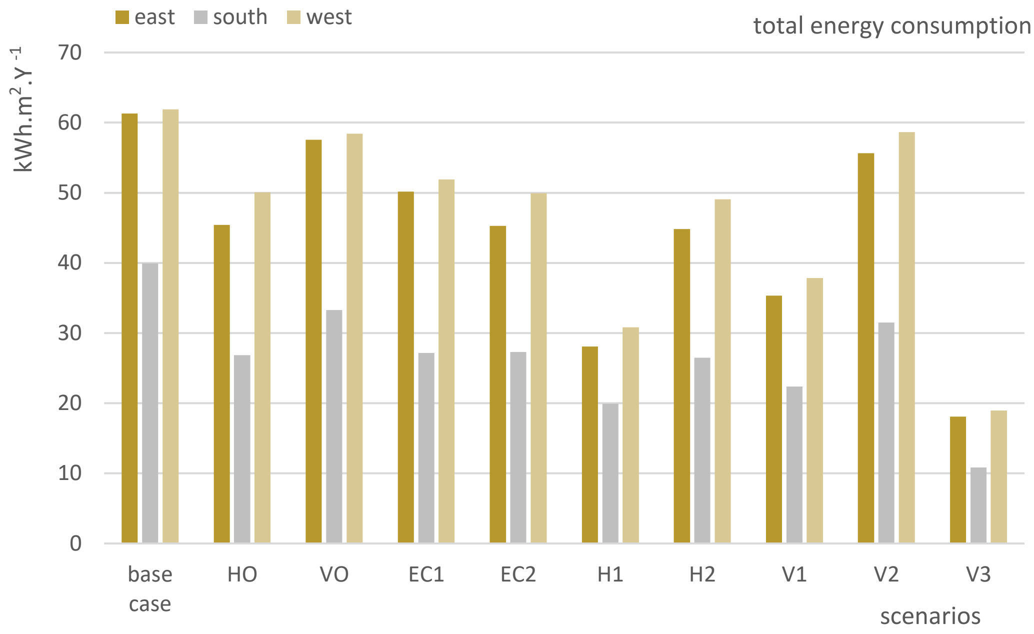

Figure 221. Comparison of simulated yearly total energy consumption (kWh.m^2.Y^{-1}) of the base case scenario all scenarios

Table 18. Total shading effectiveness [%] for total energy/conditioned area [kWh/m^2] in east, south and west direction.

Scenarios	EAST	SOUTH	WEST
BC	-	-	-
HO	-25.89	-32.83	-19.08
VO	-6.09	-16.73	-5.55
EC1	-18.14	-31.93	-16.10
EC2	-26.14	-31.59	-19.29
H1	-54.16	-50.11	-50.21
H2	-26.85	-33.71	-20.69
V1	-42.37	-44.03	-38.85
V2	-9.21	-21.18	-5.18
V3	-70.48	-72.84	-69.40

0%; -20%	-20%; -40%	-40%; -60%	-60%; -80%

5.3 Antalya, Turkey

5.3.1. Indoor air temperature

The proposed scenarios belong to three different categories of shading design. To begin with, an analysis of the results within each category is conducted, followed by a ranking of all proposed scenarios. The simulation results show that within the "I Category" different scenarios (HO, VO, EC1 and EC2) have different impact depending on the east south or west orientation for a typical summer day (refer to ***Figure 119***, ***Figure 121*** and ***Figure 123***). In the east orientation, a decrease in air temperature up to 3.19 °C with the impact of EC1 scenario. While in the south and west a decrease up to 2.68 °C and 4.88 with the EC2 scenario (see ***Table 19***).

The simulation results show that the "II Category" scenarios (H1 and H2) have almost the same impact in every direction for a selected summer day (refer to ***Figure 125*** and ***Figure 127***). But the one that has a better performance is H1 with a decrease in air temperature up to 4.2 °C (see ***Table 19***).

The simulation results show that the "III Category" scenarios (V1, V2 and V3) have different impact depending on the east south or west orientation for a selected summer day (refer to ***Figure 131***, ***Figure 133*** and ***Figure 135***). In the east orientation what performs better is V3 with an air temperature decrease up to 1.95 °C while in the south and west orientation the scenario that performs better is V1 with an air temperature decrease up to 1.88 °C south and 2.79 °C west (see ***Table 19***).

A comparison of simulation results within categories was made. What also interests us in further studies is which of all these scenarios performs best and which is most appropriate for a particular orientation making that and within a given situation in future proposals may have a combination of them depending on the orientation.

According to the above detailed analysis for each category we can make a selection of the best scenario and the one which has less impact for a selected summer day. In the east orientation, the one that has the greatest impact in lowering the temperature is H1 with 3.55 °C followed by EC2 scenario in south direction with

2.68 °C and in west direction EC1 scenario with 4.88 °C (refer to ***Table 19***). However, for all scenarios no significant change in temperature is registered in east, south and east orientation for a typical winter day.

Table 19. Simulation results of air temperature for a typical summer day (3rd August)

	East, Peak hour; 9:00			**South, Peak hour; 12:00**			**West, Peak hour; 15:00**		
T[°C]	Exterior	Interior	ΔT	Exterior	Interior	ΔT	Exterior	Interior	ΔT
BC	26.45	33.71	-7.26	30.90	33.56	-2.66	32.75	37.53	-4.78
HO	26.45	31.68	-5.23	30.90	31.26	-0.36	32.75	33.97	-1.22
VO	26.45	31.21	-4.76	30.90	31.85	-0.95	32.75	34.56	-1.81
EC1	26.45	30.52	-4.07	30.90	30.99	-0.09	32.75	32.65	0.10
EC2	26.45	31.60	-5.15	30.90	30.70	0.20	32.75	33.82	-1.07
H1	26.45	30.16	-3.71	30.90	30.78	0.12	32.75	33.33	-0.58
H2	26.45	31.38	-4.93	30.90	30.97	-0.07	32.75	33.97	-1.22
V1	26.45	32.27	-5.82	30.90	31.68	-0.78	32.75	34.74	-1.99
V2	26.45	33.15	-6.70	30.90	32.17	-1.27	32.75	36.05	-3.30
V3	26.45	31.76	-5.31	30.90	32.29	-1.39	32.75	36.31	-3.56

5.3.2. Energy performance

An overall comparative analysis of monthly heating, cooling and total loads for three categories is carried out as follows. As illustrated in ***Figure 222*** no significant improvement in heating performance during cold months (January, February, March, April, October, November, December) is noted with the use of HO, VO, EC1, EC2, H1, H2, V1 and V2 scenarios in east, south and west orientation. However, similar to Almeria's climate a significant decrease in heating energy consumption with 25% up to 50% is registered with V3 scenario in east and west orientations (refer to ***Table 20***).

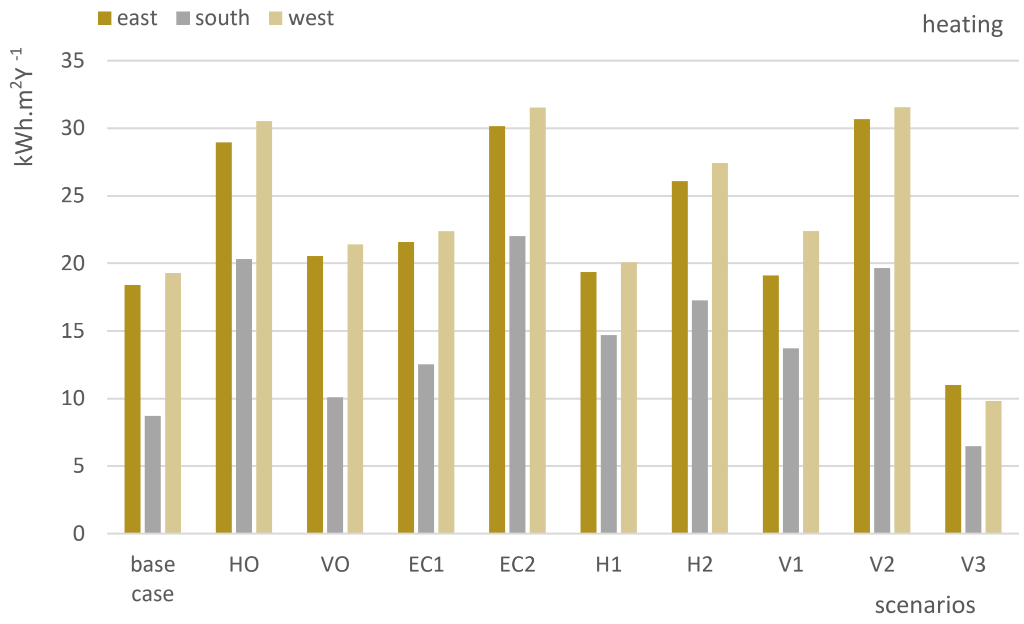

Figure 222. Comparison of simulated yearly heating loads (kWh.m^2.Y^{-1}) of the base case scenario all scenarios

Table 20. Shading effectiveness [%] for heating loads in east, south and west direction.

Scenarios	EAST	SOUTH	WEST
BC	-	-	-
HO	57.22	133.32	58.25
VO	11.64	15.88	10.89
EC1	17.29	43.84	15.88
EC2	63.82	152.77	63.36
H1	5.10	68.54	4.09
H2	41.61	97.97	42.15
V1	3.75	57.28	-23.92
V2	66.60	125.47	63.49
V3	-40.41	-25.81	-49.08

0%; -20%	-20%; -40%	-40%; -60%	-60%; -80%
0%; +50%	+50%; +100%	+100%; +150%	+150%; +200%

The benefit of shade was proven during the peak summer months from May to September. As illustrated in ***Figure 223*** significant improvement in cooling performance during warm months (May, June, July, August, September) is noted with the use of all shading design scenarios in east, south and west orientation. However, a significant decrease in cooling energy consumption up to 74.02% is registered V3 scenario in all orientation (refer to ***Table 21***). However, a significant decrease is registered also with H1 scenario reaching its best performance in south orientation with 81.90%.

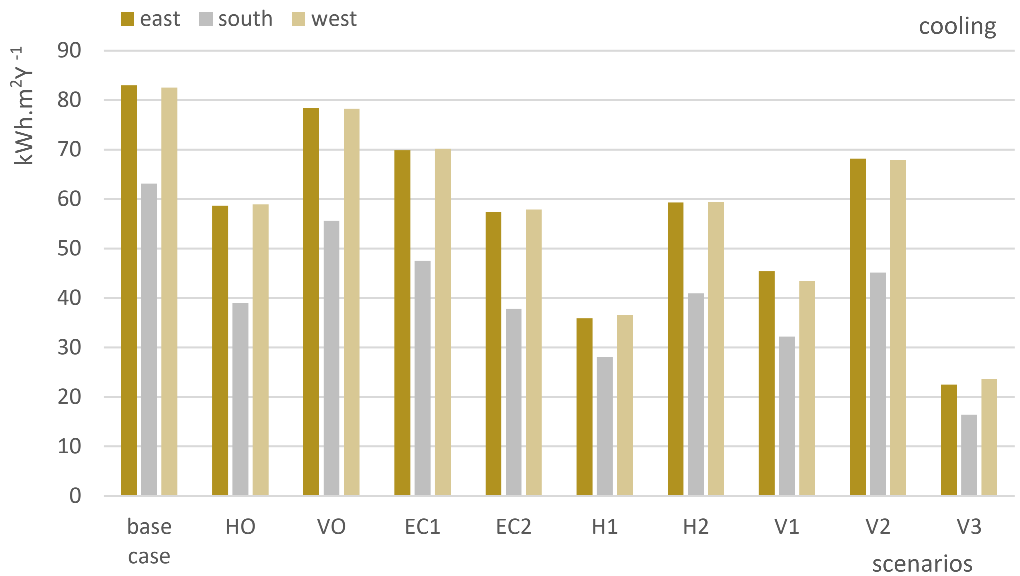

Figure 223. Comparison of simulated yearly cooling loads (kWh.m^2.Y^{-1}) of the base case scenario all scenarios

Table 21. Shading effectiveness [%] for cooling loads in east, south and west direction

Scenarios	EAST	SOUTH	WEST
BC	-	-	-
HO	-29.31	-38.23	-28.62
VO	-5.54	-11.86	-5.21
EC1	-15.85	-24.66	-14.97
EC2	-30.88	-40.05	-29.90
H1	-56.76	-81.90	-55.71
H2	-28.56	-35.15	-28.04
V1	-45.33	-48.95	-71.94
V2	-17.85	-28.49	-17.77
V3	-72.87	-74.02	-71.45

0%; -20%	-20%; -40%	-40%; -60%	-60%; -80%

Furthermore, a panoramic comparison of annual heating load, cooling load, total energy consumption, and savings in cooling load and total energy consumption with respect to the base case for all shading devices, in east south and west orientation is presented in ***Table 22*** and ***Figure 224***. There is dramatic increase in heating load of the base case in all cases, but this did not affect the saving in the total energy consumption. This is attributed to the fact that, as per the prevailing climate of the study area, the heating load of the building is low (20-50%) compared to the cooling load (70-80%) (see ***Table 23***). Therefore, the impact of external shading devices on cooling load is highly significant compared to the heating load. This ascertains the fact that the choice of proper shading strategy of a building depends mainly on the climatic location.

Table 22. Annual simulation results obtained for all the scenario

	Annual heating demand			**Annual cooling demand**			**Annual energy demand**		
	Total heating [kWh]	Heating/ conditioned area [kWh/m2]	Shading effective-ness [%]	Total cooling [kWh]	Cooling/ conditioned area [kWh/m2]	Shading effective-ness [%]	Total energy demand [kWh]	Total energy/ conditioned area [kWh/m2]	Total Shading effectiveness [%]
BC_E	6002.31	18.41	-	27055.69	83.00	-	33057.99	101.41	-
HO_E	9437.04	28.95	**57.22**	19127.00	58.67	**-29.31**	28564.04	87.62	**-13.59**
VO_E	6701.17	20.56	**11.64**	25557.58	78.40	**-5.54**	32258.75	98.96	**-2.42**
EC1_E	7039.91	21.60	**17.29**	22768.48	69.84	**-15.85**	29808.39	91.44	**-9.83**
EC2_E	9833.25	30.16	**63.82**	18701.80	57.37	**-30.88**	28535.04	87.53	**-13.68**
H1_E	6308.22	19.35	**5.10**	11698.73	35.89	**-56.76**	18006.95	55.24	**-45.53**
H2_E	8499.98	26.07	**41.61**	19329.70	59.30	**-28.56**	27829.68	85.37	**-15.82**
V1_E	6227.49	19.10	**3.75**	14790.28	45.37	**-45.33**	21017.77	64.47	**-36.42**
V2_E	9999.69	30.67	**66.60**	22226.70	68.18	**-17.85**	32226.39	98.86	**-2.52**
V3_E	3576.79	10.97	**-40.41**	7339.16	22.51	**-72.87**	10915.95	33.49	**-66.98**
BC_S	2839.76	8.71	-	20571.50	63.10	-	23411.26	71.82	-
HO_S	6625.61	20.32	**133.32**	12707.34	38.98	**-38.23**	19332.94	59.31	**-17.42**
VO_S	3290.65	10.09	**15.88**	18131.41	55.62	**-11.86**	21422.06	65.71	**-8.50**
EC1_S	4084.73	12.53	**43.84**	15497.75	47.54	**-24.66**	19582.48	60.07	**-16.35**
EC2_S	7177.97	22.02	**152.77**	12331.76	37.83	**-40.05**	19509.73	59.85	**-16.67**
H1_S	4786.00	14.68	**68.54**	9147.89	11.42	**-81.90**	6495.89	19.93	**-72.25**
H2_S	5621.79	17.25	**97.97**	13340.83	40.92	**-35.15**	18962.62	58.17	**-19.00**
V1_S	4466.41	13.70	**57.28**	10501.48	32.21	**-48.95**	14967.90	45.92	**-36.07**
V2_S	6402.74	19.64	**125.47**	14710.81	45.13	**-28.49**	21113.55	64.77	**-9.81**
V3_S	2106.87	6.46	**-25.81**	5344.00	16.39	**-74.02**	7450.86	22.86	**-68.17**
BC_W	6289.35	19.29	-	26905.83	82.54	-	33195.17	101.83	-
HO_W	9952.58	30.53	**58.25**	19204.85	58.91	**-28.62**	29157.43	89.44	**-12.16**
VO_W	6974.52	21.39	**10.89**	25505.11	78.24	**-5.21**	32479.64	99.63	**-2.16**
EC1_W	7288.13	22.36	**15.88**	22877.77	70.18	**-14.97**	30165.90	92.54	**-9.13**
EC2_W	10274.26	31.52	**63.36**	18862.25	57.86	**-29.90**	29136.51	89.38	**-12.23**
H1_W	6546.86	20.08	**4.09**	11917.03	36.56	**-55.71**	18463.89	56.64	**-44.38**
H2_W	8940.03	27.42	**42.15**	19360.54	59.39	**-28.04**	28300.57	86.81	**-14.74**
V1_W	4784.95	14.68	**-23.92**	7548.72	23.16	**-71.94**	12333.68	37.83	**-62.84**
V2_W	10282.66	31.54	**63.49**	22123.58	67.87	**-17.77**	32406.24	99.41	**-2.38**
V3_W	3202.77	9.82	**-49.08**	7682.62	23.57	**-71.45**	10885.39	33.39	**-67.21**

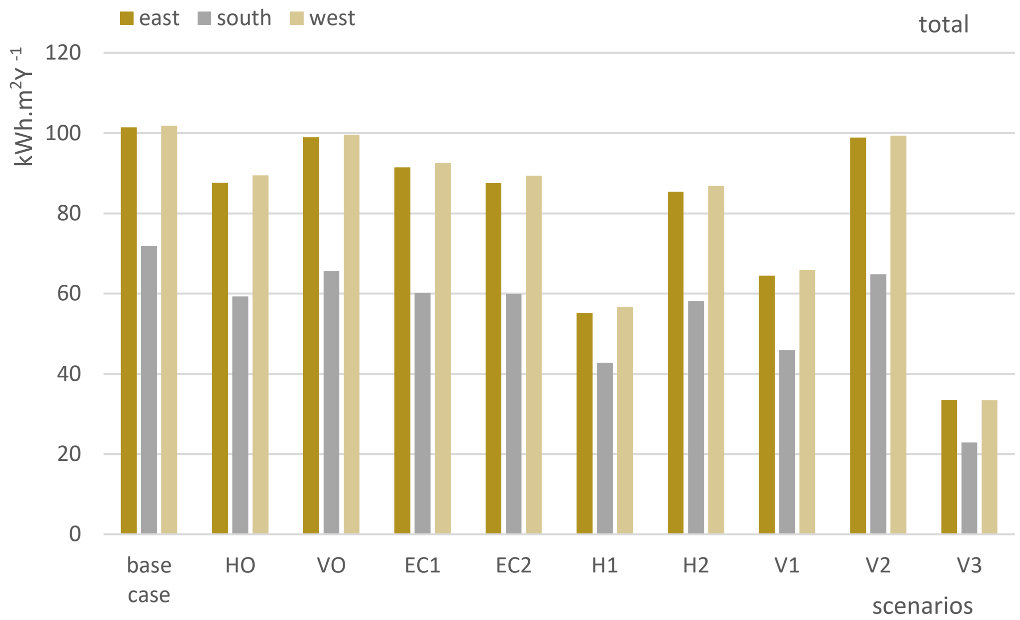

Figure 224. Comparison of simulated yearly total energy consumption (kWh.m^2.Y^{-1}) of the base case scenario all scenarios

Table 23. Total shading effectiveness [%] for total energy/conditioned area [kWh/m^2] in east, south and west direction.

Scenarios	**EAST**	**SOUTH**	**WEST**
BC	-	-	-
HO	-13.59	-17.42	-12.16
VO	-2.42	-8.50	-2.16
EC1	-9.83	-16.35	-9.13
EC2	-13.68	-16.67	-12.23
H1	-45.53	-72.25	-44.38
H2	-15.82	-19.00	-14.74
V1	-36.42	-36.07	-62.84
V2	-2.52	-9.81	-2.38
V3	-66.98	-68.17	-67.21

0%; -20%	-20%; -40%	-40%; -60%	-60%; -80%

5.4 Naples, Italy

5.4.1. Indoor air temperature

The proposed scenarios belong to three different categories of shading design. To begin with, an analysis of the results within each category is conducted, followed by a ranking of all proposed scenarios. The simulation results show that within the "I Category" different scenarios (HO, VO, EC1 and EC2) have different impact depending on the east south or west orientation for a typical summer day (refer to ***Figure 166***, ***Figure 168*** and ***Figure 169***). In the east and west orientation, a decrease in air temperature up to 2.99 °C and 4.44 °C with the impact of EC1 scenario. While in the south a decrease up to 4.02 degrees with the EC2 scenario (see ***Table 24***).

The simulation results show that the "II Category" scenarios (H1 and H2) have almost the same impact in every direction except H2 scenario which performs better in east orientation for a selected summer day (refer to ***Figure 172*** and ***Figure 175***).

The simulation results show that the "III Category" scenarios (V1, V2 and V3) have different impact depending on the east south or west orientation for a selected summer day (refer to ***Figure 178***, ***Figure 180*** and ***Figure 182***). In the east orientation what performs better is V3 with an air temperature decrease up to 2.32 °C while in the south and west orientation the scenario that performs better is V1 with an air temperature decrease up to 2.63 °C south and 3.21 °C west (see ***Table 24***).

A comparison of simulation results within categories was made. According to the above detailed analysis for each category we can make a selection of the best scenario and the one which has less impact for a selected summer day. In the east and west orientation, the one that has the greatest impact in lowering the temperature is H1 with 3.86 °C east and 5.71 °C west while in the south direction it is EC2 4.02 °C similar to Tirana's climate (refer to ***Table 24***). However, for all scenarios no significant change in temperature is registered in east, south and east orientation for a typical winter day.

Table 24. Simulation results of air temperature for a typical summer day (3rd August)

	East, Peak hour; 9:00			**South, Peak hour; 12:00**			**West, Peak hour; 15:00**		
T[°C]	Exterior	Interior	ΔT	Exterior	Interior	ΔT	Exterior	Interior	ΔT
BC	22.00	29.60	-7.60	26.23	30.87	-4.64	28.23	34.01	-5.79
HO	22.00	27.35	-5.35	26.23	26.95	-0.72	28.23	30.45	-2.22
VO	22.00	27.22	-5.22	26.23	28.50	-2.28	28.23	31.02	-2.79
EC1	22.00	26.61	-4.61	26.23	27.73	-1.50	28.23	29.57	-1.35
EC2	22.00	27.31	-5.31	26.23	26.85	-0.62	28.23	30.24	-2.02
H1	22.00	25.74	-3.74	26.23	27.20	-0.98	28.23	28.30	-0.08
H2	22.00	27.04	-5.04	26.23	27.31	-1.09	28.23	30.38	-2.16
V1	22.00	27.72	-5.72	26.23	28.24	-2.02	28.23	30.80	-2.58
V2	22.00	28.35	-6.35	26.23	28.94	-2.72	28.23	31.91	-3.68
V3	22.00	27.28	-5.28	26.23	28.93	-2.71	28.23	32.57	-4.34

5.4.2. Energy performance

An overall comparative analysis of monthly heating, cooling and total loads for three categories is carried out as follows. As illustrated in ***Figure 225*** no significant improvement in heating performance during cold months (January, February, March, April, October, November, December) is noted with the use of HO, VO, EC1, EC2, and V2 scenarios in east, south and west orientation. However, a significant decrease in heating energy consumption with 5% up to 52% is registered with H1, V1, and V3 scenario (refer to ***Table 25***). The position and angle of H1, V1, and V3 shading devices design bring more heat gain into the building during cold months.

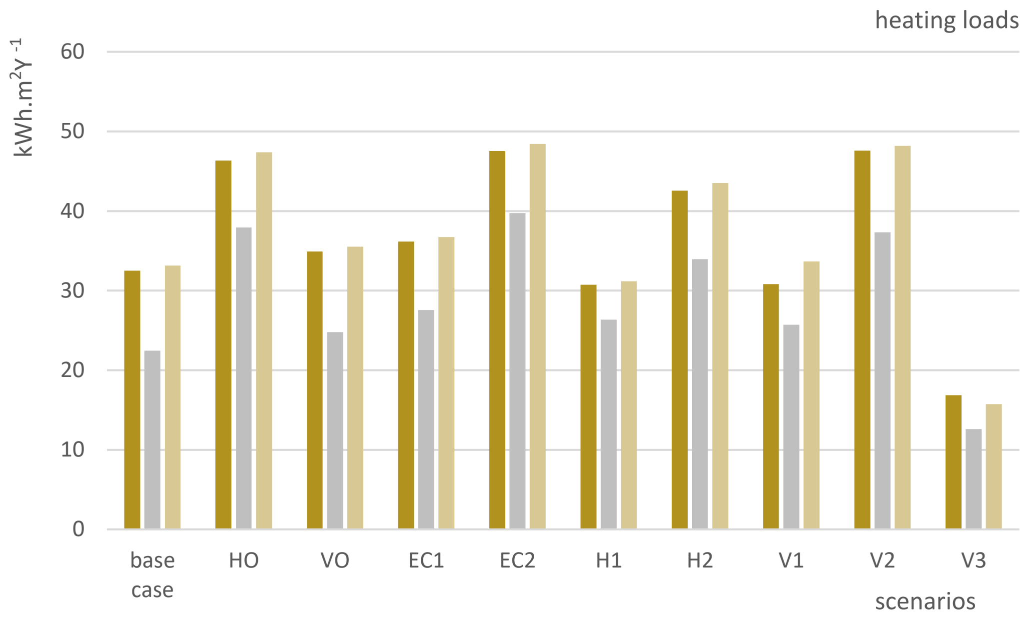

Figure 225. Comparison of simulated yearly heating loads (kWh.m^2.Y^{-1}) of the base case scenario all scenarios

Table 25. Shading effectiveness [%] for heating loads in east, south and west direction.

Scenarios	EAST	SOUTH	WEST
BC	-	-	-
HO	42.46	68.99	43.03
VO	7.38	10.33	7.25
EC1	11.18	22.74	10.86
EC2	46.15	76.98	46.17
H1	-5.52	17.47	-5.90
H2	30.90	51.25	31.33
V1	-5.21	14.49	1.68
V2	46.28	66.37	45.42
V3	-48.10	-43.86	-52.55

0%; -20%	-20%; -40%	-40%; -60%	-60%; -80%
0%; +20%	+20%; +40%	+40%; +60%	+60%; +80%

The benefit of shade was proven during the peak summer months from May to September. As illustrated in ***Figure 226*** significant improvement in cooling performance during warm months (May, June, July, August, September) is noted with the use of all shading design scenarios in east, south and west orientation. However, a significant decrease in cooling energy consumption up to 80 % is registered V3 scenario in south orientation (refer to ***Table 26***). However, a significant decrease is registered also with H1 scenario reaching its best performance in south orientation with 70.42%.

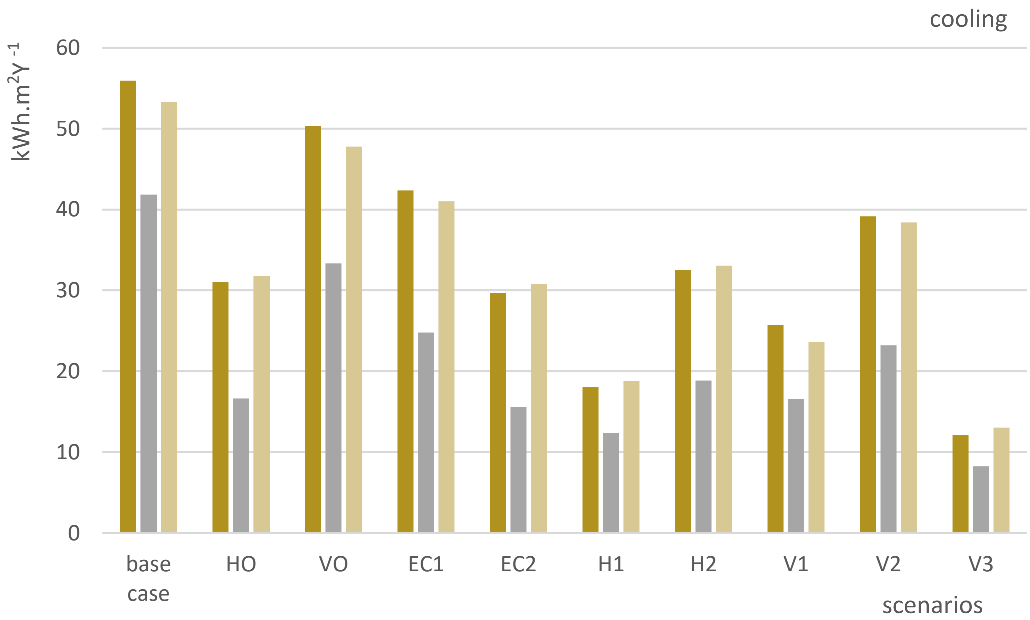

Figure 226. Comparison of simulated yearly cooling loads (kWh.m^2. Y^{-1}) of the base case scenario all scenarios

Table 26. Shading effectiveness [%] for cooling loads in east, south and west direction

Scenarios	EAST	SOUTH	WEST
BC	-	-	-
HO	-44.51	-60.25	-40.30
VO	-9.98	-20.40	-10.30
EC1	-24.32	-40.78	-23.02
EC2	-46.91	-62.74	-42.27
H1	-67.79	-70.42	-64.68
H2	-41.85	-54.91	-37.94
V1	-54.07	-60.44	-55.61
V2	-30.04	-44.51	-27.88
V3	-78.37	-80.30	-75.53

0%; -20%	-20%; -40%	-40%; -60%	-60%; -80%

Furthermore, a panoramic comparison of annual heating load, cooling load, total energy consumption, and savings in cooling load and total energy consumption with respect to the base case for all shading devices, in east south and west orientation is presented in ***Table 27*** and ***Figure 227***. Therefore, the impact of external shading devices on cooling load is highly significant compared to the heating load. This ascertains the fact that the choice of proper shading strategy of a building depends mainly on the climatic location.

Table 27. Annual simulation results obtained for all the scenario

	Annual heating demand			**Annual cooling demand**			**Annual energy demand**		
	Total heating [kWh]	Heating/ conditioned area [kWh/m2]	Shading effective-ness [%]	Total cooling [kWh]	Cooling/ conditioned area [kWh/m2]	Shading effective-ness [%]	Total energy demand [kWh]	Total energy/ conditioned area [kWh/m2]	Total Shading effectiveness [%]
BC_E	10600.34	32.52	-	18238.29	55.95	-	28838.63	88.46	-
HO_E	15101.16	46.32	**42.46**	10119.81	31.04	**-44.51**	25220.97	77.37	**-12.54**
VO_E	11383.02	34.92	**7.38**	16418.99	50.37	**-9.98**	27802.01	85.28	**-3.59**
EC1_E	11785.96	36.15	**11.18**	13802.63	42.34	**-24.32**	25588.59	78.50	**-11.27**
EC2_E	15492.23	47.52	**46.15**	9682.09	29.70	**-46.91**	25174.31	77.22	**-12.71**
H1_E	10015.38	30.72	**-5.52**	5873.78	18.02	**-67.79**	15889.16	48.74	**-44.90**
H2_E	13875.85	42.57	**30.90**	10605.52	32.53	**-41.85**	24481.37	75.10	**-15.11**
V1_E	10047.77	30.82	**-5.21**	8376.23	25.69	**-54.07**	18424.00	56.52	**-36.11**
V2_E	15505.85	47.57	**46.28**	12758.74	39.14	**-30.04**	28264.59	86.70	**-1.99**
V3_E	5501.09	16.88	**-48.10**	3944.45	12.10	**-78.37**	9445.54	28.97	**-67.25**
BC_S	7316.67	22.44	-	13646.89	41.86	-	20963.56	64.31	-
HO_S	12364.25	37.93	**68.99**	5424.88	16.64	**-60.25**	17789.13	54.57	**-15.14**
VO_S	8072.48	24.76	**10.33**	10863.03	33.32	**-20.40**	18935.51	58.09	**-9.67**
EC1_S	8980.16	27.55	**22.74**	8081.04	24.79	**-40.78**	17061.20	52.34	**-18.61**
EC2_S	12948.76	39.72	**76.98**	5085.29	15.60	**-62.74**	18034.05	55.32	**-13.97**
H1_S	8594.91	26.37	**17.47**	4036.49	12.38	**-70.42**	12631.40	38.75	**-39.75**
H2_S	11066.39	33.95	**51.25**	6153.01	18.87	**-54.91**	17219.40	52.82	**-17.86**
V1_S	8377.11	25.70	**14.49**	5398.87	16.56	**-60.44**	13775.97	42.26	**-34.29**
V2_S	12172.72	37.34	**66.37**	7573.33	23.23	**-44.51**	19746.04	60.57	**-5.81**
V3_S	4107.78	12.60	**-43.86**	2688.19	8.25	**-80.30**	6795.98	20.85	**-67.58**
BC_W	10798.89	33.13	-	17364.83	53.27	-	28163.72	86.39	-
HO_W	15445.83	47.38	**43.03**	10366.44	31.80	**-40.30**	25812.27	79.18	**-8.35**
VO_W	11581.84	35.53	**7.25**	15576.78	47.78	**-10.30**	27158.62	83.31	**-3.57**
EC1_W	11971.55	36.72	**10.86**	13367.39	41.01	**-23.02**	25338.95	77.73	**-10.03**
EC2_W	15785.21	48.42	**46.17**	10024.63	30.75	**-42.27**	25809.83	79.17	**-8.36**
H1_W	10161.28	31.17	**-5.90**	6133.61	18.82	**-64.68**	16294.89	49.99	**-42.14**
H2_W	14182.12	43.50	**31.33**	10777.27	33.06	**-37.94**	24959.40	76.56	**-11.38**
V1_W	10980.42	33.68	**1.68**	7708.95	23.65	**-55.61**	18689.36	57.33	**-33.64**
V2_W	15703.86	48.17	**45.42**	12522.93	38.42	**-27.88**	28226.79	86.59	**0.22**
V3_W	5124.31	15.72	**-52.55**	4248.63	13.03	**-75.53**	9372.95	28.75	**-66.72**

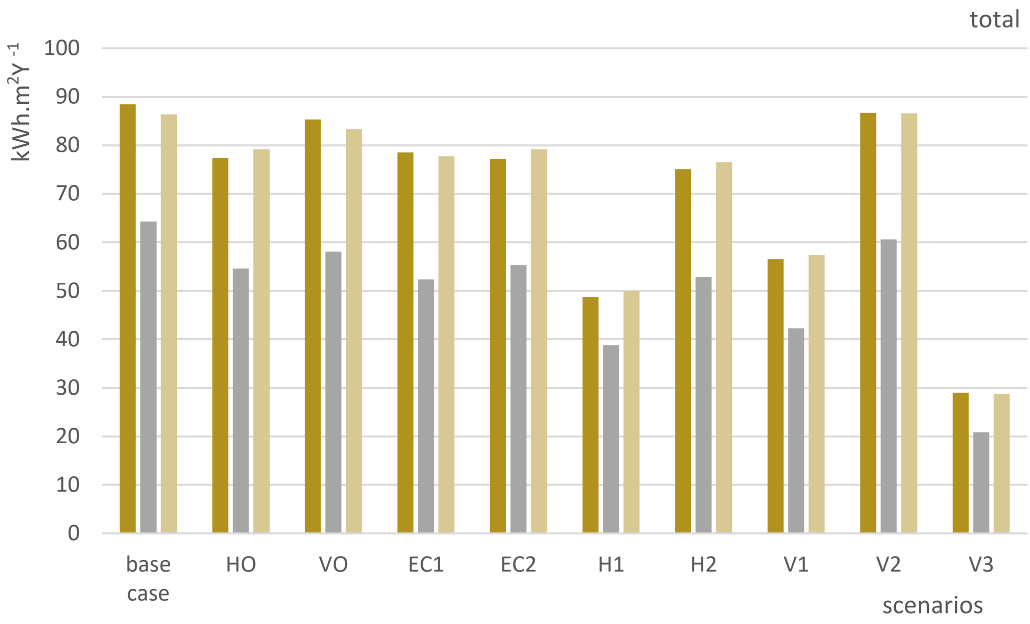

Figure 227. Comparison of simulated yearly total energy consumption ($kWh.m^2.Y^{-1}$) of the base case scenario all scenarios

Table 28. Total shading effectiveness [%] for total energy/conditioned area [kWh/m^2] in east, south and west direction.

Scenarios	**EAST**	**SOUTH**	**WEST**
BC	-	-	-
HO	-12.54	-15.14	-8.35
VO	-3.59	-9.67	-3.57
EC1	-11.27	-18.61	-10.03
EC2	-12.71	-13.97	-8.36
H1	-44.90	-39.75	-42.14
H2	-15.11	-17.86	-11.38
V1	-36.11	-34.29	-33.64
V2	-1.99	-5.81	0.22
V3	-67.25	-67.58	-66.72

0-20%	20-40%	40-60%	60-80%

5.5 Locations comparison

Considering that shading is effective in the summer session, the overall cooling demand and thermal comfort for a typical summer day are evaluated and compared below. ***Figure 228*** compares the simulated cooling demand (kWh.m^{-2}. Y^{-1}) for south oriented typologies in four locations in Mediterranean context. All typologies have similar performance in four locations studied. Even though Antalya and Tirana have "humid" dry-summer subtropical climate and mild rainy winter they display the highest cooling demand.

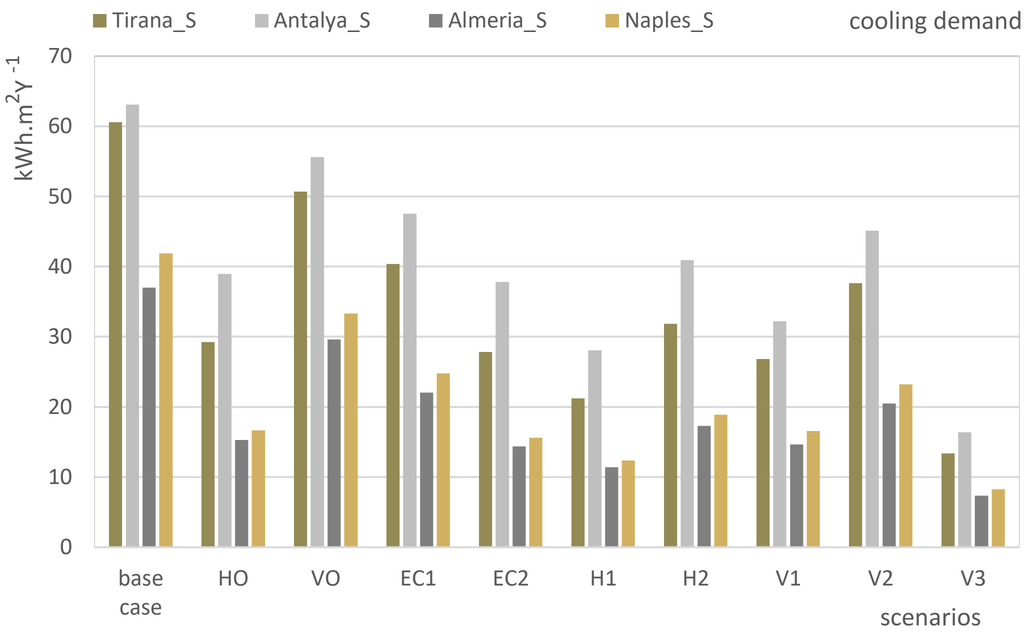

Figure 228. Comparision of annual simulated cooling demand (kWh.m^{-2}. Y^{-1}) in south orientation typologies in four selected locations

Simulated results based on location are found also on hotel room overheating in a typical summer day, as shown in ***Table 29.*** Antalya is ranked first, followed by Naples, Almeria and Tirana. None of locations remains within the comfort temperatures in the studied summer day but we realize contribution of the implemented scenarios as a passive design.

Table 29. Hotel room overheating for a typical summer day (3rd August)

	Tirana			Almeria			Antalya			Naples		
Scenarios	**east**	**south**	**west**	**east**	**south**	**west**	**east**	**south**	**west**	**east**	**south**	**west**
BC	6.71	6.30	6.55	6.82	4.67	5.19	10.16	8.73	10.00	6.95	5.90	6.57
HO	4.3	3.54	5.49	4.64	2.39	3.52	8.48	7.34	8.27	4.56	3.00	4.76
VO	5.31	4.43	5.60	5.20	3.15	4.23	9.02	7.31	8.42	5.24	4.00	4.90
EC1	4.92	3.89	5.05	4.57	2.72	3.81	8.43	6.71	6.92	4.69	3.50	4.00
EC2	4.71	3.45	5.23	2.31	2.31	3.45	8.40	6.57	8.20	4.50	2.88	4.59
H1	4.44	3.64	4.46	3.40	2.38	3.06	7.70	6.57	7.63	3.53	2.99	2.67
H2	4.82	3.70	5.12	2.96	2.42	3.43	8.28	6.87	8.15	4.37	3.20	4.56
V1	5.41	4.24	5.30	5.16	2.91	3.46	9.04	7.22	8.32	4.95	3.84	4.51
V2	5.39	4.26	6.00	5.53	2.89	3.95	9.17	7.34	9.11	5.00	3.92	5.18
V3	4.83	4.25	5.92	4.63	2.96	3.98	8.53	7.36	8.88	4.56	3.84	5.20

CHAPTER 6

CONCLUSIONS

6.1 Conclusions

The success of shading device design depends entirely on building's use and local climatic conditions. To prevent improper applications, designers need accurate and detailed information to ensure choosing the correct shading devices techniques referring Mediterranean regions. For this reason, proposed strategies are developed with the aim of initiating an analytical and quantitative approach to evaluate the thermal and energy performance of shading device systems. The study analyses several scenarios for further evaluation of shading devices already implemented on hotel building envelopes, even though rarely evaluated in previous studies. The new proposals are an enhancement of the previously proposed studies by adding contributions outlined as below:

- Considering that all selected regions belong to the Mediterranean climate which is characterized by hot summers all the proposed scenarios as a shading function have a positive impact on both energy performance and thermal performance.
- From the comparison of simulated yearly total energy consumption ($kWh.m^2. Y^{-1}$) of the base case scenario and all scenarios we notice the same ranking in all Mediterranean regions studied starting from the starting with the one that has the least impact to the one that has the most impact: VO scenario followed by EC1, V2, H2, HO, EC2, H1, and V1.
- The climate of Tirana with mild and rainy winter displays the highest energy demand. Followed by, Antalya's "humid" dry-summer subtropical and mild rainy winter climate displays a similar performance to that of Tirana with an average difference of 10 $kWh.m^{-2}. Y^{-1}$ in east orientation. Continuing with Naples with a humid subtropical climate. Almeria is the only city in Europe

with a true hot desert climate one of the driest zones on either shore of the Mediterranean coast. We can still observe from the simulation results that it requires less energy demand with an average difference of 40 kWh.m^{-2} compare to other Mediterranean regions.

- Approximately a maximum of 68.32% up to 80.3% for the humid subtropical climate of Tirana, Antalya and Naples while 72.84% for the a hot semi-arid climate of Almeria of total energy consumed can be reduced through the selection of the proper shading design. Results highlight that V3 scenario has a significant influence in all three orientations, with the greatest impact towards the south.
- There is dramatic increase in heating load of the base case in all cases, but this did not affect the saving in the total energy consumption. This is attributed to the fact that, as per the prevailing climate of the study area, the heating load of the building is low (6-59%) compared to the cooling load (76-80%). Therefore, the impact of external shading devices on cooling load is highly significant compared to the heating load. This ascertains the fact that the choice of proper shading strategy of a building depends mainly on the climatic location. For instance, in a cooling dominated climate, attention should be given to reducing the cooling load, and vice versa in a heating dominated climate (Alhuwayil et. al., 2018).
- The presence of shading systems as passive design lowers the air temperature values for a typical summer day from to 2.68 °C up to 5 °C better with H1, EC1 and EC2 scenarios. However, they belong to the same Mediterranean climate implemented shadings vary on the orientation and region (Aldawoud, 2012).

6.2 Recommendations for future research

Therefore, the results demonstrate that shading device applications can provide significant thermal and energy savings. Nonetheless, the model development and analysis are in accordance with the relevant scientific studies and experiments, taking into account the influence of climatic conditions, shading parameters (spacing, depth, angle), construction properties, HVAC, and internal loads, resulting in optimal model performance. Several priority areas for further investigations are therefore suggested.

- Further studies relating to best scenarios H1, EC1, EC2 and V3 with different shading parameters (spacing, depth and angle).
- Considering exterior and indoor glass surface temperature in the simulations results.
- Future research may consider them as moveable due to adverse impact as passive design during the cold months.
- Including impact of shading system on daylighting and visual comfort.

REFERENCES

Aldawoud, A. (2013). Conventional fixed shading devices in comparison to an electrochromic glazing system in hot, dry climate. *Energy and Buildings*, *59*, 104–110. https://doi.org/10.1016/j.enbuild.2012.12.031

Alhuwayil, W. K., Abdul Mujeebu, M., & Algarny, A. M. M. (2019). Impact of external shading strategy on energy performance of multi-story hotel building in hot-humid climate. Energy, 169, 1166–1174https://doi.org/10.1016/j.energy.2018.12.069

Al-Masrani, S. M., & Al-Obaidi, K. M. (2019, June 1). Dynamic shading systems: A review of design parameters, platforms and evaluation strategies. Automation in Construction. Elsevier B.V. https://doi.org/10.1016/j.autcon.2019.01.014

Al-Tamimi, N. A., & Fadzil, S. F. S. (2011). The potential of shading devices for temperature reduction in high-rise residential buildings in the tropics. In Procedia Engineering (Vol. 21, pp. 273–282). Elsevier Ltd. https://doi.org/10.1016/j.proeng.2011.11.2015

Arifin, N. A., & Denan, Z. (2015). An Analysis of Indoor Air Temperature and Relative Humidity in Office Room with Various External Shading Devices in Malaysia. Procedia - Social and Behavioral Sciences, 179, 290–296. https://doi.org/10.1016/j.sbspro.2015.02.432

Atzeri, A., Cappelletti, F., & Gasparella, A. (2014). Internal versus external shading devices performance in office buildings. In Energy Procedia (Vol. 45, pp. 463–472). Elsevier Ltd. https://doi.org/10.1016/j.egypro.2014.01.050

Cho, J., Yoo, C., & Kim, Y. (2014). Viability of exterior shading devices for high-rise residential buildings: Case study for cooling energy saving and economic feasibility analysis. Energy and Buildings, 82, 771–785. https://doi.org/10.1016/j.enbuild.2014.07.092

Choi, S. J., Lee, D. S., & Jo, J. H. (2017). Lighting and cooling energy assessment of multi-purpose control strategies for external movable shading devices by using shaded fraction. Energy and Buildings, 150, 328–338. https://doi.org/10.1016/j.enbuild.2017.06.030

Ghosh, A., & Neogi, S. (2018). Effect of fenestration geometrical factors on building energy consumption and performance evaluation of a new external solar shading device in warm and humid climatic condition. Solar Energy, 169, 94–104. https://doi.org/10.1016/j.solener.2018.04.025

Gratia, E., & De Herde, A. (2007). The most efficient position of shading devices in a double-skin facade. Energy and Buildings, 39(3), 364–373. https://doi.org/10.1016/j.enbuild.2006.09.001

Hernández, F. F., Cejudo López, J. M., Peña Suárez, J. M., González Muriano, M. C., & Rueda, S. C. (2017). Effects of louvers shading devices on visual comfort and energy demand of an office building. A case of study. In Energy Procedia (Vol. 140, pp. 207–216). Elsevier Ltd. https://doi.org/10.1016/j.egypro.2017.11.136

Idchabani, R., El Ganaoui, M., & Sick, F. (2017). Analysis of exterior shading by overhangs and fins in hot climate. In Energy Procedia (Vol. 139, pp. 379–384). Elsevier Ltd. https://doi.org/10.1016/j.egypro.2017.11.225

Jin, Q., Overend, M., & Thompson, P. (2012). Towards productivity indicators for performance-based façade design in commercial buildings. Building and Environment, 57, 271–281. https://doi.org/10.1016/j.buildenv.2012.05.009

Kandar, M. Z., Nimlyat, P. S., Abdullahi, M. G., & Dodo, Y. A. (2019). Influence of inclined wall self-shading strategy on office building heat gain and energy performance in hot humid climate of Malaysia. Heliyon, 5(7). https://doi.org/10.1016/j.heliyon.2019.e02077

Kirimtat, A., Koyunbaba, B. K., Chatzikonstantinou, I., & Sariyildiz, S. (2016, January 5). Review of simulation modeling for shading devices in buildings. Renewable and Sustainable Energy Reviews. Elsevier Ltd. https://doi.org/10.1016/j.rser.2015.08.020

Lee, J., & Chang, J. D. (2015). Influence on Vertical Shading Device Orientation and Thickness on the Natural Ventilation and Acoustical Performance of a Double Skin Facade. In Procedia Engineering (Vol. 118, pp. 304–309). Elsevier Ltd. https://doi.org/10.1016/j.proeng.2015.08.431

Li, Z., Zhang, S., Chang, J., Zhao, F., Zhao, Y., & Gao, J. (2020). Simulation study on light environment performance and heat gain of applying a bimetal automatic shading device to rooms. Energy and Buildings, 211. https://doi.org/10.1016/j.enbuild.2020.109820

Lin, Y. H., Tsai, K. T., Lin, M. D., & Yang, M. D. (2016). Design optimization of office building envelope configurations for energy conservation. Applied Energy, 171, 336–346. https://doi.org/10.1016/j.apenergy.2016.03.018

Liu, S., Kwok, Y. T., Lau, K. K. L., Chan, P. W., & Ng, E. (2019). Investigating the energy saving potential of applying shading panels on opaque façades: A case study for residential buildings in Hong Kong. Energy and Buildings, 193, 78–91. https://doi.org/10.1016/j.enbuild.2019.03.044

Mandalaki, M., Zervas, K., Tsoutsos, T., & Vazakas, A. (2012). Assessment of fixed shading devices with integrated PV for efficient energy use. Solar Energy, 86(9), 2561–2575. https://doi.org/10.1016/j.solener.2012.05.026

Manzan, M. (2014). Genetic optimization of external fixed shading devices. Energy and Buildings, 72, 431–440. https://doi.org/10.1016/j.enbuild.2014.01.007

Mendis, T., Huang, Z., Xu, S., & Zhang, W. (2020). Economic potential analysis of photovoltaic integrated shading strategies on commercial building facades in urban blocks: A case study of Colombo, Sri Lanka. Energy, 194. https://doi.org/10.1016/j.energy.2020.116908

Planas, C., Cuerva, E., & Alavedra, P. (2018). Effects of the type of facade on the energy performance of office buildings representative of the city of Barcelona. Ain Shams Engineering Journal, 9(4), 3325–3334.

Rungta S. (2011). Design guide: Horizontal shading devices and light shelves. ⟨http://www.public.asu.edu/~kroel/www558/Shaily%20Vipul%20Assignment%203.pdf⟩.

Saranti, A., Tsoutsos, T., & Mandalaki, M. (2015). Sustainable Energy Planning. Design Shading Devices with Integrated Photovoltaic Systems for Residential Housing Units. In Procedia Engineering (Vol. 123, pp. 479–487). Elsevier Ltd. https://doi.org/10.1016/j.proeng.2015.10.099

Shahdan, M. S., Ahmad, S. S., & Hussin, M. A. (2018). External shading devices for energy efficient building. In IOP Conference Series: Earth and Environmental Science (Vol. 117). Institute of Physics Publishing. https://doi.org/10.1088/1755-1315/117/1/012034

Touma, A. A., & Ouahrani, D. (2018). The selection of brise soleil shading optical properties for energy conservation and glare removal: A case study in Qatar. Journal of Building Engineering, 20, 510–519. https://doi.org/10.1016/j.jobe.2018.08.020

Valladares-Rendón, L. G., Schmid, G., & Lo, S. L. (2017, April 1). Review on energy savings by solar control techniques and optimal building orientation for the strategic placement of façade shading systems. Energy and Buildings. Elsevier Ltd. https://doi.org/10.1016/j.enbuild.2016.12.073

Wong, N. H., & Istiadji, A. D. (2003). Effects of External Shading Devices on Daylighting and Natural Ventilation. Eighth International IBPSA Conference Eindhoven, Netherlands August 11-14, 2003, 475–482.

Himçi, Gridi   Impact of external shading strategy on energy performance of hotel buildings in Mediterranean climate